Molar dentition of the docodontan *Haldanodon* (Mammaliaformes) as functional analog to tribosphenic teeth

DISSERTATION

zur Erlangung des Doktorgrades (Dr. rer. nat.)

der Mathematisch-Naturwissenschaftlichen Fakultät

der Rheinischen Friedrich-Wilhelms-Universität Bonn

vorgelegt von

JANKA J. BRINKKÖTTER

aus Berlin

Bonn 2018

Angefertigt mit Genehmigung der Mathematisch-Naturwissenschaftlichen Fakultät der

Rheinischen Friedrich-Wilhelms-Universität Bonn

1. Gutachter: Prof. Dr. Thomas Martin

2. Gutachter: Prof. Dr. P. Martin Sander

Tag der Promotion: 14. Dezember 2018

Erscheinungsjahr: 2019

List of abbreviations

d – deciduous tooth
M – upper molar
m – lower molar
P – upper premolar
p – lower premolar

m – mesial
buc – buccal
dex – dextral
sin – sinistral

L – length
W – width

fr. – fragment

List of contents

Abstract

A virtual reconstruction of the mastication cycle of the Late Jurassic docodont *Haldanodon exspectatus* shows that the power stroke has two phases. Phase 1 is a steep upward motion from buccal to lingual of the lower molars into centric occlusion where the upper molar occludes in between two lower molars. The second phase is either a downward palinal motion following centric occlusion (phase 2) or a separate upward proal motion (phase 1b). In phase 1 the lingual flanks of the upper molar main cusps and the buccal flanks of the lower molar main cusps pass each other in a shear-cutting motion. At the same time, cusp b of the distal lower molar performs crushing within the "pseudotrigon basin" of the upper molar. At the very end of phase 1, cusp Y slides into the "pseudotalonid basin" to conduct a grinding function. As soon as the mesial border of the basin is worn down it slides over the rim, causing cusp b to actually contact the "pseudotrigon basin" and perform grinding as well. Consequently, the majority of crushing and probably also grinding in *Haldanodon* takes place within the large "pseudotrigon basin" of the upper molar. During the palinal downward movement of phase 2 the distal crests of the mesially situated lower molar pass the mesial flank of cusp X in a "shear-grinding" motion. In the proal upward movement of phase 1b true shear-cutting is performed and cusp b of the distal molar simultaneously also conducts crushing within the "pseudotrigon basin". A similar chewing stroke is also very likely for the other docodont taxa. Nevertheless, slight differences in molar morphology indicate that some of them were much more specialized in crushing and grinding. They either focused it on the lower molar by adding a distal basin, sometimes even accompanied by an additional cusp on the upper molar, or equally distributed it to upper and lower molar by developing relatively low cusps that allow simultaneous crushing and grinding within "pseudotalonid" and "pseudotrigon basin". All in all, crushing and even grinding was much more prominent in docodont molars than postulated in previous studies.

A comparison of molar functions of the presumably insectivorous *Haldanodon* with the tribosphenic taxa *Didelphis* (omnivorous) and *Monodelphis* (insectivorous) shows that in *Didelphis* grinding lasts much longer than in *Monodelphis*, but *Haldanodon* spends even less time on this function. Therefore, grinding is obviously more distinct in both tribosphenic taxa than in *Haldanodon*. This is not necessarily true for crushing, which lasts throughout the entire phase 1 in all taxa. In case of a separate upward power stroke, *Haldanodon* also spends the entire phase 1b on this function. Then the amount of crushing would not differ that much from *Didelphis* although its basins are better enclosed and much larger than those of *Haldanodon* are. In comparison to *Monodelphis* crushing probably was at least equally distinct since compared to *Didelphis* its basins of are much smaller, shallower and less closed. In other

docodont taxa with better enclosed “pseudotalonid” and “pseudotrigon basins” and additional distal basins on the lower molars crushing certainly was more distinct than in *Monodelphis* and maybe even equally distinct as in *Didelphis*. However, although docodont molars were functionally similar to early tribosphenic molars, their thin enamel layer made them much more prone to abrasion and the concomitant loss of function.

Kurzfassung

Eine virtuelle Rekonstruktion des Mastikationszykluses des oberjurassischen Docodonten *Haldanodon exspectatus* zeigt einen zweiphasigen Kauschlag. Phase 1 ist eine steile, von bukkal nach lingual verlaufende Aufwärtsbewegung der unteren Molaren in die zentrale Okklusion, wobei der obere Molar zwischen zwei unteren Molaren okkludiert. Die zweite Phase ist entweder eine direkt auf die zentrale Okklusion folgende palinale Abwärtsbewegung (Phase 2) oder eine eigenständige proale Aufwärtsbewegung (Phase 1b). In Phase 1 bewegen sich die lingualen Flanken der oberen Haupthöcker scherschneidend entlang der bukkalen Flanken der unteren Haupthöcker. Zur gleichen Zeit greift Höcker b des distalen unteren Molaren quetschend ins „Pseudotrigonbecken“ des oberen Molaren. Erst ganz am Ende der ersten Phase fährt Höcker Y reibend ins „Pseudotalonidbecken“. Sobald dessen mesiale Begrenzung abradiert ist, rutscht der Höcker jedoch über den Beckenrand hinaus, wodurch die Lücke zwischen Höcker b und dem „Pseudotrigonbecken“ geschlossen wird. Dieser Kontakt führt zu einer zusätzlichen reibenden Komponente. Somit findet ein Großteil des Quetschens und wahrscheinlich auch des Reibens im „Pseudotrigonbecken“ des oberen Molaren statt. Während der palinalen Abwärtsbewegung von Phase 2 „scher-reiben“ die distalen Grate des mesial gelegenen unteren Molaren an der mesialen Flanke des Höcker X entlang. Während der proalen Aufwärtsbewegung von Phase 1b findet echtes Scherschneiden statt und Höcker b des distalen Molaren greift zeitgleich ein weiteres Mal quetschend ins „Pseudotrigonbecken“. Andere Docodontenarten hatten sehr wahrscheinlich einen ähnlicher Kauschlag. Unterschiede in der Zahnmorphologie zeigen jedoch an, dass einige Arten viel stärker auf Quetschen und Reiben spezialisiert waren. Sie fokussierten diese Funktionen vor allem auf die unteren Molaren, indem sie zusätzlich ein distales Quetschbecken und manchmal sogar einen dort hineingreifenden Zahnhöcker im oberen Molaren ausbildeten. Andere Arten nutzten sowohl die oberen als auch die unteren Molaren, da ihre relativ niedrigen Zahnhöcker das gleichzeitige Stattfinden von Quetschen und Reiben in „Pseudotalonid-“ und „Pseudotrigonbecken“

erlaubten. Somit waren die Molaren der Docodonten wesentlich besser für Quetschen und sogar Reiben geeignet als allgemein angenommen.

Ein Vergleich der molaren Funktionen von *Haldanodon* (wahrscheinlich insektivor) mit denen der tribosphenischen Taxa *Didelphis* (omnivor) und *Monodelphis* (insektivor) zeigt, dass bei *Didelphis* Reiben wesentlich mehr Zeit in Anspruch nimmt als bei *Monodelphis*, *Haldanodon* jedoch noch weniger Zeit auf diese Funktion verwendet. Daher ist bei beiden tribosphenischen Taxa Reiben offensichtlich stärker ausgeprägt als bei *Haldanodon*. Quetschen wird bei allen drei Taxa die komplette Phase 1 hindurch ausgeführt. Falls *Haldanodon* einen eigenständigen aufwärts gerichteten Kauschlag genutzt haben sollte, wurde auch die gesamte Phase 1b für Quetschen verwendet. In diesem Fall würde die Quetschfunktion sich nicht wesentlich von der von *Didelphis* unterscheiden, obwohl dessen Becken besser abgeschlossen und viel größer sind als diejenigen von *Haldanodon*. Im Vergleich zu *Monodelphis* war die Quetschfunktion von *Haldanodon* dann wahrscheinlich sogar mindestens gleich stark ausgeprägt, weil die Becken von *Monodelphis* wesentlich kleiner, flacher und weniger gut abgeschlossen sind als diejenigen von *Didelphis*. Bei Docodontenarten mit besser abgeschlossenen „Pseudotalonid-“ und „Pseudotrigonbecken“ und zusätzlichen distalen Becken im unteren Molaren war Quetschen mit Sicherheit ausgeprägter als bei *Monodelphis* und vielleicht sogar ähnlich ausgeprägt wie bei *Didelphis*. Obwohl die Molaren der Docodonten den frühen tribosphenischen Molaren funktionell sehr ähnlich waren, machte ihre dünne Schmelzschicht sie viel anfälliger für Abrasion und den damit einhergehenden Funktionsverlust.

1 Aim of study

In the stem line of the Theria, which include extant placentals and marsupials, the development of the tribosphenic tooth morphology is regarded as key to the success of this mammalian subclass: in addition to the shear-cutting function the dentition also gained a crushing and grinding function by evolving a crushing basin (talonid) on the lower and an interlocking cusp (protocone) on the upper molar. This enabled the therians to process their food more efficiently due to the decreased particle size generated by chewing (Crompton 1971, Prothero 1981, Luo et al. 2001, Evans and Sanson 2003, Woodburne et al. 2003, Kielan-Jaworowska et al. 2004, Lopatin and Averianov 2006, Luo 2007, Luo et al. 2007, Davis 2011). The smaller the food particles entering the digestive system, the larger the surface area digestive acids can affect. This does not only allow faster absorption of nutrients but also is an important premise to efficiently process plant materials (Gingerich 1973, Rensberger 1973, Moore and Sanson 1995). However, in mammalian history three other lineages had independently developed such a crushing basin on the lower and an interlocking cusp on the upper molars. Their dentitions are regarded as functional analogs to the tribosphenic dentition. The earliest representatives with such a "pseudotribosphenic" tooth morphology are the docodonts (Simpson 1929, Crompton & Jenkins 1968, Hopson and Crompton 1969, Jenkins 1969, Gingerich 1973, Krusat 1980, Kermack et al. 1987, Butler 1988, Butler 1997, Wang et al. 1998, Pfretzschner et al. 2005, Luo 2007, Luo and Martin 2007, Luo et al. 2007, Davis 2011, Schultz et al. 2017).

The aim of this study is to compare the docodont tooth morphology to that of the tribosphenids, which are considered functionally similar (Simpson 1929, Patterson 1956, Sigogneau-Russell 2003, Averianov and Lopatin 2008, Wang and Li 2016). To accomplish this, first the docodont chewing cycle has to be reconstructed in detail. *Haldanodon* is the most suitable docodont taxon for this task since dozens of very well-preserved jaw specimens and hundreds of isolated molars are available. This is favorable to get reliable results including proportions of matching upper and lower teeth, location and size of facets, and striation patterns. The high number of specimens is also suited for a review of previous studies on the occlusion and possible ways of mastication movements in *Haldanodon* and other docodonts conducted with much less material. In this study, for the first time an attempt is made to virtually reconstruct the chewing movement of *Haldanodon* in an objectively testable manner exceeding mere hypothesis. This is done using 3D-models and the Occlusal Fingerprint Analyser (OFA), a software developed by the DFG research unit 771. This software is also used to quantify the amount of crushing and grinding taking place within the "pseudotalonid basin" for the first time. The results are compared to an OFA-analysis of the dentitions of the extant marsupials *Didelphis* and

Monodelphis as representatives of a tribosphenic tooth morphology. The classical comparative taxon *Didelphis* is omnivorous (Gardner 1982, Schwermann 2015) while *Monodelphis* prefers a more insectivorous diet (Casella and Cáceres 2006, Schwermann 2015), similar to that postulated for *Haldanodon* (Martin 2000, Martin and Nowotny 2000). With this, functional similarities and differences, particularly concerning crushing and grinding, of the tribosphenic dentition compared to that of the docodonts can finally be objectively tested.

2 Introduction

2.1 Systematical position of the Docodonta

The docodonts are mammaliaforms currently known only from Laurasia (Lillegraven and Krusat 1991, Kielan-Jaworowska et al. 2004, Ji et al. 2006, Luo 2007, Luo and Martin 2007, Averianov et al. 2010, Davis 2011, Rougier et al. 2014, Luo et al. 2015). The order Docodonta is named after the lingually expanded upper molars (from the Greek words *dokos* – "beam, rafter" and *odon* – "tooth") (Simpson 1929, Patterson 1956, Hopson and Crompton 1969, Krebs 1975, Kron 1979, Martin and Nowotny 2000, Averianov and Lopatin 2006, Hu et al. 2007). Docodont mandibles still show the Meckelian groove and a mandibular trough, indicating the presence of small, mechanically dysfunctional bone fragments. Therefore, docodonts indeed possessed fully functional secondary jaw joints replacing the primary ones but did not yet establish the mammalian middle ear, which is why they are placed just outside the Mammalia sensu stricto (Krebs 1975, Kron 1979, Henkel and Krusat 1980, Krusat 1980, Lillegraven and Krusat 1991, Martin and Nowotny 2000, Ruf et al. 2013). Their fossil record starts in the Middle Jurassic with six undisputed taxa and continues through the Late Jurassic with four taxa into the late Early Cretaceous with only one undisputed taxon (Maschenko et al. 2002, Kielan-Jaworowska et al. 2004, Martin and Averianov 2004, Lopatin and Averianov 2005, Pfretzschner et al. 2005, Ji et al. 2006, Luo and Martin 2007, Davis 2011). Most docodont taxa are known from mandibles and isolated teeth only (Simpson 1928, 1929, Kron 1979, Kielan-Jaworowska et al. 2004, Luo and Martin 2007, Rougier et al. 2014). Until recently more or less well-preserved skulls were only known from *Haldanodon* (Henkel and Krusat 1980, Lillegraven and Krusat 1991, Ruf et al. 2013), the postcranial only from *Haldanodon* and *Castorocauda* (Henkel and Krusat 1980, Krusat 1991, Martin 2005, Ji et al. 2006). However, in 2015 two additional taxa – *Docofossor* and *Agilodocodon* – have been described from partial skeletons with partially preserved skulls and complete upper and lower dentitions (Luo et al. 2015, Meng et al. 2015).

The first description of a docodont was that of *Docodon* (= *Diplocynodon*) by Marsh (1880, 1881), who referred this taxon to the "Pantotheria" (a paraphyletic group believed to be ancestral to Metatheria and Eutheria). Within this order he established a new family with the presently invalid, since preoccupied, name "Diplocynodontidae" (Marsh 1887). Simpson (1925) finally erected a distinct family Docodontidae, which he regarded as part of the "Pantotheria" as well (Simpson 1925, 1929). The first one to question the "pantothere" reference of the docodonts had been Gidley (1906) but he did not pursue the idea any further.

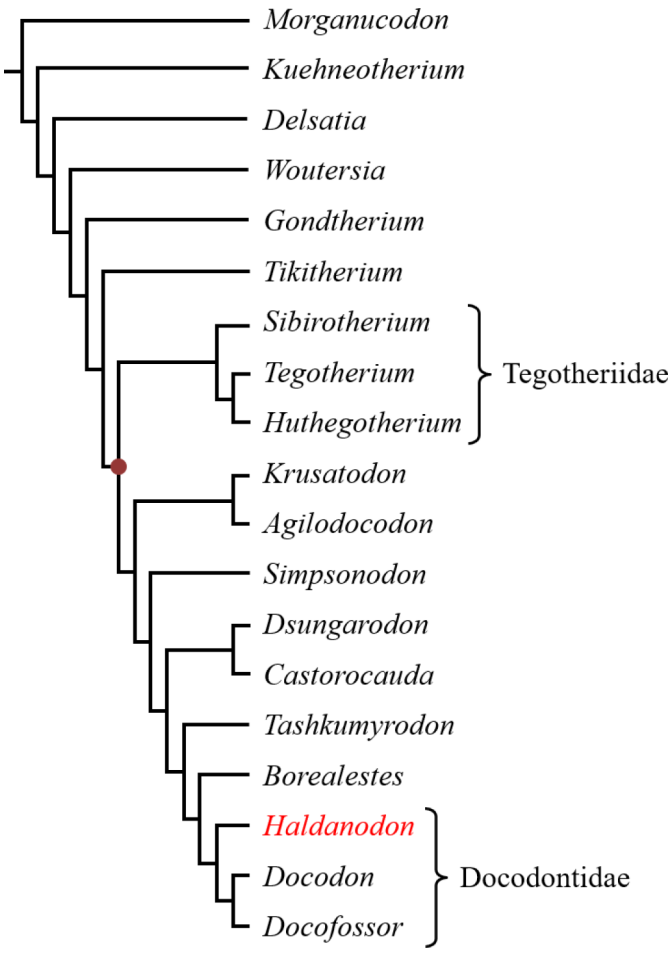

Fig. 1: Phylogeny of docodonts and their nearest relatives derived from dental characters (based on Meng et al. 2015). Red dot – Docodonta.

Kretzoi (1946) then considered them to be an independent order but his arguments for the separation from the "Pantotheria" were proven to be incorrect by Simpson (1961). However, meanwhile a new definition and diagnosis of the nontherian order Docodonta had been given by Patterson (1956), which is presently still valid.

Formerly docodonts were regarded as sister taxon to morganucodontids because the main cusp row of the lower molars of *Morganucodon* was considered to be homologous to the buccal cusps of docodont lower molars (Kühne 1950, Patterson 1956, Crompton and Jenkins 1968, Hopson and Crompton 1969, Jenkins 1969, Gingerich 1973, Kermack et al. 1973, Krebs 1975, Krusat 1980, Pascual et al. 2000, Averianov and Lopatin 2006). This was rebutted by Kemp (1983) who revealed that a straight arrangement of the main cusps is already present in many premammaliaform cynodonts. Later studies also showed that while most basicranial and postcranial characters are more derived in the docodont *Haldanodon* than in *Morganucodon*, some of them actually are more derived in morganucodontids. This makes it extremely improbable that they were the ancestors of docodonts (Lillegraven and Krusat 1991, Wible and Hopson 1993, Luo 1994, Rougier et al. 1996, Ruf et al. 2013). A new hypothesis places docodonts next to Late Triassic "symmetrodont" mammaliaforms like *Woutersia*, *Delsatia*, *Tikitherium*, and *Kuehneotherium* (fig. 1). The reason is a strikingly similar cusp morphology

in both upper and lower molars assuming that the distal broadening of the docodont molars was acquired by developing an additional disto-lingual cusp (Sigogneau-Russell and Hahn 1995, Butler 1997, Sigogneau-Russell and Godefroit 1997, Martin and Averianov 2004, Pfretzschner et al. 2005, Averianov et al. 2010). Sigogneau-Russell and Godefroit (1997) even suggested including *Delsatia* into Docodonta, as the oldest known docodont taxon. Most other studies, however, do not consider this taxon to be a docodont but closely related to them (e.g. Ji et al. 2006, Luo and Martin 2007, Meng et al. 2015). In *Tikitherium* from India the "talon-like platform" of the upper molar (the only specimen so far) already is so advanced that Datta (2005) considered it to be the earliest presumably "pseudotribosphenic" dentition. A phylogenetic analysis of the tooth morphology by Luo and Martin (2007) confirms *Tikitherium* as sister taxon to the docodonts. It places both taxa next to *Woutersia* and *Delsatia*, thus greatly supporting the "symmetrodont" hypothesis (see also Ji et al. 2006, Meng et al. 2015).

So far there are eleven taxa placed within docodonts without doubt: the Middle Jurassic taxa *Borealestes* from Great Britain (Waldman and Savage 1972, Sigogneau-Russell 2003), *Castorocauda* from China (Ji et al. 2006), *Hutegotherium* from Siberia (Averianov et al. 2010), *Krusatodon* from Great Britain (Sigogneau-Russell 2003), *Simpsonodon* (= *Cyrtlatherium*) from Great Britain, Siberia and Kyrgyzstan (Freeman 1979, Kermack et al. 1987), and *Tashkumyrodon* from Kyrgyzstan (Martin and Averianov 2004), the Late Jurassic taxa *Docodon* (= *Diplocynodon* / *Dicrocynodon*, *Enneodon* / *Ennacodon*) from Great Britain and North America (Marsh 1881, Simpson 1929), *Dsungarodon* (= *Acuodulodon*) from China (Pfretzschner et al. 2005, Hu et al. 2007), *Haldanodon* from Portugal (Kühne and Krusat 1972, Krusat 1980, Lillegraven and Krusat 1991, Martin 2005), and *Tegotherium* from China and Mongolia (Tatarinov 1994), and the Early Cretaceous taxon *Sibirotherium* from Siberia (Maschenko et al. 2002).

Simpsonodon actually is a junior synonym of *Cyrtlatherium* (Freeman 1979). Unfortunately, the lower molars described by Freeman are milk teeth (Sigogneau-Russell 2001, Averianov 2004, Kielan-Jaworowska et al. 2004, Martin and Averianov 2004) and therefore their characters are not sufficient to define a taxon. This is why the younger name is preferred (Luo and Martin 2007, Averianov et al. 2010).

Until very recently, *Itatodon* (Lopatin and Averianov 2005, Averianov and Lopatin 2006) from the Middle Jurassic of Siberia was also commonly assigned to the docodonts (Lopatin and Averianov 2005, Averianov and Lopatin 2006, Hu et al. 2007, Luo and Martin 2007, Lopatin et al. 2009, Averianov et al. 2010, Martin and Averianov 2010, Meng et al. 2015). Martin and Averianov (2010) also added a new genus *Paritatodon* from the Middle Jurassic of Kyrgyzstan. Although the holotype, a left lower molar, was formerly described as a shuotheriid by

Sigogneau-Russell (1998), Martin and Averianov (2010) noticed its striking similarity to *Itatodon* and placed it within the docodonts instead. Wang and Li (2016), though, pointed out that the molar morphology of both *Itatodon* and *Paritatodon* is much more similar to that of the Middle and Late Jurassic *Shuotherium* (Chow and Rich 1982) from China and Great Britain than to that of the other docodont taxa. Therefore, they reassign both taxa to the shuotheriids. There have been a few attempts to include *Shuotherium* into Docodonta as well, because it also possesses a mesially situated "pseudotalonid" (Kermack et al. 1987, Tatarinov 1994). However, it is nowadays widely accepted that this was a convergent development and it is usually regarded as the sister taxon to australosphenids (Luo et al. 2001, Luo et al. 2002, Rauhut et al. 2002, Martin and Rauhut 2005, Ji et al. 2006, Luo 2007) (see also 2.3.1).

There is one clade that separates from the other docodont taxa in almost all phylogenetic analyses: the endemic Asian family Tegotheriidae, comprising *Tegotherium* and *Sibirotherium* (Martin and Averianov 2004, Averianov and Lopatin 2006, Ji et al. 2006, Hu et al. 2007, Luo and Martin 2007, Averianov et al. 2010, Meng et al. 2015). According to the most recent analyses by Averianov et al. (2010) and Meng et al. (2015) the recently described *Hutegotherium* is most certainly also part of this family (fig. 1). For some time, *Tashkumyrodon* was included as well (Martin and Averianov 2004, Ji et al. 2006), sometimes together with *Itatodon* (Lopatin and Averianov 2005, Averianov and Lopatin 2006), but both taxa were excluded by later studies (Hu et al. 2007, Luo and Martin 2007, Lopatin et al. 2009, Averianov et al. 2010, Meng et al. 2015). The only exceptions are Martin and Averianov (2010) who also added their newly erected taxon *Paritatodon* to the tegotheriids as sister taxon to *Itatodon*. In place of *Tashkumyrodon* and *Itatodon*, Lopatin et al. (2009) as well as Averianov et al. (2010) consider *Krusatodon* to be part of this family. Sigogneau-Russell (2003) even suggested *Krusatodon* as direct ancestor of *Tegotherium*, while Ji et al. (2006) and Meng et al. (2015) regard this taxon as closer related to *Simpsonodon*, *Castorocauda* and *Dsungarodon*, Luo and Martin (2007) as sister taxon to *Itatodon* (which is not part of the tegotheriids in their phylogeny). Opposing opinions also exist for the position of the tegotheriids within Docodonta: some authors regard them as the most derived group (Averianov and Lopatin 2006, Hu et al. 2007, Averianov et al. 2010), others place the separation of tegotheriids at the very base of the docodont tree (Ji et al. 2006, Luo and Martin 2007, Meng et al. 2015).

Most phylogenetic analyses show another distinct family, the Docodontidae. It comprises *Docodon* and *Haldanodon* (Pfretzschner et al. 2005, Ji et al. 2006, Luo and Martin 2007, Averianov et al. 2010, Meng et al. 2015). Some authors also place *Borealestes* within this clade (Pfretzschner et al 2005, Ji et al. 2006, Averianov et al. 2010). Sigogneau-Russell (2003) separates *Haldanodon* and *Docodon* but sees *Borealestes* as direct ancestor to *Haldanodon*.

Luo and Martin (2007) consider *Borealestes* to be closer related to *Tashkumyrodon* and instead include *Dsungarodon* into docodontids.

However, most other phylogenetic analyses place *Dsungarodon* in a clade with *Simpsonodon* (Pfretzschner et al. 2005, Averianov and Lopatin 2006, Ji et al. 2006, Averianov et al. 2010). Averianov and Lopatin (2006) added *Castorocauda*, Pfretzschner et al. (2005) *Krusatodon* to the same clade, Ji et al. (2006) both taxa.

Two recently described taxa from China were also referred to the docodonts by the respective authors: the Middle Jurassic *Agilodocodon* (Meng et al. 2015) and the Late Jurassic *Docofossor* (Luo et al. 2015). According to the phylogenetic analysis by Meng et al. (2015, see also Supplementary Materials) *Agilodocodon* is the sister taxon of *Krusatodon* and *Docofossor* that of *Docodon* (including it into Docodontidae and restricting this family to these two taxa plus *Haldanodon*) (fig. 1).

Sigogneau-Russell (2003) also included the Middle to Late Jurassic *Peraiocynodon* (Simpson 1928) from Great Britain as sister taxon to *Docodon*. However, this taxon was excluded again by Averianov (2004) because he argued that both species of this genus are based on deciduous teeth – the larger one probably belonging to *Krusatodon*, the smaller one to *Docodon*. That *Peraiocynodon* actually might be a milk dentition of *Docodon* had also been remarked by previous authors (Butler 1939, Patterson 1956, Kermack et al. 1987). Therefore, *Peraiocynodon* is not regarded as a valid taxon by most authors, with the exception of Hu et al. (2007) who recognize it as the most basal docodont. The recent study by Schultz et al. (2017), who among other things examined the deciduous lower premolars of *Docodon* in great detail, strongly supports the assumption that *Peraiocynodon* and *Docodon* are indeed different taxa. A similar case is that of the Late Jurassic *Acuodulodon* (Hu et al. 2007) from China, which is regarded as a juvenile specimen of *Dsungarodon* by Martin et al. (2010) but recognized as valid taxon by Averianov et al. (2010). There are also two questionable docodonts reported from Gondwana. The first one is *Gondtherium* (Prasad and Manhas 2001, 2007) from the Middle Jurassic of India which was included into Docodonta by the describing authors and by Luo and Martin (2007) who placed it at the base of non-tegotheriids. Averianov et al. (2010), however, pointed out that this taxon is only known from a single upper premolar and thus should be excluded from further consideration. (Originally, also a lower molar had been described by Prasad and Manhas (2001) which was included into the study by Luo and Martin (2007) who also reinterpreted the upper premolar as upper molar). Meng et al. (2015) nevertheless included *Gondtherium* into their phylogeny but placed it outside of the Docodonta as a closely related taxon in between *Woutersia* and *Tikitherium*. The other disputed Gondwanan taxon is *Reigitherium* (Bonaparte 1990) from the Late Cretaceous of South America. It would also be

the youngest known docodont taxon by far. Originally placed within Dryolestoidea (Bonaparte 1990), *Reigitherium* was placed within docodonts by Pascual et al. (2000) and then reassigned to Dryolestoidea by Rougier and Apesteguia (2004), respectively announced to have an unknown position within Mammalia by Kielan-Jaworowska et al. (2004). A recent study by Harper and Rougier (2017) strongly supports its affiliation with the dryolestids.

Until their extinction in the Early Cretaceous docodonts were a quite diverse, widespread, and abundant order with taxa occupying very diverse ecological niches, as suggested by taxa known not only from dental but also from skeletal remains: *Agilodocodon* possessed arboreal adaptations (Meng et al. 2015), *Docofossor* most certainly had a subterranean lifestyle comparable to that of extant golden moles (Luo et al. 2015), *Haldanodon* had subterranean and possibly semiaquatic adaptations comparable to that of extant desmans and the monotreme *Ornithorhynchus* (Krusat 1991, Martin and Nowotny 2000, Martin 2005, Ruf et al. 2013), and *Castorocauda* was certainly semiaquatic (Ji et al. 2006).

2.2 Definition of terms

2.2.1 Abrasion and Attrition

There are two types of wear affecting the teeth during mastication – abrasion and attrition (Hunter 1778, Stones 1948). The terms are originally taken from dental medicine and were first applied to fossil teeth by Butler (1972). A third type of wear commonly distinguished by dentists, erosion or corrosion, is caused by acidic fluids (like fruit juice, cola type beverages, and gastric acid) and therefore mostly effective in modern human dentitions (Eccles 1982, Grippo et al. 2004, Barbour and Rees 2006). This is why it can be neglected for fossil teeth.

“Abrasion” refers to **tooth wear resulting from contact of the tooth surface with food particles and grit or sand** during the mastication process **(food-tooth contact)**. This eventually makes the cusps become dull (Butler 1972, Rensberger 1973, Kay and Hiiemäe 1974, Krusat 1980). Abrasion is not restricted to the occlusal surface but can also occur on the buccal and lingual sides as the food particles are forced against them by the cheeks, lips, and tongue (Grippo et al. 2004). Abrasion usually occurs in the early stages of mastication when the food is compressed between the teeth, but the teeth are not yet in contact with each other (Crompton and Hiiemäe 1970, Butler 1972, Krusat 1980).

“Attrition” on the other hand refers to **tooth wear resulting from repetitious occlusal contact of the tooth with its antagonist (tooth-tooth contact)**. This causes the development of wear

facets with a distinctly smooth, flat surface (Butler 1972, Greaves 1973, Rensberger 1973, Kay and Hiiemäe 1974, Krusat 1980, Eccles 1982, Moore and Sanson 1995, Grippo et al. 2004). They are usually crossed by more or less parallel running striae caused by microscopic food particles and grit that are caught between the teeth during mastication. Therefore, these striations are an indicator for the orientation of the jaw movement (Butler 1972, Greaves 1973, Gingerich 1973, Krusat 1980, Costa and Greaves 1981). However, they are not indicating the direction of movement because it could be either way parallel to them (Greaves 1973, Costa and Greaves 1981). Striations observed on the tooth surface that do not run parallel are most likely caused by abrasion (Rensberger 1978, Moore and Sanson 1995).

The direction of the jaw movement can be deduced from exposed dentine. During mastication, it is worn down faster than enamel because it is much softer (Rensberger 1973, Costa and Greaves 1981, Eccles 1982, Barbour and Rees 2006). If dentine is exposed, this leads to the formation of indentations, where the scoured dentine is encompassed by enamel. This is why the wear of dentine even on attritional surfaces is usually dominated by abrasion – it does not get in contact with the antagonistic tooth surface any more (Rensberger 1973, Costa and Greaves 1981). However, the dentine at the leading edge of these indentations, where the occluding surface of the antagonist and therefore the abrasive food particles arrive first, is protected by the preceding enamel and connects smoothly with it. At the trailing side in contrast there is a characteristic step in between the elevated enamel and the dentine, where the food particles are pressed against the more resistant following enamel border and abrade the dentine to form a step. Therefore, the movement of the chewing stroke can be deduced from the leading edge towards the trailing edge (Greaves 1973, Rensberger 1973, Costa and Greaves 1981).

2.2.2 Wear facets

In this study, any surface formed by tooth-tooth-contact, that is attrition, is referred to as (wear) facet. Therefore, wear facets can also be present on dentine provided that the attrition outweighs the abrasion and the dentine surface is worn smooth. Wear caused by abrasion is not considered to be a facet in this study.

2.2.3 Mastication functions

2.2.3.1 Shear-cutting

Traditionally, shear-cutting is said to require two relatively flat surfaces which move across one another in a plane oblique or perpendicular to the occlusal plane which results in the building of two sharp edges (Rensberger 1973). Referred to teeth this means that parts of the occluding upper and lower tooth slide across each other in a direction nearly parallel to their planes of contact (Kay and Hiiemäe 1974). According to Moore and Sanson (1995) only shear produces wear facets since it is dominated by attrition.
This study defines "**shear-cutting**" as "**two surfaces moving past each other with close contact of antagonistic structures in a lateral movement relative to the surfaces**".

2.2.3.2 Crushing

The traditional definition describes crushing as two planar surfaces being brought together, which creates stresses in a direction nearly perpendicular to the approaching or actual plane of contact between them (Rensberger 1973, Kay and Hiiemäe 1974). In this kind of definition, it does not matter whether the antagonistic structures actually contact each other (actual plane of contact) or do not do that (approaching plane of contact). However, if the stresses need to be perpendicular to the plane of contact, this contact can only occur at the very end of the crushing motion. This fact is emphasized by Butler (1972) as well as Moore and Sanson (1995) who state that the crushing function involves only very little tooth-to-tooth contact and therefore does not produce any wear facets. The cusps involved are worn solely by abrasion.
This study combines these uses of the term "**crushing**" and defines it as "**compression between two surfaces without contact of antagonistic structures and without lateral movement relative to the surfaces**". According to this definition the antagonistic structures do not necessarily have to be planar. In *Didelphis*, for example, the hypoconid conducts a crushing function within the trigon basin. Neither do they have to be horizontal to the occlusal surface of the tooth as demanded by Moore and Sanson (1995). Therefore, also flanks of cusps can become crushing surfaces if the jaw movement is lateral – the flanks then are moving straight towards each other, so relative to them the movement is not lateral.

2.2.3.3 Grinding

Grinding is usually seen as a combination of shear-cutting and crushing (Kay and Hiiemäe 1974, Moore and Sanson 1995, Spears and Crompton 1996) or interpreted as (nearly) horizontal shear-cutting (Butler 1972). Consequently, Spears and Crompton (1996) even wanted to abandon the term "grinding", although this view is not widely accepted throughout the literature.

Traditionally grinding is defined as a motion of flat or irregular surfaces across one another in a plane more or less parallel to the occlusal plane, the resulting stresses having components both perpendicular and parallel to the plane of approaching or actual contact between the teeth (Rensberger 1973, Kay and Hiiemäe 1974). According to Butler (1972) in contrast to the crushing function the grinding function does involve close tooth-to-tooth contact producing clearly distinguishable wear facets.

This study closely follows the use of the term "**grinding**" as crushing with a shear-cutting component, that is "**compression between two surfaces with close contact of antagonistic structures and with a certain amount of lateral movement relative to the surfaces**". The protocone for example conducts a grinding function within the talonid in basal tribosphenic teeth.

2.3 Morphology of "pseudotribosphenic" molars

2.3.1 Convergent development of crushing basins on the lower molars in mammalian history

The term "tribosphenic" (from the Greek words *tribein* – to rub (for grinding) and *sphen* – wedge (for shear-cutting)) was first introduced by Simpson (1936) to describe the ancestral dentitions of crown therians: they developed a lingual cusp on the upper molar (the protocone) occluding into a distal basin on the lower molar (the talonid basin). This protocone of the upper molar acts like a pestle, the talonid basin of the lower molar like a mortar; both together perform a crushing and grinding function. From this type of molar evolved all the various types of molars found in modern mammals (Simpson 1936, Patterson 1956, Mills 1966, Crompton and Hiiemäe 1970, Butler 1972, Prothero 1981, Luo et al. 2001, Datta 2005, Lopatin and Averianov 2006, Luo 2007, Luo et al. 2007, Davis 2011).

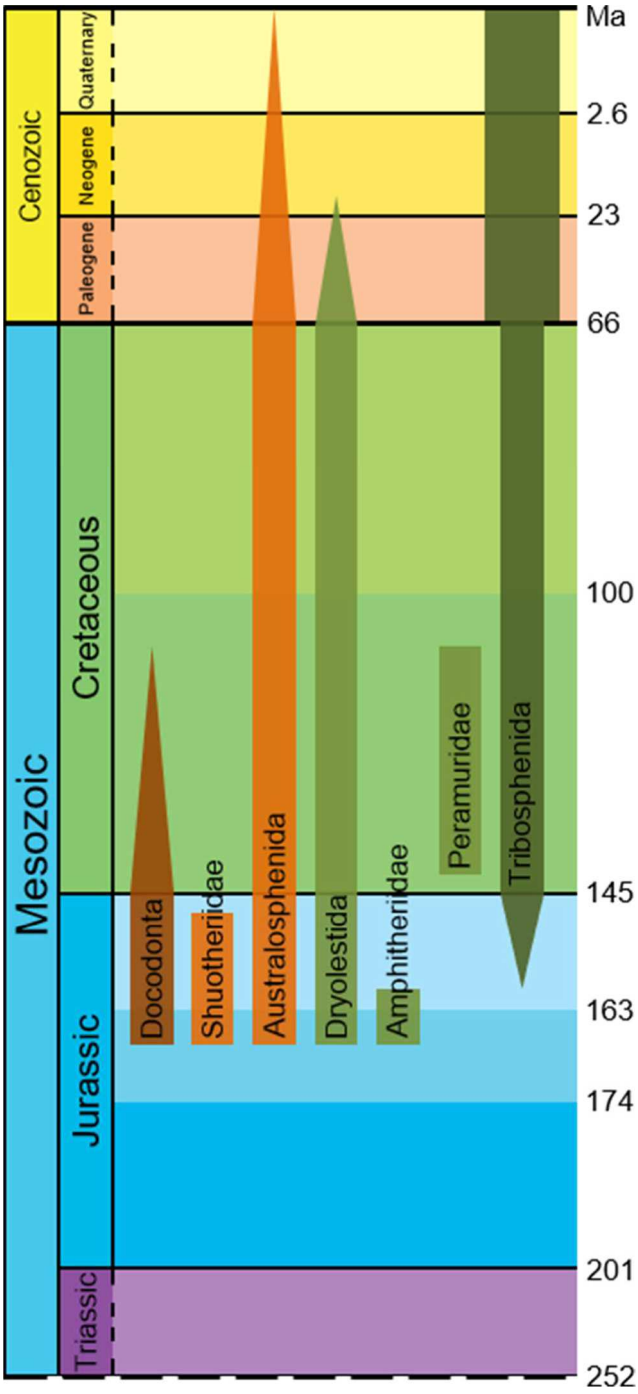

Fig. 2: Chronological distribution of the "pseudotribosphenic" docodonts (brown), shuotheriids, and australosphenids (both orange), the pretribosphenic dryolestids, amphitheriids, and "peramurids" (all light green), and the tribosphenids (dark green) (based on data derived from Chow and Rich 1982, Flynn et al. 1999, Lopatin and Averianov 2009, Averianov et al. 2010, Martin et al. 2010, Davis 2011, Luo et al. 2011, Chimento et al. 2012).
Docodonts and shuotheriids possess a mesially situated "pseudotalonid basin" on the lower as well as a "pseudoprotocone" on the upper molar to fit into this basin. The "pseudotalonid basin" of the australosphenids is situated distally like the talonid basin of the tribosphenids. Their upper molars probably lacked a "pseudoprotocone". Dryolestids and amphitheriids have an unicuspid talonid, "peramurids" a bicuspid one with an incipient basin. None of these pretribosphenic taxa had yet developed a protocone. Only tribosphenids possess a fully basined, tricuspid talonid and a protocone to fit into this basin.
Note that docodonts successfully coexisted with all "pseudo-" and pretribosphenic taxa until the rise of the tribosphenids.

In tribosphenids, the talonid was developed earlier than the protocone (Crompton 1971, Sigogneau-Russell 1998, Averianov and Lopatin 2008, Davis 2011). At first, it was formed rather like an additional crest than a basin and was used to increase the functional area for shear-cutting in the dentition (Davis 2011, Schultz 2011). This increase was mainly achieved by the overlapping of the molars in occlusion. Previously, the shear-cutting had been restricted to the mesial and distal margins of the crown by interlocking, more or less triangular molars (Davis 2011). With the development of a basined talonid and the protocone and the addition of a transverse jaw movement during mastication the talonid also gained a grinding function (Crompton and Hiiemäe 1970, Davis 2011). This talonid-protocone interaction which combines

shear-cutting, crushing, and grinding therefore is considered to be a key dental innovation for more effective herbivory and omnivory, a vital factor for the basal diversification of the Tribosphenida, comprising marsupials, placentals and their ancestors (Crompton 1971, Prothero 1981, Luo et al. 2001, Rauhut et al. 2002, Evans and Sanson 2003, Woodbourne et al. 2003, Kielan-Jaworowska et al. 2004, Datta 2005, Lopatin and Averianov 2006, Luo 2007, Luo et al. 2007, Davis 2011).

However, by now there is evidence that in mammalian history a crushing basin in the lower molar similar to the talonid basin developed at least three times independently before the occurrence of the tribosphenids in the Late Jurassic: in docodonts (Middle Jurassic to Early Cretaceous), shuotheriids (Middle to Late Jurassic), and australosphenids (since Middle Jurassic, including the extant monotremes) (fig. 2). This was accompanied by the development of an additional cusp in the upper molar, the "pseudoprotocone", which fits into this "pseudotalonid basin", conducting a crushing and grinding function like a pestle in a mortar (Hopson and Crompton 1969, Chow and Rich 1982, Kermack et al. 1987, Butler 1988, Sigogneau-Russell 1998, Wang et al. 1998, Luo et al. 2001, Sigogneau-Russell et al. 2001, Datta 2005, Luo 2007, Luo et al. 2007, Lopatin et al. 2009, Davis 2011). Thus, the "pseudotribosphenic" tooth morphology just like the tribosphenic molars allowed to combine shear-cutting, crushing and grinding in a single chewing stroke (Evans and Sanson 2003, Luo and Martin 2007, Davis 2011). This enabled these taxa to process food much more efficiently due to the reduction of particle size during mastication and the resulting increased surface area of the particles entering the digestive system, on which digestive fluids act more rapidly (Gingerich 1973, Rensberger 1973, Krusat 1980, Moore and Sanson 1995).

In contrast to the distally situated talonid of the tribosphenids, the "pseudotalonid" of docodonts and shuotheriids is situated mesially (Kermack et al. 1987, Datta 2005, Luo 2007, Luo et al. 2007, Davis 2011). Australosphenids (including the ancestors of the nowadays toothless monotremes) have a distally situated "pseudotalonid", which is why it was considered to be homologous to the tribosphenic talonid for a long time. However, Kielan-Jaworowska et al. (1998) and Rich et al. (1998) showed that there actually are some differences. This finally led to the formulation of the dual origin hypothesis by Luo et al. (2001), who implied that the "talonid" of the australosphenids rather developed independently from that of the tribosphenids. This view is supported by recent studies and phylogenetic analyses (Sigogneau-Russell et al. 2001, Luo et al. 2002, Rauhut et al. 2002, Martin and Rauhut 2005, Rougier et al. 2007, Davis 2011). Martin and Rauhut (2005) as well as Davis (2011) are of the opinion that despite the morphological resemblance the "pseudotalonid" of the australosphenids is also not functional homologous to the tribosphenic talonid. According to them it lacks a grinding function, because

even on strongly worn lower molars facets do not form within the basin but only on the shear-cutting surfaces of the teeth. An upper molar of any australosphenid has yet to be found; until then the presence or absence of a "pseudoprotocone" that might have had occluded into the basin will remain obscure.

A similar problem is the relationship of the "pseudotalonid basins" of docodonts and shuotheriids, which are both mesially situated. Some authors like Martin and Averianov (2004), Pfretzschner et al. (2005), Luo and Martin (2007), and Wang and Li (2016) do not consider them homologous while others like Kermack et al. (1987) and Sigogneau-Russell (2003) do. This depends on the view of cusp homology the authors base their statements on: Sigogneau-Russell (2003) sees cusp g as cusp b. In this case both the docodont and the shuotheriid "pseudotalonid basin" would be situated mesial to the a-b crest. Otherwise the "pseudotalonid basin" of the docodonts would be situated lingually of the a-b crest and therefore would not be homologous to the shuotheriid one.

Martin and Averianov (2004) as well as Averianov and Lopatin (2006) suggest that the "pseudotalonid" was also independently acquired twice within Docodonta: Since the tegotheriids – in their definition including *Tegotherium*, *Sibirotherium*, and *Tashkumyrodon* (and the questionable docodont *Itatodon* in Averianov and Lopatin 2006) – unlike the other docodonts did not reduce cusp e, it is included into the "pseudotalonid" in these taxa. Therefore, the mesial border of the "pseudotalonid basin" is not formed by crest b-g but by crests b-e and e-g. However, in more recent phylogenetic analyses *Tashkumyrodon* as well as other docodonts formerly regarded as tegotheriids like *Krusatodon* are closer related to the other docodonts than to the tegotheriids (Luo and Martin 2007, Lopatin et al. 2009; Meng et al. 2015). According to Meng et al. (2015: Supplementary Materials) a "pseudotalonid" mesially bordered by crest b-e is present not only in the tegotheriids (*Tegotherium*, *Hutegotherium*, and *Sibirotherium* in their definition) but also at the very base of the non-tegotheriid docodonts (*Krusatodon* and the newly discovered *Agilodocodon*) and in the middle of the non-tegotheriid branch (*Tashkumyrodon* and *Borealestes*).

2.3.2 "Pseudotalonid basin", "pseudoprotocone", and "pseudotrigon basin" on docodont molars

As mentioned above, the "pseudotalonid basin" is a basin structure similar to the talonid basin on the lower molars of non-tribosphenids. In docodonts it is situated mesially. In *Haldanodon* it is placed in between cusps a, b, and g and opens in mesio-lingual and distal direction, because

the a-g crest and the b-g crest are not very distinctive; in some of the other docodont taxa cusp e is also included into the “pseudotalonid” (fig. 3, for a detailed discussion see 6.1.1).
The lingually situated cusp X of the upper molar is also called the “pseudoprotocone“. Due to the common use of this term it is also employed in this study, although it is highly controversial (fig. 3, for a detailed discussion see 6.1.2).
The “pseudotrigon basin“ of docodont upper molars is situated distally in between the buccal cusps A and C and the lingual cusps X and Y. In *Haldanodon* it opens in distal direction, because it lacks crest C-Y (fig. 3).

3 Material

3.1 Docodonta

Docodonts were chosen as representatives of a “pseudotribosphenic” molar morphology, because they are the most primitive taxon in the mammalian lineage to have evidently developed a crushing basin on the lower molars and an interlocking conus on the upper molars (Sigogneau-Russell and Hahn 1995, Butler 1997, Sigogneau-Russell and Godefroit 1997, Martin and Averianov 2004, Pfretzschner et al. 2005, Ji et al. 2006, Luo and Martin 2007, Averianov et al. 2010, Davis 2011, Rougier et al. 2014, Meng et al. 2015). This makes a comparison with the “true” tribosphenic tooth morphology most interesting. A second reason is the quantity of the available material. However, this mostly belongs to one genus, *Haldanodon*, with a single species, *Haldanodon exspectatus* (Kühne 1968, Kühne and Krusat 1972). Comprising hundreds of isolated teeth, as well as many mandibles with more or less complete tooth rows, a few skulls, an almost complete skeleton, and some additional isolated postcranial remains, *Haldanodon* is the best known docodont taxon by far (Kühne and Krusat 1972, Henkel and Krusat 1980, Krusat 1980, Lillegraven and Krusat 1991, Martin and Novotny 2000, Martin 2005, Luo et al. 2007, Ruf et al. 2013). The other taxa are mostly known from few isolated teeth or jaw fragments. The only exceptions are two recently described specimens of two different docodont taxa represented by partial skeletons, including partially preserved skulls and complete upper and lower dentitions (Luo et al. 2015, Meng et al. 2015). These dentitions, however, are still partially embedded and therefore not suited for a detailed study of the docodont mastication movement. Comparisons of *Haldanodon exspectatus* with other docodont taxa mostly depend on information derived from literature. A few isolated molars of *Dsungarodon* and *Tegotherium* from the Sino-German Project collection (SGP) are currently housed in the Steinmann-Institut für Geologie, Mineralogie und Paläontologie, Rheinische Friedrich-Wilhelms-Universität Bonn, Germany. These specimens were also used for comparisons, as well as a cast of the holotype of *Tashkumyrodon* (ZIN 85279; Zoological Institute of the Russian Academy of Sciences in St. Petersburg, Russia).

3.1.1 *Haldanodon exspectatus* KÜHNE AND KRUSAT 1972

The genus *Haldanodon* comprises a single species: *Haldanodon exspectatus*. It was chosen as representative for docodonts because of the high quantity and quality of available material. All

specimens derive from a single locality: the Guimarota coal mine in the vicinity of Leiria, Portugal. It is dated as Kimmeridgian (Middle Late Jurassic, 151 – 154 Ma) (Helmdach 1971, Schudack 2000). Animal and plant fossils indicate a subtropical forest-swamp on the coast of a brackish lagoon as original habitat (Helmdach 1971, Krusat 1980, Martin 2000). This marshy environment in combination with some adaptations in the skull and postcranium – most obvious in the humerus – suggests a fossorial and possibly semiaquatic lifestyle for *Haldanodon*, comparable to that of extant desmans and the monotreme *Ornithorhynchus* (Lillegraven and Krusat 1991, Martin and Nowotny 2000, Martin 2005, Ruf et al. 2013). Its diet probably consisted mainly of insect larvae and worms (Martin 2000, Martin and Nowotny 2000).

The first fossils were collected from 1959 until the closure of the mine in 1961. From 1973 to 1982 it was reopened for paleontological excavations (Krebs 1988, Krebs 2000, Martin 2000, Martin 2005). During more than ten years of screen washing and picking the coal a vast number of Mesozoic fossils could be recovered, thereof hundreds of jaw fragments and isolated teeth of *Haldanodon*. 52 mandible fragments, 16 maxilla fragments and 102 isolated teeth (67 lower and 35 upper molars) were included in this study (for a detailed list of specimens see appendix tab. 1-5). Most of the specimens of *Haldanodon* and other Mesozoic mammals from the Guimarota coal mine are currently housed in the collection of the Steinmann-Institut für Geologie, Mineralogie und Paläontologie, Rheinische Friedrich-Wilhelms-Universität Bonn (Gui Mam; specimens figured in Krusat 1980: VJ).

A complete upper tooth row of *Haldanodon* is composed of six incisors, a canine, three premolars, and five molars. M4 sometimes is vestigial, M5 always is. The lower tooth row consists of four incisors, a canine, three premolars, and four to six molars. Of those m5 and m6 are vestigial without exception (Martin and Nowotny 2000, Nowotny et al. 2001, Luo and Martin 2007). This study focuses exclusively on the molars since they perform the main function during mastication.

3.2 Marsupialia

3.2.1 *Didelphis* LINNAEUS 1758

The marsupial taxon *Didelphis* was chosen as representative for a tribosphenic tooth morphology, because it is one of the very few Recent taxa which still show a largely unmodified tribosphenic pattern. Furthermore, its dentition and mastication movement are well-studied (i.a. Hiiemäe and Jenkins 1969, Crompton and Hiiemäe 1970, Hiiemäe and Crompton 1971, Stern

et al. 1989, Thomason et al. 1990, Cornay and Mead 2012, Schwermann 2015). This is why it also has been frequently used as tribosphenic comparative taxon in many previous studies (e.g. Clemens 1966, Hiiemäe and Jenkins 1969, Crompton and Hiiemäe 1970, Butler 1972, Crompton 1995, Schwermann 2015).

The genus *Didelphis* comprises six species with partially overlapping distributions in South, Central, and North America (Wilson and Reeder 2005). Therefore, it is one of the very few marsupial taxa living outside Australia. All *Didelphis* species are solitary, nocturnal, terrestrial to arboreal animals that preferably live in humid woodlands (Gardner 1973, McManus 1974, Gardner 1982). The size of the best-studied species *Didelphis virginiana* amounts to averagely 42 cm (74 cm including the tail) and its weight to approximately 2.5 kg (Gardner 1982). All species are omnivorous and their diet comprises mainly insects, carrion, fruits, and grass or leaves (Hamilton 1958, Gardner 1973, McManus 1974, Gardner 1982). *Didelphis* possesses five upper and four lower incisors, as well as one canine, three premolars, and four molars in the upper as well as the lower tooth row (Thenius 1989).

The tooth-tooth-contact diagram for the tribosphenic molars of *Didelphis* is based on an OFA project kindly provided by Dr. Achim H. Schwermann (LWL-Museum für Naturkunde, Münster, Germany). In his doctoral thesis, among other taxa, he analyzed the mastication movement of *Didelphis* in detail (Schwermann 2015). The provided project uses scans of the right m1-m2 and M1 of the same specimen of *Didelphis virginiana* (SMF 77266) from the collection of the Senckenberg Forschungsinstitut in Frankfurt am Main, Germany.

3.2.2 *Monodelphis* BURNETT 1829

The didelphid *Monodelphis* was chosen as an additional comparative taxon since its mainly insectivorous diet is more similar to that postulated for *Haldanodon* than that of the omnivorous *Didelphis*. Its dentition and masticatory movement has been studied in detail by Schwermann (2015).

The genus *Monodelphis* comprises 18 species. Their distribution is restricted to South America and the southernmost Central America (Wilson and Reeder 2005). Just like the *Didelphis* species they are solitary animals that are mainly active during night time and prefer a more or less heavily vegetated habitat (Streilein 1982, Macrini 2004). The best-known species *Monodelphis domestica* is also often kept as laboratory animal. With a head and body length of averagely 14 cm (21 cm including the tail) and a weight of about 70 g it is much smaller than *Didelphis virginiana* (Redford and Eisenberg 1992, Macrini 2004). In comparison to *Didelphis*,

Monodelphis prefers a much more insectivorous to carnivorous diet (Streilein 1982, Busch and Kravetz 1991, Macrini 2004, Casella and Cáceres 2006).

Complete upper and lower dentitions of *Monodelphis* have the same tooth formula as those of *Didelphis*, that is five upper and four lower incisors, one canine, three premolars, and four molars (Macrini 2004).

The contact diagram for *Monodelphis*, too, is based on an OFA project kindly provided by Dr. Achim H. Schwermann (LWL-Museum für Naturkunde, Münster, Germany). The OFA project uses scans of the left m1-m2 and M1 of a *Monodelphis sorex* specimen (ZMB MAM 35496) from the collection of the Museum für Naturkunde in Berlin, Germany.

4 Methods

4.1 Terminology

4.1.1 Cusps and crests

4.1.1.1 Docodonta

The nomenclature of docodont tooth morphology has somewhat varied over time. Simpson (1961) was the first one to name the cusps, using roman numerals (cusps I to IV on the upper, cusps X to XVI on the lower molars). However, this approach was not followed in later studies. Instead, Crompton and Jenkins (1968) introduced a terminology using single letters to refer to cusps based on morganucodontid molar terminology, following the hypothesis of morganucodontids as sister taxon to docodonts. Upper molar cusps are referred to with capital letters (e.g. A, B), lower molar cusps with lower case letters (e.g. a, b).

Sigogneau-Russell (2003) developed yet another nomenclature based on Kermack et al. (1987), naming the cusps and crests according to their positions on the molars (e.g. main cusp, mesio-labial cusp, antero-main crest, lingual cingulum). For upper molars, the names are capitalized (e.g. Mesio-Labial Cusp, Anterior Crest). This descriptive approach is a lot more independent from phylogenetic relationships. However, it is quite inconvenient to use in written text and figure labels and most other authors prefer to keep to capital and lower-case letters, which is why this terminology is not used in this study.

This study follows the most recent nomenclature of Luo and Martin (2007), based on Butler (1997). He maintained the use of single letters but altered the name of some cusps to match the hypothesis of *Woutersia* as sister taxon to docodonts. Luo and Martin (2007) additionally renamed cusp f as cusp df (for “docodont cusp f”) to distinguish it from cusp f of morganucodonts, kuehneotheriids, and crown therians, which is not homologous.

On upper molars of *Haldanodon* the cusps of the buccal row from mesial to distal are named B (= E in Crompton and Jenkins 1968), A, C, and D with A being the main cusp. The lingual cusps are X and Y, the latter much smaller than X and more distally situated. Cusps A, C, X, and Y enclose the “pseudotrigon basin” (for a detailed discussion see 6.1.2). On lower molars of *Haldanodon* the cusps of the buccal row from mesial to distal are named b, a, and d, with a being the main cusp. The cusps of the lingual row from mesial to distal are named e, g (= h in Crompton and Jenkins 1968), c (= g), and df (= f). Cusps a, b, and g enclose the “pseudotalonid

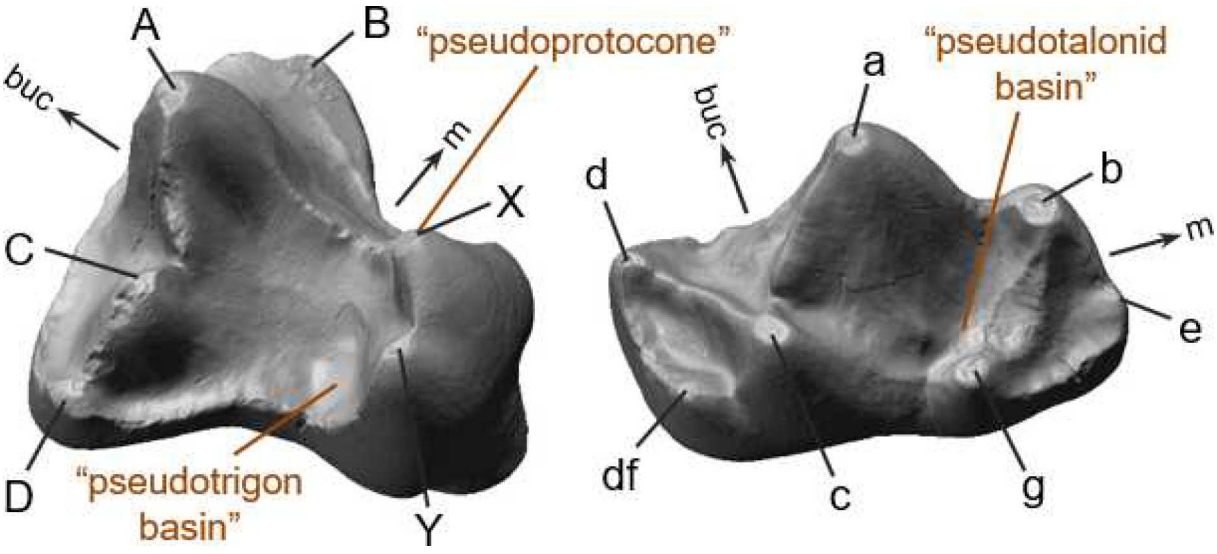

Fig. 3: Terminology of docodont molar cusps and basins, as shown by *Haldanodon* (based on Luo and Martin 2007). Left: Upper molar terminology (model: Gui Mam 3113, dP dex.; dPs usually show a much better developed cusp Y than permanent molars). Right: Lower molar terminology (model: Gui Mam 3142, m sin.).

basin" (for a detailed discussion see 6.1.1). Crests are referred to by the names of the connected cusps, e.g. A-B, d-df, etc. (fig. 3).

4.1.1.2 *Didelphis* and *Monodelphis*

The commonly used nomenclature for tribosphenic molar cusps has been established by Osborn (1888a, 1888b, 1907). Since *Didelphis* and *Monodelphis* mostly retained the basic tribosphenic pattern, it is also applicable for these taxa. On upper molars the mesio-buccal cusp is named paracone, the disto-buccal cusp metacone, and the lingual cusp protocone. These three cusps enclose the trigon basin. On lower molars the mesio-buccal cusp is the protoconid, the disto-buccal cusp the hypoconid, and the lingual cusps from mesial to distal are named paraconid, metaconid, entoconid, and hypoconulid. Paraconid, protoconid and metaconid form the trigonid triangle. Hypoconid, hypoconulid, and entoconid enclose the talonid basin (fig. 5).

4.1.2 Wear facets

4.1.2.1 Docodonta

The only terminology of wear facets available for *Haldanodon* is that of Crompton and Jenkins (1968). They show the hypothetical development of tooth morphology and correlated wear facets from *Eozostrodon*, a morganucodontid, to *Docodon* with a hypothetical intermediate stage partially based on *Haldanodon*. The figure illustrating this development was later reused by Hopson and Crompton (1969) who directly assigned this hypothetical stage to *Haldanodon*. However, the terminology applied by Crompton and Jenkins (1968) is easily confused with that of wear facets on tribosphenic teeth introduced by Crompton (1971), because both are based on Arabic numerals. Crompton's facet terminology is still commonly used for basal mammals. However, Crompton and Jenkins' docodont facets are not meant to be homologous to the tribosphenic facets. Instead, they reflect the assumed ancestry of morganucodontids to docodonts and therefore are phylogenetically prejudiced. That is why the numbering of facets on the upper molar of *Haldanodon* begins with facet 2 due to the assumed loss of the morganucodontid cusp B in docodonts which carries the morganucodontid facet 1. On the lower molar of *Haldanodon*, facet 3 and 4 are assumed to be lost due to a complete reduction of the morganucodontid cusp c. This is why in *Haldanodon* according to Crompton and Jenkins (1968) and Hopson and Crompton (1969) facet 1 of the lower molar contacts the merged facets 3 and 4 of the upper molar. Facet 2 and the additionally developed docodont facets 5 to 8 all have an equivalent on lower and upper molar. Since nowadays docodonts are not regarded as sister taxon to morganucodontids but rather to "symmetrodonts" (see 2.1), this terminology is not used in this study.

The only other docodont wear facet terminology was introduced by Jenkins (1969) and is based on *Docodon*. However, it is rather confusing with facets 1 to 13 on the lower and facets 14 to 21 on the upper molar. Therefore, matching facets on upper and lower molars are not recognizable in the text. Some of them with coherent but differently orientated surfaces are even further divided with additional letters (e.g. 1a, 1b, 1c). Furthermore, Jenkins did not distinguish between abrasion and attrition surfaces – facets 1a, 9a, 14, and 19a for example are situated at the tip of cusps and are formed by abrasion, not attrition. These facts are the cause why this terminology is not used in this study as well.

All other studies on docodont occlusion and wear prefer not to name the facets but rather depict and paraphrase them (e.g. Hopson and Crompton 1969, Kron 1979, Krusat 1980, Butler 1997, Sigogneau-Russell and Godefroit 1997) or use the terminology postulated by Jenkins

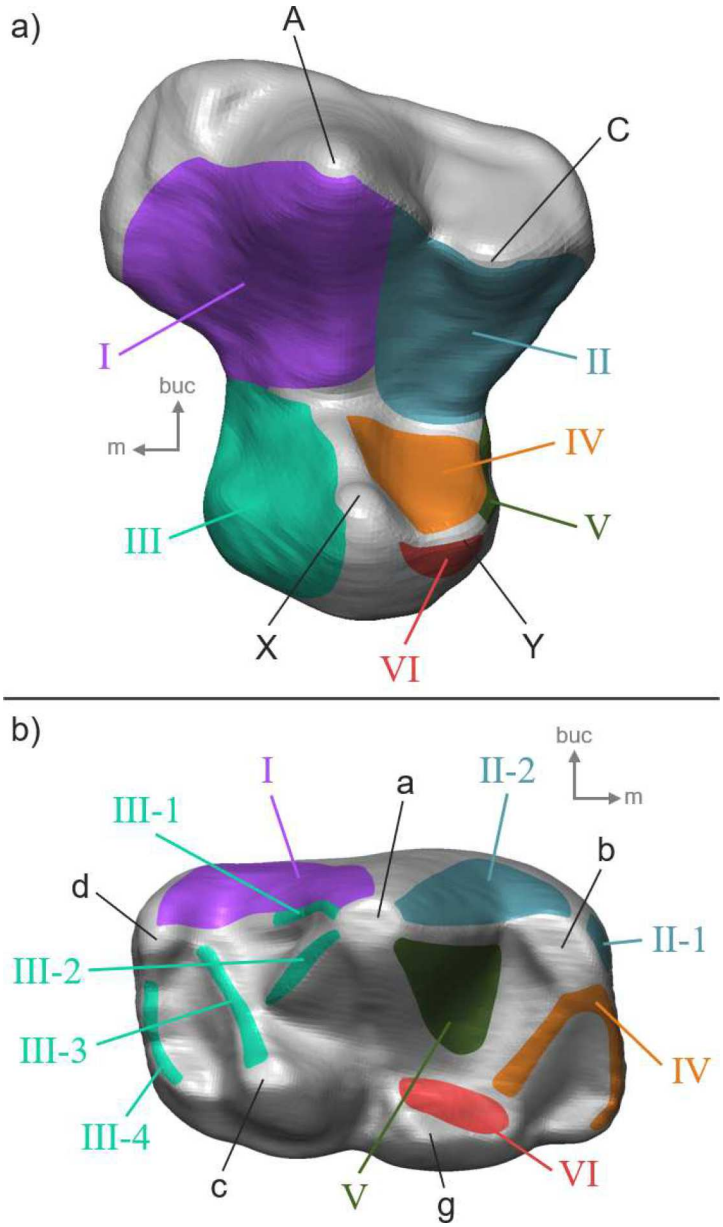

Fig. 4: Terminology of wear facets on *Haldanodon* molars, occlusal view.
a) Upper molar (model: M2 of Gui Mam 30/79).
b) Lower molar (model: m3 of Gui Mam 6/82).
Wear facets were given roman numerals to distinguish them from tribosphenic wear facets after Crompton (1971).

(1969) (e.g. Gingerich 1973, Butler 1988, Maschenko et al. 2002, Pfretzschner et al. 2005). The only ones to follow Crompton and Jenkins' (1968) facet terminology are Schultz et al. (2017). Regarding the described difficulties with the existing wear facet terminologies, in this study a self-compiled terminology is used: The facets on the upper molar are named I to VI, from mesial to distal and from buccal to lingual. Roman numerals are used to emphasize the difference to Crompton's tribosphenic facets, which, as mentioned above, are not homologous to the docodont facets. Corresponding facets on the lower molar have the same number. In cases where two or more facets of the lower molar contact the same facet on the upper molar an Arabic numeral is added (e.g. II-1 and II-2) from mesial to distal to distinguish between the partial facets, if necessary. Additionally, corresponding facets on upper and lower molars have the same color in all figures (facet I: light violet, facet II: grey blue, facet III: turquoise, facet IV: orange, facet V: olive, facet VI: light red) (fig. 4).

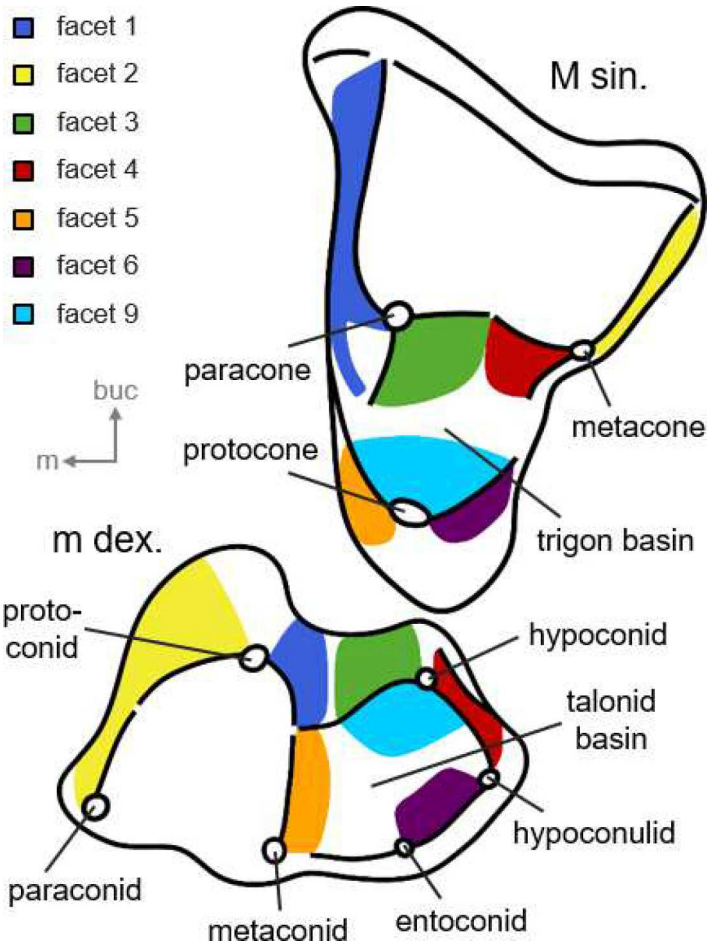

Fig. 5: Terminology of tribosphenic molar morphology and wear facets, occlusal view. Facet position and terminology are based on Crompton (1971) and amendments made by Kay and Hiiemäe (1974). Facet color scheme according to Schwermann (2015).

4.1.2.2 *Didelphis* and *Monodelphis*

A still commonly used wear facet terminology for tribosphenic teeth and their predecessors based on Arabic numerals was established by Crompton (1971). It originally included only six facets but was later expanded by Kay and Hiiemäe (1974). This terminology is easily applicable for *Didelphis* and *Monodelphis* with their almost unaltered tribosphenic tooth morphology and has also been used in the most recent study on their dentition by Schwermann (2015). The facets on the molars of *Didelphis* and *Monodelphis* are colored according to his color scheme (facet 1: dark blue, facet 2: yellow, facet 3: green, facet 4: red, facet 5: light orange, facet 6: violet, facet 9: light blue) (fig. 5).

4.2 Measurements

Images taken with a digital camera (model Axio-Cam HRc) mounted on a Zeiss Stereomicroscope (model Axio Zoom.V16) served as base for the measurements. Tooth rows

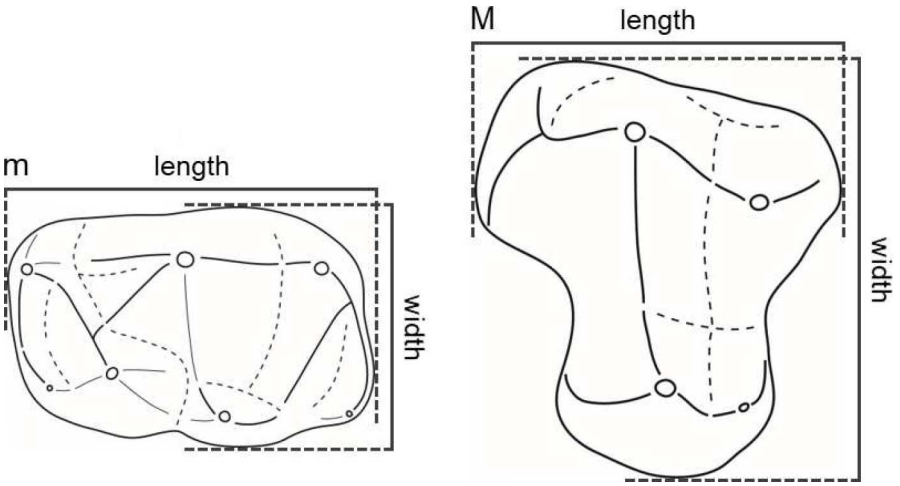

Fig. 6: Measuring points for measurements of molar length and width in *Haldanodon* (left: lower molar, right: upper molar).

were positioned in occlusal view with mesial facing left. Of each tooth row an image focused on the basal outline of the molars was taken with the Zeiss software ZEN pro 2011. The length of the molar row was then measured three times successively with the virtual caliper of ZEN; the scale had been imbedded into the image information. The software converted pixel-size into micrometer with an accuracy of more than 0.001 mm. Each molar of the tooth row was also measured separately. For this, it was arranged in occlusal view parallel to its buccal side and with mesial to the left. The image was focused on the basal outline of the molar and was taken in the highest possible magnification. Then length and width were measured in micrometers with the virtual caliper three times successively at the molar's longest and widest position (fig. 6). Finally, the measurements of tooth rows and molars were converted into millimeter and recorded with Microsoft Excel 2010 for further analyses.

4.3 Recording of striations with scanning electron microscope (SEM)

Some molars with well-preserved facets were recorded with the scanning electron microscope (SEM) CamScan MV 2300. Previously, the isolated teeth had each been mounted separately in occlusal view on a plug using conductive carbon cement as adhesive. The chosen specimens were coated with gold in the Cressington Sputter Coater 108auto for three minutes at a voltage of 30 to 40 mA and a pressure of about 0.05 mbar. Afterwards, several SEM images were taken with the BSE detector of the CamScan and Vega©Tescan in the Resolution Scan Mode with quintuple speed at a voltage of 18.7 kV or 19.8 kV. These images included shots taken from occlusal view as well as shots from the molars tilted in an angle of 70° to 80° into buccal view and rotated around the z-axis. At intervals of about 45° several shots of the same view in different focusing distances were taken. Striations visible in the images were then marked in

red with the image editing program GIMP 2.6.12. The general directions of the observed striations were transferred onto the 3D-prints of lower and upper molars, which were used to manually test possible ways of occlusion (see 4.4). The most likely movement indicated by these striations was used as base for an OFA analysis (see 4.5).

4.4 CT scans, reconstruction, and printing of 3D-models

Fifty-four specimens of isolated teeth were scanned with synchrotron-microtomography at the European Synchrotron Radiation Facility (ESRF) in Grenoble (France) as part of the project EC-440 („Analysis of the chewing cycle in Mesozoic Mammals“). The scans were run with the Beamline ID19, a monochromatic X-ray, a moderate phase contrast, and an energy of 25 keV (kiloelectronvolt). The resulting voxel size was 2.07 µm.

CT scans of the jaw fragments were done at the Steinmann-Institut (University of Bonn) with a Phoenix|x-ray v|tome|x s 240. Most specimens were scanned with the 180 kV nanotube, 55 to 80 kV, and 100 to 170 µA. The resulting voxel size was 8.21 to 14.99 µm. This is also the case for specimen Gui Mam 6/82, from which the lower molar models for the virtual reconstruction of the mastication movement with the OFA were taken (see 4.5). It was scanned with a voltage of 60 kV and a current of 170 µA and has a voxel size of 13.22 µm. Upper and lower jaw of specimen Gui Mam 30/79 were scanned with the 240 kV microtube, 100 kV, and 100 µA. The resulting voxel size was 18.50 µm for the upper jaw, from which the upper molar model for the OFA reconstruction was taken, respectively 11.05 µm for the lower jaw. In all cases the image-stacks were generated with the Phoenix|x-ray software datos|x.

Avizo 7.1 was used to convert these image stacks into 3D-models. If necessary, the raw 3D-models were then further processed with Polyworks 2014 IR 11, for example to remove remaining artefacts, to reduce the size of the models, or to scale them. Polyworks was also used to color facets observed on the original molars for comparison with the contact areas displayed by the Occlusal Fingerprint Analyser (see 4.6).

A few selected 3D-models were printed with the Objet Eden 260V using FullCure 720 as body matrix and FullCure 705 as supporting matrix. These palm-sized models can be colored with water soluble aquarelle pencils as needed. Therefore, it was possible to mark facets and striations on the models, which then could be compared to each other or manually tested for best fit in occlusion.

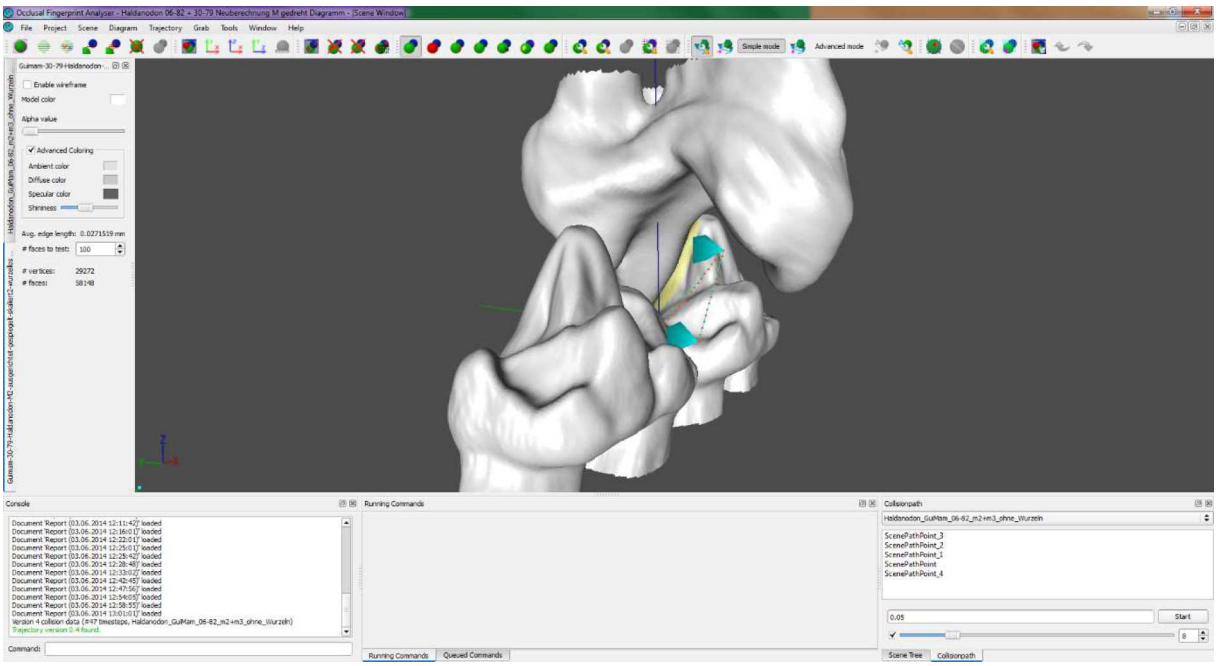

Fig. 7: Screenshot of the user interface for the Occlusal Fingerprint Analyser (OFA) software, version 1.7. The path which sets the movement of the lower molars during mastication is shown as orange dots.

4.5 Occlusal Fingerprint Analyser (OFA)

The Occlusal Fingerprint Analyser (OFA) is an open source software developed by ZiLoX IT (based in Wallhausen, Germany) on behalf of the DFG research unit 771. It detects the collision of two 3D-objects moving along a specified path and adjusts this path to avoid one model permeating the other. It also displays the calculated collision area on each object and performs various analyses (fig. 7). Therefore, it is well suited to simulate and verify possible mastication cycles and to provide data on tooth-tooth contact (that is forming of facets).

In this study OFA version 1.7 was used to test whether the assumed mastication path of *Haldanodon* creates collision areas similar to the observed facets on the model of an upper molar (based on the M2 of Gui Mam 30/79) and a model of two lower molars (based on m2 and m3 of Gui Mam 6/82). The 3D-models of the molars were isolated from an upper and a lower tooth row with reliably determinable tooth positions. This also guaranteed the correct alignment of m2 and m3 in relation to each other. Since matching upper and lower molar rows from one individual were not available, two rows belonging to different individuals with a comparable abrasion stage had to be used for the OFA analysis. The upper molar model had to be scaled with Polyworks 2014 IR 11 to match the size of the model of the lower molars (see also 6.2). To obtain the correct alignment of upper and lower molars towards each other the models were first aligned separately with Polyworks 2014 IR 11. For this, they were imbedded into a model of the entire tooth row, also including the jaw bones as far as they are preserved.

This model was then aligned with the occlusal planes of the lower molars pointing upwards and those of the upper molars pointing downwards. Afterwards, the models of M2 and m2+m3 were isolated again and reloaded into the OFA with the respective coordinates. For fine tuning the lower molars were then brought into centric occlusion, and the upper molar was slightly rotated to allow maximum contact of the teeth. Starting from centric occlusion, the lower molars were then moved along the anticipated mastication path separately for each phase. Both movements were connected before running the OFA analysis.

The OFA analysis does not only simulate the specified chewing motion, but also detects and colors the collision area in between the molar models for as long as they are in contact. The colors for the contact areas are randomly chosen for each time step by the program. However, they can be manually recolored to match the color chosen for the represented facet. Furthermore, two or more detached contact areas actually belonging to the same facet can be merged manually. They are still visualized as distinct parts, but the sizes of the areas are added together. This is necessary for the creation of a tooth-tooth-contact diagram, which displays the size of the contact areas in mm^2 at a given time step as a bar diagram. The height of the bars correlates with the size of the contact area, the color with the respective facet. Since the bars correlated with the facets are not displayed in consecutive order, in this study the diagram was rearranged with the image editing program GIMP 2.6.12. With the contact diagram, a statement regarding the development of the amount of contact for a distinct facet throughout the mastication movement is possible (see 5.5, 6.4.5, and 6.5.1 - 6.5.2). Since each facet can be associated with a certain function, it is also an indirect approach to quantify the amount of crushing and shear-cutting (see 6.4.6 and 6.5.1 - 6.5.2).

5 Results

5.1 *Haldanodon* molars

5.1.1 Determination of position for isolated molars

The *Haldanodon* molar rows included into this study – if fully preserved – consist of four upper respectively four to five, seldom six lower molars. To be able to create a virtual simulation of the chewing stroke of *Haldanodon* as realistic as possible, matching tooth positions of the molar models had to be ensured. To enable the inclusion of the isolated molar specimens into the material from which to choose the most suitable models, an attempt was made to refer isolated molars to their former tooth position in the dental row. For this, ten upper and 42 lower molar rows with known tooth positions and well-preserved molars were measured as described in 4.2. Length measurements of seven upper molar rows include M1 to M3 and range from 3.8 mm to 5.71 mm with a mean length of 4.85 mm (see appendix tab. 6). M4 was excluded from the length measurements of the molar rows, because otherwise the sample size would have been further reduced to three out of the ten specimens. The M2 of the right maxilla Gui Mam 30/79 was entirely excluded from the study, because with a length of 1.44 mm and a width of 1.71 mm it is significantly smaller than any of the other M2 (see below).

The mean lengths of the upper molar positions do not differ much (see appendix tab. 8): M2 (1.90 mm) is only slightly longer than M3 (1.81 mm), M4 (1.75 mm), and M1 (1.73 mm). However, they differ more significantly in mean width: M2 (2.21 mm) is wider than M3 (1.98 mm), M1 (1.84 mm), and M4 (1.46 mm). For comparison of the overall size of the different molar positions, for every specimen the values of length and width were added up. The mean values reflect the size distribution of molar positions within the same tooth row: M2 is always the largest molar followed by M3, M1 and M4 (fig. 8). Only in one specimen (Gui Mam 18/80) M3 is slightly longer than M2. In three specimens M1 is slightly larger than M3 – in two (Gui Mam 41/45, Gui Mam 16/78) both in length and width, in one (Gui Mam 60/76) only in length but not in width. In one specimen (Gui Mam 25/82) M4 is longer than both M3 and M1; their widths are not comparable, since that of M3 and M1 could not be measured (see appendix fig. 1 + 2).

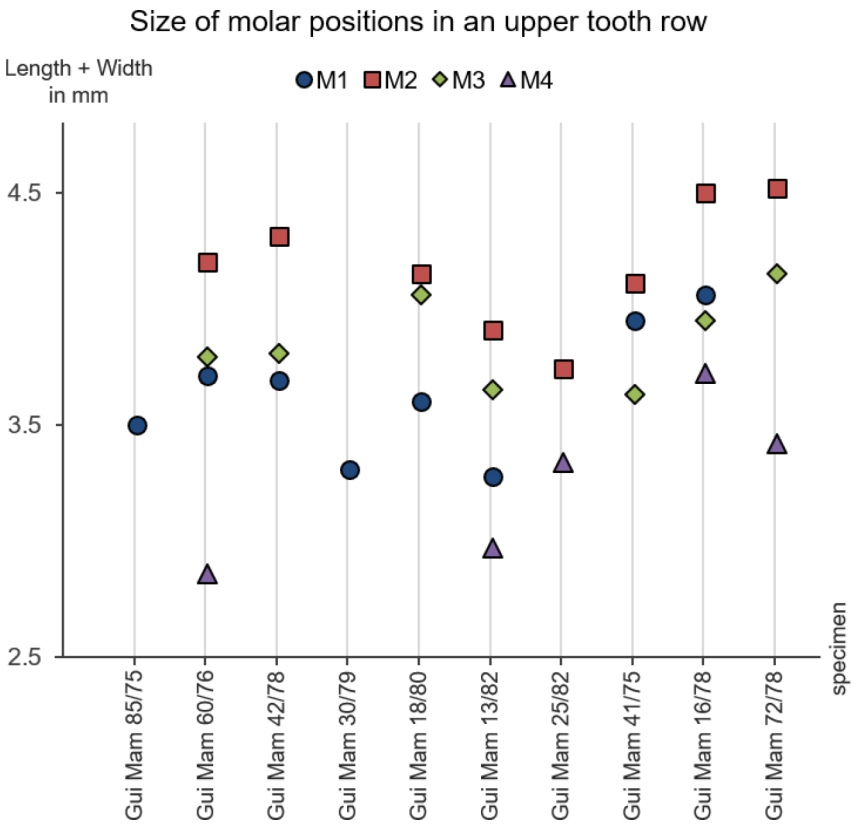

Fig. 8: Size distribution of the molar positions within upper *Haldanodon* tooth rows. For each position molar lengths and widths were added up to determine the overall size of the molars (for a separated illustration of lengths and widths see appendix fig. 1+2). Measurements only include well-preserved molars with certainly determinable positions.

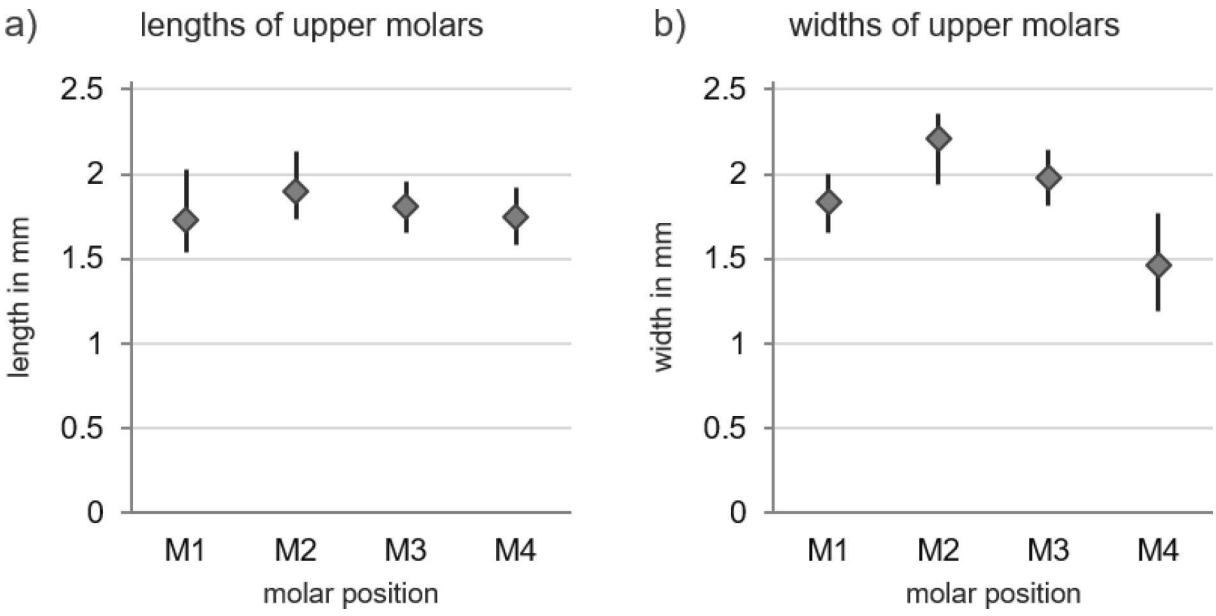

Fig. 9: Ranges of lengths and widths within upper molar positions in *Haldanodon*. Measurements only include well-preserved molars with certainly determinable positions. a) Ranges of lengths. All upper molar positions show considerably overlapping values with similar means. b) Ranges of widths. Although the mean values are well distinguished the ranges considerably overlap with at least one other molar position.

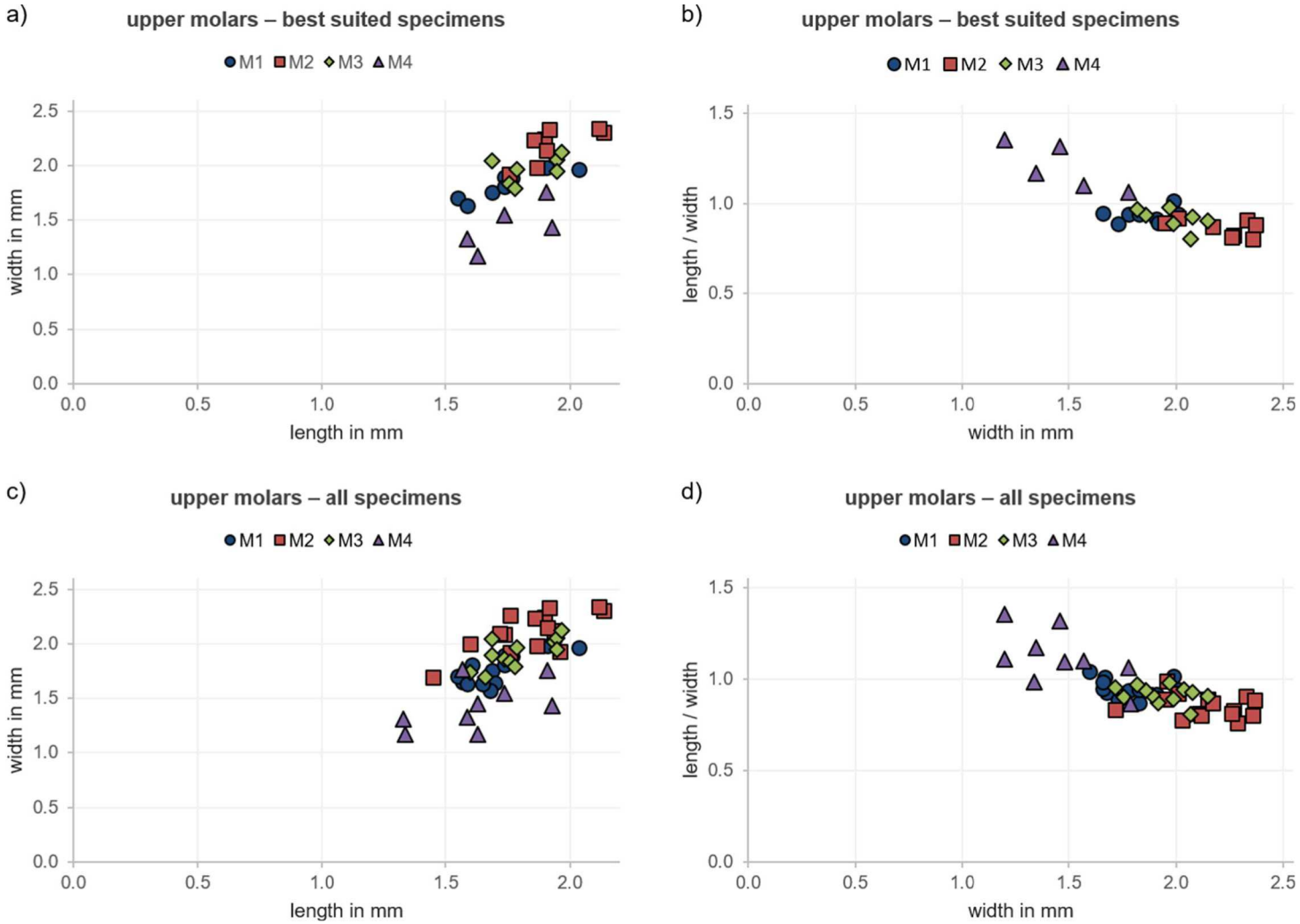

Fig. 10: a) + c) Plot of length against width of upper molar positions in *Haldanodon*. b) + d) Plot of width against length/width of upper molar positions. It further emphasizes the size differences in between the molar positions. a) and b) only include well-preserved molars with certainly determinable positions. M4, the smallest M1s and the largest M2s separate from the other molar positions. c) and d) additionally include estimated values of less well-preserved molars and molars with uncertain position. Only the smallest M4s and largest M2s clearly separate from the other molar positions.

The size of an upper molar correlates with the size of the other molars in the tooth row – specimens with a relatively large M1 also have large molars in the following positions, specimens with a small M1 also have relatively small molars in the following positions. The only molar position not following this trend is that of M4 which can be smaller in an otherwise rather large row than in a row with comparatively low values.

Although the mean widths of upper molar positions show some significant disparities and the size distribution within the molar rows is very stable, there is a great overlap in values of the same tooth positions among different molar rows. The range of width of M1 (1.65 – 2.00 mm) lies well within that of M2 (1.94 – 2.36 mm), M3 (1.81 – 2.14 mm), and M4 (1.19 – 1.77 mm). The range of width of M2 additionally lies within that of M3. The ranges of length show an even greater overlap: The values of all molar positions, that is M1 (1.54 – 2.03 mm), M2 (1.73 – 2.13 mm), M3 (1.65 – 1.96 mm), and M4 (1.58 – 1.92 mm), greatly overlap with those of the other molar positions (fig. 9).

Therefore, it is almost impossible to distinguish upper molar positions by a simple plot of length against width, with the exception of M4, the smallest M1s and largest M2s (fig. 10a). An index of length/width plotted against width emphasizes the size differences but does not give a better resolution (fig. 10b). If measurements of seven more upper molar rows with not as well-preserved molars and / or uncertain tooth positions are included into the plot, the resolution even lessens, so that only the smallest M4s and largest M2s can be certainly distinguished from the other molar positions (fig. 10c + d).

Length measurements of the lower molar row include m1 to m4. In 21 out of the 42 lower molar rows all of these molar positions are preserved. Their measurements range from 5.62 mm to 7.43 mm with a mean length of 6.38 mm (see appendix tab. 07). The last molar positions m5 and m6 were not included into these measurements, because they erupt at a relatively late ontogenetic stage. Therefore, they are not yet present in younger adult specimens.

Lower molar positions differ significantly in both mean length and mean width (see appendix tab. 9): m2 (1.80 mm) is the longest molar of the row, followed by m3 (1.76 mm), m1 (1.58 mm), m4 (1.43 mm), m5 (1.12 mm), and m6 (0.92 mm). The differences in mean width are less distinct but still noticeable with m3 (1.22 mm) as the widest molar followed by m2 (1.14 mm), m4 (1.03 mm), m1 (0.95 mm), m5 (0.85 mm) and m6 (0.80 mm).

Like with the upper molars, for every specimen the values of length and width were added up to determine the overall size of the different lower molar positions. The mean values reflect the size distribution of molar positions within the same tooth row: in most rows, m3 is slightly larger than m2, followed by m1, m4, m5, and m6 (fig. 11). In 16 out of 28 comparable molar rows m2 is slightly larger than m3, thereof twelve only in length. In five of these rows

additionally m1 is wider than m3. Only in one of these specimens (VJ 1001) m1 is also longer than m3, but not wider. In 14 out of 23 molar rows m4 is larger than m1, thereof ten only in width. These ten molars are also wider than m2 of the same molar rows, in two of which (Gui Mam 34/74, Gui Mam 1/80) m5 is also significantly wider than m1 (see appendix fig. 3 + 4).
The sizes of m1-m3 correspond well within the tooth row – if m1 is relatively large, so are the following molar positions, if m1 is relatively small, the following positions tend to be small as well. The last molar positions do not follow this pattern and can be distinctly larger (mostly in length) in small molar rows than in larger ones. This trend is most obvious in m5. There are only three m6 included into the study, but this tooth position seems to correspond well to that of m5.
Like in the upper molar positions, the overlap of the ranges of length and width in lower molar positions is great, although the means of these measurements show significant differences and the size distribution within the molar rows is relatively stable. The range of length of m1 (1.37 – 1.70 mm) lies well within that of m2 (1.64 – 1.93 mm), m3 (1.29 – 2.04 mm), and m4 (1.05 – 1.68 mm). The range of length of m2 additionally lies within that of m3 and m4, that of m3 also within that of m4 and m5 (0.82 – 1.37 mm). The range of length of m4 additionally overlaps with that of m5 and m6 (0.72 – 1.11 mm), and that of m5 also lies within the range of length of m6. The ranges of width show an even greater overlap: m1 (0.83 – 1.08 mm) overlaps with all following molar positions, that is m2 (0.99 – 1.26 mm), m3 (1.04 – 1.45 mm), m4 (0.72 – 1.29 mm), m5 (0.63 – 1.06 mm), and m6 (0.65 – 0.96 mm). The positions of m2 and m3 also overlap with all following molar positions but m6, the range of width of m4 additionally with both m5 and m6, and m5 with that of m6 (fig. 12).
Therefore, like with the upper molars it is difficult to distinguish lower molar positions by a simple plot of length against width, with the exception of the smallest m1s and m2s and the largest m3s (fig. 13a). However, it is at least possible to estimate whether a molar is more likely to belong to the first molar positions m1-m3 or more likely to belong to the last molar positions m4-m6. An index of length / width against length or width only slightly emphasizes the size differences (fig. 13b). Although these differences become more indistinct if measurements for not as well-preserved molars and eight more lower molar rows with uncertain molar positions are included, they are still present (fig. 13c + d).

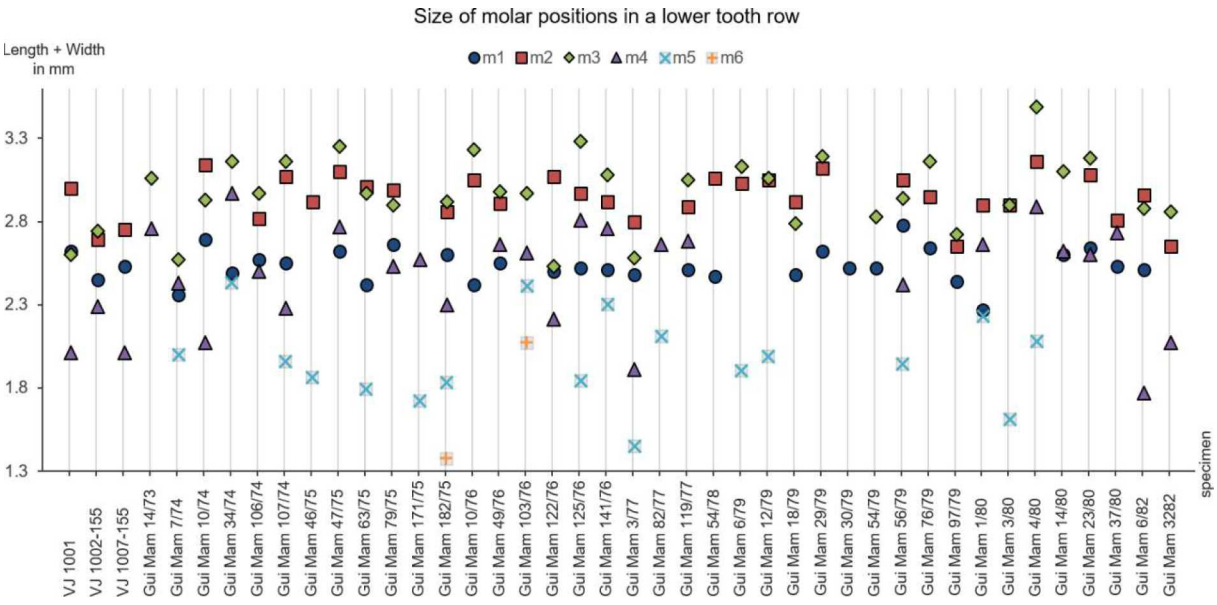

Fig. 11: Size distribution of the molar positions within lower *Haldanodon* tooth rows. For each position molar lengths and widths were added up to determine the overall size of the molars (for a separated illustration of lengths and widths see appendix fig. 3+4). Measurements only include well-preserved molars with certainly determinable positions.

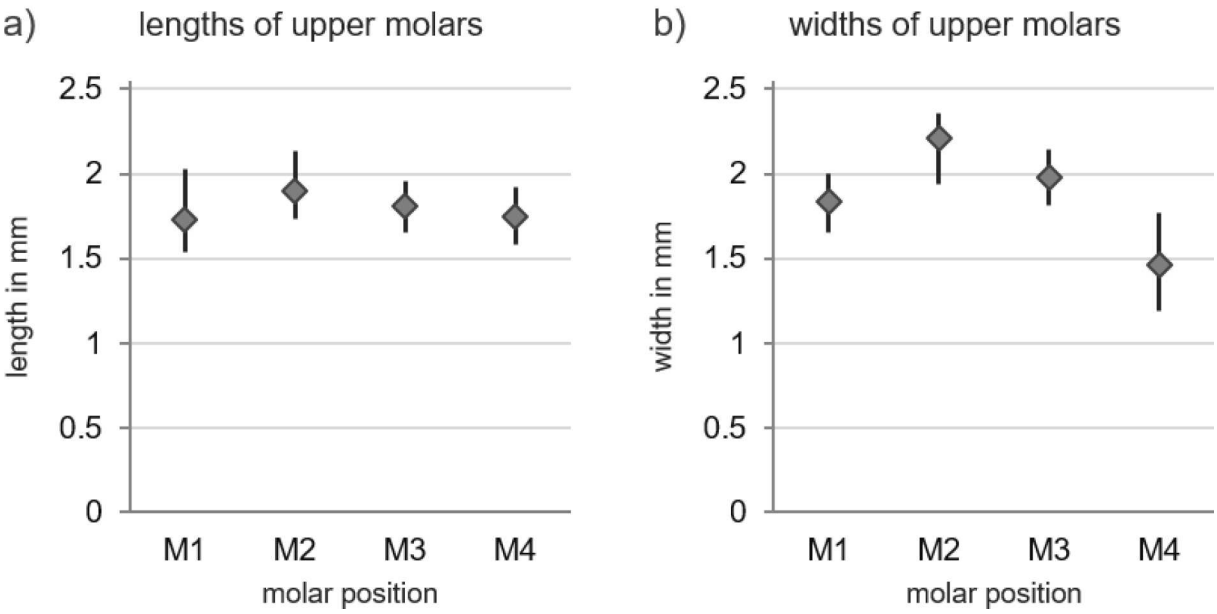

Fig. 12: Ranges of lengths and widths within lower molar positions in *Haldanodon*. Measurements only include well-preserved molars with certainly determinable positions. a) Ranges of lengths. Although the mean values are more or less well distinguished the ranges considerably overlap with most of the other molar positions. b) Ranges of widths. Mean values are less well distinguished and the ranges considerably overlap with each other.

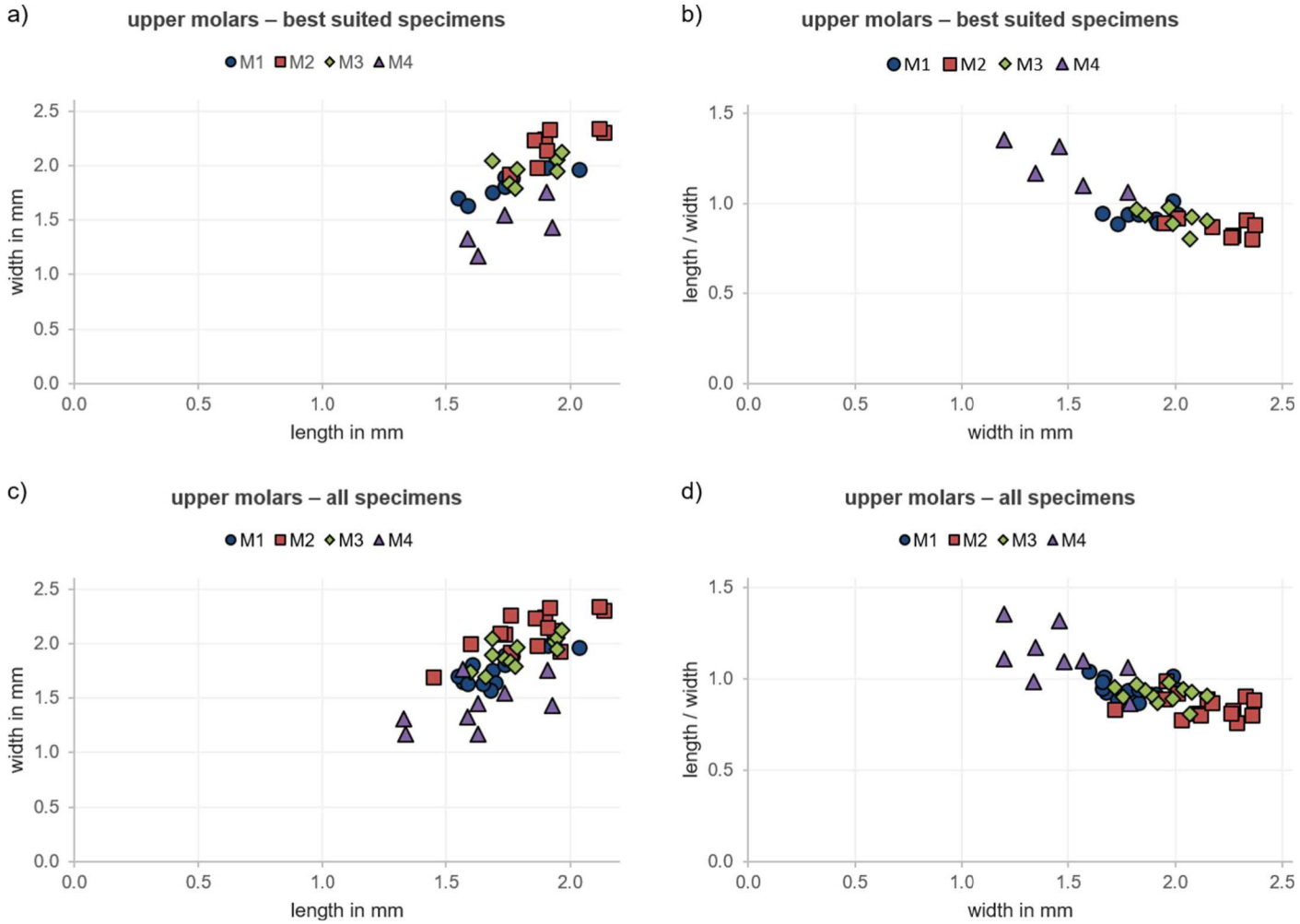

Fig. 13: a) + c) Plot of length against width of lower molar positions in *Haldanodon*. b) + d) Plot of length against length/width of lower molar positions. It slightly emphasizes the size differences in between the molar positions. a) and b) only include well-preserved molars with certainly determinable positions. The smallest m1s and m2s as well as the largest m3s separate from the other molar positions. The first molar positions m1-m3 separate quite well from the last molar positions m4-m6. c) and d) additionally include estimated values of less well-preserved molars and molars with uncertain position. The smallest m1s and m2s as well as the largest m3s still separate from the other molar positions. Also, the first molar positions m1-m3 still separate quite well from the last molar positions m4-m6.

5.1.2 Abrasion patterns of molar rows

During the process of taking measurements from various molar positions in a molar row to be able to refer isolated molars to their former tooth position (see also 4.2 and 5.1), a peculiar abrasion pattern of the studied molar rows became apparent. In some molar rows the wear increases in mesial direction – that is, the first molar of the row is worn more heavily than the second one, which in turn is more heavily worn than the third one. However, other molar rows show the reversed pattern with wear increasing in distal direction. In this case, the first molar of the row is less heavily worn than the second one which in turn is less heavily worn than the third one (fig. 14 + 15). It therefore seemed to be worthwhile to study the abrasion pattern of the molar row in more detail.

5.1.2.1 Definition of wear stages

Only molar rows with three or more mostly intact molars were included into the study to enable the determination of the direction of increasing wear within the row. On the lower molar row m5 and m6 were excluded from consideration because they always are vestigial.
Molar rows were roughly classified by three different degrees of wear: low, medium, and high (fig. 16 + 17). In rows with a low degree of wear the least strongly worn molar only shows first signs of wear on cusps and crests with very little exposure of dentine, if any at all. In rows with a medium degree of wear on the least worn molar the cusps and crests are connected by exposed dentine but are still clearly distinguishable. In rows with a high degree of wear on the least worn molar the boundaries between cusps and crests become indistinct, because they fuse. Ultimately, the tooth morphology completely brakes down and dentine is exposed all over the occlusal surface.
Furthermore, the wear gradient of each molar row was determined. If least and strongest worn molar are less than one degree of wear apart, the molar row is considered to have a small gradient (fig. 16c, 17b + c). The rows in which the least and strongest worn molar are one or more degrees of wear apart are considered to have a large gradient (fig. 16a + b, 17a).

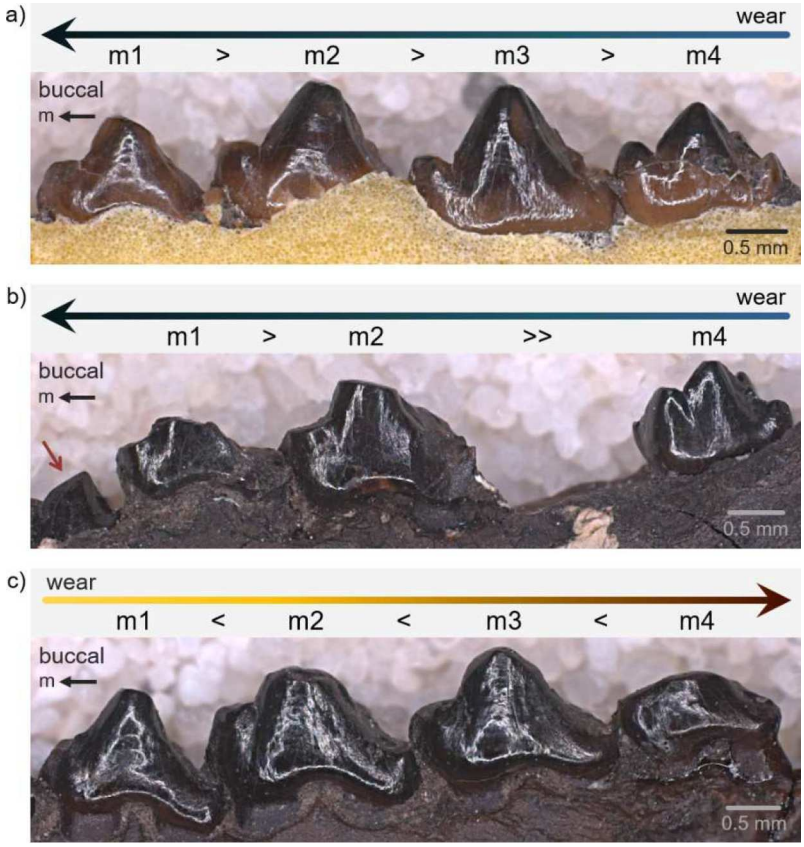

Fig. 14: Direction of wear in lower molar rows of *Haldanodon*, buccal view. a) Mesially increasing wear gradient with the preceding molar more heavily worn than the following one (Gui Mam 14/80). b) Mesially increasing wear gradient in a juvenile specimen (Gui Mam 33/77); red arrow indicates erupting p3. c) Distally increasing wear gradient with the preceding molar less heavily worn than the following one (Gui Mam 23/80, inverted).

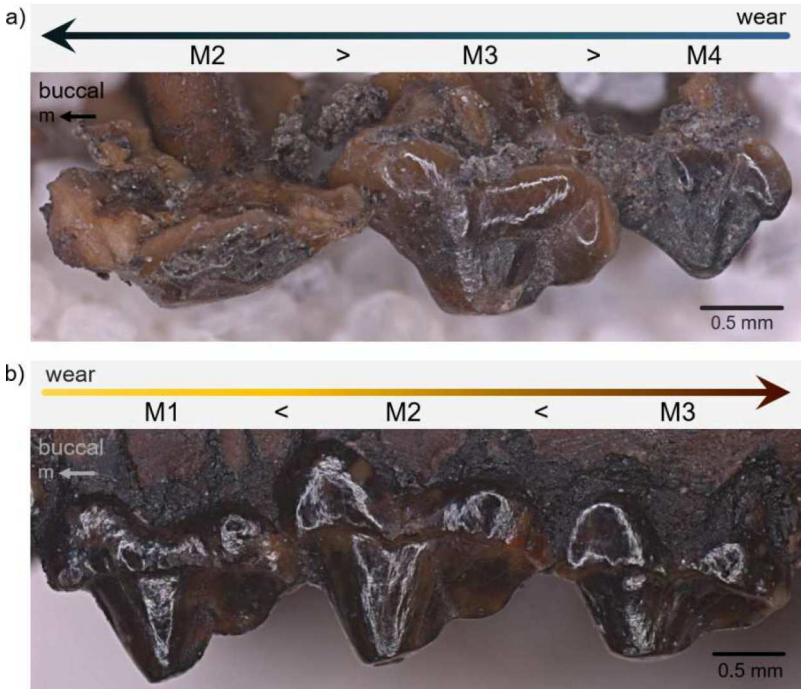

Fig. 15: Direction of wear in upper molar rows of *Haldanodon*, buccal view. a) Mesially increasing wear gradient with the preceding molar more heavily worn than the following one (Gui Mam 58/79). b) Distally increasing wear gradient with the preceding molar less heavily worn than the following one (Gui Mam 42/78, inverted).

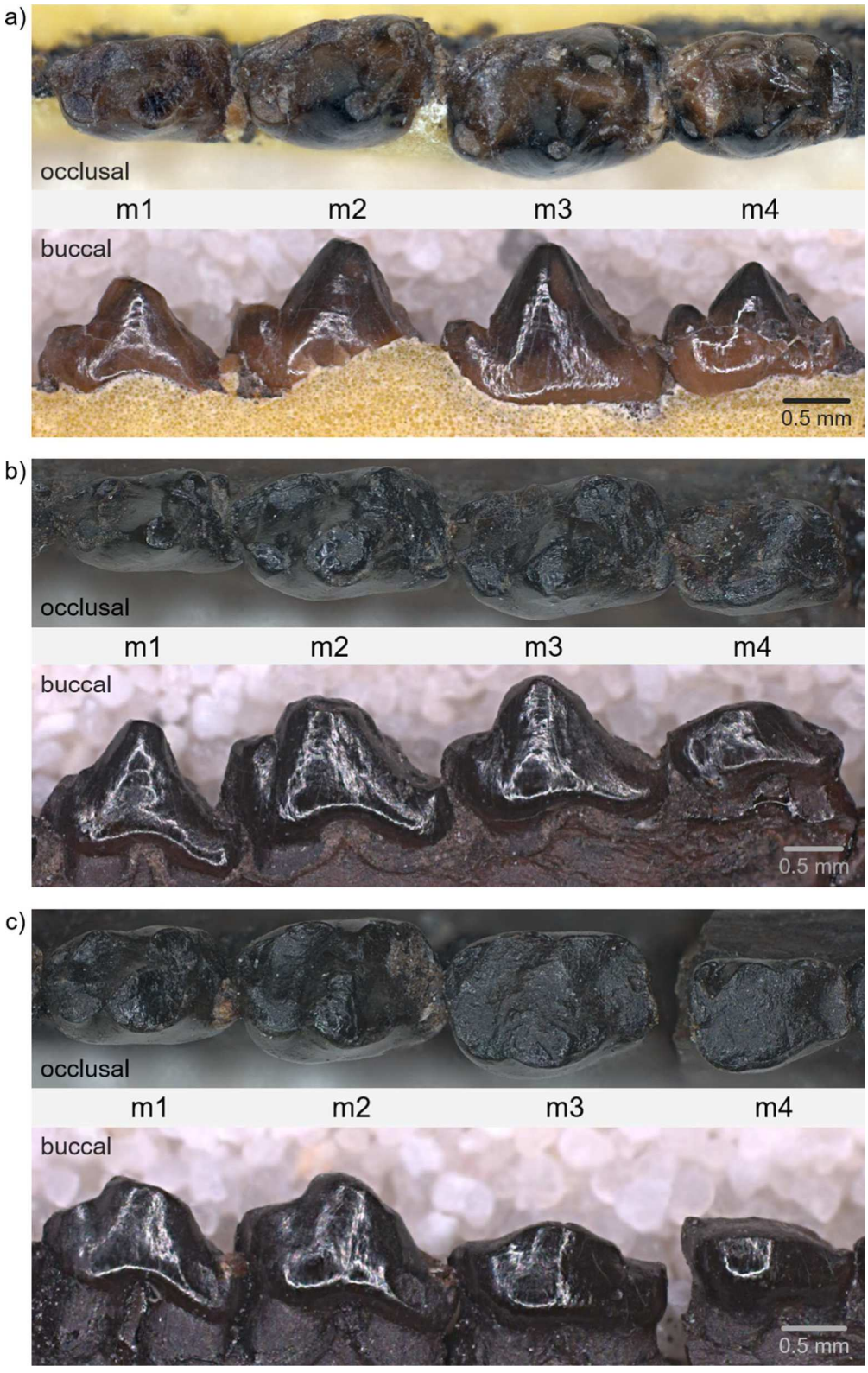

Fig. 16: Degree of wear in lower molar rows of *Haldanodon*. a) Low degree of wear with only very little exposure of dentine on cusps and crests of the least worn molar (m4). The molar row also shows a large, mesially increasing wear gradient (m1: medium to high degree of wear, m4: low degree of wear) (Gui Mam 14/80). b) Medium degree of wear with cusps and crests connected by exposed dentine on the least worn molar (m1). The molar row also shows a large, distally increasing wear gradient (m1: medium degree of wear, m4: high degree of wear) (Gui Mam 23/80, inverted). c) High degree of wear with indistinct boundaries in between cusps and crests of the least worn molar (m1). The molar row also shows a small, distally increasing wear gradient (m1: high degree of wear, m4: high degree of wear) (Gui Mam 182/75, inverted).

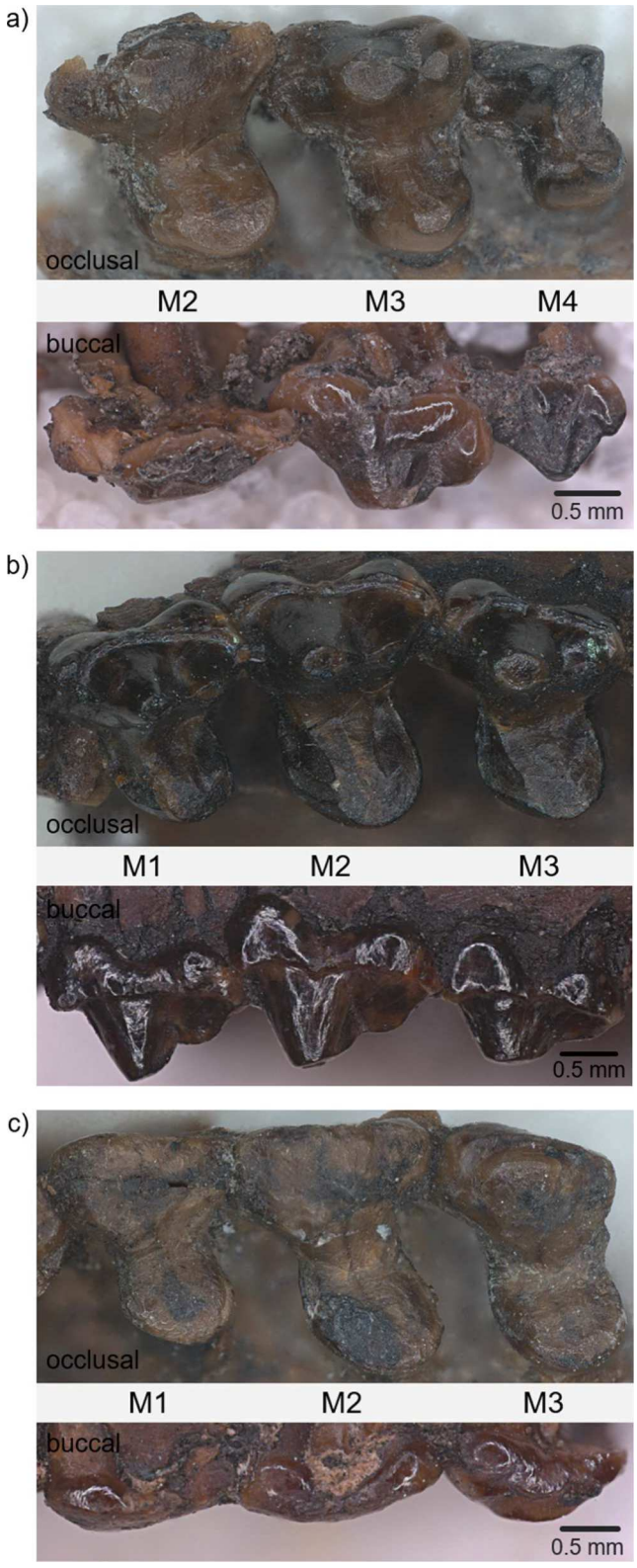

Fig. 17: Degree of wear in upper molar rows of *Haldanodon*. a) Low degree of wear with only very little exposure of dentine on cusps and crests of the least worn molar (M4). The molar row also shows a large, mesially increasing wear gradient (M2: high degree of wear, M4: low degree of wear) (Gui Mam 58/79). b) Medium degree of wear with cusps and crests connected by exposed dentine on the least worn molar (M1). The molar row also shows a small, distally increasing wear gradient (M1: medium degree of wear, M3: medium to high degree of wear) (Gui Mam 42/78, inverted). c) High degree of wear with indistinct boundaries in between cusps and crests of the least worn molar (M3). The molar row also shows a small, mesially increasing wear gradient (M1: high degree of wear, M3: high degree of wear) (Gui Mam 18/80).

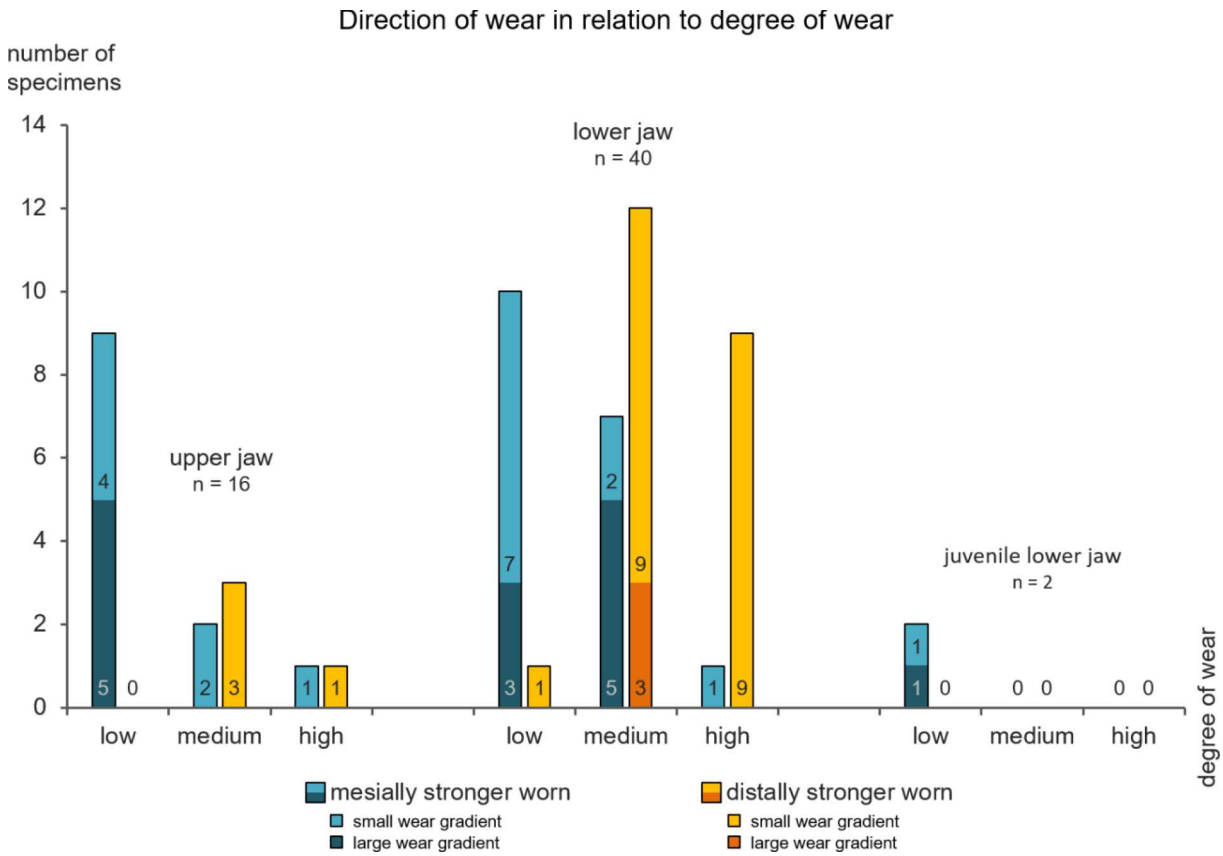

Fig. 18: Diagram showing the correlation of the direction of wear within a molar row (mesially (blue) or distally (orange) stronger worn) and the degree of wear of the molar row (low, medium or high) in *Haldanodon*. It also shows the distribution of small (light blue / light yellow) and large (dark blue / dark orange) wear gradients among the molar rows in correlation to both direction and degree of wear. The majority of mesially stronger worn molar rows shows a low degree of wear in both upper and lower jaws. Distally stronger worn molar rows show a medium to high degree of wear. Large wear gradients are mostly present in mesially stronger worn molar rows and only in specimens with a low to medium degree of wear.

5.1.2.2 Wear pattern

To examine the abrasion patterns of the molar rows, 40 lower and 16 upper jaws of *Haldanodon* were studied. As mentioned above only molar rows with three or more mostly intact teeth were included into the study to get a reliable assessment of the direction of increasing wear within the molar row.

Two distinctly different abrasion patterns were observed for the lower jaws. In 18 lower molar rows the wear increases in mesial direction. However, in 22 lower molar rows wear increases in the opposite direction, that is towards distal. Altogether, 45% of the lower molar rows are mesially stronger and 55% distally stronger worn. The direction of wear is strongly correlated to the degree of wear within the molar row. Ten out of eleven rows with a low degree show a mesially increasing wear gradient. In contrast to that, nine out of ten rows with a high degree

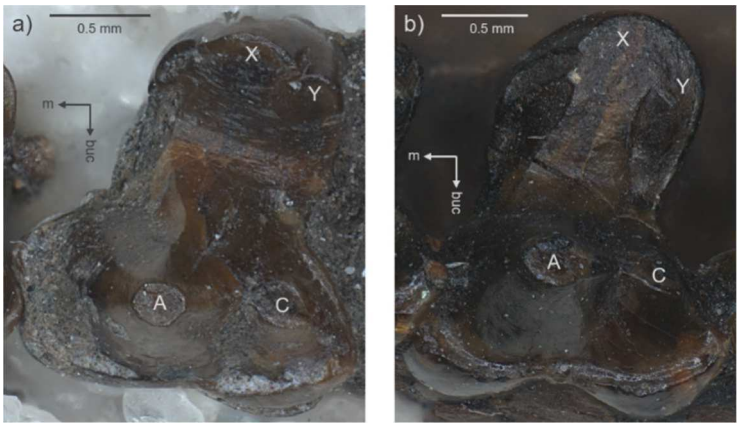

Fig. 19: Abrasion patterns of crest X-Y in upper *Haldanodon* molars. a) Worn only on the buccal side, forming a sharp crest (M2 of Gui Mam 13/82). b) Worn flat, forming a broad crest (M2 of Gui Mam 42/78).

of wear show a distally increasing wear gradient. Rows with a medium degree are more often stronger worn in distal direction (twelve) than in mesial direction (seven). The majority of the lower molar rows (29 specimens = >70%) show a small wear gradient. The large wear gradients are restricted to rows with a low (3) or medium (8) degree of wear. Thereof, all of the rows with a low and five of the rows with a medium degree are mesially stronger worn (fig. 18).

Two juvenile lower jaw specimens (VJ 1005-155, Gui Mam 33/77) added to the study have a mesially stronger worn molar row with a low degree of wear. However, one of them (Gui Mam 33/77) shows an especially large wear gradient with the first molar already heavily abraded (fig. 14b). The other one (VJ 1005-155) has a small wear gradient.

The 16 upper molar rows included into this study also show the same two opposing abrasion patterns as the lower molar rows. Twelve upper molar rows have a mesially increasing wear gradient and four a distally increasing one. With this, 75% of the upper molar rows are mesially stronger worn and 25% distally stronger worn. The correlation with the degree of wear is less distinct but still present. In all of the nine molar rows with a low degree, wear is increasing in mesial direction. Out of the two rows with a high degree, one shows a mesially increasing wear gradient and one a distally increasing one. Rows with a medium degree also are more often stronger worn in distal direction (three) than in mesial direction (two). Here, too, most of the rows (11 specimens = ~70%) show a small wear gradient. All five rows showing a large gradient have a low degree of wear increasing in mesial direction (fig. 18).

The upper molar rows additionally show another noticeable abrasion pattern, independent from degree or direction of wear or wear gradient. In two specimens crest X-Y is clearly worn flat in a horizontal plane on all molars, forming a broad crest at the lingual side of the “pseudotrigon basin” (Gui Mam 85/75, Gui Mam 42/78). On the other hand, in two specimens this crest is worn only on the buccal side on all molars, forming a sharp edge at the lingual side of the “pseudotrigon basin” (Gui Mam 20/76, Gui Mam 13/82) (fig. 19). The other specimens show a less distinct disparity but either tend towards a flatly worn crest X-Y (seven) or a buccally worn one (four).

5.1.3 Position of facets

To determine the most probable way of occlusion for the virtual simulation of the chewing stroke of *Haldanodon* with the OFA, facet positions had to be investigated. This was also necessary to verify whether the collision areas displayed by the OFA match the facets actually observed on the original specimens.

The upper molar has six facets (fig. 4a, fig. 20). Facet I is the largest one and is situated on the lingual flank of cusp A. In its full extent it entirely covers the mesio-lingual part of the buccal half of the upper molar from crest A-B and crest A-X down to the base of the mesial cingulum as well as the upper half of the disto-lingual flank of cusp A. Facet II is situated on the lingual flank of cusp C and the lower half of the disto-lingual flank of cusp A. Fully developed, it covers most of the disto-lingual part of the buccal half of the upper molar (and with this the buccal part of the "pseudotrigon basin") including the distal cingulum. Facet I and II are often fused without showing any sign of where one ends and the other begins. Facet III is situated on the mesial flank of cusp X, which is also called the "pseudoprotocone". In its maximum extent, it covers all of the lingual half of the upper molar mesially of crest A-X down to the base of the mesial cingulum and also circles around the mesio-lingual flank of cusp X. Facet IV is situated on the buccal flank of cusp Y. It covers most of the lingual half of the upper molar in between crests X-Y and A-X (and with this the lingual part of the "pseudotrigon basin") with the exception of the upper third of the disto-buccal flank of cusp X. In its full extend, it is adjacent to facet V, which completely covers the lingual part of the distal cingulum, from the apex of cusp Y downward. Facet VI is a small facet situated on the lingual flank of cusp Y directly below its apex. The described facets are not always present on all of the upper molar specimens and sometimes the facets on either the buccal or the lingual half are much more developed than those on the other half are.

The lower molar has six facets matching the ones on the upper molar (fig. 4b, fig. 20). Facet I is situated on the disto-buccal flank of main cusp a and extends towards the mesio-buccal flank of cusp d. It completely covers the flanks of the cusps from the apices throughout the deep groove in between them down to the disto-buccal tooth rim. Facet II is usually divided into two separated parts. Facet II-1 is a small facet situated on the mesial flank of cusp b directly below its apex. Facet II-2 is situated on the mesio-buccal flank of cusp a and the disto-buccal flank of cusp b; it mainly covers the steep, shallow groove in between those cusps and in contrast to facet I ends well above the buccal tooth rim. Facet III is not continuously developed as well. Facet III-1 is situated directly above facet I on the disto-buccal flank of cusp a; the two are separated by the faint crest in between cusp a and the deep distal groove. Facet III-2 covers

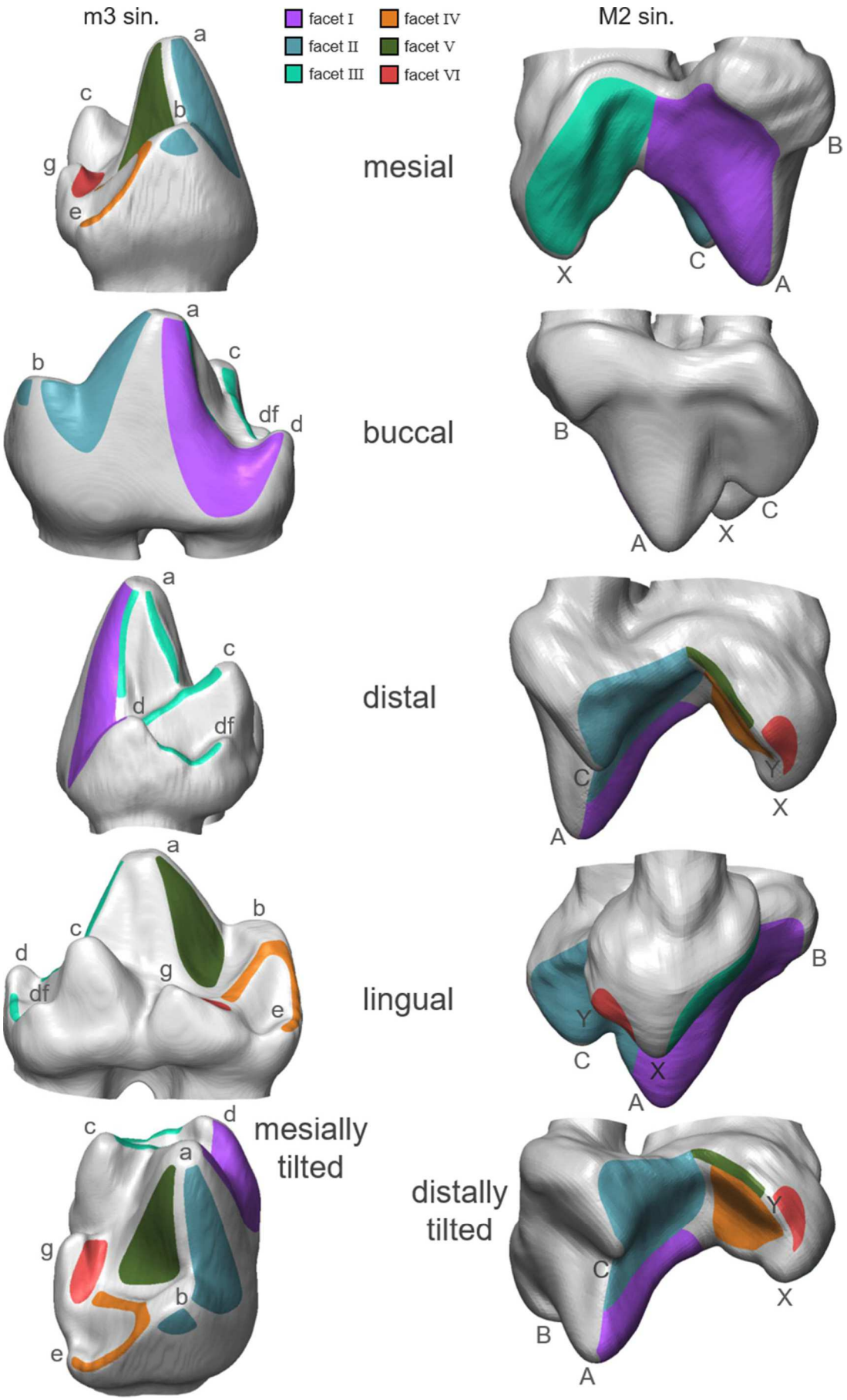

Fig. 20: Position of wear facets on *Haldanodon* molars as seen from different views (for occlusal view see fig. 4). Left: lower molar (model: m3 of Gui Mam 6/82). Right: upper molar (model: M2 of Gui Mam 30/79). Corresponding wear facets have the same color.

crest a-c, facet III-3 crest c-d, and facet III-4 crest d-df. Facet IV is located on the crests b-e and b-g, joining directly below the apex of cusp b. Facet V covers the entire mesio-lingual flank of cusp a beginning directly below its apex and running along crest a-b but does not quite reach the bottom of the "pseudotalonid basin". Facet VI is the smallest facet and is situated on the lingual side of the "pseudotalonid basin" which is made up of the buccal flank of cusp g. On the lower molar, too, not all of the specimens always show all of the facets.

5.1.4 Striation patterns and trailing edges

To determine the most probable way of movement of the lower molar models in the virtual simulation of the chewing stroke, striation patterns and trailing edges had to be examined on original molar specimens.

Three distinctly different directions of striae were observed on SEM-images of upper and lower molars (fig. 21). The first striation pattern consists of striae that run vertical. These are present on facets I and II. On upper facet I they are covering crest A-X and the distal flank of cusp A (e.g. Gui Mam 3125, Gui Mam 3231, Gui Mam 3261) (fig. 22). On lower facet I vertical striae can only be found on the upper part above the disto-buccal groove, but they are usually not very distinct (e.g. Gui Mam 3176, Gui Mam 3203, Gui Mam 3206, Gui Mam 3213) (fig. 23). On upper facet II vertical striae are only present on the upper part covering the flanks of cusps A and C (e.g. Gui Mam 3231, Gui Mam 3242, Gui Mam 3243, Gui Mam 3261) (fig. 24). As mentioned in 5.3, on many upper molar specimens facets I and II are fused. Striations continue smoothly from one facet onto the other without even a slight change in direction (e.g. Gui Mam 3125, Gui Mam 3231, Gui Mam 3243). On lower facet II vertical striae are always present on the lower part of facet II-2 covering the mesio-buccal groove (e.g. Gui Mam 3168, Gui Mam 3170, Gui Mam 3172, Gui Mam 3174, Gui Mam 3176, Gui Mam 3178, Gui Mam 3203, Gui Mam 3208) (fig. 25).

The second striation pattern consists of striae inclining in mesial direction. These are present on facet IV as well as upper facet III and lower facets I, II, V, and maybe VI. As mentioned above, striations on the upper part of lower facet I above the disto-buccal groove usually run vertical. However, on the lower part below the groove the striae always distinctly incline towards mesial (e.g. Gui Mam 3170, Gui Mam 3172, Gui Mam 3203, Gui Mam 3213) (fig. 22). On lower facet II mesially inclining striae are only present on the upper part of facet II-2 above the mesio-buccal groove (e.g. Gui Mam 3168, Gui Mam 3170, Gui Mam 3172, Gui Mam 3176, Gui Mam 3178, Gui Mam 3203). If striae are mesially inclined, they show a distinctly lower

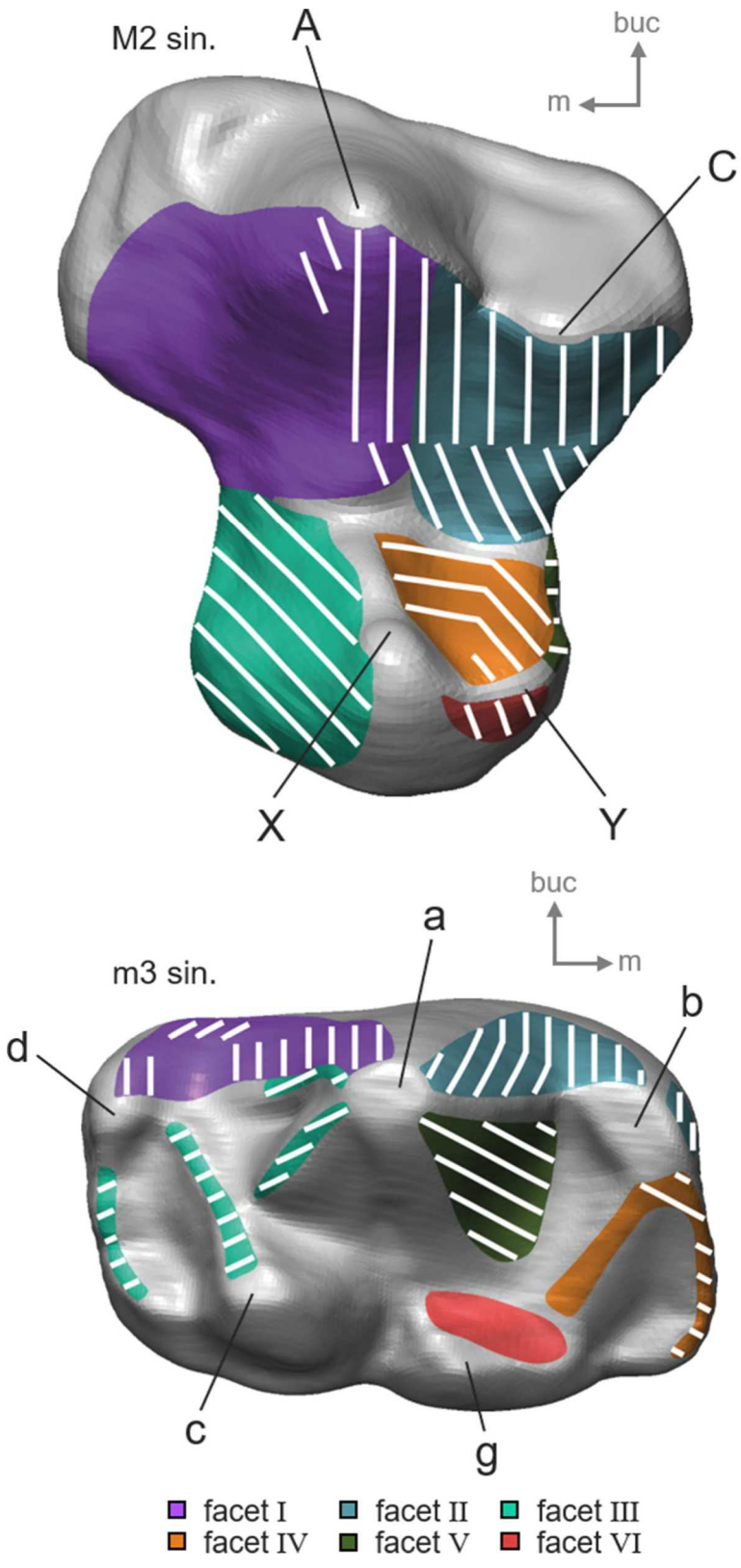

Fig. 21: Striations as observed on upper and lower *Haldanodon* molars, occlusal view. Corresponding upper and lower facets have the same color. There are three distinct striation patterns. Vertically running striae are present on upper and lower facets I and II. Mesially inclining striae are present on upper facets III and IV as well as lower facets I, II, IV, and V. On upper facet III and IV they are parallel, so are they on lower facets IV and V. On lower facet I they are much more inclined than on lower facet II. Distally inclining striae are present on upper facets I, II, IV, V, and VI as well as lower facet III. On upper facets I, II, and VI they are parallel as well as on upper facets IV and V on which they run almost horizontal. (upper molar model: M2 of Gui Mam 30/79, lower molar model: m3 of Gui Mam 6/82)

degree of inclination than those on the lower part of lower facet I. On the level of the mesio-buccal groove they turn abruptly vertical, which is usually accompanied by the formation of a sharp edge in between the two parts of lower facet II-2 (fig. 25). On one of the examined specimens (Gui Mam 3188) the striae on the lowermost part of facet II-2 abruptly turn towards mesial again. They are also divided by a faint edge from the rest of the facet. On upper facet III mesially inclining striae always cover all of it and are rather steep (e.g. Gui Mam 3123, Gui Mam 3191, Gui Mam 3228, Gui Mam 3231, Gui Mam 3242, Gui Mam 3245, Gui Mam 3252, Gui Mam 3262, Gui Mam 3265) (fig. 26). Striae on upper facet IV only incline towards mesial on the distal part below cusp Y. They usually run almost vertical and only slightly incline towards mesial (e.g. Gui Mam 3228, Gui Mam 3242, Gui Mam 3245, Gui Mam 3262, Gui Mam 3265) (fig. 28). Thus, they run more or less parallel to the striae on upper facet III (e.g. Gui Mam 3228, Gui Mam 3245). On lower facet IV mesially inclining striae can only be observed right below the tip of cusp b and on crest b-e (e.g. Gui Mam 3168, Gui Mam 3170, Gui Mam 3176, Gui Mam 3203). Crest b-g often shows a distinct polished surface but no striations at all (fig. 29). On lower facet V mesially inclining striae are present all over it (e.g. Gui Mam 3168, Gui Mam 3172, Gui Mam 3174, Gui Mam 3176, Gui Mam 3177, Gui Mam 3188, Gui Mam 3203, Gui Mam 3206) (fig. 31). They usually run parallel to facet IV (e.g. Gui Mam 3168, Gui Mam 3176, Gui Mam 3203). On lower facet VI striae are very faint but seem to incline in mesial direction (e.g. Gui Mam 3176) (fig. 33).

The third striation pattern consists of striae inclining in distal direction. These are present on upper facets I, II, IV, V, and VI as well as lower facet III. On upper facet I, the part on the mesial flank of cusp A often shows a distinct polished surface right below the tip of the cusp. Striations on this part are usually heavily overprinted by abrasion but in contrast to the distal part of the facet seem to incline in distal direction (e.g. Gui Mam 3125, Gui Mam 3191, Gui Mam 3221, Gui Mam 3231, Gui Mam 3261) (fig. 22). On upper facet II, striae usually are vertical on the flanks of the cusps but then turn more or less abruptly towards distal at their base within the “pseudotrigon basin” (e.g. Gui Mam 3125, Gui Mam 3231, Gui Mam 3242, Gui Mam 3243, Gui Mam 3261, Gui Mam 3262) (fig. 24). They run more or less parallel to the distally inclining striae on upper facet I. On lower facet III, distally inclining striae are present on all parts of the facet (e.g. Gui Mam 3172, Gui Mam 3174, Gui Mam 3176, Gui Mam 3203, Gui Mam 3208, Gui Mam 3213) (fig. 27). On many specimens the striae are additionally more or less slightly oriented towards lingual (e.g. Gui Mam 3172, Gui Mam 3174, Gui Mam 3203, Gui Mam 3213). Striations on upper facet IV incline towards distal on its mesial part below cusp X. In contrast to the steep mesially inclining striae on its distal part they almost run horizontal (e.g. Gui Mam 3228, Gui Mam 3242, Gui Mam 3245, Gui Mam 3251, Gui Mam

3252, Gui Mam 3262, Gui Mam 3265) (fig. 28). Striae on upper facet V are almost horizontal as well and only show a very slight inclination towards distal (fig. 30). Thus, they run more or less parallel to the striae on the mesial part of upper facet IV (e.g. Gui Mam 3228, Gui Mam 3262, Gui Mam 3265). On upper facet VI striae seem to show about the same degree of distal inclination than those on upper facet II (e.g. Gui Mam 3130, Gui Mam 3191, Gui Mam 3242, Gui Mam 3252, Gui Mam 3265) (fig. 32).

Striations cannot only be observed on facets but also frequently cover other parts of the molars. However, these striae do not show any clearly distinguishable orientation but rather cross each other in more or less diverse angles. Especially if dentine is exposed, undirected striae can also be present on the facets, partially interfering with the oriented striations.

Exposed dentine usually either connects very smoothly with the enclosing enamel or is deeply scoured at all sides. Therefore, smooth leading and stepped trailing edges at the enamel-dentine junction usually cannot be distinguished on neither lower nor upper molars. The only exceptions that show clearly visible leading and trailing edges on many lower molar specimens are the mesio-lingual border of the “pseudotalonid basin” and the buccal extension of the disto-buccal groove in between cusps a and d. If present, the leading edge within the “pseudotalonid basin” always lies on the distal side of crest b-g and the trailing edge on the mesial one (e.g. Gui Mam 3172, Gui Mam 3174, Gui Mam 3178, Gui Mam 3188, Gui Mam 3203, Gui Mam 3206) (fig. 34). This is always accompanied by a considerable outward downslope of the dentine field, which therefore breaks through crest b-g (e.g. Gui Mam 3104, Gui Mam 3142, Gui Mam 3168, Gui Mam 3170, Gui Mam 3172, Gui Mam 3174, Gui Mam 3176, Gui Mam 3177, Gui Mam 3178, Gui Mam 3188, Gui Mam 3203, Gui Mam 3208). Gui Mam 3172 additionally seems to show a vague leading edge on the basal part of crest b-e and a vague trailing edge above. If present, the leading edge of the disto-buccal groove lies on the lingual side of the dentin field exposed within and below the groove. The accompanying trailing edge is situated on the buccal side (e.g. Gui Mam 3170, Gui Mam 3203, Gui Mam 3213) (fig. 35). On some lower molar specimens vague leading edges might also be present on the distal side of some of the distal crests accompanied by vague trailing edges on the mesial side of the same crests (e.g. Gui Mam 3172, Gui Mam 3174, Gui Mam 3188) (fig. 36). On the upper molar, a slight leading edge might be present on the mesial side of the mesial cingulum with the accompanying trailing edge on the distal side of the same cingulum (e.g. Gui Mam 3242, Gui Mam 3245) (fig. 37).

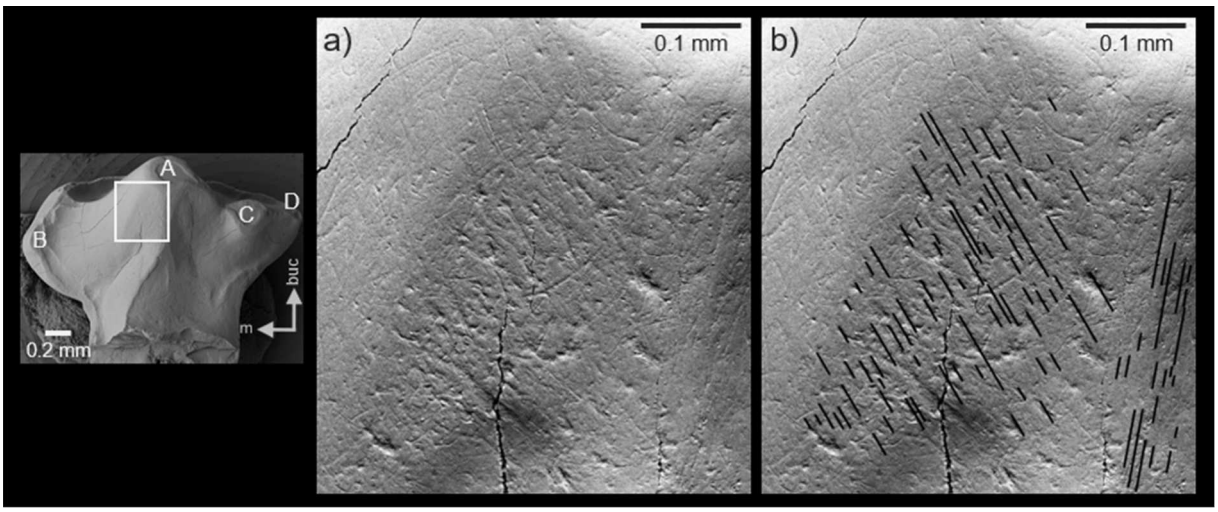

Fig. 22: Striations on facet I of a *Haldanodon* upper molar specimen (Gui Mam 3125, M sin.). Parallel striae incline in distal direction on the mesio-lingual flank of cusp A and run vertical on crest A-X. a) Magnified facet. b) Magnified facet with marked striae.

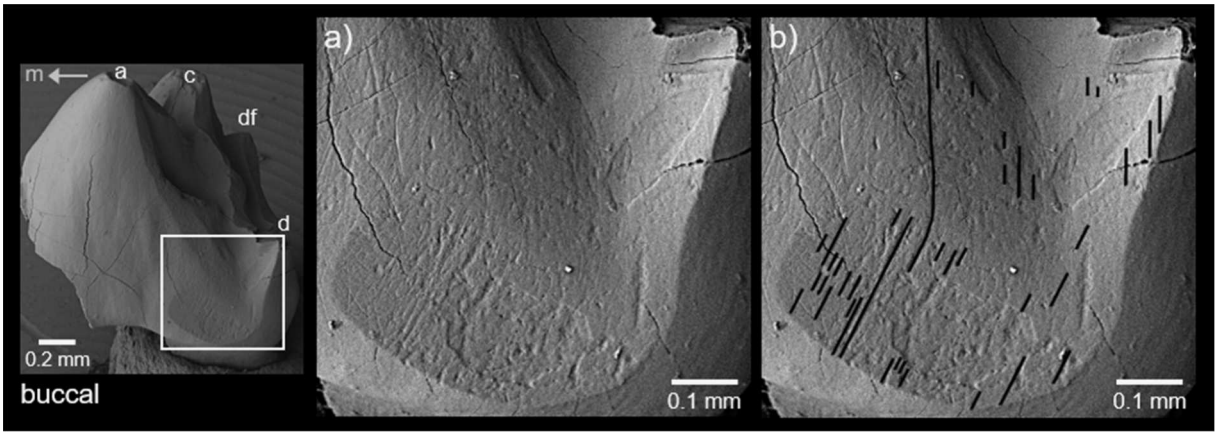

Fig. 23: Striations on facet I of a *Haldanodon* lower molar specimen (Gui Mam 3213, m dex. inverted). Parallel striae run vertical on the upper part and abruptly change direction towards mesial on the lower part. a) Magnified facet. b) Magnified facet with marked striae.

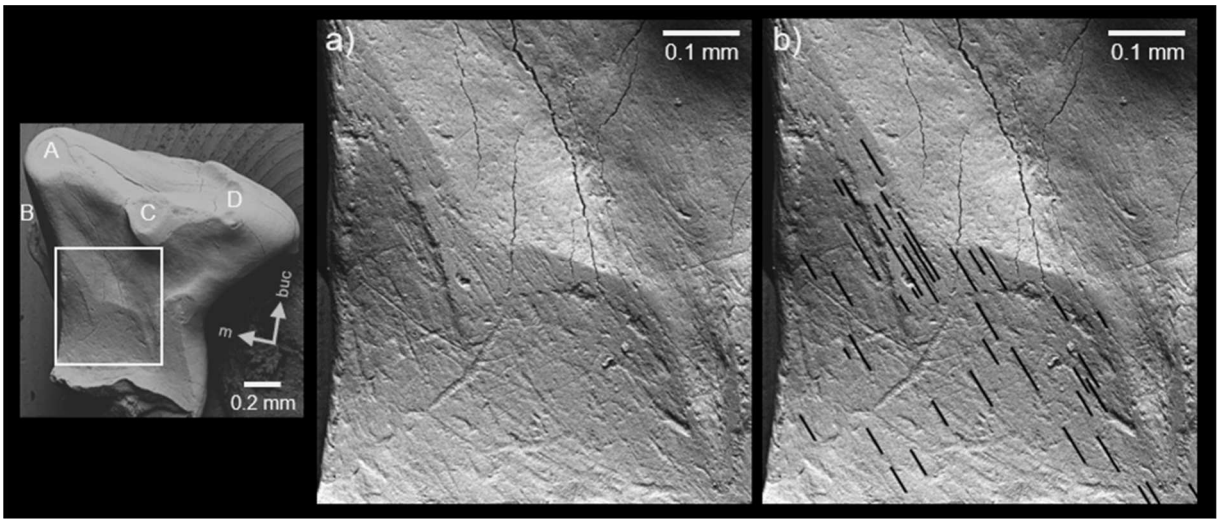

Fig. 24: Striations on facet II of a *Haldanodon* upper molar specimen (Gui Mam 3125, M sin.). Parallel striae incline in distal direction. a) Magnified facet. b) Magnified facet with marked striae.

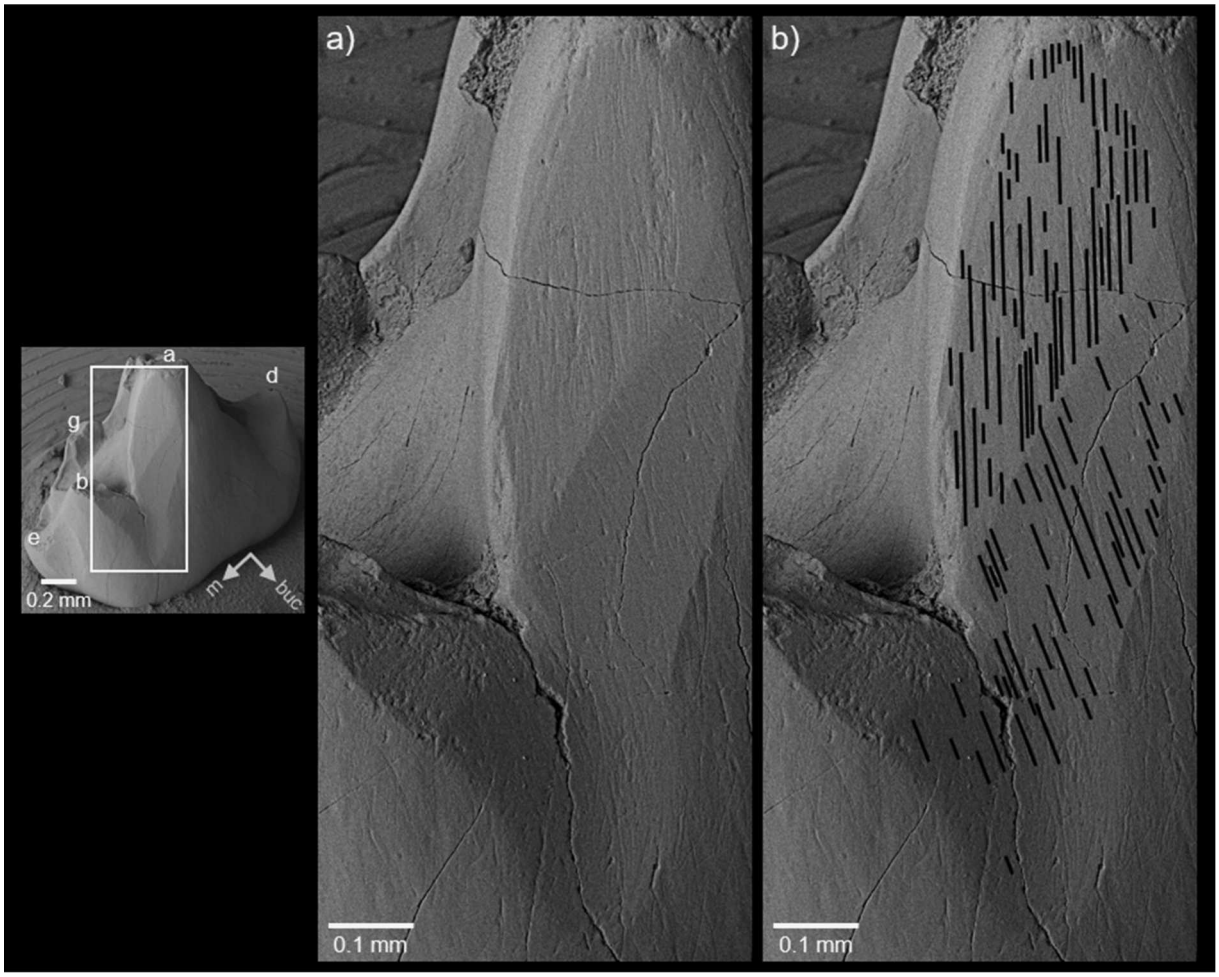

Fig. 25: Striations on facet II-2 of a *Haldanodon* lower molar specimen (Gui Mam 3203, m dex. inverted). Parallel striae slightly incline towards mesial on the upper part and abruptly turn vertical on the lower part. Both parts are separated by a sharp edge. a) Magnified facet. b) Magnified facet with marked striae.

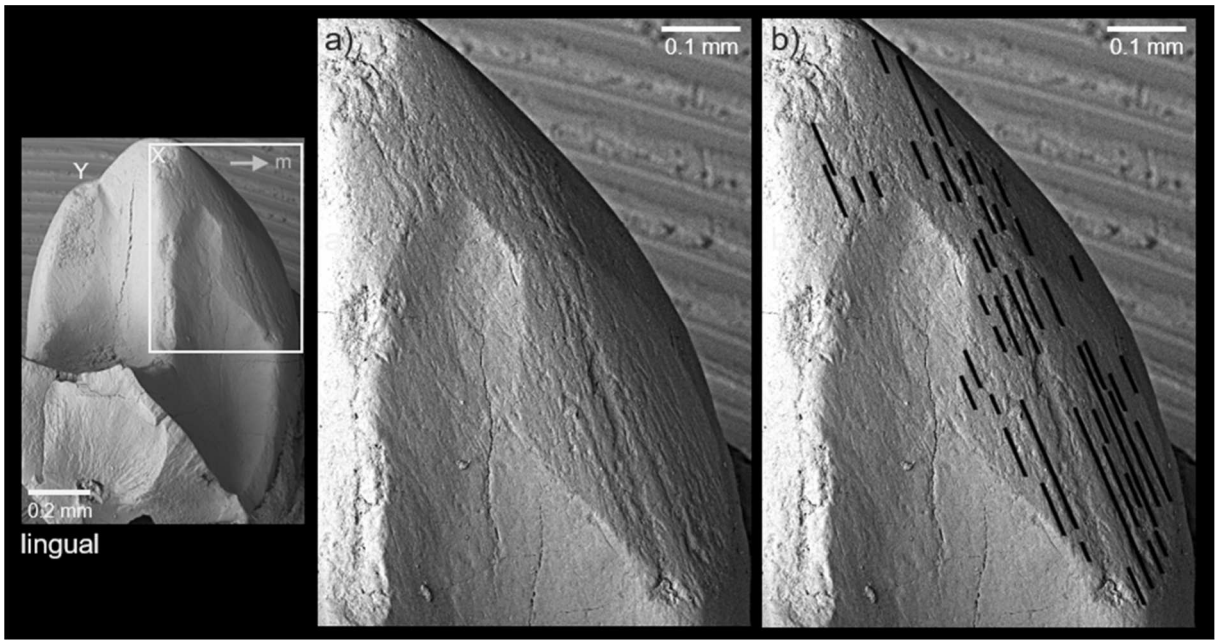

Fig. 26: Striations on facet III of a *Haldanodon* upper molar specimen (Gui Mam 3262, M dex. inverted). Parallel striae slightly incline in mesial direction. a) Magnified facet. b) Magnified facet with marked striae.

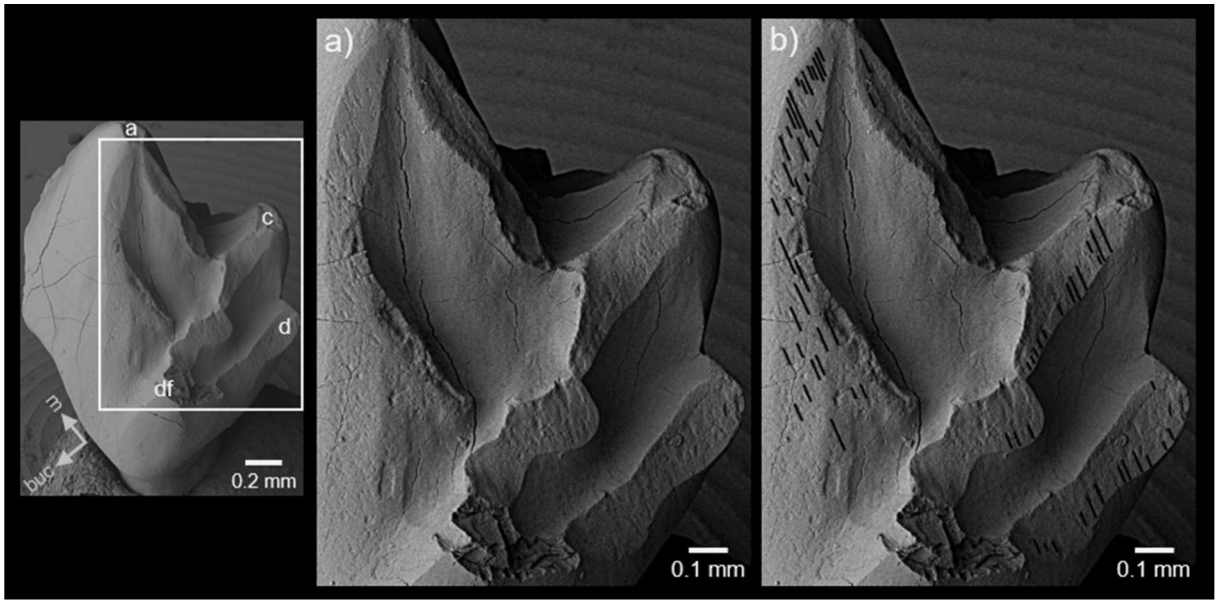

Fig. 27: Striations on facet III of a *Haldanodon* lower molar specimen (Gui Mam 3213, m dex. inverted). Parallel striae incline in distal direction. a) Magnified facet. b) Magnified facet with marked striae.

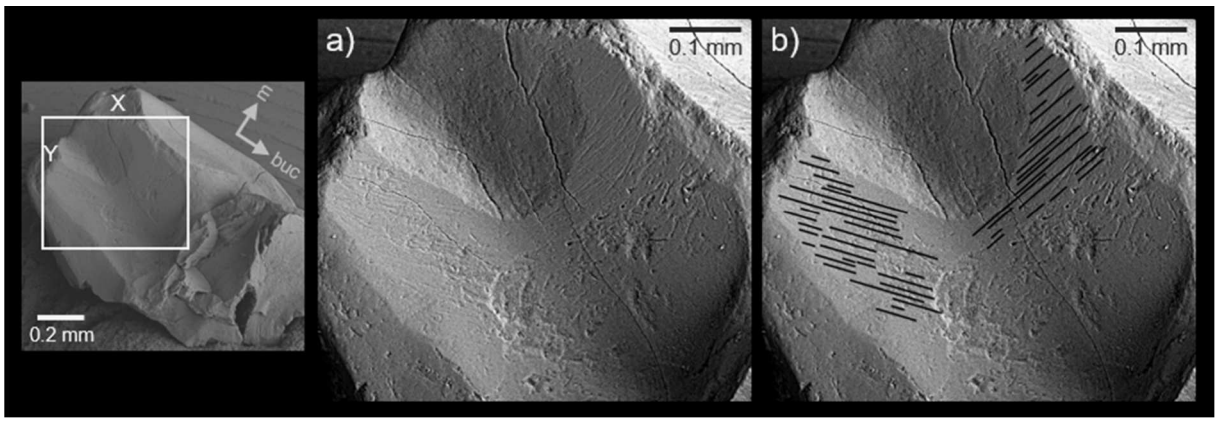

Fig. 28: Striations on facet IV of a *Haldanodon* upper molar specimen (Gui Mam 3245, M sin.). Parallel striae slightly incline in mesial direction below cusp Y and run almost horizontal with a slight inclination towards distal below cusp X. a) Magnified facet. b) Magnified facet with marked striae.

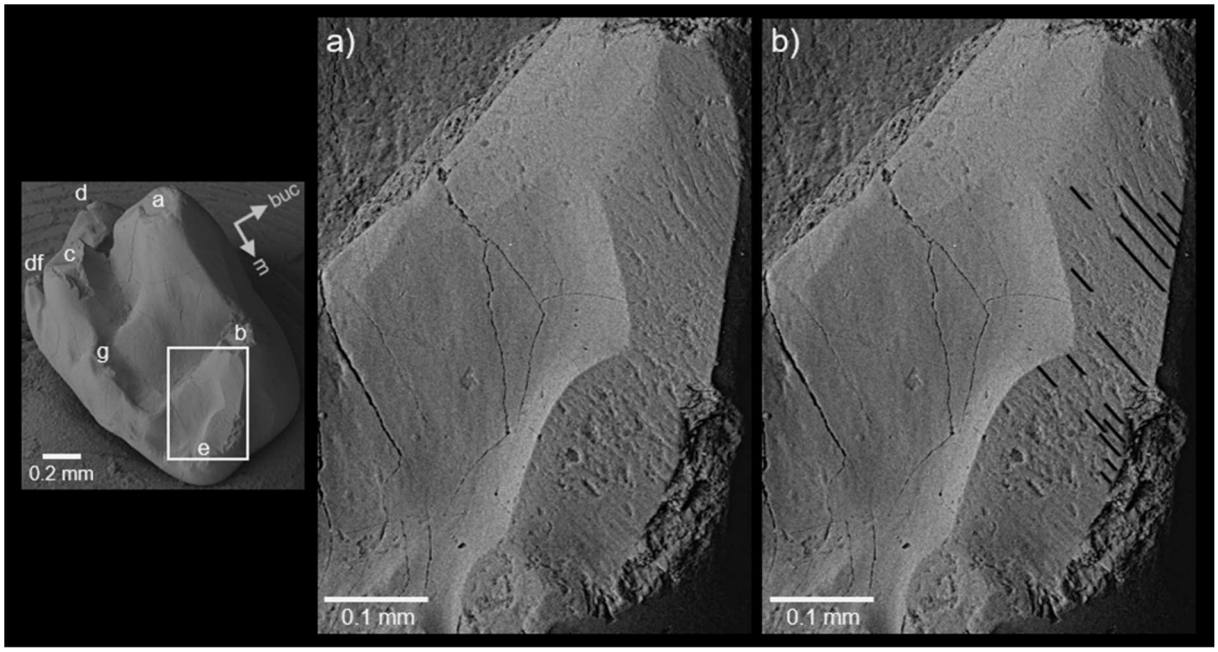

Fig. 29: Striations on facet IV of a *Haldanodon* lower molar specimen (Gui Mam 3203, m dex. inverted). Parallel striae incline in mesial direction on crest b-e. a) Magnified facet. b) Magnified facet with marked striae.

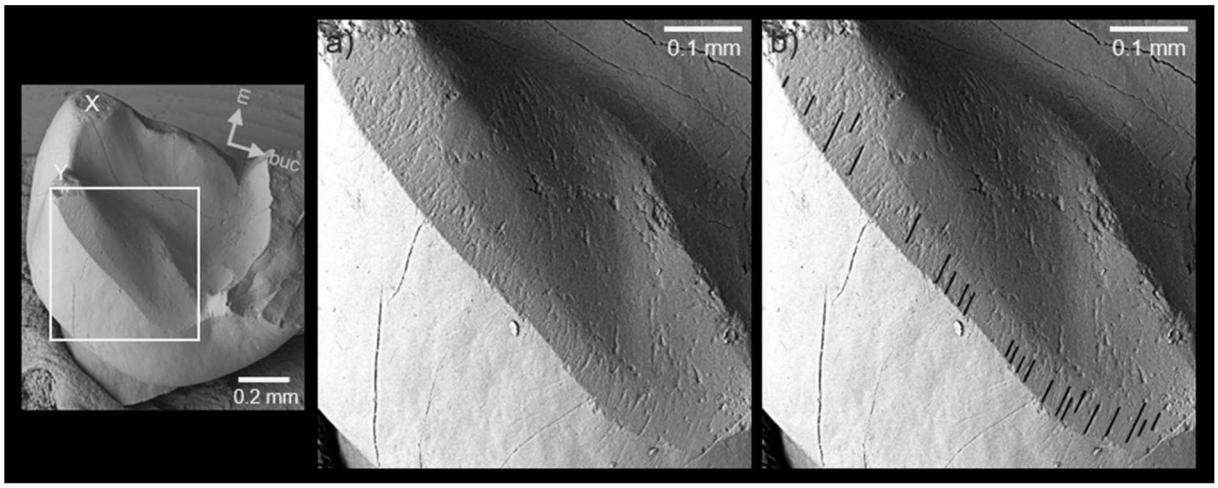

Fig. 30: Striations on facet V of a *Haldanodon* upper molar specimen (Gui Mam 3228, M dex. inverted). Parallel striae slightly incline in distal direction. a) Magnified facet. b) Magnified facet with marked striae.

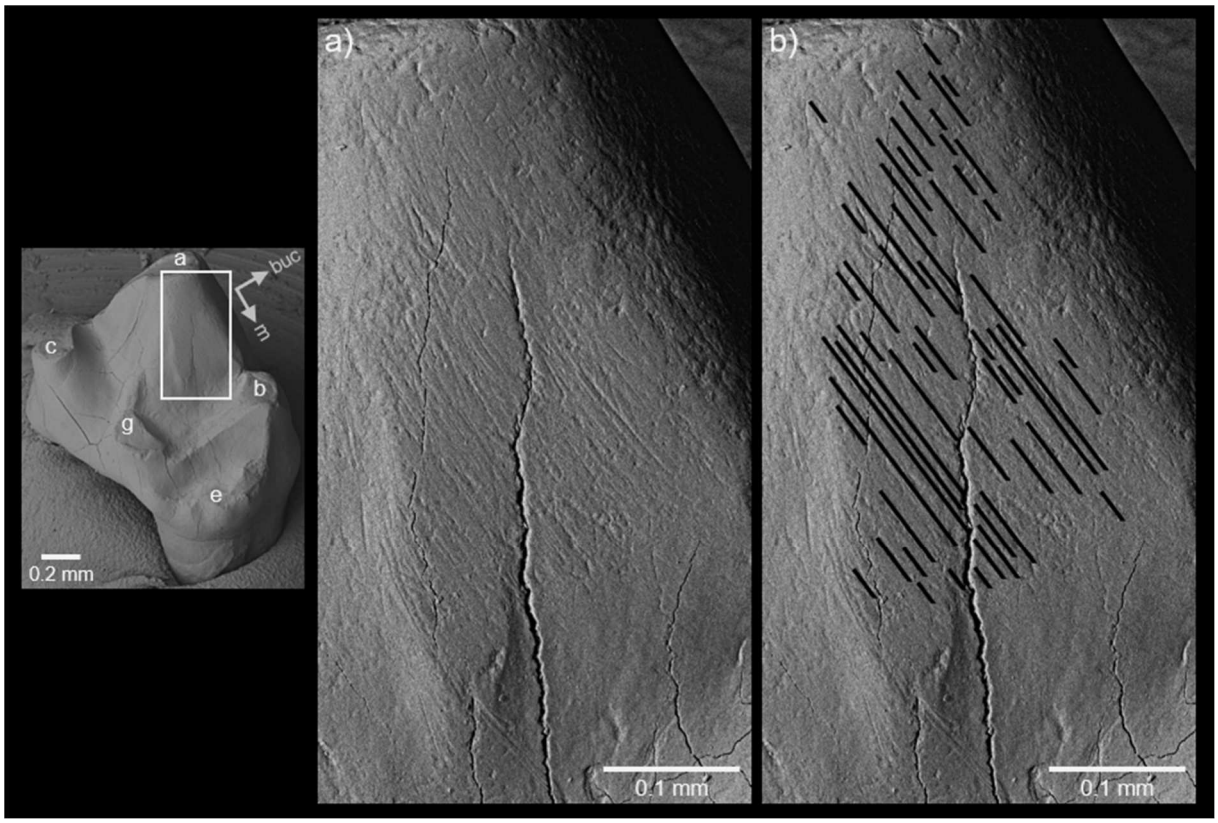

Fig. 31: Striations on facet V of a *Haldanodon* lower molar specimen (Gui Mam 3174, m dex. inverted). Parallel striae incline in mesial direction. a) Magnified facet. b) Magnified facet with marked striae.

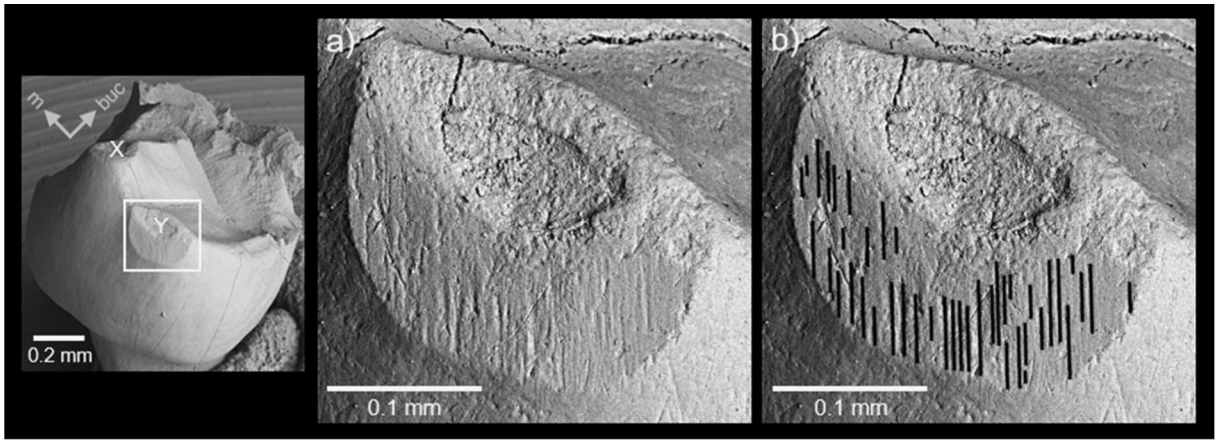

Fig. 32: Striations on facet VI of a *Haldanodon* upper molar specimen (Gui Mam 3265, M sin.). Parallel striae incline in distal direction. a) Magnified facet. b) Magnified facet with marked striae.

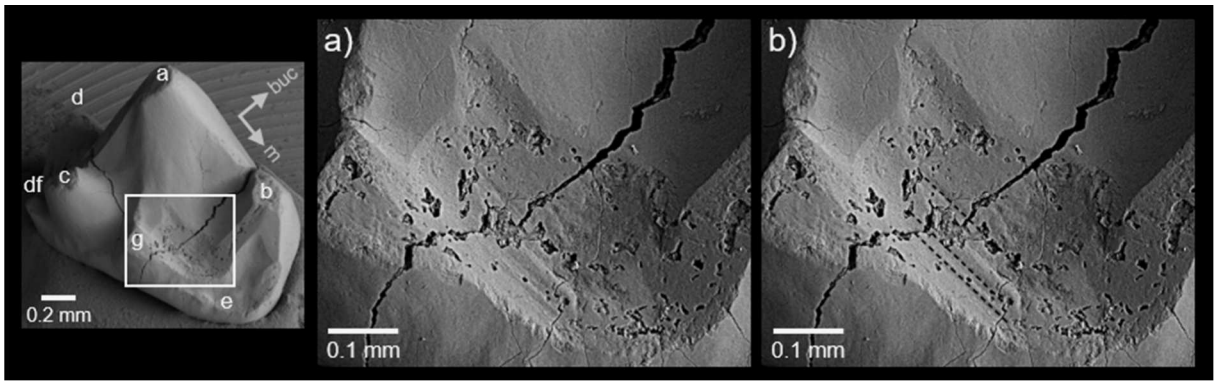

Fig. 33: Potential striations on facet VI of a *Haldanodon* lower molar specimen (Gui Mam 3176, m sin.) inclining in mesial direction. a) Magnified facet. b) Magnified facet with marked striae.

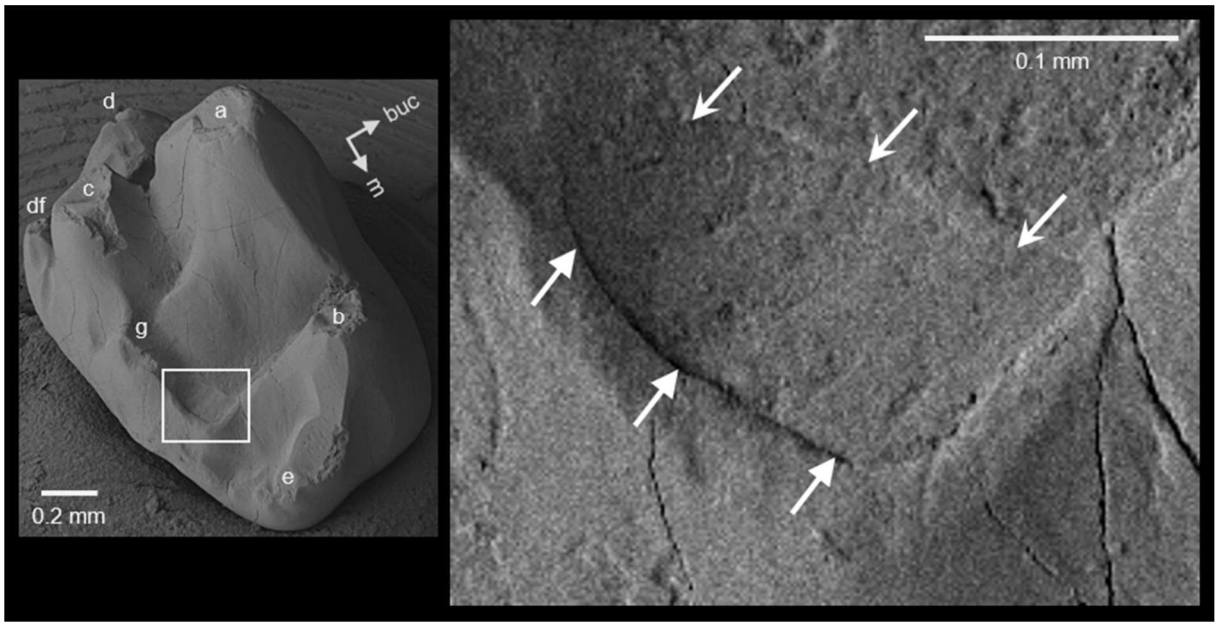

Fig. 34: Leading and trailing edge within the "pseudotalonid basin" of a *Haldanodon* lower molar specimen (Gui Mam 3203, m dex. inverted). The leading edge (narrow arrows) is situated on the buccal side of crest b-g, the trailing edge (wide arrows) on the lingual one. Crest b-g builds up the mesial border of the "pseudotalonid basin" and is completely worn down. The exposed dentine field shows an outward downslope.

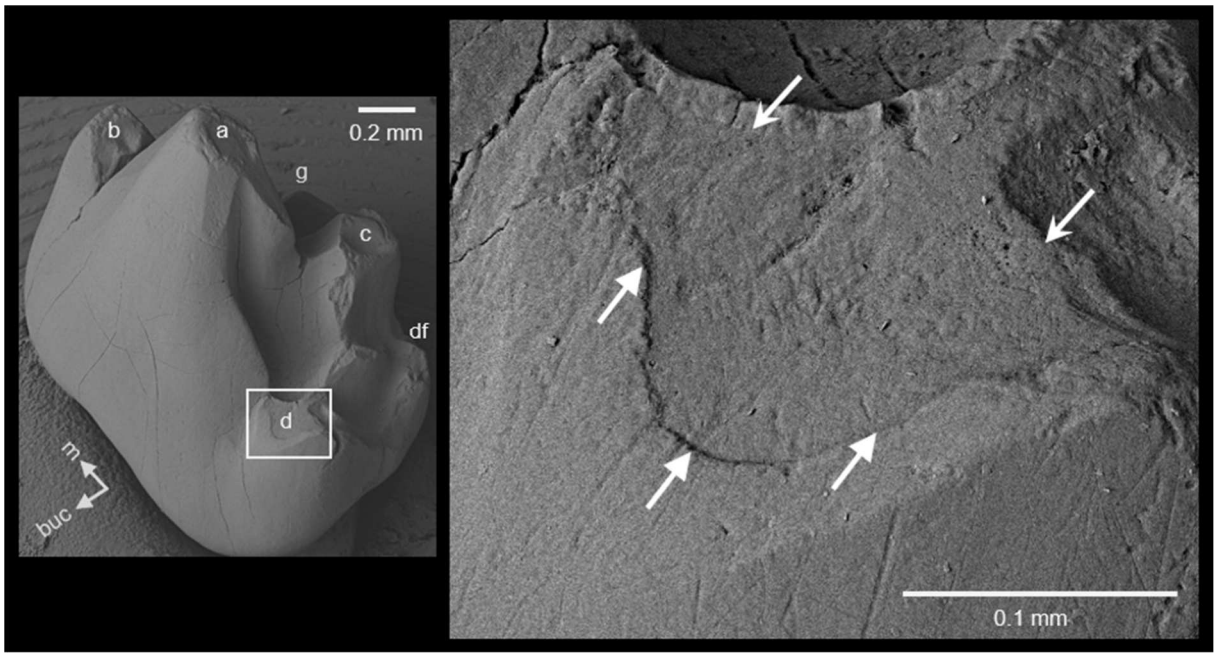

Fig. 35: Leading and trailing edge within the disto-buccal groove of a *Haldanodon* lower molar specimen (Gui Mam 3203, m dex. inverted). The leading edge (narrow arrows) is situated on the lingual side of cusp d, the accompanying trailing edge (wide arrows) on the buccal side.

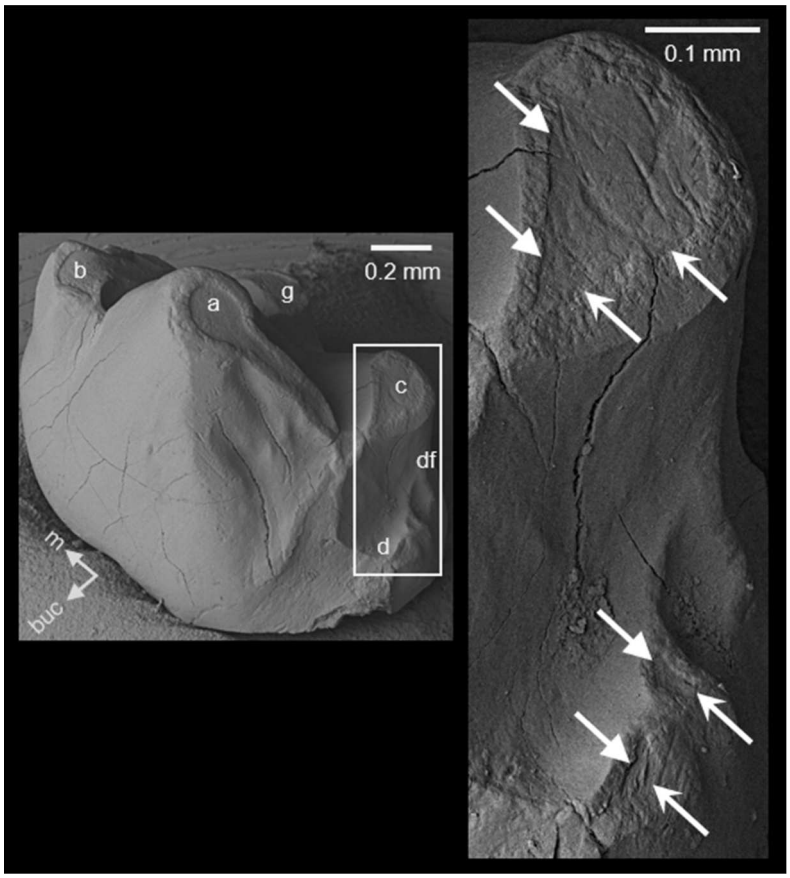

Fig. 36: Leading and trailing edges on the distal crests of a *Haldanodon* lower molar specimen (Gui Mam 3174, m dex. inverted). The leading edge (narrow arrows) is situated on the distal side of crests c-d and d-df, the trailing edge (wide arrows) on the mesial side.

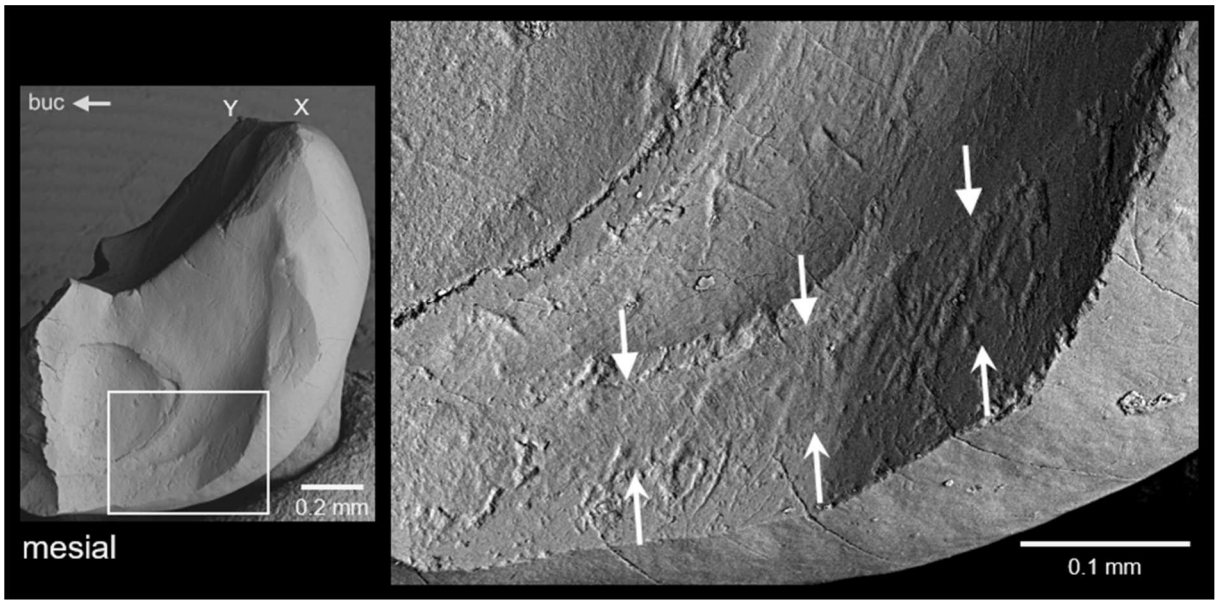

Fig. 37: Vague leading and trailing edge on the lingual part of the mesial cingulum of a *Haldanodon* upper molar specimen (Gui Mam 3242, M sin.). The leading edge (narrow arrows) is situated on its cervical side, the accompanying trailing edge (wide arrows) on its apical side.

5.2 Tooth-tooth-contact diagrams

5.2.1 *Haldanodon*

The Occlusal Fingerprint Analyser (OFA) was used to create a bar diagram showing the development of the sizes of the contact areas in between upper and lower molars over the duration of the chewing stroke (see also 4.5). For the program to be able to detect these areas, first the postulated mastication movement of *Haldanodon* had to be simulated. According to the facet positions and striations on the molars observed in this study, it definitely had two phases (see 6.4). Phase 1 consisted of a lateral upward movement of the lower molars from buccal to lingual and ended in centric occlusion with the lower molars resting in between the upper molars. For the second phase there are two different possible scenarios: either it had been a palinal downward movement directly following phase 1 (phase 2) or a separate proal upward movement ending in centric occlusion as well (phase 1b).

The contact diagram of phase 1/1a is divided into 17 time steps. For the scenario with the downward resumption of the mastication movement the count of time steps continues to 46, with centric occlusion separating phase 1 from phase 2 in between time steps 17 and 18 (fig. 38). The scenario with two separate upward movements also requires two separate contact diagrams. That for phase 1a terminates after the 17^{th} time step, that for phase 1b starts over with 29 time steps (fig. 39). In both diagrams centric occlusion takes place at the very end and also marks the end of the respective power stroke. Six facets are represented in the contact diagrams: facet I (light violet), facet II (grey blue), facet III (turquoise), facet IV (orange), facet V (olive), and facet VI (light red). Facet I with up to 0.36 mm² has the largest contact area, followed by facet III with up to 0.33 mm², and facet II with up to 0.24 mm². The smallest facets are facet VI with a contact area of up to 0.14 mm², facet IV with a contact area of up to 0.07 mm², and facet V with a contact area of up to 0.02 mm².

The first facet coming into contact with its antagonist on the upper molar in phase 1/1a is facet II, immediately followed by facet I in time step 2. The contact area of both facets more or less steadily increases until time step 10, and then it more or less steadily decreases again until the respective facet loses contact. For facet I, this is the case at time step 15, shortly before centric occlusion. Facet II loses contact right at the beginning of phase 2 at time step 18, if the chewing movement continues. Otherwise it loses contact with the opening of the jaw after centric occlusion. Facets III to VI almost simultaneously get in contact at the very end of phase 1/1a – facets III, IV, and VI at time step 16 and facet V at time step 17. Facets IV, V, and VI show their largest contact area at the very beginning of phase 2 at time step 18, respectively the very

end of phase 1b at time step 29 and only stay in contact for a very short time. In phase 2, they lose contact at its beginning: facet V at time step 18, facet VI at time step 19, and facet IV at time step 20. The contact area of facet III rapidly increases until time step 20, but then only slowly decreases again with some fluctuations. The loss of contact of facet III at time step 46 marks the end of phase 2. In the scenario with two separate upward movements, facets III to VI lose contact immediately after centric occlusion in phase 1a at time step 17. The first facet to get into contact in phase 1b is facet III, followed by facet IV at time step 27, facet VI at time step 28, and facet V at time step 29. All of these facets steadily increase in contact until they abruptly lose it after centric occlusion at time step 29. All in all, the facet with the longest time of contact is facet III with 31 (2+29) time steps, followed by facet II with 18 (17+1) time steps, facet I with 14 (14+0) time steps, facet IV with five time steps (2+3), facet VI with four time steps (2+2), and finally facet V with only two (1+1) time steps.

5.2.2 *Didelphis*

The power stroke of *Didelphis* comprises of two phases, separated by centric occlusion. Phase 1 is a more or less lateral movement of the lower molars from disto-buccal to mesio-lingual into centric occlusion. The lateral movement is continued in phase 2 in lingual direction.
All in all, the chewing motion of *Didelphis* consists of 44 time steps with centric occlusion separating the phases in between time steps 34 and 35. Phase 1 is divided into 34 time steps, phase 2 into ten (fig. 40). Five facets are shown in the contact diagram: facet 1 (dark blue), facet 2 (yellow), facet 3 (green), facet 6 (violet), and facet 9 (light blue). Facets 2 and 9 with a contact area of up to 0.7 mm² each are the largest facets. With up to 0.49 mm² facet 6 is the third largest facet, followed by facet 3 with a contact area of up to 0.35 mm². Facet 1 with a contact area of up to 0.24 mm² is the smallest one.
Facet 2 is the first facet to get into contact, immediately followed by facet 1 at time step 2. Facet 2 steadily increases its contact area until time step 16; afterwards its contact area rapidly decreases again until it loses contact at time step 21. Facet 1 steadily increases its contact area until time step ten, and then it slowly decreases again with a second small peak at time step 18. It loses contact simultaneously with facet 2 at time step 21. At the same time as facets 1 and 2 lose contact, facet 6 establishes contact with its antagonist. It steadily increases contact until time step 27. At time step 28 the size of the contact area of facet 6 abruptly drops to almost zero. Then it rapidly recovers until time step 31 and stays almost level until centric occlusion. Facet 6 abruptly loses contact at the very beginning of phase 2 at time step 35. At the end of

phase 1 the last two facets come into contact: facet 3 at time step 32 and facet 9 at time step 33. Facet 3 rapidly increases in size until centric occlusion after which it abruptly loses contact. Except for the one time step of facet 6, facet 9 is the only facet to continue its contact into phase 2. It increases in size only slowly until time step 41 and then very rapidly until its peak at time step 43. The loss of contact of facet 9 at time step 44 also marks the end of phase 2 and the power stroke. All in all, facet 2 has the longest contact with 21 (21+0) time steps, closely followed by facet 1 with 20 (20+0) time steps. Facet 6 maintains contact for 15 (14+1) time steps and facet 9 for twelve (2+10). Facet 3 has the shortest contact by far with only three (3+0) time steps.

5.2.3 *Monodelphis*

The power stroke of *Monodelphis* is very similar to that of *Didelphis*. It also has two phases, separated by centric occlusion. Like in *Didelphis*, phase 1 is a more or less lateral movement of the lower molars from disto-buccal to mesio-lingual. In phase 2, the lateral movement is continued in lingual direction as well.

The power stroke of *Monodelphis* consists of 42 time steps with centric occlusion occurring in between time steps 27 and 28. Thereof, phase 1 occupies 27 time steps and phase 2 has 15 time steps (fig. 41). There are three facets shown in the diagram: facet 1 (dark blue), facet 2 (yellow), and facet 9 (light blue). Facet 2 with up to 0.2 mm² is by far the largest facet, followed by facet 1 with up to 0.07 mm², and facet 9 with up to 0.05 mm². Facet 2 is also the first facet to get into contact, directly followed by facet 1 at time step 3. The contact area of facet 2 first increases slowly until time step 8 and then rapidly until it reaches its peak at time step 17. Then it decreases slowly until the facet abruptly loses contact at time step 21. The contact area of facet 1 slowly increases until time step 8. Afterwards it slowly decreases again with a second small peak at time step 17. Facet 1 does not lose contact before centric occlusion at time step 27. Just before centric occlusion, facet 9 gets into contact at time step 26. It is the only facet that continues the contact into phase 2, slowly increasing its contact area until time step 34 and then decreasing it just as slowly until its loss of contact at time step 42 marks the end of the phase and the power stroke. Facet 1 is the facet with the longest contact, lasting for 25 time steps (25+0), followed by facet 2 with a contact lasting 21 time steps (21+0), and facet 9 with a contact lasting 17 time steps (2+15).

Fig. 38 (next page): Tooth-tooth-contact diagram for *Haldanodon* showing the size of the contact area for each lower molar facet during a certain time step throughout the chewing stroke from first to last contact of the molars. This contact diagram is based on the reconstruction of the masticatory movement as a bi-phased power stroke, with a lateral upward movement of the lower molars into centric occlusion (phase 1) followed by a palinal downward movement (phase 2). (lower molar model: m3 of Gui Mam 6/82)

Fig. 39 (next page): Tooth-tooth-contact diagram for *Haldanodon* showing the size of the contact area for each lower molar facet during a certain time step throughout the chewing stroke from first to last contact of the molars. This contact diagram is based on the reconstruction of the masticatory movement as two independent power strokes, one consisting of a lateral upward movement of the lower molars into centric occlusion (phase 1a), and another consisting of a proal upward movement of the lower molars into centric occlusion (phase 1b). Centric occlusion is followed by a vertical opening of the jaw which results in an immediate loss of contact of the antagonistic molars. Both power strokes can be used alternatively. (lower molar model: m3 of Gui Mam 6/82)

Fig. 40 (page after next): Tooth-tooth-contact diagram for *Didelphis* showing the size of the contact area for each lower molar facet during a certain time step throughout the chewing stroke from first to last contact of the molars. *Didelphis* has a bi-phased power stroke, with a mesio-lingual upward movement of the lower molars into centric occlusion (phase 1) followed by a lingual downward movement (phase 2). (lower molar model: m2 of SMF 77266; red facet 4 is not in contact in this OFA simulation)

Fig. 41 (page after next): Tooth-tooth-contact diagram for *Monodelphis* showing the size of the contact area for each lower molar facet during a certain time step throughout the chewing stroke from first to last contact of the molars. *Monodelphis* has a bi-phased power stroke very similar to that of *Didelphis*, with a mesio-lingual upward movement of the lower molars into centric occlusion (phase 1) followed by a lingual downward movement (phase 2). (lower molar model: m2 of ZMB MAM 35496; green facet 3, red facet 4, and violet facet 6 are not in contact in this OFA simulation)

Fig. 38

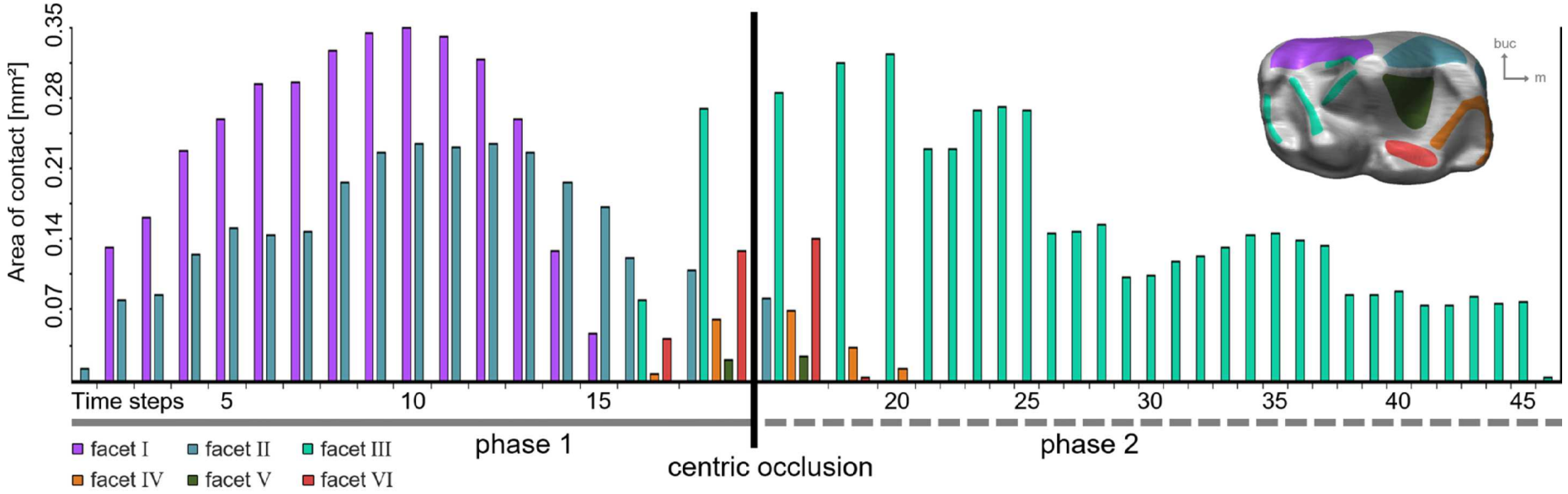
Area of contact [mm²]
0.07
0.14
0.21
0.28
0.35
Time steps
5
10
15
20
25
30
35
40
45
phase 1
phase 2
centric occlusion
facet I
facet II
facet III
facet IV
facet V
facet VI
buc
m

Fig. 39

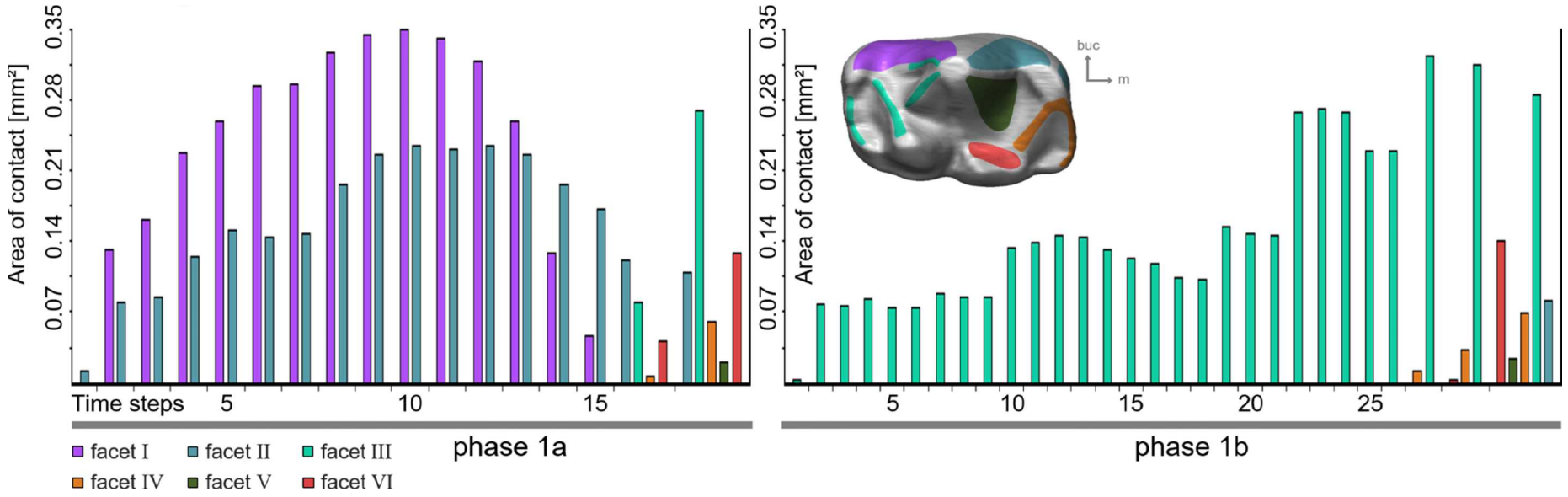
Area of contact [mm²]
0.07
0.14
0.21
0.28
0.35
Time steps
5
10
15
20
25
phase 1a
phase 1b
facet I
facet II
facet III
facet IV
facet V
facet VI
buc
m

Fig. 40

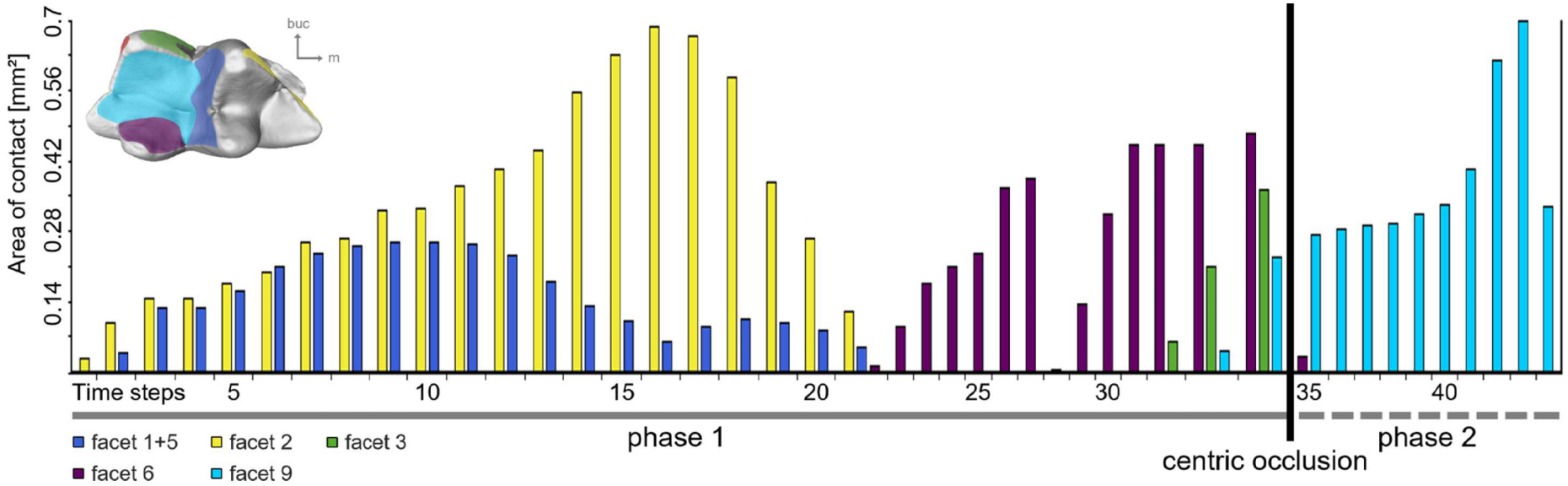
buc
m
Area of contact [mm²]
0.14
0.28
0.42
0.56
0.7
Time steps
5
10
15
20
25
30
35
40
phase 1
phase 2
centric occlusion
facet 1+5
facet 2
facet 3
facet 6
facet 9

Fig. 41

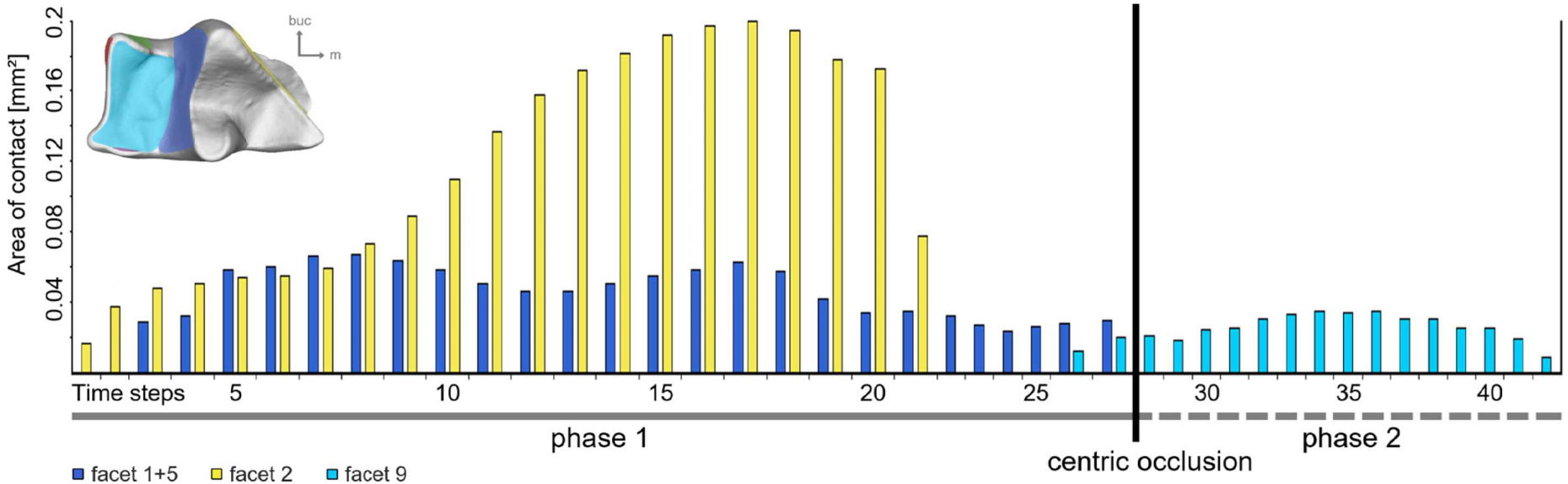
buc
m
Area of contact [mm²]
0.04
0.08
0.12
0.16
0.2
Time steps
5
10
15
20
25
30
35
40
phase 1
phase 2
centric occlusion
facet 1+5
facet 2
facet 9

6 Discussion

6.1 Location of basins and “pseudoprotocone” on docodont molars

6.1.1 Location of basins on the lower molars

The location of the docodont “pseudotalonid basin” has been the subject of discussion for a long time. Most authors locate it in between cusps a, b, and g. In this case, its margin is formed by crest a-b at the buccal, crest a-g at the distal, and crest b-g at the mesial side (Kermack et al. 1987, Sigogneau-Russell 2003, Martin and Averianov 2004, Pfretzschner et al. 2005, Averianov et al. 2010). However, other authors like Jenkins (1969), Krusat (1980) and Meng et al. (2015: Supplementary Materials) locate the “pseudotalonid basin” in between cusps a, b, and c (= g in Krusat 1980!) with crests a-b, a-c, and b-c building the boundary.

On various isolated lower molars of *Haldanodon* included in this study, striations were only observed in between cusps a, b, and g, as suggested by the majority of authors. Cusp c is clearly not part of the boundary of the “pseudotalonid basin” in this taxon. The basin is not closed but opens in mesio-lingual and distal direction, because crests a-g and b-g are not very distinctive. This is why some authors do not consider it a basin at all and therefore postulate that *Haldanodon* did not possess a “pseudotalonid basin” (Kermack et al. 1987, Pfretzschner et al. 2005, Averianov and Lopatin 2006). However, this study does not follow this opinion, because a small depression can be observed in between the cusps of unworn and slightly worn molars. Furthermore, a small amount of grinding does take place within this region as long as cusp g is not completely worn down (see 6.4.6).

In some of the other docodont taxa, additionally cusp e is included into the “pseudotalonid”. In that case crest b-g is not developed and the mesial margin is bordered by crest b-e, the lingual margin by crest g-e (Maschenko et al. 2002, Martin and Averianov 2004, Pfretzschner et al. 2005, Hu et al. 2007, Luo and Martin 2007, Lopatin et al. 2009, Averianov et al. 2010, Meng et al. 2015: Supplementary Materials). This is why the “pseudotalonid” of these taxa sometimes is considered to be convergent to that of the other docodonts (see also 2.3.1).

There are many authors who assume that docodonts actually had two basins on the lower molars – a mesial and a distal one, the latter often referred to as “talonid” (Jenkins 1969, Krusat 1980, Pascual et al. 2000, Sigogneau-Russell 2003, Ji et al. 2006, Hu et al. 2007, Luo and Martin 2007, Averianov et al. 2010, Meng et al. 2015: Supplementary Materials, Wang and Li 2016). Some of these authors see both basins as half-basins, which combined between two adjacent molars function as a large “intermolar” crushing basin (Jenkins 1969, Krusat 1980, Pascual et

al. 2000). There are also some authors like Tatarinov (1994) and Pfretzschner et al. (2005) who consider the tegotheriids to be the only taxa with two basins on the lower molars. In all cases the distal basin is placed in between cusps a, c, and d (Jenkins 1969, Averianov et al. 2010), a few authors also add cusp df to the borderline (Krusat 1980, Hu et al. 2007, Luo and Martin 2007).

In this study, at least *Haldanodon* is not considered to possess a distal basin as defined above. The structure in between cusps a, c, and d is not regarded as a basin, because it is continuously sloping down towards the disto-buccal rim of the molar and therefore closer resembles a groove. A basin in between cusps a, c, d, and df as postulated by Krusat (1980) explicitly for *Haldanodon* would be disrupted by crest c-d. The only distal structure that might resemble a very small basin is that in between cusps c, d, and df with crests c-d and d-df building the margin. Since it is rather small and clearly offset from the following lower molar, it should not be seen as part of an intermolar basin.

However, this does not exclude the existence of a distal basin in between cusps a, c, d, and df in other docodont taxa (see also 6.4.7). In *Docodon* and *Simpsonodon*, for example, crest c-d is much weaker and crest a-d slightly better developed than in *Haldanodon*. Therefore, the distal part of their lower molars might be considered to form a broad, shallow, distally opening basin. In tegotheriids (*Tegotherium*, *Hutegotherium*, and *Sibirotherium*) crest c-d is absent and crest a-d is very well-developed. In their case, crests a-c, a-d, c-df, and d-df enclose an undoubtedly well-build distal basin.

6.1.2 Location of “pseudotrigon basin” and “pseudoprotocone” on the upper molars

The “pseudotrigon basin” is also referred to as “pseudotalon basin” by some authors (Averianov et al. 2010, Martin and Averianov 2010, Martin et al. 2010a). The arrangement of cusps enclosing the basin in the docodonts closer resembles that of the tribosphenic trigon (build by protocone, paracone and metacone) than the heel-like talon (build by the hypocone). This is why the term “pseudotrigon basin” is preferred in this study, although it is made up of four and not of three cusps.

In contrast to the location of the “pseudotalonid basin” on the lower molars, that of the “pseudotrigon basin” on the upper molars is not seen as very controversial. For all docodont taxa, the “pseudotrigon basin” is consistently specified throughout the literature as being situated in between cusps A and C at the buccal and cusps X and Y at the lingual border. The mesial border is built by crest A-X, the distal one by crest C-Y (Kermack et al. 1987,

Pfretzschner et al. 2005, Hu et al. 2007, Lopatin et al. 2009, Martin et al. 2010a). The only major point of discussion is whether *Haldanodon* possesses a "real" "pseudotrigon basin" since in this taxon it lacks a distinct crest C-Y and therefore opens in distal direction. This is why Pfretzschner et al. (2005) postulate that *Haldanodon* does not have a "pseudotrigon basin". However, in this study *Haldanodon* is considered to have a real basin, although rather shallow, since the lowest point is located somewhat mesial of the distal tooth rim and the slope of crest A-X does not just level off at the distal margin of the molar.

Much more controversial is the term "pseudoprotocone". Usually, it is referred to the lingually situated cusp X, because its position on the upper molar is similar to that of the tribosphenic protocone. This is also why it sometimes is regarded to interlock with the "pseudotalonid basin" and therefore to have the same grinding function (Hu et al. 2007, Luo 2007, Davis 2011, Rougier et al. 2014). However, the majority of authors do not consider it as functionally homologous to the protocone of the tribosphenids. According to them in centric occlusion cusp X actually rests mesio-lingually of the "pseudotalonid basin" and cusp Y is the one that occludes within the basin (Crompton and Jenkins 1968, Hopson and Crompton 1969, Jenkins 1969, Gingerich 1973, Kron 1979, Krusat 1980, Kermack et al. 1987, Butler 1988, Pfretzschner et al. 2005, Luo and Martin 2007). Kermack et al. (1987) therefore consider cusp Y and not cusp X as equivalent to the protocone. Nevertheless, in this study cusp X is labeled "pseudoprotocone" to prevent misunderstandings due to the much more common use of the term for this cusp. However, part of this study was also to reexamine whether the function this term implies is actually performed by this cusp, this time by virtually reconstructing the actual mastication movement (see 6.4).

6.2 Determination of position for isolated *Haldanodon* molars

According to other studies, the upper molar row of *Haldanodon* consists of up to five molars, whereof M5 is vestigial and lacks the distal half and with it the "pseudotrigon basin" (Kron 1979, Krusat 1980, Martin and Nowotny 2000, Luo and Martin 2007). However, none of the 16 upper jaw specimens included in this study possesses more than four molars, all of them fully developed. This indicates that M5 most likely erupted at a relatively late ontogenetic stage just as m5 and m6 of the lower molar row. This ontogenetic stage probably is not represented within the studied specimens because even in the much larger sample of 52 mandibles only half of the specimens possess m5 and only three specimens m6. However, in some of the upper jaw specimens the maxillary bone distal of M4 is not preserved, so it cannot be excluded that it

might have shown at least the alveoli of M5. In any case, since M5 is not present in the studied specimens, it has been excluded from further consideration.

The order of molar size in the upper molar row of *Haldanodon* determined in this study differs from that provided by Krusat (1980). According to this study M2 is always the largest molar followed by M3, M1 and M4, whereas according to him M4 should be larger than M1. The few specimens available for Krusat (1980) apparently were not preserved well enough to allow width measurements; therefore, he only measured the lengths of the molars. Considering only the means of the length measurements, M4 indeed is slightly longer than M1 (see appendix tab. 8). However, in this case the mean values are misleading since they derive from nine M1 but only five M4. In four upper molar row specimens both M1 and M4 are preserved – in two of them M4 actually is shorter. In one specimen M1 and M4 are equally long. Only in one of these four specimens M4 is actually longer than M1. However, in this last specimen M4 is also longer than M3, so it seems to be unusually large (unfortunately, the width of M1 and M3 of this specimen could not be measured for comparison). Since M4 is always considerably less wide than M1, in overall size M1 is always larger than M4 (fig. 8).

The order of molar size in lower molar rows reported by Krusat (1980) differs from that determined in this study as well. In this study m3 is the largest molar, followed by m2, m1, m4, m5, and m6 (fig. 11). According to Krusat (1980) m2 should be larger than m3. Most probably, he evaluated the order of size by the lengths of the molars. This would match the fact that although m3 is the largest molar in overall size, in more than half of the specimens' m2 is longer than m3. In most of these specimens this is compensated by the much greater width of m3 compared to m2. A similar case is the order of m1 and m4 since m1 is larger in overall size but in more than half of the specimens m4 is wider. This is compensated by the much greater length of m1 in comparison to m4.

Since teeth stop growing once they have erupted, the extreme size differences of the molar rows of almost two millimeters in between the smallest and largest row most probably reflects relatively high size differences in adult *Haldanodon* individuals. Most certainly, these differences are much too great to be explained by abrasion of the occlusal surface during ontogeny. Furthermore, some of the smallest tooth rows are only slightly worn and some of the larger ones heavily worn. This size variability was also observed by Krusat (1980) who found it particularly noticeable that some of the jawbones and teeth are up to one third larger in one specimen than in the other. Averianov and Lopatin (2006) as well as Lopatin et al. (2009) made the same observation in other docodont taxa and presume that possibly the range of individual and sex variation in docodonts was much greater than it is in extant mammals.

High individual size variability is also indicated by the observation that within the same molar row the order of size with very few exceptions is always the same (fig. 8 + 11) – while on the other hand the great range of length and width measurements within one molar position leads to a remarkable overlap of values in between different molar positions (fig. 9 + 12). Inclusion of measurements derived from less well-preserved molar rows indicate that a larger sample might further obliterate the differences between molar positions. Nevertheless, this also might be an effect of the more precarious measurements due to estimated molar contours or uncertain molar positions. Since it is impossible to determine whether an isolated molar originally comes from a large or a small tooth row, it is also impossible to confidently refer isolated molars to their former position in the dental row by simple length and width measurements (fig. 10 + 13). A distinction between buccal and lingual length as well as mesial and distal width might get better results. This probably better conveys visually observed shape differences, at least in lower molars: m1 and especially m2-m3 are broadest mesially at the “pseudotalonid” region, m4-m6 are mesially and distally more or less equally wide. However, this approach was not further pursued in this study.

The high independence of the size of the last molar positions (M4 and m5-m6) from the size of the preceding molars indicates that these positions are in the state of being reduced. This is further indicated by the tooth morphology of these molars. That of M4 and m4 can vary from fully developed cusps and basins to a reduced cusp number and almost nonexistent basins; m5 always shows a simpler tooth morphology, and m6 is rather knob-like (see also Krusat 1980, Luo and Martin 2007).

The original purpose to try to refer isolated molars to their former tooth positions had been to be able to also consider isolated material as models for the OFA analysis. For the lower molar model, the positions m2 and m3 were chosen, because they are the largest molars in the lower row with the best developed “pseudotalonid basin”. They both occlude with M2 (see 6.4.3), which is also the largest molar of the upper row with the largest “pseudotrigon basin”. Since it is not possible to confidently determine the former tooth position of isolated molars, models were chosen only from jaw specimens with reliably determinable tooth positions. The molar rows also were required to show a very low degree of wear so that the tooth morphology had not been altered by abrasion. Unfortunately, the sizes of the most suitable m2, m3 (Gui Mam 6/82) and the only suitable M2 (Gui Mam 30/79) do not match. The chosen m2 and m3 fall right within the average size of their respective tooth position, while the chosen M2 is significantly smaller than the average size. Therefore, the upper molar 3D-model had to be scaled to match that of the lower molar models. Since the average length of M2 more or less equals the average length of m2, even if comparing lowest and highest values, the length of the

M2 model of Gui Mam 30/79 was scaled to the same length as that of the m2 model of Gui Mam 6/82. Length and width ratios of upper and lower molar models then matched the observed ratios in between the respective molar positions (e.g. average width M2 ≥ average length m2 or m3, average length M2 ~ average length m2 or m3; see appendix tab. 10).

6.3 Wear patterns of *Haldanodon* molar rows

Haldanodon has a diphyodont tooth replacement with m1 erupting first, followed one by one by the more distal molars (Henkel and Krusat 1980, Krusat 1980, Martin and Nowotny 2000, Nowotny et al. 2001, Martin et al. 2010b). Since the tooth erupting first is exposed to wear from abrasion and attrition longer than the following teeth, molar rows should be mesially stronger worn. This is always the case in modern brachydont mammals: m1 is always slightly to considerably stronger worn than m2, which in turn is stronger worn than m3. The reversed case in which later erupted molars are stronger worn than earlier erupted ones is not known from any extant taxon. This is why the existence of distally stronger worn molar rows as observed for *Haldanodon* is unique, as was also noted by Krusat (1980).

Even more exceptional is the existence of both mesially and distally stronger worn molar rows within the same species (fig. 14 + 15), which is not yet described for any other extant or fossil mammalian taxon. Krusat (1980) did not mention that he also observed mesially stronger worn molar rows within the few specimens available for his study. Nevertheless, in this study including much more specimens this observation was not only made for the lower but also for the upper molar rows and therefore is certainly not an artifact of some kind. However, the difference in the ratio of mesially to distally stronger worn molar rows is great, with 75% of the upper but only 45% of the lower molar rows being mesially stronger worn. This is probably attributed to the smaller number of upper molar rows – more than twice as much lower molar rows were included in the study. Furthermore, most of the distally stronger worn molar rows are more or less heavily abraded and there are only very few strongly worn upper jaw specimens.

The degree of wear of the molar row is determined by the degree of wear of the least worn molar in this study, because this takes best into account the two opposing directions of increasing wear observed in this study. A specification by the degree of wear of a predetermined molar position, e.g. m2 / M2, is not suitable in this case since the results might be biased by whether the row has a mesially or distally increasing wear gradient. Additionally, a classification by the degree of wear of the least worn molar is more likely to reflect the

ontogenetic age of the specimen, which otherwise might be obscured by a high abrasion rate leading to a large wear gradient. A very good example is one of the juvenile specimens (Gui Mam 33/77) in which m1 is almost completely worn down but m4 has just erupted and therefore shows almost no signs of wear. Despite its undoubtedly young ontogenetic age, this specimen certainly would not be assigned to a low degree of wear, if evaluated by the wear of any of the preceding molars.

There is a remarkable correlation between direction of wear (mesially or distally stronger) and degree of wear (low, medium, high) (fig. 18). Molar rows with a low degree of wear are almost always mesially stronger worn (10/11 lower and 9/9 upper molar rows) whereas molar rows with a high degree of wear are almost always distally stronger worn (9/10 lower and 1/2 upper molar rows). Molar rows with a medium degree of wear are more often distally stronger worn (12/19 lower and 3/5 upper molar rows), but also frequently include mesially stronger worn specimens (7/19 lower and 2/5 upper molar rows). Since, as explained above, the degree of wear is an indicator for the ontogenetic age of the specimens, this implies a change of direction of wear during ontogeny from mesially stronger worn in young individuals to distally stronger worn in old individuals. Therefore, a molar row initially would be mesially stronger worn but with increasing age of the individual would become more and more distally stronger worn. Krusat (1980) might have come to a similar conclusion because the only specimen in his study that clearly is not distally stronger worn is a juvenile (VJ 1005-155). If this did not exceed his expectations, he might not have considered its direction of wear deviating from his observations made on the other specimens worth mentioning. In any case, the hypothesis of a change of direction of wear during ontogeny is supported by the fact that the other juvenile specimen (Gui Mam 33/77) added in this study also is mesially stronger worn regardless of the high degree of its overall wear. Additionally, the only exception of a lower jaw specimen being distally stronger worn despite its low degree of wear (Gui Mam 7/74) possesses five molars and therefore must have been older than suggested by its wear (since m5 and m6 erupt at a relatively late ontogenetic stage). All other lower molar rows with five or six molars have at least a medium degree of wear.

This change in the direction of wear might be explained by a distal shift of the chewing focus in interaction with a relatively thin enamel layer and highly abrasive food. A distally situated chewing focus (as also postulated by Krusat (1980) to explain his observations) would cause the last molar at a time to be subject of the strongest abrasion. Since the enamel of docodont teeth is relatively thin, this molar would “pass” the degree of wear of the previous one over time if the abrasion rate was high enough. This is also why a large gradient is only found within molar rows with a low or sometimes also medium degree of wear. The majority of these

specimens is mesially stronger worn. Since it takes time for the distal molars to "pass" the wear of the mesial ones, which are also further abraded at the same time, the wear gradient in a distally stronger worn molar row cannot easily get large. A distally situated chewing focus is also indicated by the fact that the premolars are not very heavily worn even in specimens with strongly worn molars as also noted by Krusat (1980).

Abrasion rates indeed must have been very high in *Haldanodon* dentitions. This is not only shown by many teeth and tooth rows worn down to small stumps but also by traces of beginning abrasion on molars that are not fully erupted and therefore have not yet contacted their antagonists (Krusat 1980). Since *Haldanodon* presumably was a semiaquatic borrower that searched for worms and insect larvae, the sediment particles taken in together with its prey most likely caused this high abrasion (Martin 2000, Martin and Nowotny 2000). The degree of overall wear and therefore the time in which the teeth were worn down seems to vary highly between different individuals. In the juvenile specimen mentioned above (Gui Mam 33/77), for example, m1 and m2 are already more heavily worn than in most of the adult specimens although p3 is just beginning to erupt. In contrast to that, one of the lower jaw specimens with five molars is only slightly worn (Gui Mam 7/74). More generally said, a large gradient in the molar row also indicates an exceptionally high abrasion rate and a small gradient indicates a comparatively low abrasion rate. In upper molar rows, another indicator for significantly varying abrasion rates in between individuals are the two different abrasion patterns of crest X-Y (fig. 19). A flatly worn crest suggests that abrasion dominated over attrition, a sharp crest that in contrast attrition dominated over abrasion. However, this contradicting abrasion pattern might also be attributed to individual differences concerning the occlusion of upper and lower molars. Anyway, the highly varying abrasion rates might be caused by the preference of different food sources or a different substrate in which the individual searched for food. That could represent either individual preferences or different populations.

A change of the direction of wear from mesially stronger worn to distally stronger worn molar rows during ontogeny might have been unique for *Haldanodon* even among docodonts. Other docodont taxa do not seem to show this pattern. At least, for none of the docodonts other than *Haldanodon* unusual wear patterns were reported. According to Sigogneau-Russell (2003), in *Borealestes* the molar row of the type jaw (m1-m4) shows the regular abrasion pattern, that is wear increases in mesial direction. Since the molar row seems to be only slightly worn (Waldman and Savage 1972: fig. 2), a mesially increasing wear gradient indeed is to be expected in any case. However, Kermack et al. (1987) also observed the regular abrasion pattern in *Simpsonodon*, although the molars of the at that time only preserved lower jaw fragment (m1-m2) are rather heavily worn (see also Kermack et al 1987: fig. 11). According to Hu et al.

(2007), in all docodont taxa the degree of wear of the molar rows decreases from mesial to distal. They postulate a mesially situated chewing focus, which they believe is why mesial molars are worn down faster. This clearly contradicts the observations on *Haldanodon* molar rows made in this study. Since it is probable that *Haldanodon* was not the only docodont taxon having a distally situated chewing focus, it is more likely that the front molars just had been in use longer than the following molars due to their earlier eruption. This would furthermore indicate that molars covered by a relatively thin enamel layer indeed are not the only factor necessary to cause a change of the direction of wear in a molar row during ontogeny. It also requires exceptionally high abrasion rates like those found in *Haldanodon*, which are very high even compared to other docodont molars.

6.4 Reconstruction of the mastication cycle of *Haldanodon*

6.4.1 Previous studies on various docodont taxa

Concerning the occlusion and function of docodont molars, some studies have been conducted throughout the last century. Simpson (1929, 1933, 1936) was the first one to note the "peculiar and highly modified morphology" of docodont molars. He was also the first to illustrate upper and lower docodont molars in occlusion, based on two different specimens of *Docodon*, the only known taxon at that time (Simpson 1929: fig. 27). In his model of occlusion both the "pseudoprotocone" as well as the accessory cusp Y were occluding within the distal "talonid" basin of the lower molar. The broad mesial cingulum contacted the "pseudotalonid" of the same lower molar. Therefore, cusp d was the cusp occluding within the "pseudotrigon basin", and cusp b pounded into the gap in between the upper molars. From Simpson's point of view, the molars of *Docodon* were not capable of efficient shear-cutting due to the lack of obvious shearing crests. He suggested they primarily performed a crushing function, because of their more or less well-developed basins. Nevertheless, he labeled it "a premature and ill-fated effort toward the production of broad-crowned crushing or grinding teeth from the more ancient piercing insectivorous type" (Simpson 1929: p. 85).

Crompton and Jenkins (1968) were the first ones to conduct a more detailed study of occlusion in docodonts on *Docodon* and *Haldanodon*, including the matching of facets on upper and lower molars. They strictly opposed this hypothesis of a distinct crushing function as well as Simpson's model of occlusion of one upper with one single lower molar. Instead, they postulated that the upper molars of docodonts actually showed an alternating occlusion pattern

with the upper molars occluding in between the lower molars (Crompton and Jenkins 1968: fig. 7). In this model of occlusion, the mesial part of an upper molar contacts the distal part of a lower molar and the distal part of an upper molar contacts the mesial part of the following lower molar. To make this possible, according to Crompton and Jenkins (1968) in *Docodon* only the "pseudoprotocone" occluded within the distal basin. Since *Haldanodon* does not possess a distal basin, they probably actually meant the "pseudoprotocone" of this taxon to occlude in between the lower molars instead. However, this did not become quite clear, because in contrast to the extent of the facets they did neither figure nor describe the occlusion in detail. In any case, according to the facets, in both taxa cusp Y was the cusp that contacted the "pseudotalonid basin" of the following lower molar. Furthermore, cusp b of this lower molar occluded within the "pseudotrigon basin" and not in between two upper molars (Crompton and Jenkins 1968: fig. 7). In contrast to Simpson (1929), Crompton and Jenkins (1968) regarded the complex tooth morphology of the docodonts as an attempt to increase shear-cutting surfaces with the development of additional crests. They did not mention crushing or grinding, but Jenkins (1969) later admitted a minor crushing function taking place on the interiors of the lower molars. Crompton and Jenkins (1968) also noted that at least in *Docodon* the mesial facets of the lower molars could not have been in contact with their antagonists on the upper molars at the same time as the distal facets. They regarded this as evidence of a mesio-distal motion component during jaw closure and therefore postulated a complex masticatory movement, which they did not specify any further.

This was taken up by Jenkins (1969) in his detailed study on the occlusion of *Docodon* molars. He was the first to illustrate the postulated movement of the lower molars during mastication. For this, he did not only figure the stage of centric occlusion from different views but also the stage when the lower molars are just getting into contact (Jenkins 1969: fig. 4). He described the masticatory movement as a primarily orthal chewing stroke with a small amount of mesio-distal movement, ending in centric occlusion. In his illustration, he depicted the mesio-distal component as a proal motion (Jenkins 1969: fig. 4A-D).

Additionally to this upward and proal shear-cutting movement, a second phase was proposed by Gingerich (1973) in his review of Jenkins study. He based this on the observation of opposing orientations of striae on the *Docodon* lower molars. In his opinion, these indicated an independent upward and palinal movement into centric occlusion (Gingerich 1973: fig. 2). According to him, a downward proal movement would not have made sense from a functional point of view. An upward movement in distal direction on the other hand could have been used to puncture and separate large pieces of food. Gingerich (1973) shared the view of the previous

authors that shear-cutting was the main function of the docodont dentition. Nevertheless, he also admitted a very limited amount of grinding at the end of the shear-cutting stroke.

The statement that docodonts mainly relied on shear-cutting to break up their food was relativized by Kron (1979) and Krusat (1980). They pointed out that even though that might have been the case in younger individuals, due to abrasion and the resulting lack of cusps and crests older individuals only were able to perform simple crushing and grinding. Krusat (1980) in his detailed study about the dentition and skull of *Haldanodon* also emphasized that the crushing function in docodont molars was generally much more important than suggested by previous studies. He even postulated a more or less well-developed grinding function performed by cusp b within the "pseudotrigon basin" and by cusp Y within the "pseudotalonid basin". This conclusion was supported by Kermack et al. (1987) in their description of a new docodont taxon, *Simpsonodon*, which shows extensive wear in its very well-developed "pseudotalonid" and "pseudotrigon basins". Both studies placed the "pseudoprotocone" within the gap in between two lower molars in centric occlusion (Krusat 1980: fig. 29, Kermack et al. 1987: fig. 45), therefore not considering it to play a significant role in molar functions. Concerning the mastication movement, Krusat (1980) was convinced the facet positions in *Haldanodon* rather suggested that the mesio-distal movement postulated by Jenkins (1969) and Gingerich (1973) was only a minor component of a mainly lingually directed, lateral movement.

Butler (1988) came to the same conclusion by reanalyzing the positions of the facets found on *Docodon* molars by Jenkins (1969). In his opinion, the mesio-distal motion component had been a palinal one. He furthermore postulated that the lateral movement had not ended in centric occlusion but had continued in a second phase (Butler 1988: fig. 2). He did not believe in the possibility of two distinct upward movements as suggested by Gingerich (1973). Instead, he assumed that the downward movement was mainly used to carry the food towards the tongue. Additionally, at its beginning, the distally situated crests of the lower molar might have ground against the mesial surface of cusp X. This would imply that there actually were two crushing areas on the lower molar, one on the distal end and one within the "pseudotalonid basin". Therefore, according to Butler (1988) in docodonts crushing had been at least as important as shear-cutting, particularly since he regarded the crests as not sharp enough for effective shear-cutting.

Pfretzschner et al. (2005) were the first to actually reconstruct the masticatory movement of docodont molars in a biomechanical experiment. For this, they mounted an epoxy cast of a lower molar on a micromanipulator and manually let it occlude with the cast of an upper molar fixed on a metal axis. The resulting movement was studied under a stereomicroscope. Pfretzschner et al. (2005) had assigned both molars used for this study to *Dsungarodon*, but the

upper molar was later reassigned to *Tegotherium* by Martin et al. (2010a). Pfretzschner et al. (2005) did not only describe their concept of occlusion in detail but also figured several distinct stages of the power stroke (Pfretzschner et al. 2005: fig. 5). A video of the resulting movement is also available upon request (T. Martin, personal comment 2018). In any case, the authors proceeded from the assumption of a two-phased chewing stroke, similar to that postulated by Butler (1988). The first phase was a lateral movement in which the buccal sides of the lower molars moved along the buccal cusps of the upper molar in a shear-cutting motion. At the same time cusp b conducted a crushing function within the "pseudotrigon basin". It also might have been a grinding function, if cusp a indeed had been much lower than in *Haldanodon*. This cusp is broken off in the at that time only available lower molar specimen of *Dsungarodon*. Unlike Krusat (1980), Pfretzschner et al. (2005) did not believe that a grinding function could have been conducted within the "pseudotrigon basin" of *Haldanodon*, because cusp b was actually not large enough to reach it. In any case, according to Pfretzschner et al. (2005), crushing also took place in between the lingual flank of cusp b and the buccal flanks of cusps X and Y. As postulated in previous studies, in centric occlusion cusp Y occluded within the "pseudotalonid basin" and cusp b within the "pseudotrigon basin". The "pseudoprotocone" cusp X, however, according to them did neither occlude right in between the lower molars nor did it contact the distal half of the more mesially situated molar. Instead, Pfretzschner et al. (2005) assumed that at least in *Dsungarodon* it occluded at the lower end of a deep and well-developed groove in between crests b-g and b-e mesial of the "pseudotalonid basin". In the second phase, a continuation of the lateral movement in downward direction, cusp X was guided along the groove, conducting a grinding function. This movement of cusp X along the groove prevented any proal or palinal motion component. At the same time, grinding also occurred when cusp b slid along the buccal flanks of cusps X and Y as well as when crest A-X moved along the distal end of the mesial lower molar.

The most recent study was conducted by Schultz et al. (2017). They re-examined the various postulated mastication movements for *Docodon* from previous studies, mainly Jenkins (1969) and Gingerich (1973). They virtually simulated the resulting chewing cycles using 3D-models derived from µCT scans and an updated version of the OFA, which is also capable of simulating the rotation of the lower molars during mastication around the long axis of the mandible. The applied lower molar models derive from m3-m5 of two different specimens and had to be slightly matched in size to each fit the upper molar model derived from M3-M4 of a third specimen. Additionally to the detailed description in the text they also provided several illustrations and a video of the reconstructed mastication movements (Schultz et al. 2017: figs. 12-14, Supplementary Information Video S2). Schultz et al. (2017) actually interpreted Jenkins

(1969) hypothesis as bi-phased. The resulting chewing stroke began with a steep proal upward movement into centric occlusion followed by a less steep lateral downward movement towards lingual with a distinct palinal motion component. The lateral component of the downward motion had to be much more distinct than originally postulated by Jenkins (1969) in order for the molars to stay in contact during the downward movement. However, a mere orthal opening of the jaw like it might have been originally intended by Jenkins (1969) would not have produced any lingual contacts at all. The bi-phased scenario, on the other hand, required a change of direction of the lower molar movement in an unrealistic sharp angle compared to recent mammals (Schultz et al. 2017: fig. 12). Furthermore, the contact areas displayed by the OFA were much smaller than the actually observed sizes of the facets they represented. As opposing hypothesis, Schultz et al. (2017) chose Gingerich's (1973) proposal for an independent steep palinal and slightly lateral upward movement into centric occlusion. They interpreted this chewing cycle as bi-phased as well and added a continuation as a shallower lateral downward movement with a distinct palinal component. The change of direction in between the first and the second phase was rather moderately angled and therefore much more probable than that required for Jenkins' hypothesis (Schultz et al. 2017: fig. 12). Furthermore, according to the OFA analysis the total contact area was distinctly larger than for the Jenkins scenario. This is why Schultz et al. (2017) strongly supported Gingerich's (1973) hypothesis for a palinal orientation of the chewing stroke in *Docodon*. However, they also postulated that a disto-lingual mastication movement probably was a derived functional feature for the *Docodon-Haldanodon* clade and not necessarily applicable to other docodont taxa.

6.4.2 Position of facets on molars

There are two previous studies, which explicitly deal with the position of facets on *Haldanodon* molars: Hopson and Crompton (1969) and Krusat (1980). Thereof, Hopson and Crompton (1969) adopt the facets from Crompton and Jenkins (1968). They showed the hypothetical development of tooth morphology and correlated wear facets from *Eozostrodon*, a morganucodontid and at that time postulated ancestor of docodonts, to *Docodon*. To demonstrate this progress, they introduced a hypothetical intermediate stage, which they claimed to be partially based on *Haldanodon*. Hopson and Crompton (1969) directly assign this hypothetical stage to *Haldanodon* and adopt the figure, only simplifying the pattern of the facets.

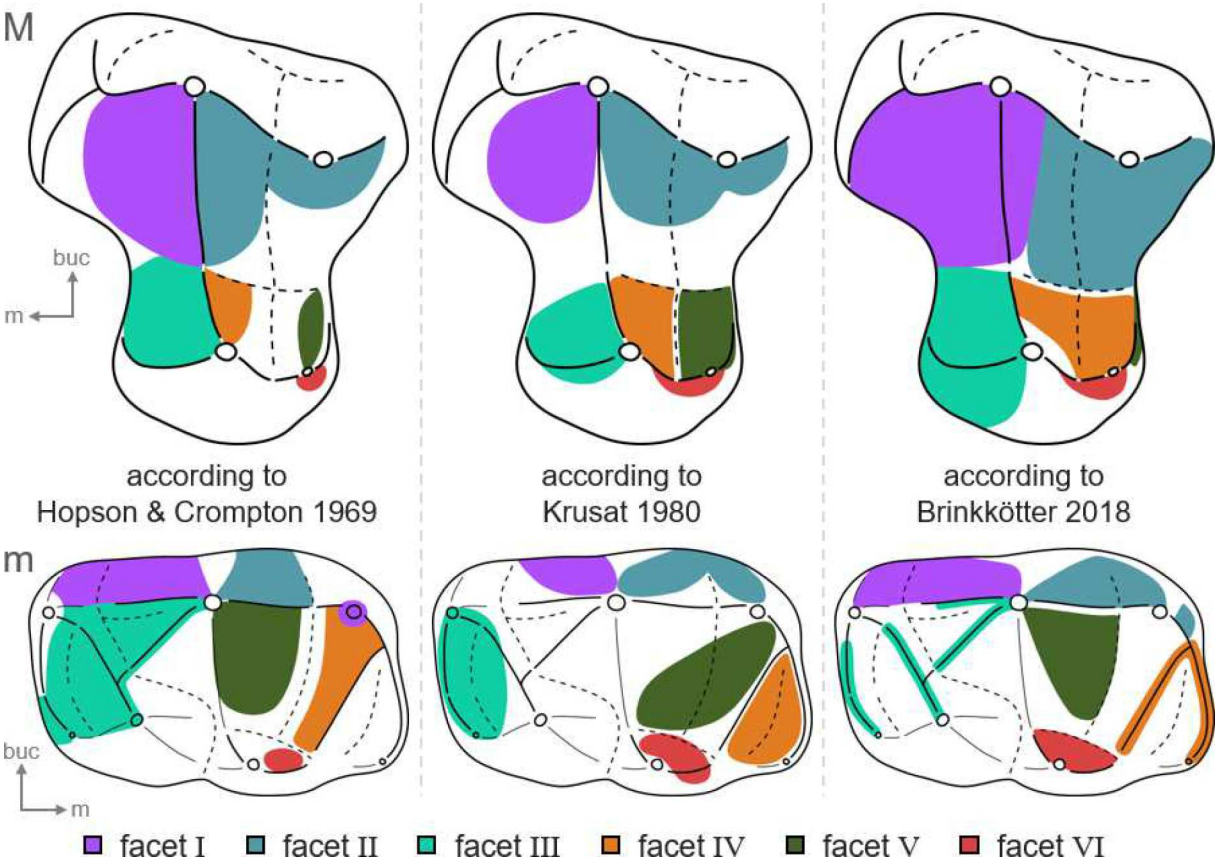

Fig. 42: Comparison of facet positions on *Haldanodon* molars as postulated by Hopson and Crompton (1969) (left), Krusat (1980) (middle), and the present study (right). For better comparison facet positions were conferred from the original figures to a unified molar draft (occlusal view). According to the present study upper facet I also includes the disto-lingual flank of cusp A and stretches onto the buccal part of the mesial cingulum, upper facet II also stretches onto the buccal part of the distal cingulum, and upper facet V is restricted to the lingual part of the distal cingulum. Lower facets I and II also include the buccal grooves, lower facet III is restricted to the distal crests and lower facet IV to the mesial ones.

Hopson and Crompton (1969) as well as Krusat (1980) locate facet I (= facet 2 in Crompton and Jenkins 1968) of the upper molar on the mesio-lingual flank of cusp A. According to them, it does not include the mesial cingulum. However, in this study the buccal part of the mesial cingulum of many upper molar specimens shows a distinctly polished enamel surface. Therefore, facet I does not only cover the mesio-lingual flank of cusp A but certainly also extends onto the cingulum. Unlike depicted in the earlier studies, it also passes crest A-X to include the disto-lingual flank of cusp A as well. That this part actually belongs to facet I and not facet II situated immediately next to it is mainly indicated by the occlusion pattern inferred from the positions of the other facets and the tooth morphology (see 6.4.3). The matching facet I on the lower molar is differently located by Hopson and Crompton (1969) and Krusat (1980). According to Krusat (1980) it only covers the disto-buccal flank of main cusp a down to the buccal tooth rim. According to Hopson and Crompton (1969), it also covers a large part of the mesio-buccal flank of cusp d, although it does not reach the apex of the cusp. This is much

closer to the location of facet I observed in this study, the only difference being that it does reach the apex of cusp d. In any case, facet I definitely extends throughout the groove in between cusps a and d as indicated by corresponding polished surfaces and striations on all but the least worn lower molar specimens.

According to Hopson and Crompton (1969) and Krusat (1980), facet II of the upper molar (= facet 3, 4) also is situated on the lingual flank of cusp C but additionally covers the disto-lingual flank of cusp A. However, as mentioned above, in this study the facet on the disto-lingual flank of cusp A is mostly part of facet I. In both earlier studies facet II does not reach far into the "pseudotrigon basin" and does not cover the distal cingulum. Nevertheless, parallel striations within the "pseudotrigon basin" and on the distal cingulum clearly indicate the presence of a facet on these parts of the molar. Additionally, even slightly worn molars show a distinct polishing of the distal cingulum. Facet II on the lower molar (= facet 1) is not divided into two separate parts in both other studies. Hopson and Crompton (1969) locate it only on the mesio-buccal flank of cusp a and extend it down to the buccal tooth rim. Krusat (1980) additionally includes the buccal flank of cusp b, but explicitly excludes the groove in between the cusps. Instead, he joins the two parts of the facet halfway down to the buccal tooth rim. However, within the groove most of the striations belonging to facet II could be observed in this study.

Both other studies, too, locate facet III (= facet 5) of the upper molar on the mesio-buccal flank of cusp X (also called the "pseudoprotocone"). According to Krusat (1980), it passes around the mesio-lingual flank of cusp X, which is exactly how it could be observed in this study. The location of the matching facet III on the lower molar, however, is entirely differently specified in the earlier studies. Both studies do not divide this facet into four separate parts, which only cover the distal crests. According to Hopson and Crompton (1969), facet III covers the entire area in between cusps a and d at the buccal and cusps c and df at the lingual side. The apices of cusps c and df are also included into the facet while those of cusps a and d are not. Only the lingual part of crest d-df is included into the facet. According to Krusat (1980), by contrast, facet III only covers all of crest d-df including the apices of the cusps as well as the distal half of crest c-d. Striations and abrasion marks, however, clearly show that attrition is limited to the crests and does not include the areas in between them or the tips of the cusps. Otherwise the distal half of the lower molar would have had to be worn flat, which was only observed for very heavily worn lower molar specimens.

Facet IV (= facet 6) of the upper molar is located on the disto-buccal flank of cusp X in the previous studies as well. The only difference is that it does not reach as far down into the "pseudotrigon basin"; in Hopson and Crompton (1969) it is a relatively small facet directly below the buccal part of crest A-X. On the lower molar the differences for the location of facet

IV are much greater. Hopson and Crompton (1969) locate it on the lingual flank of cusp b, extending from the apex to the bottom of the "pseudotalonid basin"; with this, it is covering the mesio-buccal side of the basin. Krusat (1980), in contrast, locates facet IV mesio-lingually of the "pseudotalonid basin" in between crests b-e and b-g. This is closer to the position of facet IV observed in this study, which clearly is restricted to the crests b-e and b-g: Striations are only present on these crests and not in the area in between them or within the "pseudotalonid basin".

Hopson and Crompton (1969) locate facet V (= facet 7) of the upper molar on the buccal flank of cusp Y, extending it into the "pseudotrigon basin" but not onto the distal cingulum. Krusat (1980) at least additionally includes the lingual part of the distal cingulum, although unlike this study he does not restrict the facet to it. However, striations found within the "pseudotrigon basin" can all be referred to facet IV. Additionally, facet V on the cingulum has a distinctly different angle than facet IV and therefore both are always separated by a sharp edge. On the lower molar, Hopson and Crompton (1969) locate facet V on the mesio-lingual flank of cusp a as well. Krusat (1980), in contrast, locates facet V on the lingual flank of cusp b, covering most of the "pseudotalonid basin". However, in this study striations referable to facet V were observed neither on the lingual flank of cusp b nor within the "pseudotalonid basin".

Facet VI (= facet 8) of the upper molar is situated on the buccal flank of cusp Y directly below its apex in both previous studies as well. On the lower molar, both other studies like the present one locate facet VI on the buccal flank of cusp g, within the "pseudotalonid basin". According to Krusat (1980), it crosses the b-g crest and covers the mesio-lingual flank of cusp g as well. However, no striations or enamel polishing could be observed in this area of the lower molar.

A seventh facet like it apparently is present on *Docodon* molars on the lingual flank of cusp X, respectively the buccal flank of cusp c (Crompton and Jenkins 1968, Hopson and Crompton 1969) is not developed on *Haldanodon* molars.

Crompton and Jenkins (1968) as well as Hopson and Crompton (1969) additionally depict a facet located directly on top the apex of cusp b. Crompton and Jenkins (1968) originally intend it to contact the distal flank of cusp C of the upper molar (part of facet II). However, they do not explain the lower jaw movement required to enable such a contact. Hopson and Crompton (1969) instead match the facet on top of cusp b with the facet on the mesio-lingual flank of cusp A (facet I). However, this disagrees with the assumption that the mesial half of the upper molar contacts the distal half of the lower molar. Krusat (1980) regards this facet as an abrasion facet and discards it from further consideration. Since the tip of cusp b is not worn smooth and does not show any oriented striations, this study follows Krusat's opinion and does not regard the abrasion mark as a real facet.

In general, the present study observes the facets to be much more restricted to crests and grooves than it is the case in both earlier studies. Nevertheless, positions of the upper facets are quite similar in all of the studies (fig. 42). The more or less minor differences probably can be referred to individual variations on the respective specimens and the varying quantity of the studied material. The differences in facet position on the lower molar, however, are much greater, particularly concerning the "pseudotalonid basin". In the previous studies the positions of facets seem to be much more influenced by assumptions about how the lower molar might occlude with the upper molar than by actual observations. With the exception of facet IV and the abrasion facet on cusp b, this study generally agrees more with the positions given by Crompton and Jenkins (1968), respectively, Hopson and Crompton (1969). Facet IV is the only facet that better fits the facet scheme of Krusat (1980).

6.4.3 Occlusion of molar dentition

The observed facets on upper and lower molars and especially their tooth morphology can only be matched assuming that the upper molars occluded in between the lower molars (fig. 20 + 43). This is in accordance with previous studies on various docodont taxa, which all postulate an alternating occlusion pattern (Crompton and Jenkins 1968, Hopson and Crompton 1969, Jenkins 1969, Gingerich 1973, Krusat 1980, Kermack et al. 1987, Butler 1988, Sigogneau-Russell 2003, Pfretzschner et al. 2005, Schultz et al. 2017). Therefore, the mesial part of the upper molar contacted the distal part of a lower molar and the distal part of the upper molar contacted the mesial part of the following lower molar. As consequence, in *Haldanodon* M1 contacted the distal part of m1 and the mesial part of m2, M2 the distal part of m2 and the mesial part of m3, M3 the distal part of m3 and the mesial part of m4, M4 the distal part of m4 and the mesial part of m5, and M5 the distal part of m5 and the mesial part of m6, if any of the latter were present. In centric occlusion crest A-X of the upper molar rested more or less in between the lower molars. In *Haldanodon*, according to observations made in the present study, the only distal lower cusp that did not lie mesial of this crest is cusp d. This is the only difference to previous studies on the dentition of *Haldanodon* by Crompton and Jenkins (1968), Hopson and Crompton (1969) and Krusat (1980). These earlier studies place cusp d mesially of crest A-X in centric occlusion, which therefore rests precisely in between the lower molars. However, the contact between one lower molar and the following lower molar is not a straight line but slightly angled. Therefore, the distalmost cusp on the lingual side (df) is situated farther mesial than the distalmost cusp on the buccal side (d). Since crest A-X is straight, cusp d must have

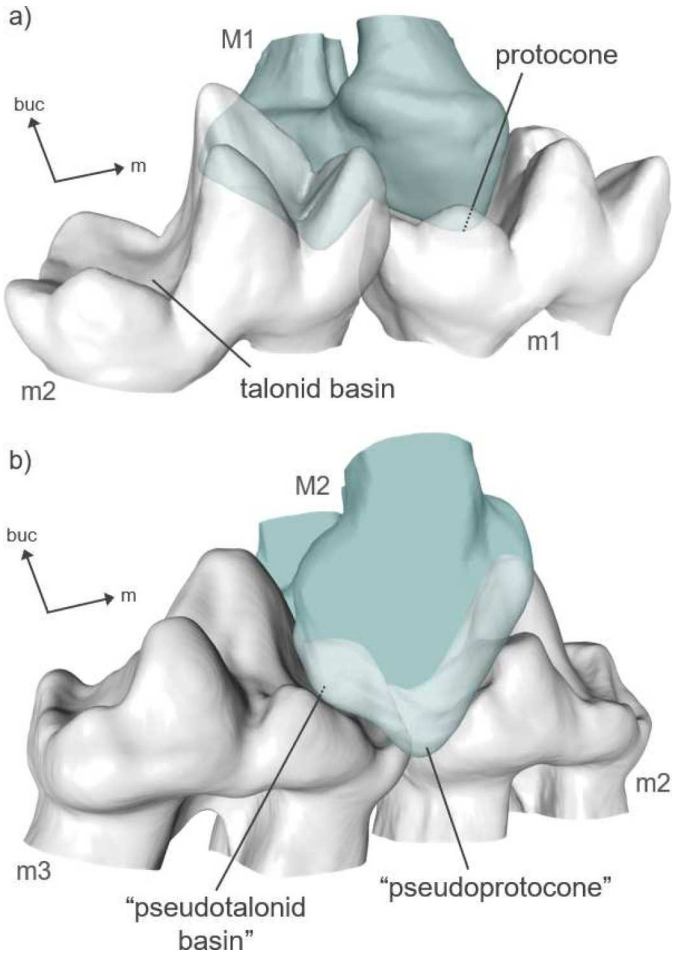

Fig. 43: Molars in centric occlusion. a) *Didelphis* (molar models: M1 and m1+m2 of SMF 77266). The upper molar occludes in between two lower molars with the protocone resting within the talonid basin. b) *Haldanodon* (upper molar model: M2 of Gui Mam 30/79, lower molar models: m2+m3 of Gui Mam 6/82). The upper molar occludes in between two lower molars with the "pseudoprotocone" resting mesio-lingually of the "pseudotalonid basin". Therefore, the "pseudoprotocone" of *Haldanodon* and other docodonts is not a functional homolog to the protocone of *Didelphis* and other tribosphenic taxa since it does not occlude within the "pseudotalonid basin". The cusp actually resting within this basin in centric occlusion is the more distally situated small cusp Y.

occluded distally of it. In any case, the upper molar is much broader distally of crest A-X than it is mesially of it. This is why the distal part of a lower molar was less overlapped than the mesial part of the following lower molar. Thereby the lingual flanks of the main cusps on the buccal half of the upper molar occluded the buccal sides of the lower molars. The lingual half of the upper molar contacted the interior of the lower molars. In this position, cusps a of the lower molars fitted exactly into the notch dividing the buccal and the lingual half of the upper molar on their respective sides.

An occlusion of the upper molar in between two lower molars implies that the "pseudoprotocone" (large cusp X) actually occluded mesio-lingually of the "pseudotalonid" and not within its basin (see also Krusat 1980, Kermack et al. 1987, Butler 1988, Sigogneau-Russell 2003, Pfretzschner et al. 2005) (fig. 43). This is also implied by the position of facet IV, which covers the disto-buccal flank of cusp X on the upper molar and crests b-g and b-e on the lower molar. These crests are situated mesially of the "pseudotalonid basin". Facet VI on the lingual flank of cusp Y and the lingual side of the "pseudotalonid basin" clearly indicates that the cusp actually occluding into the "pseudotalonid basin" was the more distally situated small cusp Y. This matches well with many of the previous studies on other docodont taxa (Crompton and Jenkins 1968, Hopson and Crompton 1969, Jenkins 1969, Gingerich 1973,

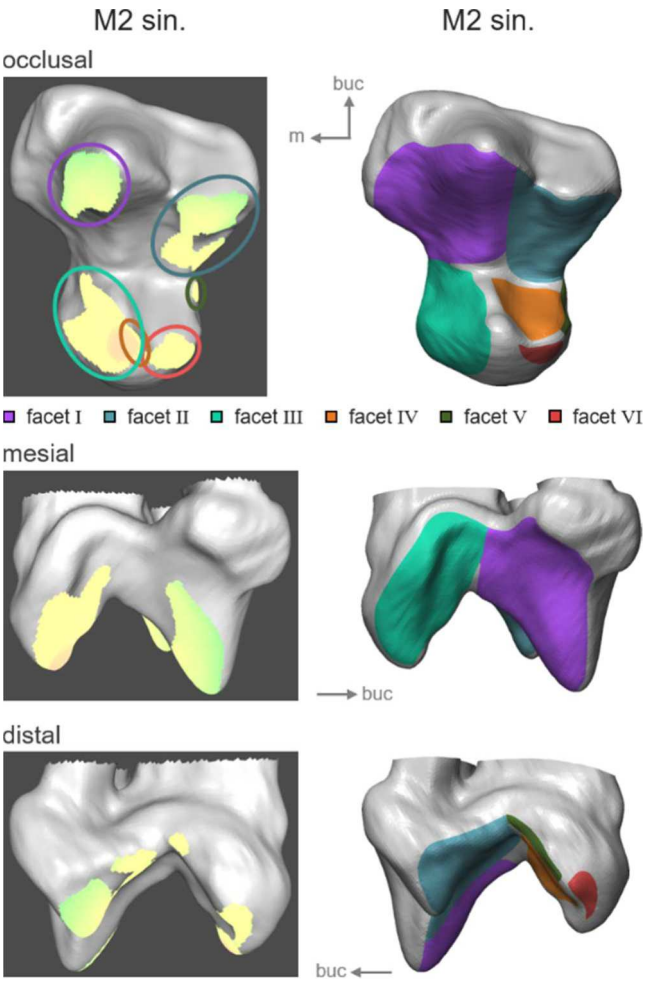

Fig. 44: Contact areas on the upper molar of *Haldanodon* as displayed by the OFA (left) in comparison to observed wear facet positions (right). Contact area size includes all time steps. In occlusal view contact areas are circled in the same color as the corresponding facets. Overlapping areas of different facets are not in contact simultaneously during the chewing stroke. (molar model: M2 of Gui Mam 30/79)

Kermack et al. 1987, Pfretzschner et al. 2005). For *Haldanodon*, the placement of facet VI is more or less the same in the earlier studies, leading to the same implication. However, neither Crompton and Jenkins (1968) nor Hopson and Crompton (1969) actually show the molars of *Haldanodon* in occlusion or give a detailed explanation in the text. Therefore, it remains uncertain whether they intend the "pseudoprotocone" cusp X to occlude within the "pseudotalonid basin" at any time of the chewing stroke. The corresponding placement of facet VI suggests that in centric occlusion cusp Y rested within the basin. However, the placement of facet IV on the disto-lingual flank of cusp b, which makes up one side of the "pseudotalonid basin", implies that they mean cusp X at least to pass by during occlusion. Contrary to that, Krusat (1980) clearly intends this cusp to have occluded in between two lower molars without passing through the "pseudotalonid basin": he places facet IV much more mesially on the lower molars than both previous studies. Therefore, the present study agrees more with his conclusion for the occlusion. That cusp X did not occlude within the "pseudotalonid basin" at any time of the chewing cycle is also indirectly suggested by facet II. It strongly indicates that cusp C occluded buccally in between cusps a and b. Since the "pseudotalonid basin" is situated lingually in between these cusps, it is unlikely that cusp X – which is situated more mesially in

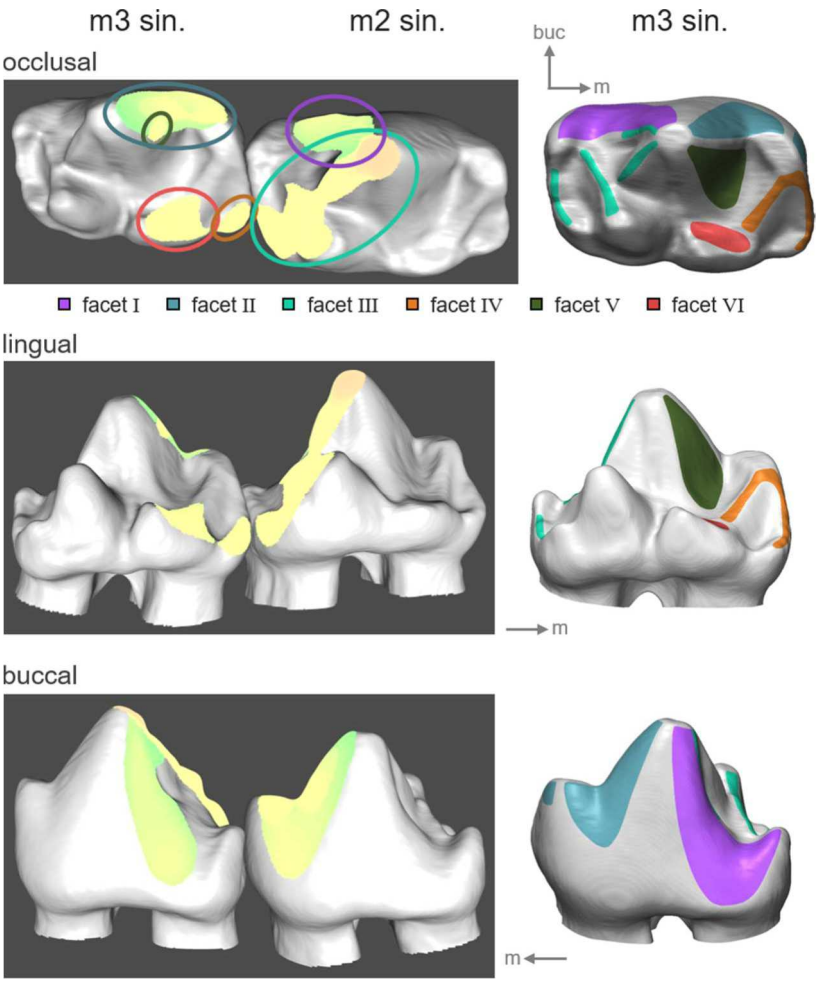

Fig. 45: Contact areas on the lower molars of *Haldanodon* as displayed by the OFA (left) in comparison to observed wear facet positions (right). Contact area size includes all time steps. In occlusal view contact areas are circled in the same color as the corresponding facets. Overlapping areas of different facets are not in contact simultaneously during the chewing stroke. (molar models: m2+m3 of Gui Mam 6/82)

relation to cusp C – occluded within this basin. Cusp Y, however, is situated directly opposite to cusp C.

Such an alternating occlusional pattern of an upper molar occluding in between two lower molars with cusp Y resting within the “pseudotalonid basin” is confirmed by the OFA analysis: The collisions detected between 3D-models of an upper and two lower molars mostly correspond to the observed facets (fig. 44 + 45).

The OFA analysis also revealed that main cusp a of the lower molar occluded well beyond the dental crown-root-boundary of the upper molar, thus creating a considerable “overbite” (fig. 43). This simulated over-occlusion most probably is not an artifact of inaccurate scaling that makes the upper molar model too small for the model of the lower molars, because according to the measurements the proportions of the models are matching (see 6.2). An over-occlusion also is a good explanation for the expansion of upper facet I onto the mesial cingulum and of upper facet II onto the distal cingulum. Since the cingula are situated not far above the crown-root-boundary of the upper molar, this would otherwise be impossible to such a great extent. Moreover, the presumption of an over-occlusion is supported by the presence of pits in the maxilla in between the upper molars (fig. 46). They most probably formed to compensate the overbite. Krusat (1980) only notes a deep pit in the maxilla in between the last precanine and

Fig. 46: Pits in the maxilla between adjacent upper molars (indicated by arrows). They compensate the "overbite" of the lower molars during centric occlusion in *Haldanodon* (depicted specimen: Gui Mam 18/80).

the canine, which received the lower canine. However, in their study about the cranio-mandibular anatomy of *Haldanodon* Lillegraven and Krusat (1991) also describe the presence of deep, rounded pits in the maxilla between adjacent upper molars and assume they served to take in the tall lower molar cusps. Moreover, similar pits in between the molars are commonly known from other early Mesozoic mammals, which did not yet develop a centric occlusion to stop the molars from over-occlusion (Hopson and Crompton 1969, Crompton 1974, Kermack et al. 1981, Gow 1986, Crompton 1995, Butler 1997, Schwermann 2015, Bi et al. 2016: Supplementary Information).

According to the OFA analysis, main cusp A of the upper molar likewise protruded beyond the dental crown-root-boundary of the lower molar. Indeed, facet I of the lower molar is developed right down to this boundary in many specimens. Additionally, the lower molars distinctly protrude beyond the buccal rim of the mandible on the lower jaw specimens. Therefore, an overbite of the upper molars on the buccal side of the lower molars should not have posed a problem, even though the mandible rim was covert with gums in the living animal.

6.4.4 Striation patterns on molars

Parallel running striae are an indicator for the orientation of the jaw movement during mastication (see 2.2.1). Therefore, the three different striation patterns observed on *Haldanodon* molars signal a change of direction in the mandible movement at least twice during the chewing stroke. This contradicts previous studies on other docodont taxa that assumed either a mere proal respectively palinal motion (Jenkins 1969, Gingerich 1973) or a mere lateral one (Krusat 1980, Butler 1988, Pfretzschner et al. 2005). A change of direction during the chewing motion furthermore makes a bi-phased power stroke very probable. This contrasts with many previous

studies as well, because they postulated a single chewing stroke ending in centric occlusion (Crompton and Jenkins 1968, Hopson and Crompton 1969, Jenkins 1969, Krusat 1980).

The presence of striae inclining in opposite directions towards either mesial or distal implies two phases for the power stroke (fig. 21). While both striation patterns were formed by either a proal movement (towards mesial) or a palinal movement (towards distal), they could not have formed at the same time. This leaves two possible explanations. On the one hand two separate upward power strokes ending in centric occlusion – one of them palinal and the other proal. On the other hand, a bi-phased power stroke with an upward movement towards either palinal or proal into centric occlusion followed by a downward movement in the same direction. The vertical striae suggest another change of direction into a lateral movement from buccal to lingual or the other way around. Since they are always associated with the distally inclining striae on the upper and the mesially inclining striae on the lower molar, they must have formed during the same phase as them (fig. 21). This means that only one of the proal or palinal movements was related to the lateral movement, because striations on matching facets of upper and lower molar incline in opposite directions: If the lower molar moves towards distal during jaw closure, striations on the upper molar deviate in distal direction while on the lower molar they deviate in mesial direction.

Facets I and II formed during the same movement, because they are the only facets on which vertical striae are present. This is also implied by their frequent fusion on the upper molar with striations continuing smoothly from one facet onto the other without even a slight change of orientation. That the movement of the lower jaw might have started out in a proal or palinal direction is suggested by the mesially inclining striae on the upper part of the usually dichotomous lower facet II-2. A predominantly palinal upward movement into centric occlusion also has been proposed by Schultz et al. (2017) for the entire *Docodon-Haldanodon* clade. However, in *Haldanodon* striations on lower facet I on the same height usually run vertical and rather imply a lateral movement without any proal or palinal motion component. This also matches the presence of vertical striae on the upper parts of upper facets I and II. A strictly lateral movement is also indicated by the likewise vertical striae on the lower part of lower facet II-2. Additionally, it is better supported by the tooth morphology since the mesio-buccal groove of the lower molar is straight and does not allow a considerable deviation from the lateral movement once it establishes contact with cusp C. An explanation for the presence of mesially inclining striae on the upper part of lower facet II-2 might be that this part does not contact the flank of cusp C but rather the distal cingulum. Its curvation and the very localized contact might lead to the formation of slightly inclined striae even though the movement was merely lateral. This would also explain the absence of matching distally inclining striae on the

upper part of upper facet II. The mesially inclining striae on lower facet I on the part situated beneath the disto-buccal groove, by contrast, most probably do indicate a rather abrupt change of direction into a more proal or palinal oriented movement. This is not only because their inclination is much more significant than that of striae on the upper part of lower facet II-2. Additionally, they seem to have distally inclining counterparts on upper facet I on the mesial flank of cusp A. A change of direction towards proal or palinal is also indicated by the distally inclining striae on upper facet II at the bases of the cusps. Only a very small area of lower facet II, probably at the very tip of cusp b, must have remained in contact to create these striae. All of this strongly suggests that a proal or palinal motion component was only added at the very end (or the very beginning) of a mainly lateral movement.

Facet III formed during a different proal or palinal movement since it shows the opposing striation pattern with mesially inclining striae on the upper and distally inclining striae on the lower molar. It probably also had a minor lateral motion component. This is indicated by the slight lingual orientation of striae on lower facet III. Furthermore, if it had been a mere proal or palinal movement, striae on upper facet III should run vertical in a 90° angle to the vertical striae on facets I and II.

Facet IV seems to have been in contact during both movements – the more lateral one indicated by facets I and II as well as the more proal or palinal one indicated by facet III. The almost horizontal, distally inclining striae on the mesial part of upper facet IV more or less match the mesially inclining striae on the mesial part of lower facet IV. Their orientation associates them with the proal or palinal phase of the lateral movement, although the inclination is not as steep as on facets I and II. The mesially inclining striae on the distal part of upper facet IV, however, must have formed at the same time as those on upper facet III since they run parallel. Matching distally inclining striae would be expected on the distal part of lower facet IV, which unfortunately does not show any striae on the examined lower molar specimens.

Fig. 47 (next page): Two possible ways of reconstructing the masticatory movement in *Haldanodon*. a) Reconstruction as a single power stroke with two phases separated by centric occlusion, lingual view. Phase 1 is a lingually directed upward movement of the lower molars into centric occlusion. Phase 2 is a distally and slightly lingually directed downward movement of the lower molars until loss of contact. This would be the first time in mammalian history that a bi-phased power stroke had been developed. b) Reconstruction as two separated, alternatively used power strokes ending in centric occlusion, lingual view. Phase 1a is a lingually directed upward movement of the lower molars into centric occlusion. Phase 1b is a mesially and slightly buccally directed upward movement of the lower molars into centric occlusion. Centric occlusion is followed by a simple downward jaw opening, resulting in immediate loss of contact. Two alternatively used power strokes are not yet known from any other extant or fossil mammalian taxon, which would make such a masticatory movement unique. (upper molar model: M2 of Gui Mam 30/79, lower molar models: m2+m3 of Gui Mam 6/82)

1: first contact, 2: halfway through the upward movement, 3: centric occlusion, 4: halfway through the downward movement, 5: last contact

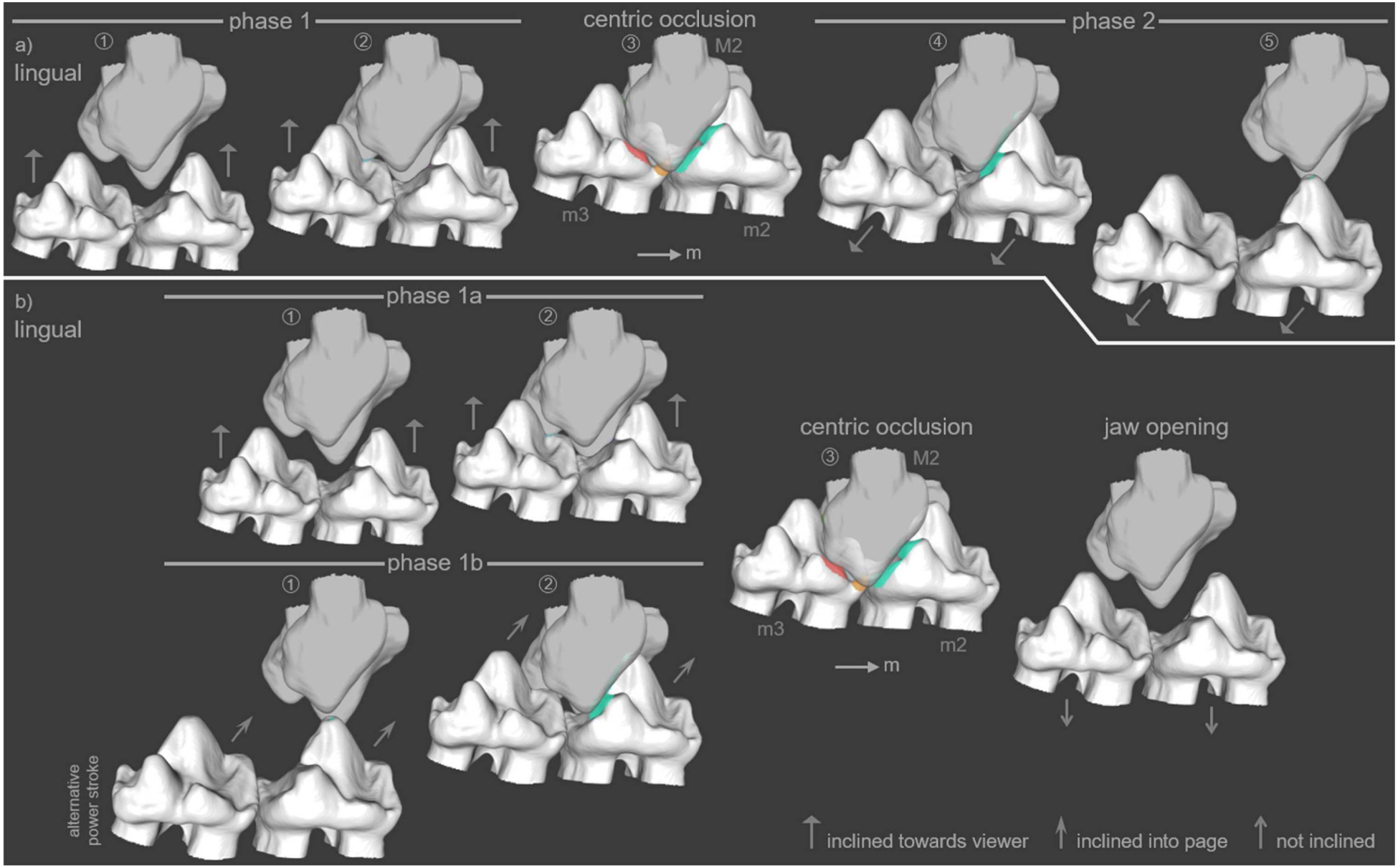
a)
lingual
phase 1
centric occlusion
phase 2
①
②
③
M2
④
⑤
m3
m2
m
b)
lingual
phase 1a
phase 1b
centric occlusion
jaw opening
alternative
power stroke
inclined towards viewer
inclined into page
not inclined

phase 1
centric occlusion
phase 2
a) occlusal
b) buccal
c) mesial
①
②
③
④
⑤
m2
m3
M2
m
buc
inclined towards viewer
inclined into page
not inclined

Fig. 48 (previous page): Masticatory movement of *Haldanodon* in a bi-phased scenario as seen from a) occlusal, b) buccal, and c) mesial view. Phase 1 is a lingually directed upward movement of the lower molars into centric occlusion. Phase 2 is a distally and slightly lingually directed downward movement of the lower molars until loss of contact. Holes in the upper molar model in occlusal view represent cut-off roots. (upper molar model: M2 of Gui Mam 30/79, lower molar models: m2+m3 of Gui Mam 6/82) 1: first contact, 2: halfway through the upward movement, 3: centric occlusion, 4: halfway through the downward movement, 5: last contact

This is probably because crest b-g confines the "pseudotalonid basin" and therefore is much more prone to interference by abrasion than crest b-e.

Facet V formed during the proal or palinal phase of the lateral movement because it does not only show the same striation pattern with distally inclining striae on upper facet V and mesially inclining ones on lower facet V. Moreover, on both upper and lower facet striae also clearly run parallel to those on the mesial part of facet IV, strongly suggesting that they all formed at the same time.

Facet VI formed during the proal or palinal phase of the lateral movement as well. This is indicated by the distal inclination of striae on upper facet VI which furthermore seems to be parallel to that of striae on the lower part of upper facet II. Lower facet VI probably does not show any striations at all because of its location within the "pseudotalonid basin" where abrasion is especially high. The undirected striae which are present all over the molars and often also interfere with the parallel striations on the facets are caused by abrasion (see 2.2.1). As explained in chapter 6.3, abrasion was very high for *Haldanodon* teeth. Therefore, it can even equal or surpass the attrition leading to the presence of many undirected striae unrelated to the direction of the mastication movement on the facets. That exposed dentine seldom shows any leading and trailing edges but usually is deeply scoured at all sides might also be the result of a high abrasion rate in combination with relatively thin enamel that is easily demolished. When attrition is more dominant, thin enamel probably is also the reason why dentin connects smoothly with it on all sides.

All in all, the striations observed on facets I and II indicate a mostly lateral movement of the lower jaw with a distinct proal or palinal motion component only at the beginning or the end of this movement. This proal or palinal motion component is also indicated by facets IV, V, and VI. Facet III and upper facet IV on the other hand indicate a mostly proal or palinal movement in an opposing direction with a slight lateral motion component.

Leading and trailing edges on many lower molar specimens with dentine exposed within the disto-buccal groove in between cusps a and d show that the lateral movement must have been directed upwards. This is because the leading edge always is situated above the trailing edge (fig. 35). Therefore, the upper part of the groove must have gotten into contact earlier than the lower part, which is only possible in an upward movement. In consequence, the additional proal

or palinal motion component must have been a palinal one: In an upward movement only a distally directed motion creates a striation pattern where striae incline towards distal on the upper and mesial on the lower molar. Thus, the initially lateral movement abruptly changed its course towards distal at the very end of the power stroke just before centric occlusion. Such a late change of direction is probably enabled by the loss of contact of the straight mesio-buccal groove on the lower molar, which previously prevented a deviation from the lateral course. Since facets IV, V, and VI do not show any vertical striae, they only were in contact during this last phase. Indeed, all of these facets are situated on the interior of the lower molar. Due to the greater width of the upper molar they only could get in contact at the very end of the lateral movement. In fact, facet IV should not show any striae related to this palinal upwards movement at all because the lingual flank of cusp b could only contact the buccal flank of cusp Y when this cusp came to rest within the “pseudotalonid basin” in centric occlusion. However, the change of direction into a palinal movement apparently allowed cusp Y to slip out of the mesially opening “pseudotalonid basin”, creating the mesially inclined striae on lower and the distally inclined striae on upper facet IV. That cusp Y did indeed not necessarily rest within the “pseudotalonid basin” during centric occlusion is also indicated by the mesial downslope of dentine exposed within the basin. It is often accompanied by a distinct leading edge on the buccal side of crest b-g and a trailing edge on the lingual one (fig. 34). Both edges probably would not be as distinct if they were solely caused by abrasion induced by escaping food particles. Moreover, food particles were most certainly also pressed through the small gap at the distal end of the basin in between cusp g and the lingual flank of cusp a, which usually does not show any signs of abrasion at all.

The opposing proal or palinal movement indicated by facet III and upper facet IV might have been directed downwards. This is suggested by vague leading edges on the distal crests of the lower molar (facet III) that seem to be situated below vague trailing edges (fig. 36). There also seems to be a vague leading edge below a vague trailing edge on crest b-e (facet IV). A downward movement would also match the pattern on the mesial cingulum of the upper molar with vague leading edges above vague trailing edges (fig. 37). However, leading and trailing edges in these cases are not nearly as distinct as those within the “pseudotalonid basin” and the disto-buccal groove. Therefore, they are much less reliable. This is why this proal or palinal movement also might have been directed upwards as well, although a downward movement seems to be more probable. In any case, if the movement was downwards it must have been a palinal one since then only a movement in distal direction can produce mesially inclined striae on the upper and distally inclined striae on the lower molar. In case of an upward movement, it would have been a proal one. Both scenarios strongly imply two phases for the power stroke of

the mastication movement. The first and more probable scenario would be a lateral upward movement into centric occlusion followed by a palinal downward movement. The second, less probable scenario would be a lateral upward movement into centric occlusion followed by a simple orthal jaw opening and an independent proal upward movement ending in centric occlusion as well and also followed by an orthal jaw opening (fig. 47 + 48).

6.4.5 Mastication movement

According to Krusat (1980), *Haldanodon* possesses a power stroke with one single phase that ends in centric occlusion. This is also what Compton and Jenkins (1968) and Jenkins (1969) postulate to be the case for all docodont taxa. However, as discussed in detail in 6.4.4, the striations observed on the facets rather indicate two phases for the power stroke. Krusat (1980) furthermore assumes that during the upward movement of the lower jaw contact is established first in between the buccal half of the upper molar and the buccal side of the lower molars (facets I, II). Towards the end of the power stroke the lingual half of the upper molar contacts the interior of the lower molars (all other facets). For him, the positions and forms of the facets indicate that the movement of the lower jaw was lateral with a distinct lingual component. The striae found on the facets would imply an additional, slighter, mesio-distally directed movement. However, the striations observed in the present study rather imply that the lateral movement had a proal or palinal component only at the very end and a second proal or palinal movement was either separated by centric occlusion or entirely independent (see also 6.4.4).
For this study, the information derived from the position of the facets about the occlusion of the molars and from the orientation of the striations about the orientation of the jaw movement was synthesized into a virtual simulation of the chewing cycle with the OFA. Using this computer program, it was possible to objectively test the occlusional model to verify whether the assumed movement is indeed capable of producing the observed facets. The total area of detected collisions during the theoretical cycle compiled from the data collected in the present study matches the position of the facets observed on the specimens with only minor divergences (fig. 44 + 45). Therefore, the theoretical mastication path is assumed to be generally correct. Of course, this does not tell anything about the direction of the movement: the reversed motion would produce the same collision pattern. Nevertheless, the ancient chewing motion of *Haldanodon* could be narrowed down to two possible scenarios.
Both scenarios begin with a steep upward, lateral movement from buccal to lingual of the lower molars into centric occlusion (phase 1). The same kind of movement also has been suggested

by Krusat (1980), Butler (1988), and Pfretzschner et al. (2005). During this lateral movement, the buccal grooves of the lower molars are guided along the lingual flanks of the upper molar main cusps. That it must have been directed upwards is indicated by the leading and trailing edges observed on many lower molar specimens with dentine exposed within the disto-buccal groove in between cusps a and d (see also 6.4.4). These are caused by cusp A, which slides through the disto-buccal groove of the mesially situated lower molar, forming facet I during the process. Since cusp d runs along the disto-lingual flank of cusp A, part of upper facet I also forms on the distal side of crest A-X. Cusp C slides through the mesio-buccal groove in between cusps a and b of the distally situated lower molar, forming lower facet II-2 and the distal part of upper facet II. At the same time, cusp b of the distal molar is guided along a groove in between cusp A and C, contributing to the formation of the mesial part of upper facet II and lower facet II-1. Towards the end of the lateral movement the lingual flanks of the upper molar main cusps mainly lose contact with the lower molars. This is also indicated by the striae on these cusps (for a detailed discussion see 6.4.4). Until the lower molars contact the lingual half of the upper molar, cusp a of the mesial lower molar is guided mainly by the mesial cingulum of the upper molar. Cusp d running along the distal side of crest A-X also prevents the lower molar from deviating in mesial direction. At the same time, cusp a of the distal lower molar is guided mainly by the distal cingulum of the upper molar.

In the contact diagram created with the OFA, which displays the area of contact for each virtual facet in a specific time step (see also 4.5, 5.5; fig. 38), the steady decrease in contact during this process is clearly shown for facet I. Since cusp A is larger than cusp C, the area of contact for facet I is also larger than that for facet II. However, the area of contact for facet II does not decline as fast as that of facet I and even becomes larger than it towards the end of phase 1. This is because cusp b remains in contact with the buccal slope of the “pseudotrigon basin” longer than cusps A and C remain in contact with the buccal grooves of the lower molar. Additionally, the contact of cusp a with the mesial cingulum is not established in the OFA simulation. The markedly polished surface of the mesial cingulum on many upper molar specimens, however, clearly indicates such a contact.

As soon as the mesio-buccal groove of the distal lower molar loses contact with cusp C, the initially lateral mastication movement deflects towards distal. At least this is strongly suggested by all of the striae found on the facets involved in phase 1 (for a detailed discussion see 6.4.4). It is furthermore implied by the straight progression of the groove that most probably had been acting as a guiding structure and up until then prevented such a deviation from the lateral course. Unfortunately, this additional motion component could not be reconstructed with the OFA since it only comprises the last two (out of 17) time steps of phase 1. The fine adjustments required

to simulate this late change of direction towards palinal were not possible to achieve with the settings used for the present project. This is because the upper molar model derives from a different specimen than the lower molar models and additionally had to be scaled to match their size (see 4.5 and 6.2). This only allows a rather rough fitting. However, the differences in size and timespan of the contacts in between a lateral continuation of the power stroke and a palinal diversion are probably almost insignificant for such a small amount of time. Nevertheless, the palinal movement was manually re-enacted with 3D-prints of an upper and two lower molars to complete the observations made with the OFA if necessary. Immediately after their change of course the lower molars establish contact with the lingual half of the upper molar. The mesio-lingual flank of cusp a of the distal molar thereby continues to run along the distal cingulum, forming facet V. At the same time, the buccal flank of cusp g contacts the lingual flank of cusp Y. This cusp slides into the "pseudotalonid basin", creating facet VI in the process. That in the contact diagram the contact representing facet V only is present for one single time step at the very end of phase 1 most likely is the result of the inaccuracies in the fitting of the 3D-models. Additionally, the rotation of the lower jaw around its long axis could not be simulated with the OFA. Nevertheless, it is an important part of the mastication movement in Recent mammals (Oron and Crompton 1985, Hylander et al. 2005, Williams et al. 2011, Menegaz et al. 2015) and has been proven to increase contact area size (Schultz et al. 2017). Both, the inaccuracies in fitting as well as the lack of rotation, most probably make the contact area for this facet much too small in comparison to the observed facet size. Therefore, the contact probably also is too short in relation to the rest of the chewing stroke. Only at the very end of the lateral chewing stroke, cusp Y establishes contact with facet IV on the lingual flank of cusp b. Therefore, unless cusp Y slips out of the basin before centric occlusion, this contact does not produce any striations at all. In the case cusp Y does slide over the mesial rim of the "pseudotalonid basin", this not only causes a short prolongation of phase 1. More importantly, it also causes the closure of the gap in between cusp b and the "pseudotrigon basin". Otherwise, cusp b is too short to reach its bottom (fig. 49). But in this case, the mesio-buccal flank of cusp b is able to slide along the mesial side of the "pseudotrigon basin", creating the distally inclining striae on upper facet II. Towards the end of the power stroke, most probably the disto-buccal flank gets into contact as well, due to the slight slope of the rather shallow "pseudotrigon basin" in the direction of the distal cingulum. Just before cusp b slides over the low distal basin margin, the palinal motion is stopped by cusp X pressing against the preceding lower molar. According to the striations, the mesio-lingual side of the tip of cusp A most probably remains in contact with the area below the disto-buccal groove until the very end of phase 1 as well. However, the contact representing facet I in the OFA diagram does not even overlap with the contacts representing facets IV, V,

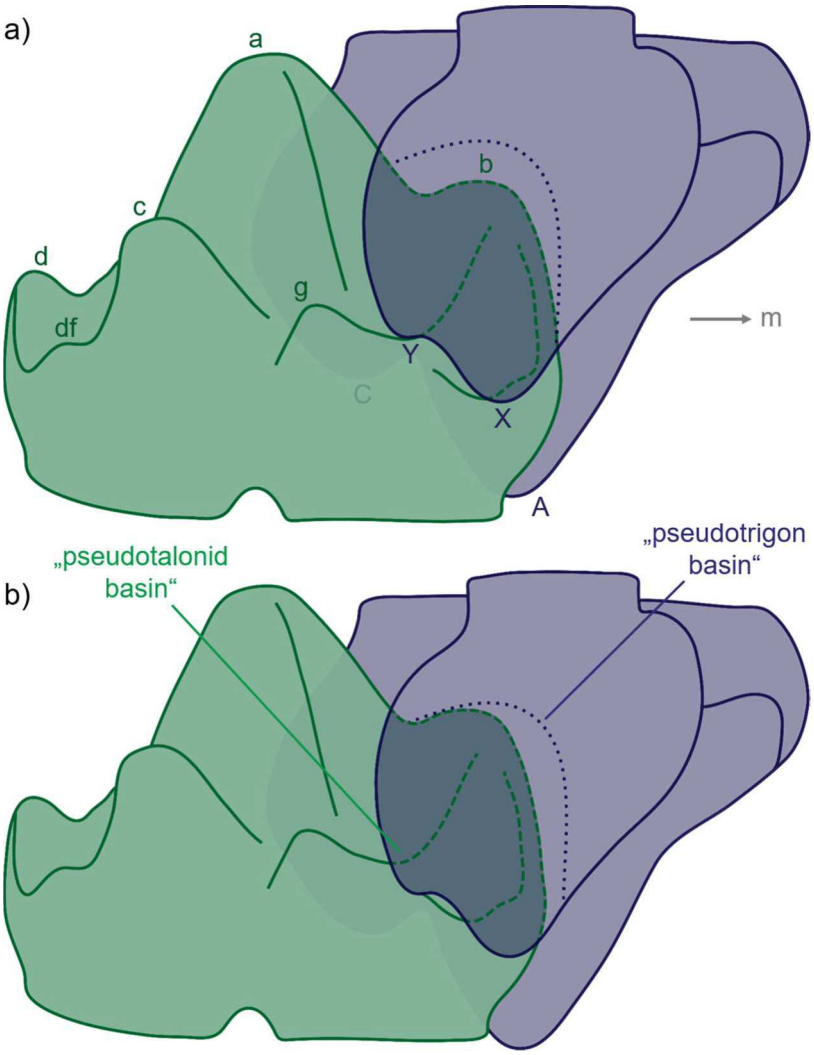

Fig. 49: Position of cusp Y in centric occlusion.
a) Cusp Y rests within the “pseudotalonid basin” as long as its mesial border is still intact.
b) Cusp Y slides out of the “pseudotalonid basin” as soon as its mesial border is fully abraded and rests mesially of it in centric occlusion. This enables cusp b of the lower molar to contact the “pseudotrigon basin” of the upper molar (dotted line) to enhance its crushing function and perform a short grinding motion.

and VI. This is probably also a result of the lack of lower molar rotation in the simulation. In contrast to the striations, the OFA analysis does show a contact for facet III in phase 1. Such a contact of the distal crests of the mesial lower molar with the mesial flank of cusp X indeed is very likely. However, any striae created by this contact are most probably overprinted during the following proal or palinal movement, which for this facet lasts much longer.

As discussed in 6.4.4, the independent proal or palinal movement could either have been a palinal downward movement directly following the lateral upward movement or an independent proal upward movement (fig. 47). Both would cause the same facet pattern. Based on Recent taxa the palinal downward movement is much more probable (see also Schultz et al. 2017). This is also suggested by vague leading and trailing edges observed on the *Haldanodon* molars. Two connected movements are also what Butler (1988) and Pfretzschner et al. (2005) postulate for the docodont chewing motion, although they both suggest a lateral continuation of the power stroke. In this first scenario with a palinal downward movement the masticatory movement of *Haldanodon* is made up of one power stroke with two phases (phase 1 and phase 2), separated by centric occlusion. Phase 1 is the steep upward lateral movement into centric occlusion, phase

2 a distally directed downward motion with only a slight lateral component continuing in lingual direction. At the beginning of this palinal motion, crest b-g of the distally situated lower molar slides along the buccal flank of cusp Y, forming the distal part of facet IV. Again, due to the unprecise fitting of the molar models, the contact area representing facet IV in the OFA simulation probably is much too small. Therefore, its contact with five time steps in total most likely is also depicted too short in the contact diagram. As indicated by the OFA analysis, facets V and VI might still have been in contact at the very beginning of the palinal movement. However, in contrast to facet IV they most certainly almost immediately lose contact and therefore do not show any striae related to the palinal movement. The vast majority of the palinal movement, however, is occupied by the movement of the distal crests of the mesially situated lower molars against the mesial flank of cusp X, forming facet III. If this scenario with a palinal downward motion were correct, this would be the first time in mammalian history that a bi-phased power stroke had been developed, long before the tribosphenids developed theirs.
Nevertheless, it is also possible that there are two distinct movements if the vague differences in height at the enamel-dentine junctions appearing to be leading and trailing edges are actually misinterpreted and do not indicate the direction of the movement. A similar occlusional model with two independent upward movements is also proposed by Gingerich (1973), although he assumes a proal and a palinal motion. From a functional point of view, the mesio-distal movement has much more meaning if performed upwards, because then the distal crests and the mesial flank of cusp X can pass each other in a shear-cutting motion. Such a shear-cutting motion is not possible or only realizable with significant effort in a downward movement. This is why Gingerich (1973) prefers the idea of two independent upward movements to explain the opposing striation pattern of mesially and distally inclining striae he also observed on *Docodon* molars. Two alternatively used power strokes are not yet known from any other extant or fossil mammalian taxon, which would make such a masticatory movement unique. This second scenario comprises two separated power strokes (phase 1a and phase 1b), which are used alternatively in the same individual. Phase 1a is the same lateral upward movement into centric occlusion as in the first scenario. Phase 1b, however, is the reversed movement of the lower jaw compared to phase 2 - an independent upward proal movement with a slight lateral component from lingual to buccal, which ends in centric occlusion as well. Both phases are followed by an orthal opening of the jaw. This means that centric occlusion with cusp Y resting within the “pseudotalonid basin” is achieved in two different ways. A proal motion also was proposed for *Docodon* by Jenkins (1969), although in contrast to Gingerich (1973) he did not consider an alternative upward movement. Two independent motions also could be another explanation besides highly varying abrasion rates why some of the upper molar rows have a

flatly and others a steeply worn crest X-Y. A flatly worn crest might indicate an emphasis on the lateral movement, a steeply worn crest an emphasis on the proal movement. In the first scenario with a palinal motion connected to the lateral one an emphasis on only one of the phases would be rather unlikely.

6.4.6 Functions performed by molars

Since the tooth morphology of *Haldanodon* molars is dominated by high cusps with steep flanks, shear-cutting obviously seems to be the dominant part of their function. This is why Crompton and Jenkins (1968) as well as Hopson and Crompton (1969) believe that the function of *Haldanodon* molars is actually completely restricted to shear-cutting. They assume that the only advantage of the relatively complex docodont tooth morphology is an increase of shear-cutting surfaces, including the broadening of the upper molar. This is opposed by Krusat (1980) and Butler (1988) who are convinced that the development of a "pseudotalonid basin" and the remarkable broadening of the upper molar in *Haldanodon* and other docodonts rather indicate a more or less derived crushing and probably grinding function. However, the importance of these crushing and grinding functions in docodont molars is commonly questioned (e.g. Jenkins 1969, Gingerich 1973, Kron 1979). Concerning *Haldanodon*, due to the small size of its "pseudotalonid basin", most authors are especially skeptical (Kermack et al. 1987, Pfretzschner et al. 2005, Averianov and Lopatin 2006). Thanks to the OFA analysis, it is now possible to estimate the relative amount of shear-cutting, crushing, and grinding occurring during the chewing stroke of *Haldanodon*.

First of all, the animation of the power stroke allows observations on how and when the molar cusps, crests and basins are getting into contact. Due to the coloring of the contact areas on the molars and the division of the movement in several time steps of equal length, these observations are relatively precise (fig. 50 + 51). The lateral upwards movement of the lower molars in phase 1 (respectively 1a) mostly consists of a shear-cutting motion when the buccal sides of the lower molar pass the lingual flanks of the upper molar main cusps. At the same time cusp b of the distal lower molar conducts a crushing function within the "pseudotrigon basin" of the upper molar. Like assumed by Pfretzschner et al. (2005), it indeed is too short to actually establish contact with the bottom of the basin. That is why, other than suggested by Krusat (1980), it does not conduct a grinding function. Crushing also takes place while the lingual flank of cusp b approaches the buccal flanks of cusp X and Y. Grinding only occurs at the very end of phase 1 immediately before centric occlusion by the time the lingual flank of

cusp Y contacts the buccal flank of cusp g and continues to slide along this flank until it reaches the base of the "pseudotalonid basin". Since in contrast to cusp b, cusp Y actually does contact its antagonistic basin, this really is a grinding function as assumed by Krusat (1980). In the case of the first scenario with a palinal downward movement following centric occlusion, for a very short time at the beginning of phase 2 cusp Y continues grinding until cusp g loses contact with it. At the same time and continuing until the molars disengage crest b-g of the distal lower molar is passing the buccal flank of cusp Y in a kind of "shear-grinding" motion. The downward movement prevents a true shear-cutting motion. At the same time, the distal crests of the mesially situated lower molar slide across the mesial flank of cusp X, performing a "shear-grinding" function as well (fig. 50). This would be the functional scenario Butler (1988) proposed for the distal part of the lower molars during the downward movement. However, that kind of grinding is not very efficient. This is because the amount of compression, which is an important part of grinding, taking place during a downward motion is much smaller than during an upward motion – at least if the food particles cannot be efficiently trapped in between two more or less flat surfaces. In the second occlusal scenario with a separated power stroke 1b, however, due to the upward movement of the lower jaw shear-cutting is performed throughout the entire phase. First, when the distal crests of the mesial lower molar pass the mesial flank of cusp X, and additionally as soon as crest b-g of the distal molar passes the buccal flank of cusp Y. Furthermore, in a proal upward motion, cusp b of the distal molar again conducts a crushing function as it approaches the "pseudotrigon basin". At the very end of the proal movement, right before it ends in centric occlusion, cusp Y also performs the grinding function within the "pseudotalonid basin" (fig. 51). Therefore, from a functional point of view the second scenario with an independent proal upward movement makes much more sense. However, comparisons with Recent taxa and the potential presence of corresponding leading and trailing edges rather indicate the first scenario with a palinal downward movement following centric occlusion for *Haldanodon* (for a detailed discussion see 6.4.4).

A further advantage of the OFA analysis is that the amount of shear-cutting and grinding can be quantified with the generation of a contact diagram. It also makes these functions comparable with other taxa processed with the OFA (see 6.5). For crushing, this is only indirectly possible, since it produces no attrition facets and the contact diagram created with the OFA shows the area of contact for each facet in a certain time step. Although a time step is not equivalent with a determinable period of time, the contact diagram shows the relative amount of time a specific function is performed during the power stroke. Additionally, the height of the bars shows how much of the respective facet is in contact at a specific time step. Since in phase 1 and 1a the shear-cutting contact of facets I and II occupies at least 15 of 17 time steps and the grinding

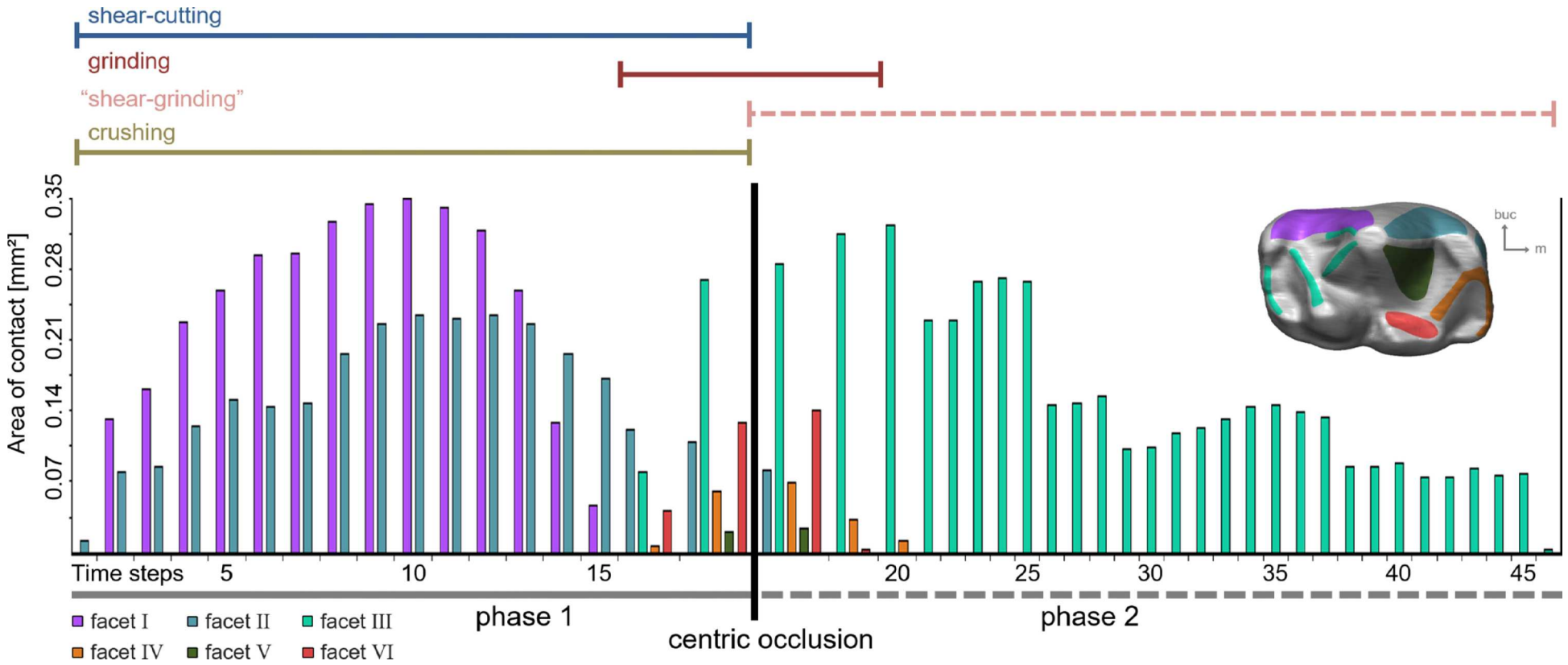

Fig. 50: Tooth-tooth-contact diagram for *Haldanodon* showing the size of the contact area for each lower molar facet during a certain time step throughout the chewing stroke from first to last contact of the molars as well as the duration of shear-cutting, grinding, and crushing functions. Since crushing produces no wear facets, the duration of this function is inferred from the animation of the chewing cycle with the OFA. This contact diagram is based on the reconstruction of the masticatory movement as a bi-phased power stroke, with a lateral upward movement of the lower molars into centric occlusion (phase 1) followed by a palinal downward movement (phase 2). Most of phase 1 is taken up by the shear-cutting contacts of facets I (light violet) and II (grey blue) as well as the crushing conducted by cusp b of the distal lower molar within the "pseudotrigon basin" of the upper molar and by the lingual flank of cusp b against the buccal flanks of cusps X and Y. Grinding facet VI (light red) only is in contact for a short time at the very end of the first and the very beginning of the second phase, simultaneously to shearing facets III (turquoise), IV (orange), and V (olive). Since 'true' shear-cutting is not possible in a downward motion, in phase 2 the shear-cutting contacts of facets III and IV become more of a "shear-grinding" contact similar to that of a grater. Crushing is not possible at all in a downward motion and therefore does not take place in phase 2. (lower molar model: m3 of Gui Mam 6/82)

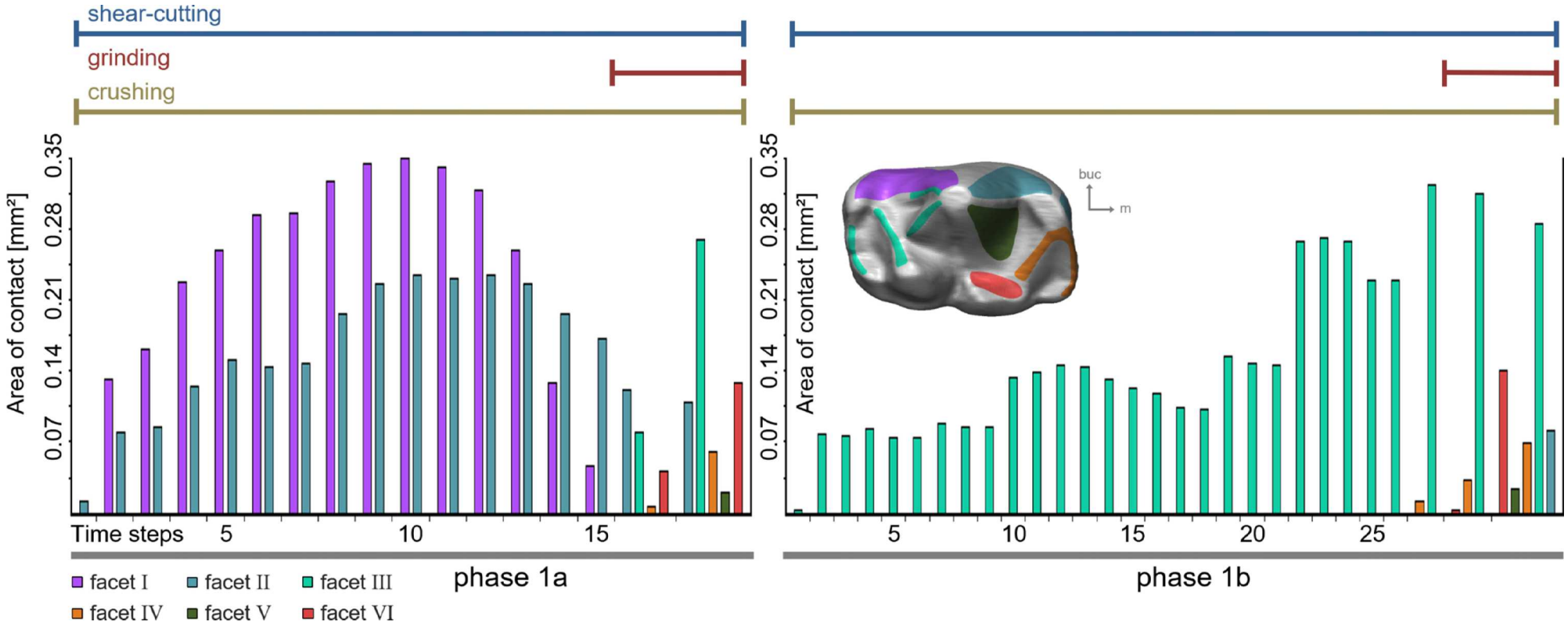

Fig. 51: Tooth-tooth-contact diagram for *Haldanodon* showing the size of the contact area for each lower molar facet during a certain time step throughout the chewing stroke from first to last contact of the molars as well as the duration of shear-cutting, grinding, and crushing functions. Since crushing produces no wear facets, the duration of this function is inferred from the animation of the chewing cycle with the OFA. This contact diagram is based on the reconstruction of the masticatory movement as two independent power strokes, one consisting of a lateral upward movement of the lower molars into centric occlusion (phase 1a), and another consisting of a proal upward movement of the lower molars into centric occlusion (phase 1b). Centric occlusion is followed by a vertical opening of the jaw which results in an immediate loss of contact of the antagonistic molars. Both power strokes can be used alternatively. Most of phase 1a is taken up by the shear-cutting contacts of facets I (light violet) and II (grey blue) as well as the crushing conducted by cusp b of the distal lower molar within the “pseudotrigon basin” of the upper molar and by the lingual flank of cusp b against the buccal flanks of cusps X and Y. Grinding facet VI (light red) only is in contact for a short time at the very end of phase 1a, simultaneously to shearing facets III (turquoise), IV (orange), and V (olive). Most of phase 1b is taken up by the shear-cutting contact of facet III as well as the crushing conducted by cusp b of the distal lower molar within the “pseudotrigon basin” of the upper molar. Grinding facet VI as well as the other shearing facets only are in contact for a short time at the very end of phase 1b. (lower molar model: m3 of Gui Mam 6/82)

contact of facet VI only takes up the last two steps, at least 88% of this phase are used for shear-cutting and only 12% account for grinding. A small amount of shear-cutting obviously also takes place during the grinding contact of phase 1, because facets III, IV and V, which are in contact at the same time as facet VI, are formed by shear-cutting. This shows that the different functions are not separated very well but rather overlap to a great extent. Observations on the animation of the chewing cycle show that throughout all of phase 1 and 1a crushing takes place within the "pseudotrigon basin". Phase 2 is clearly dominated by the "shear-grinding" contact of facet III. Although it lasts throughout the entire phase, its contact area is steadily decreasing. Only two of the 29 time steps attributed to phase 2 (7%) show the grinding contact of facet VI. Due to the downward movement of the lower jaw in this scenario, crushing does not take place at all in phase 2. In phase 1b with an independent upward movement, however, crushing is as important as shear-cutting which both persist during the entire phase. Thereby, the shear-cutting area of facet III is steadily increasing towards the end of the phase. The grinding function at the end of the phase 1b probably does not increase in comparison to phase 2.

All in all, the crushing function in *Haldanodon* molars is much more prominent than suggested so far, even in the first scenario with a downward palinal movement and all the more in the second one with an upward proal movement. Compared to shear-cutting and crushing, grinding really is a minor issue and is not even clearly separated from the shear-cutting function. Nevertheless, it is a well determinable part of the chewing process and therefore cannot be declared completely insignificant. In any case, it is obvious that although shear-cutting indeed is a very prominent function in *Haldanodon* molars, they are not at all restricted to it as suggested by Crompton and Jenkins (1968) and Hopson and Crompton (1969).

The amount of crushing and grinding occurring within the "pseudotalonid basin" is actually quite small. Not only does the basin provide only very limited space for this function due to its small size – it also quickly loses the requirements for an efficient grinding function. This is because its mesial border made up of crest b-g is worn down very fast, even before dentine is exposed on any of the other crests, enabling cusp Y to slip out of the basin during the palinal motion of phase 1. For a brief time, this loss of the mesial border actually prolongs the grinding function, since the distance cusp Y travels along the buccal flank of cusp g is longer. The "pseudotalonid basin" becomes a narrow groove during this process. However, the steeper its slope is worn, the more grinding changes into shear-cutting, at least in phase 1 and 1a. In phase 2, the grinding function is completely lost as soon as cusp Y starts sliding out of the basin. In an independent phase 1b, however, the direction of the applied force presses the lingual flank of cusp Y against the buccal flank of cusp g. This prevents cusp Y to slip out of the basin even if the mesial basin border is fully abraded. Therefore, in phase 1b the grinding function of the

“pseudotalonid basin” is maintained as long as cusp g is not completely worn down and cusp Y is not too heavily abraded. At the latest when cusp g is fully abraded, the grinding and even the crushing function within the basin cease to exist in both phase 1a and 1b. Since cusp g is very small, it is one of the first cusps to be worn down completely. Considering the exceptionally high abrasion rates of the molar enamel in *Haldanodon*, this must have happened in a very early ontogenetic stage. In the front molars, it may well have been the case before the eruption of the fourth lower molar, that is in juvenile individuals. Cusp Y is almost equally fast worn down and additionally is not always well-developed in the first place. This is why, as mentioned above, the grinding function of the “pseudotalonid basin” is almost negligible.

However, this lack of significant crushing and grinding within the “pseudotalonid basin” is compensated by the much greater amount of crushing taking place within the large “pseudotrigon basin” of the upper molar. Moreover, as soon as cusp Y begins to slide over the mesial edge of “pseudotalonid basin”, this allows cusp b to close the gap to the “pseudotrigon basin” (fig. 49). In this case, it becomes able to conduct the grinding function suggested by Krusat (1980) and furthermore indicated by the presence of the distally oriented striae within the “pseudotrigon basin”, which are far too parallel to merely be the result of food particles escaping the basin during the crushing motion. Although this grinding contact most certainly is at least as short as that of cusp Y had been within the “pseudotalonid basin”, it persists until the tooth morphology is leveled out by abrasion. Therefore, the majority of the crushing and very likely even the grinding function in *Haldanodon* molars actually took place within the “pseudotrigon basin” of the upper molar.

Crushing most probably is also the last operating function in very strongly worn molars on which the tooth morphology is more or less leveled out. Since striae imply that the two distinctly different power strokes are still performed in old individuals, there probably still is some rudimentary shear-cutting, respectively “shear-grinding” taking place on the flatly worn distal ends of the lower molars as long as they are not too rounded. According to Krusat (1980), the premolars take over the preparation of the food in old individuals, because they are less strongly worn than the molars. He also postulates a change of food preference with old age.

6.4.7 Relevance of the results for the *Haldanodon* molar dentition for other docodont taxa

The molar tooth morphology of other docodonts is generally quite similar to that of *Haldanodon*, with the same cusps in a more or less similar arrangement. The cusps can differ in proportion: for example, cusp g usually is almost as tall as cusp c, and cusp Y is much better

developed than in *Haldanodon* in almost all other taxa. A very few taxa also show small additional cusps on lower or upper molars: *Krusatodon* a small conulid buccal of cusp d (Sigogneau-Russell 2003: fig. 3); *Tegotherium* and *Hutegotherium* a small conulid lingual of cusp e (Martin et al. 2010a: fig. 10, Averianov et al. 2010: fig. 5); *Hutegotherium* and *Sibirotherium* a small accessory cusp Z on the mesial flank of cusp X (Sigogneau-Russel 2003: fig. 5, Averianov et al. 2010: fig. 4, Lopatin et al. 2009: fig. 2). The main difference in between the docodont molar dentitions, however, is how the cusps are connected to each other. The "pseudotalonid", for example, opens in mesial direction not only in *Haldanodon* but also in *Borealestes* (Sigogneau-Russell 2003: fig. 2), *Docodon* (Jenkins 1969: figs. 7, 8, Rougier et al. 2014: figs. 3, 4), and most probably *Tashkumyrodon* (Martin and Averianov 2004: figs. 2, 3). It can also be well-enclosed like in *Dsungarodon* (Pfretzschner et al. 2005: fig. 3, Martin and Averianov 2010: fig. 7), *Hutegotherium* (Averianov et al. 2010: fig. 5), *Krusatodon* (Sigogneau-Russell 2003: fig. 3), *Sibirotherium* (Maschenko 2002: figs. 1-3, Lopatin et al. 2009: pl. 12), *Simpsonodon* (Kermack et al. 1987: figs. 3-29, Averianov et al. 2010: fig. 3), and *Tegotherium* (Tatarinov 1994: fig. 1, Martin and Averianov 2010: fig. 10-12). In the tegotheriids (*Tegotherium*, *Hutegotherium*, *Sibirotherium*), in contrast to the other docodonts cusp e is included into the border of the "pseudotalonid basin". The tegotheriids are also the only docodonts with a well-enclosed distal basin on the lower molar, whereas the distal lower cusps in all other docodont taxa are connected by more or less well-developed crests in a zig-zag-pattern. The upper molars differ mostly in width and the height of the cusps. Another character unique to the tegotheriids and *Krusatodon* is the reduction or complete absence of crest A-X (Martin and Averianov 2010: figs. 8, 9, Averianov et al. 2010: fig.4, Lopatin et al. 2009: pl. 12, Sigogneau-Russell 2003: fig. 5).

Despite these differences the most important guiding structures are still present in all docodont molars. For one, those are the buccal grooves on the lower molars in combination with the row of buccal cusps on the upper molars. Although in taxa with a well-developed crest a-d like the tegotheriids the disto-buccal groove might be very shallow and steep, it is still present in these taxa. Almost all docodont taxa show at least a very well-developed facet I and most also facet II on the lower molars (Jenkins et al. 1969: fig. 6, Kermack et al. 1987: figs. 16, 29, Maschenko et al. 2002: fig. 4, Sigogneau-Russell 2003: fig. 2, Martin and Averianov 2004: fig. 2, Averianov et al. 2010: fig. 5, Martin et al. 2010a: figs. 10, 12, Rougier et al. 2014: fig. 4), implying that the buccal grooves really have had a guiding function also in the other docodonts. This hypothesis is further supported by the fact that if lower facet II is present, just like in *Haldanodon* it always also covers the interior of the mesio-buccal groove, best seen in *Sibirotherium* (Maschenko et al. 2002: figs. 1, 4), *Simpsonodon* (Kermack et al. 1987: figs. 16,

29), and *Tegotherium* (Martin et al. 2010a: figs. 10, 12). The only definite exception seems to be *Docodon*. At least the m6 of the holotype mandible YPM-VP011826 from the collection of the Yale University Peabody Museum of Natural History depicted by Jenkins (1969: fig. 6) shows a dichotomous lower facet II on the mesio-buccal flank of cusp a and the disto-buccal flank of cusp b that clearly omits the groove. This mandible was also used for the virtual reconstruction of the chewing motion in the study of Schultz et al (2017). Since it also shows alveoli for two more molars, unlike in *Haldanodon* the m6 in *Docodon* is not the ultimate molar and therefore unlikely to have been reduced much. As consequence to the location of lower facet II as well as the mesially inclining striae observed on this facet (see also Gingerich 1973: fig. 1), Schultz et al (2017) reconstructed the mastication movement of *Docodon* as a mainly palinal motion with only a small lateral component. In this kind of movement, the buccal grooves just pass by the lingual flanks of the upper buccal cusps without any guiding function whatsoever (see also Schultz et al. 2017: Supplementary Information Video S2). However, there are also a few *Haldanodon* lower molar specimens on which facet II omits the mesio-buccal groove (e.g. Gui Mam 3174), although in the vast majority of specimens it covers this groove as well. Therefore, the *Docodon* holotype might not be representative of the genus concerning the extent of lower facet II. In this case the grooves might actually have had a guiding function in *Docodon* as well. On the other hand, according to a personal comment of J. A. Schultz (2018), in the OFA simulation it was impossible to let the lower molar models occlude with both upper molar models without a very distinctive palinal motion component. Therefore, *Docodon* also might be an exception and the lower buccal grooves did not have any guiding function in this genus.

The distal crests of the lower molars are the other important guiding structure. In the tegotheriids with their small distal basin this is mainly crest a-d, in the other docodonts crests a-c and c-d. The only taxa in which these are not very distinctive, *Docodon* and *Simpsonodon*, the almost basin-like distal part is covered by heavy crenulations (Jenkins 1969: figs. 9, 15, Kermack et al. 1987: figs. 4, 5). Since both guiding structures are present in all docodont dentitions, it is not surprising that observations on isolated upper and lower molars of *Dsungarodon*, as well as lower molars of *Tashkumyrodon* and *Tegotherium* show that with the exception of facet V all facets observed on *Haldanodon* molars can also be found on these taxa at the same positions. Only in *Tegotherium*, due to the inclusion of cusp e into the border of the "pseudotalonid basin", facet IV aberrantly covers crest e-g and the crest running from cusp e to the small conulid mesial of the basin. However, those crests have the same relative position as crests b-g and b-e in *Haldanodon*.

Therefore, it is very likely that docodonts share a very similar chewing stroke. The common presence of facets I and II and their covering the interior of the grooves show that at least the lateral movement of phase 1/1a determined for *Haldanodon* is more than likely to occur in the other docodonts as well. The only exception might be *Docodon*, which as mentioned above seems to lack the guiding function of the lower buccal grooves and therefore might have had a much more distally directed first phase. A very similar chewing stroke throughout docodonts is further indicated by the study of Pfretzschner et al. (2005) who accidently used upper and lower molars of two different taxa (*Tegotherium* and *Dsungarodon*) for their analysis of the docodont mastication movement. Nevertheless, they still obtained a viable result for their postulated chewing stroke with phase 1 being almost identical to phase 1 determined in this study for *Haldanodon*. A similar chewing stroke is also further supported by the presence of vertical striae on facet II-2 of a lower molar specimen of *Tegotherium* (SGP 2004/3), which also strongly suggest a strictly lateral movement (Martin et al. 2010a: fig. 10e, personal observation).

As for the second phase, a continuation of the lateral movement in downward direction as suggested by Butler (1988) and Pfretzschner et al. (2005) is rather unlikely also for the other docodonts. According to Pfretzschner et al. (2005), during the lateral continuation cusp b slid along the buccal side of crest X-Y in a grinding motion without producing distinct wear facets. This, however, is not possible without abrasion predominating attrition. This is very improbable, because that is not even always the case on upper molars of *Haldanodon*, which were subjected to extraordinarily high abrasion rates caused by its subterranean lifestyle. Furthermore, the presence of the second phase facets III and IV even on lower *Tegotherium* molars with their enlarged “pseudotalonid basins” and small distal basins strongly implicates a second phase similar to that in *Haldanodon*. Certainly, these facets most probably were in contact during both phases as well and therefore could have been formed solely by the lateral movement. However, the additional presence of guiding crests on the distal part of the lower molar in all of the other docodont taxa makes a proal or palinal movement during the second phase similar to that of *Haldanodon* much more probable. All this rather supports the interpretation that all docodonts shared a similar mastication movement and that the *Docodon-Haldanodon* clade is not functionally derived from the other docodont taxa as assumed by Schultz et al. (2017). At the very least, the primarily palinal chewing stroke postulated for *Docodon* is not applicable for *Haldanodon*.

While the tooth morphology of docodonts in general is similar enough to assume a very similar chewing stroke, it also differs enough to assume at least a diverging focus on specific chewing functions. Pfretzschner et al. (2005) postulated three different trends of molar function within

docodonts. According to them *Borealestes*, *Haldanodon*, and *Docodon* are mainly piercing and cutting their food. These functions are best suited to process a diet comprising arthropods and other invertebrates. *Tashkumyrodon*, *Sibirotherium*, and *Tegotherium* additionally developed two large crushing basins in the lower molars. This probably allowed them to prey on armored insects such as beetles or might also be indicative of a more omnivorous diet. *Simpsonodon*, *Dsungarodon*, and to a lesser extent *Krusatodon* finally developed an extensive grinding function. This probably enabled them to distinctly increase the amount of plant material in their diet, which might also have included soft-bodied invertebrates. A grinding function for *Simpsonodon* also has been suggested by Kermack et al. (1987) and Luo et al. (2002).

Indeed, *Borealestes* and *Docodon* are the only other docodont taxa besides *Haldanodon* whose "pseudotalonid" and "pseudotrigon basins" are not closed. This is why their molar functions most probably are mainly focused on shear-cutting as well. However, their molar morphology just like that of *Haldanodon* might have allowed for much more crushing and even grinding than Pfretzschner et al. (2005) anticipate: if cusp Y also started to slip out of the "pseudotalonid basin" at the end of phase 1 as soon as its already low mesial border was completely abraded, this probably would enable cusp b to contact the "pseudotrigon basin" for a short grinding movement (for a detailed discussion see 6.4.6). In this case, *Borealestes* and *Docodon*, too, would have executed the main part of crushing and grinding within the "pseudotrigon basin" of the upper molar. A reexamination of a cast of the only known specimen of *Tashkumyrodon* showed that in contrast to the assumptions of Pfretzschner et al. (2005) its "pseudotalonid basin" is also rather open. Additionally, its distal part is covered by crests that do not enclose a distal basin. Therefore, its molars most probably were closer in function to *Haldanodon* and the other docodonts with open "pseudotalonid basins" and laterally running distal crests than to the tegotheriids. In this group, *Docodon* is the only taxon that does not have well-developed distal crests. Especially crest c-d does not run straight as in the other taxa but shows a considerable indentation in between the cusps (Jenkins 1969: figs. 9, 15). Therefore, the distal part is rather formed like a broad, shallow, distally opening basin (Rougier et al. 2014: fig. 3). Since cusp d is set slightly more distal than cusp df (Jenkins 1969: figs. 2-3, 8, Rougier et al. 2014: figs. 2-4), like in *Haldanodon* it most probably occluded distally of crest A-X. Therefore, the mesio-lingual flank of cusp A and the mesio-buccal flank of cusp X probably conducted a crushing function within this basin. Crompton and Jenkins (1968) as well Jenkins (1969) suggest that in *Docodon* the "pseudoprotocone" cusp X actually occluded within this distal basin structure rather than in between the lower molars. This was also adopted by Schultz et al. (2017) for their reconstruction of the mastication cycle of *Docodon* and the resulting OFA analysis. However, since cusp X is much larger than cusp Y, that would terminate the movement long before the

latter could contact the “pseudotalonid basin”. This is also clearly visible in the illustrations of the respective postulated chewing strokes (Jenkins 1969: fig. 4, Schultz et al. 2017: figs. 13, 14). Cusp X terminating the chewing motion early would not only cancel the crushing and grinding function of the “pseudotalonid basin”. It would also shorten the mastication movement and with this considerably reduce the shear-cutting and crushing taking place on other molar parts as well. It is rather unlikely that the grinding function gained within the “talonid” basin would really compensate for this. Thus, it is much more probable that also in *Docodon* cusp X did not occlude within the distal basin structure but in between the lower molars. In contrast to the other docodonts with mesially opening “pseudotalonid basins”, in *Docodon* the lingual flank of cusp a and the mesio-lingual flank of cusp A are covered by vertically running crenulations that reach down into the basins (Jenkins 1969: figs. 7, 9-10, 13, 15). They probably functioned as additional shearing crests. Due to the tooth morphology these crenulations on the lower molar were probably most effective during phase 1/1a in the distal basin region, and during phase 2/1b in the “pseudotalonid basin” region. With this, *Docodon* had significantly increased the shear-cutting and crushing functions of its molars in comparison to *Haldanodon*, *Borealestes*, and *Tashkumyrodon*. The majority of crushing (and grinding) most likely still took place in the “pseudotrigon basin”, but the importance of the lower molar for crushing was considerably enhanced with the addition of the distal basin. The crenulations presumably compensated the decrease in shear-cutting function of the weakened distal crests. The only other docodont taxon with a very similar basin-like structure covered by heavy crenulations on the distal part of the lower molar is *Simpsonodon* (Kermack et al. 1987: figs. 4-5, 11-29). This taxon, however, did not only enhance the crushing function of the lower molar by adding a distal basin. It also increased crushing and grinding taking place within the “pseudotalonid basin”, since its mesial border is well-developed and therefore it is well-enclosed on all sides (Kermack et al. 1987: figs. 4-5, 11-29). Thus, in *Simpsonodon* as well as in all the other docodonts with a well-enclosed “pseudotalonid basin”, it is very unlikely that cusp Y could have slipped out of the basin in any but the most heavily worn lower molars. This is also suggested by the vertically running striae observed on lower facet II-2 of the *Tegotherium* specimen SGP 2004/3. On this specimen the facet actually reaches all the way down towards the tooth rim. The striae continue to run vertical and do not show any inclination on the lower part of the facet (Martin et al. 2010a: fig. 10e, personal observation). This strongly implies that unlike in *Haldanodon* there had not been a sudden change of direction immediately before centric occlusion. This further indicates that a palinal motion component was prevented by cusp Y pressing against the mesial border of the “pseudotalonid basin”.

Usually, this would mean that at least the main grinding function is shifted to the lower molar, since cusp b can no longer get close enough to the "pseudotrigon basin" to perform more than a crushing function. *Simpsonodon*, however, has considerably decreased the height of the upper molar cusps (Kermack et al. 1987: figs. 30-44). This means cusp b most probably was able to get very close to the "pseudotrigon basin" despite cusp Y resting within the "pseudotalonid basin" in centric occlusion. It even might have still conducted a grinding function. Together with the compact appearance of upper and lower molars with the rather blunt cusps this implies that *Simpsonodon*, as suggested by Pfretzschner et al. (2005), indeed had one of the most extensive crushing and grinding functions within docodonts. To a lesser extent, this might also be true for *Dsungarodon*. This taxon has a very well-developed "pseudotalonid basin" as well but lacks the distal basin structure on the lower molar (Pfretzschner et al. 2005: fig. 3, Martin et al. 2010a: fig. 7). Nevertheless, the lingual upper molar fragments referred to *Dsungarodon* show that cusps X and Y are also not very high in comparison to other docodonts (Martin et al. 2010a: fig. 5). A similar trend is shown by the upper molars of *Krusatodon* as well, although the cusps are not as low as those of *Simpsonodon* or *Dsungarodon* are (Sigogneau-Russell 2003: fig. 5). Compared to the other docodonts, though, it developed a relatively tall cusp b (Sigogneau-Russell 2003: fig. 3). Therefore, this cusp still might have established contact with the "pseudotrigon basin" without cusp Y slipping out of the "pseudotalonid basin". In comparison to *Simpsonodon*, *Dsungarodon*, and *Krusatodon* the "pseudotalonid basin" of the tegotheriids is even larger due to the inclusion of cusp e into its border. Additionally, they all developed a small but well-enclosed distal basin on the lower molar (*Tegotherium*: Tatarinov 1994: fig. 1, Martin et al. 2010a: fig. 10, *Hutegotherium*: Averianov et al. 2010: fig. 5, *Sibirotherium*: Maschenko et al. 2002: figs. 1-4, Lopatin et al. 2009: pl. 12). As postulated by Pfretzschner et al. (2005), in *Tegotherium* this distal basin could only have been used as a crushing basin since the upper molar lacks an antagonistic cusp (Martin et al. 2010a: figs. 8-9). Furthermore, due to the well-developed crests enclosing the basin neither the lingual flank of cusp A nor the buccal flank of cusp X could have gotten even close to the bottom of the basin. The other tegotheriids, however, developed an additional accessory cusp Z on the mesial flank of cusp X (*Hutegotherium*: Averianov et al. 2010: fig. 4, *Sibirotherium*: Lopatin et al. 2009: fig. 2, pl. 12). It obviously pounded into the distal basin of the lower molar and most probably did not only perform crushing but also grinding. Still, the majority of crushing and certainly also grinding was conducted by cusp Y within the much larger "pseudotalonid basin". Since the lingual upper cusps are distinctly higher than those of *Simpsonodon* are, cusp b most probably did not come into contact with the "pseudotrigon basin". Therefore, in the tegotheriids it was only used for crushing.

Considering all this, docodonts indeed show several different functional trends as postulated by Pfretzschner et al. (2005). These are mostly defined by the differing focus on certain crushing and grinding areas. The first group consists of docodont taxa with a mesially opening "pseudotalonid", like *Borealestes*, *Docodon*, and *Haldanodon*, and probably also *Tashkumyrodon*. In these taxa the crushing and grinding function is concentrated on the "pseudotrigon basin" of the upper molar. It is conducted by cusp b, which is able to close the gap to the upper basin only if cusp Y slips out of the "pseudotalonid basin" before centric occlusion due to the abrasion of the mesial "pseudotalonid border". Nevertheless, sharp crests and high cusps indicate their molars were mainly used for shear-cutting and piercing. Only *Docodon* has a slightly higher emphasis on crushing, since it developed an additional crushing basin on the distal part of the lower molar. With this, it is also functionally close to the group comprising *Dsungarodon*, *Krusatodon*, and *Simpsonodon*, which more or less equally divide the crushing and grinding functions in between upper and lower molar. However, in contrast to *Docodon* they all possess a large, well-enclosed "pseudotalonid basin" and relatively low upper molar cusps. The low lingual cusps of the upper molar compensate for the inability of cusp Y to get over the well-build mesial border of the "pseudotalonid basin": even though cusp Y rests within the basin, cusp b can get close to the "pseudotrigon basin". With this, crushing and probably even grinding can occur simultaneously in the "pseudotalonid" and the "pseudotrigon basin". *Simpsonodon* additionally developed a crushing basin on the distal part of the lower molars. This undoubtedly makes it the taxon with the most extensive crushing and grinding function out of all docodonts. In contrast to the other docodonts, the tegotheriids completely focused their crushing and grinding on the lower molar. Since cusp b is not large enough to reach the bottom of the "pseudotrigon basin" in centric occlusion, it is very likely that the two well-enclosed lower basins are more important for these functions. For *Hutegotherium* and *Sibirotherium* with their additionally accessory cusps Z as antagonist for the distal basin this is even more probable than for *Tegotherium*. Tegotheriids all still possess relatively high cusps and very sharp crests on the lower molars. This is why, despite their increased crushing and grinding ability, shear-cutting was also an important function. In *Hutegotherium* and *Sibirotherium* it seems to be slightly less important, because they both lack crest A-X that functions as a shearing crest.

Since there were no detailed drawings or high-resolution photographs available for the dentitions of *Agilodocodon*, *Castorocauda*, and *Docofossor*, no reliable statement about their molar functions can be given in the present study. However, according to the descriptions given by the authors, they all show some unique peculiarities. The incisors of *Agilodocodon* are spatulate indicating a diet containing gum or sap (although this interpretation has been

questioned by Wible and Burrows (2016) who do not see any remarkable resemblance with the incisors of Recent exudativorous taxa). The molars are very similar to those of *Krusatodon*, with a well-developed "pseudotalonid basin" and relatively high upper and lower molar cusps (Meng et al. 2015). Therefore, *Agilodocodon* can probably be assigned to the same functional group as *Krusatodon*, *Dsungarodon*, and *Simpsonodon*. In *Castorocauda*, on the first two of its six molars all cusps are aligned in a row with the tips curving in distal direction. This was interpreted as adaptation to piscivory similar to modern seals (Ji et al. 2006). While this is unique among docodonts, a phylogenetic analysis using the dental characters of the following molars places *Castorocauda* within the same distinct group as *Krusatodon*, *Dsungarodon*, and *Simpsonodon* (Ji et al. 2006). Therefore, it is highly probable that it also belongs to the same functional group as these taxa. The molars of *Docofossor* are most similar to those of *Haldanodon* (Luo et al. 2015). Nevertheless, they might have had much less shearing potential since many crests in both upper and lower molars seem to be weak or absent (Luo et al. 2015: fig. 2, Supplementary Materials).

All in all, docodont molars show a wide variety of shear-cutting, crushing, and grinding functions. None of the docodont taxa is more or less limited to either only shear-cutting as suggested by Crompton and Jenkins (1968), Jenkins (1969), and Gingerich (1973) or only crushing as postulated by Butler (1988). Even the docodonts with a mesially opening "pseudotalonid basin" and laterally running lower distal crests like *Borealestes*, *Docodon*, *Haldanodon*, *Tashkumyrodon*, and to a lesser extent maybe also *Docofossor*, which are indeed relying mostly on shear-cutting, also conduct a fair amount of crushing and even grinding. Shear-cutting plays a significant role in *Hutegotherium*, *Sibirotherium*, and *Tegotherium* as well, although with their well-enclosed "pseudotalonid basin" and the additional lower distal basin they are much more specialized in crushing and grinding. And finally, the docodonts most adapted to crushing and grinding due to their well-enclosed "pseudotalonid basin" and relatively low cusps, *Dsungarodon*, *Krusatodon*, *Simpsonodon*, and probably also *Agilodocodon* and *Castorocauda*, still retain some shear-cutting function thanks to the laterally running lower distal crests, respectively the heavily crenulated surface of the distal lower basin in *Simpsonodon*. In any case, docodont molars certainly were far apart from being "a premature and ill-fated effort toward the production of broad-crowned crushing or grinding teeth from the more ancient piercing insectivorous type" as stated by Simpson (1929: p. 85). Instead, they quickly became functionally divers since representatives of all three functional groups are present as early as the Middle Jurassic.

6.5 Comparison of tribosphenic and docodont “pseudotribosphenic” tooth morphology

6.5.1 Comparison of molar functions in *Didelphis* and *Haldanodon*

The reconstruction of the chewing movement with the OFA allows the comparison of tooth functions of different taxa. With the resulting tooth-tooth-contact diagrams it is possible to compare the relative amount of time spent on a specific molar function during the power stroke. It is also possible to compare the development of contact area size for specific facets and the functions they represent. This is essential to estimate the efficiency of a molar function because it depends on a combination of tooth morphology (e.g. sharp or blunt crests), length of execution, and facet size. Since crushing produces no facets, facet size cannot be used to evaluate the efficiency of this function.

The *Didelphis* molars from the OFA project provided by A. H. Schwermann are slightly worn (wear stage II out of five stages, see also figs. 35 and 36 in Schwermann 2015). Therefore, their functions are well comparable to those of the *Haldanodon* molars that also only show first signs of wear.

Didelphis has a power stroke with two phases, separated by centric occlusion. Phase 1 consists of a mesio-lingual movement, which is continued in phase 2 in lingual direction. About two thirds of phase 1 are occupied by the shear-cutting contact of facets 1 and 2. It takes place when the distal flanks of proto- and metaconid glide along the mesial flanks of para- and protocone and the mesial flanks of proto- and paraconid along the distal flanks of metacone and metacrista. Simultaneously also crushing occurs within the talonid and trigon basins conducted by the approaching protocone and hypoconid. The shearing facets lose contact as soon as the buccal flank of the entoconid contacts the disto-lingual flank of the protocone. From this point onward, the protocone moves through the talonid basin in a grinding motion that results in the formation of facet 6. This grinding contact continues until centric occlusion. At the same time, the hypoconid continues its crushing function within the trigon basin. Immediately before centric occlusion its lingual flank contacts the buccal flank of the protocone. The movement of hypoconid against protocone causes the formation of facet 9. At the same time, the mesio-buccal flank of the hypoconid also contacts the disto-lingual flank of the paracone in a short shear-cutting motion producing facet 3. After centric occlusion, the protocone continues its grinding function within the talonid basin until it finally loses contact with the hypoconid. This also marks the end of the power stroke. Crushing does not take place in phase 2, due to the downward motion of the lower molars. Other than in *Haldanodon*, the efficiency of the grinding in phase 2 is not as much affected by the downward movement, because the antagonistic

surfaces involved both are flanks of cusps. They are better suited to prevent the trapped food particles from escaping than the distal crests on the lower molars of *Haldanodon*.

Facets 4 and 5 of the *Didelphis* molars do not occur in the contact diagram. In the case of facet 4, usually situated on the distal flank of the hypoconid, this facet is not developed on the original specimen. According to Schwermann (2015) the absence of facet 4 is not uncommon for *Didelphis* molars. *Didelphis* shows highly varying occlusal patterns and only few individuals actually possess all facets. Schwermann (2015) assumes the omnivorous diet could be responsible for the varieties, since different food sources with differing textures might affect the chewing pattern. Facet 5, though, is actually present on the original specimen. It is situated on the distal flank of the metaconid. However, in the virtual reconstruction of the chewing stroke it is fused with facet 1 on the distal flank of the protoconid. Therefore, the OFA is not able to distinguish between their contact areas and that of facet 5 is integrated into that of facet 1. Since both, facet 1 and facet 5, are formed by the same shear-cutting motion, it actually is not necessary to differentiate between them for this study. Furthermore, a fusion of these facets is also very common on more heavily worn molars. (For a more detailed analysis of the chewing motion and molar functions of *Didelphis* see Schwermann 2015.)

In *Didelphis*, the main shear-cutting contacts of facet 1 (+5) and 2 take up 62 % of phase 1 (21 out of 34 time steps) (fig. 52). This means 38 % of phase 1 (13 out of 34 time steps) are used primarily for grinding. Phase 2 is completely dominated by grinding (10 out of 10 time steps) without a single shear-cutting contact. In *Haldanodon* shear-cutting makes up at least 88 % of phase 1/1a (15 out of 17 time steps). Only 12 % (2 out of 17 time steps) is spent on the grinding contact of facet VI. Additionally, these 12 % are still dominated by the shear-cutting contacts of facets III to V that occur at the same time. This also does not change significantly if cusp Y slips out of the “pseudotalonid basin” immediately before centric occlusion, allowing cusp b to contact the “pseudotrigon basin” for a short grinding motion. Phase 1b is clearly dominated by the shear-cutting contact of facet III, which lasts throughout the entire phase. Only 7 % (2 out of 29 time steps) of phase 1b account for the grinding contact of facet VI. The same is true for the phase 2 scenario, the only difference being that shear-cutting is replaced by “shear-grinding”. Referred to the entire power stroke *Didelphis* spents 48 % (21 out of 44 time steps) on shear-cutting and 52 % (23 out of 44 time steps) on grinding. *Haldanodon* on the other hand spents 91 % (42 out of 46 time steps) of its power stroke solely on shear-cutting and only 9 % (4 out of 46 time steps) on grinding. Therefore, the relative amount of time spent on grinding is undoubtedly much higher in *Didelphis* than in *Haldanodon*. Even if in the phase 2 scenario for *Haldanodon* “shear-grinding” is counted as grinding and the amount of time spent on this function significantly rises to 67 % (31 out of 46 time steps), it is much more comparable to

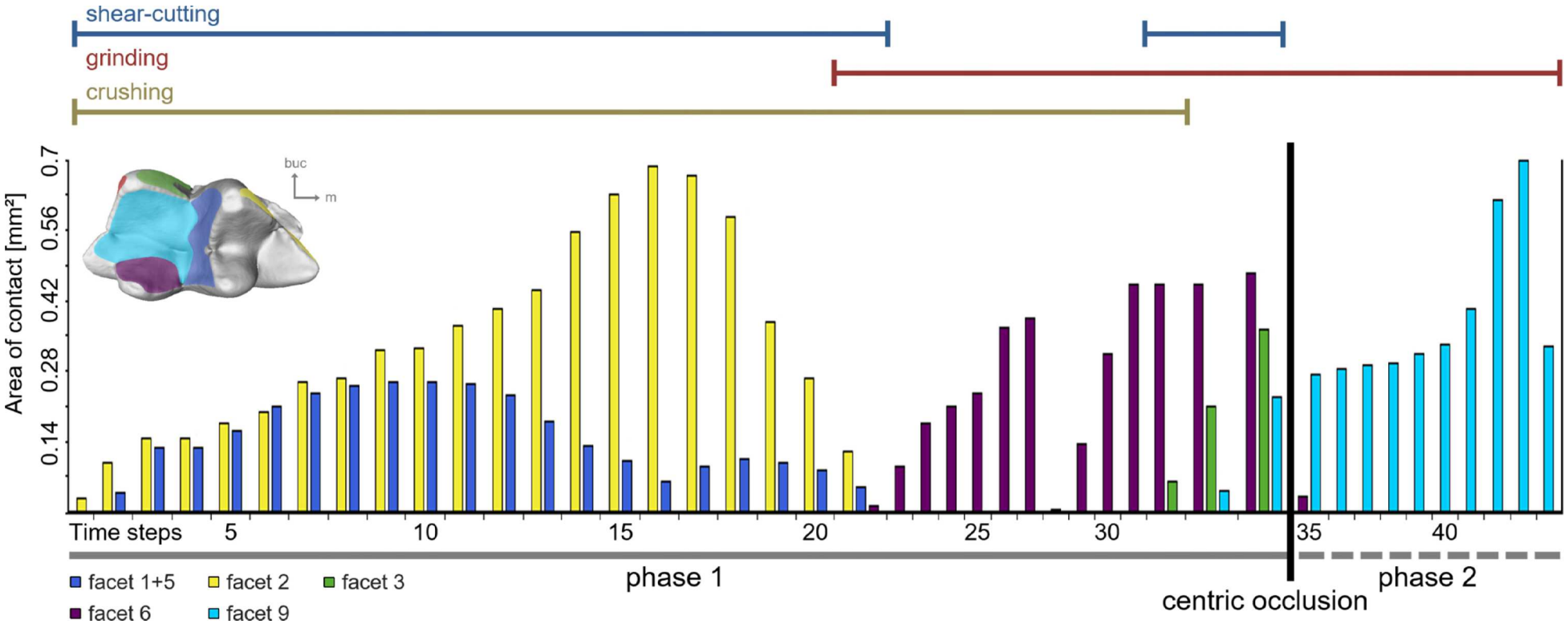

Fig 52: Tooth-tooth-contact diagram for *Didelphis* showing the size of the contact area for each lower molar facet during a certain time step throughout the chewing stroke from first to last contact of the molars as well as the duration of shear-cutting, grinding, and crushing functions. Since crushing produces no wear facets, the duration of this function is inferred from the animation of the chewing cycle with the OFA. *Didelphis* has a bi-phased power stroke, with a mesio-lingual upward movement of the lower molars into centric occlusion (phase 1) followed by a lingual downward movement (phase 2). Most of phase 1 is taken up by the shear-cutting contacts of facets 1+5 (dark blue), 2 (yellow), and 3 (green) as well as the crushing conducted by the protocone within the talonid basin (before it establishes contact with the bottom of the basin) and by the hypoconid within the trigon basin. Grinding facet 6 (violet) is in contact during the last third of phase 1. Phase 2 is completely taken up by the grinding contact of facet 9 (light blue). Crushing cannot take place in phase 2 due to the downward movement of the lower molars. Facet 4 (red) is not developed on the original specimen and therefore does not occur in the contact diagram. (lower molar model: m2 of SMF 77266)

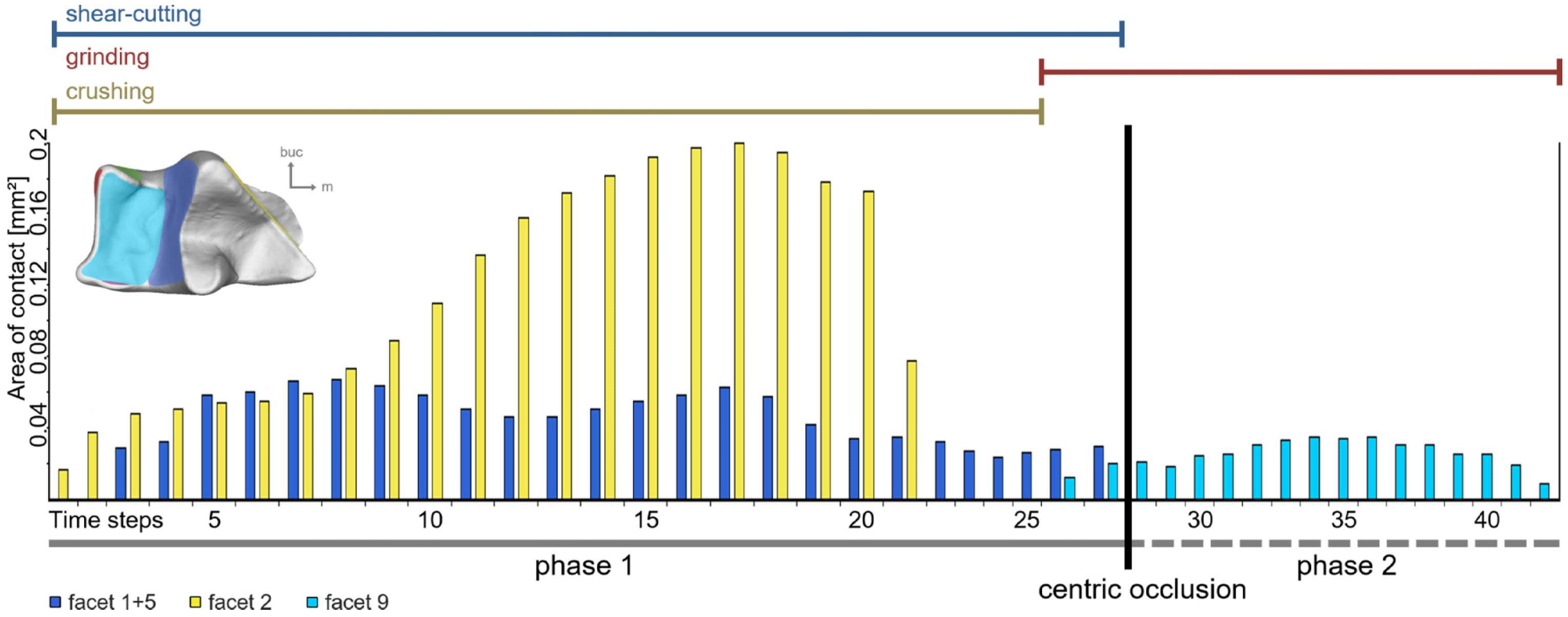

Fig 53: Tooth-tooth-contact diagram for *Monodelphis* showing the size of the contact area for each lower molar facet during a certain time step throughout the chewing stroke from first to last contact of the molars as well as the duration of shear-cutting, grinding, and crushing functions. Since crushing produces no wear facets, the duration of this function is inferred from the animation of the chewing cycle with the OFA. *Monodelphis* has a bi-phased power stroke very similar to that of *Didelphis*, with a mesio-lingual upward movement of the lower molars into centric occlusion (phase 1) followed by a lingual downward movement (phase 2). Phase 1 is taken up by the shear-cutting contacts of facets 1+5 (dark blue), and 2 (yellow) as well as the crushing conducted by the protocone within the talonid basin (before it establishes contact with the bottom of the basin) and by the hypoconid within the trigon basin. Phase 2 is completely taken up by the grinding contact of facet 9 (light blue). Crushing cannot take place in phase 2 due to the downward movement of the lower molars. The heavy wear of the specimen used for the analysis does not much interfere with the functions since it mainly concentrates on the basins. Facet 3 (green) and facet 6 (violet) are not present on the original specimen and therefore do not occur in the contact diagram. Facet 4 (red) is present on the original specimen but could not be reproduced with the OFA. (lower molar model: m2 of ZMB MAM 35496)

grinding with a grater than grinding with a mortar. Shear-cutting and grinding are also not as well separated in *Haldanodon* as in *Didelphis*: As mentioned above, in *Haldanodon* shear-cutting also takes place at the same time as grinding whereas in *Didelphis* this is only the case for a very short time when facet 3 establishes contact in addition to facet 6 and 9 immediately before centric occlusion. The importance of shear-cutting for *Haldanodon* is also shown by the fact that the main shearing facets I, II, and III are by far the largest facets (up to 0.36 mm², 0.24 mm², and 0.33 mm²). The grinding facet VI in comparison is rather small (up to 0.14 mm²). In *Didelphis*, on the contrary, shearing facets 1 and 2 (up to 0.24 mm², and 0.7 mm²) are distinctly smaller or the same size as grinding facets 6 and 9 (up to 0.49 mm², and 0.7 mm²). This also emphasizes that the grinding function is much more distinct in *Didelphis* than it is in *Haldanodon*.

Nevertheless, according to Schwermann (2015) in *Didelphis* the crushing conducted by the protocone within the talonid basin and at the same time by the hypoconid within the trigon basin is more important than the grinding functions of these cusps. This is certainly true for phase 1, since crushing is performed also during the shear-cutting contacts of facets 1(+5) and 2 within both the talonid and the trigon basin. As mentioned above, the hypoconid also continues its crushing function within the trigon basin in the time the protocone moves through the talonid basin in a grinding motion. The crushing persists until both cusps contact each other immediately before centric occlusion. Therefore, in *Didelphis* a total of 94 % of phase 1 (32 out of 34 time steps) is used for crushing. In *Haldanodon*, crushing takes place during the entire first phase. Since the amount of time spent on this function is more or less the same in both taxa, in this case the size and seclusion of the basins and other crushing surfaces is more important to determine functional differences. The crushing basins of *Didelphis* are more closed than those of *Haldanodon* are. Additionally, while trigon basin and “pseudotrigon basin” are more or less the same size, the talonid basin is proportionally much larger than the “pseudotalonid basin”. Therefore, it appears that *Didelphis* molars are more specialized in crushing than *Haldanodon* molars. This difference would be somewhat reduced if *Haldanodon* indeed used a separate upward mandible movement (phase 1b). Then, in contrast to *Didelphis*, crushing was also taking place during the second phase and would have overall persisted over a considerably longer time span than in *Didelphis*. In any case, the amount of lateral crushing (in between the lingual flank of cusp b and the buccal flanks of cusps X and Y) is also much more distinct in *Haldanodon*. All in all, while the grinding function compared to *Haldanodon* is clearly more distinct in *Didelphis* molars, both taxa do not differ that much in the amount of molar crushing function, at least in the case of an independent upward jaw movement in docodonts.

However, that *Didelphis* molars are more specialized in grinding and maybe also crushing might not necessarily be true in comparison to the molars of other docodont taxa. It is to be expected that in *Simpsonodon*, for instance, crushing and grinding will dominate both phases (see also 6.4.7). Its basins are also much better enclosed than those of *Haldanodon* are. In fact, the "pseudotalonid basin" of *Simpsonodon* is even better enclosed than the buccally opening talonid basin of *Didelphis*. Of course, it still is proportionally much smaller than the talonid basin but this is compensated to a certain degree by the presence of a second (albeit relatively open) distal basin on the lower molar. The "pseudotrigon basin" of *Simpsonodon* is proportionally at least as large and well-enclosed as the trigon basin of *Didelphis*. Therefore, compared to *Didelphis*, *Simpsonodon* molars might have been at least equally or even more specialized in crushing. This is especially the case if indeed the second phase of the docodont chewing stroke was a separate upward movement of the molars into centric occlusion.
Therefore, the difference in importance of the grinding and crushing functions of molars belonging to *Haldanodon*, *Simpsonodon*, and *Didelphis* might rather reflect the different diets consumed by these taxa. To process the probably mostly insectivorous diet of *Haldanodon* (Martin 2000, Martin and Nowotny 2000) shear-cutting and crushing are the most important functions. The diet of *Simpsonodon* probably contained a fair amount of plant material, which is processed best by grinding and crushing (Pfretzschner et al. 2005). The omnivorous diet of *Didelphis* (Gardner 1982, Schwermann 2015) requires a broad spectrum of functions to process. This is why, although *Didelphis* better embodies the original tribosphenic tooth morphology, a second comparison taxon, *Monodelphis*, was chosen for this study. Its mainly insectivorous diet (Macrini 2004, Schwermann 2015) much closer resembles the one postulated for *Haldanodon*.

6.5.2 Comparison of molar functions in *Monodelphis* and *Haldanodon*

Monodelphis belongs to the Didelphimorphia as well and its tooth morphology does not differ very much from that of *Didelphis*. For one, *Monodelphis* has slightly higher cusps with steeper flanks. More importantly, in comparison to *Didelphis* its talonid basin less resembles that of Cretaceous marsupials such as *Alphadon* and *Protolambda*. It is much smaller, shallower, and less well-enclosed (see fig. 120 in Schwermann 2015). However, this certainly is an adaptation to its insectivorous diet. To a lesser extent, this trend also can be seen within two distinct species of *Alphadon*. According to Schwermann (2015), the insectivorous *A. wilsoni* has a distinctly smaller talonid basin than the frugivorous *A. halleyi* (see also fig. 120 in Schwermann 2015). The molar morphology of *Haldanodon* with its high cusps, steep flanks, and more or less sharp

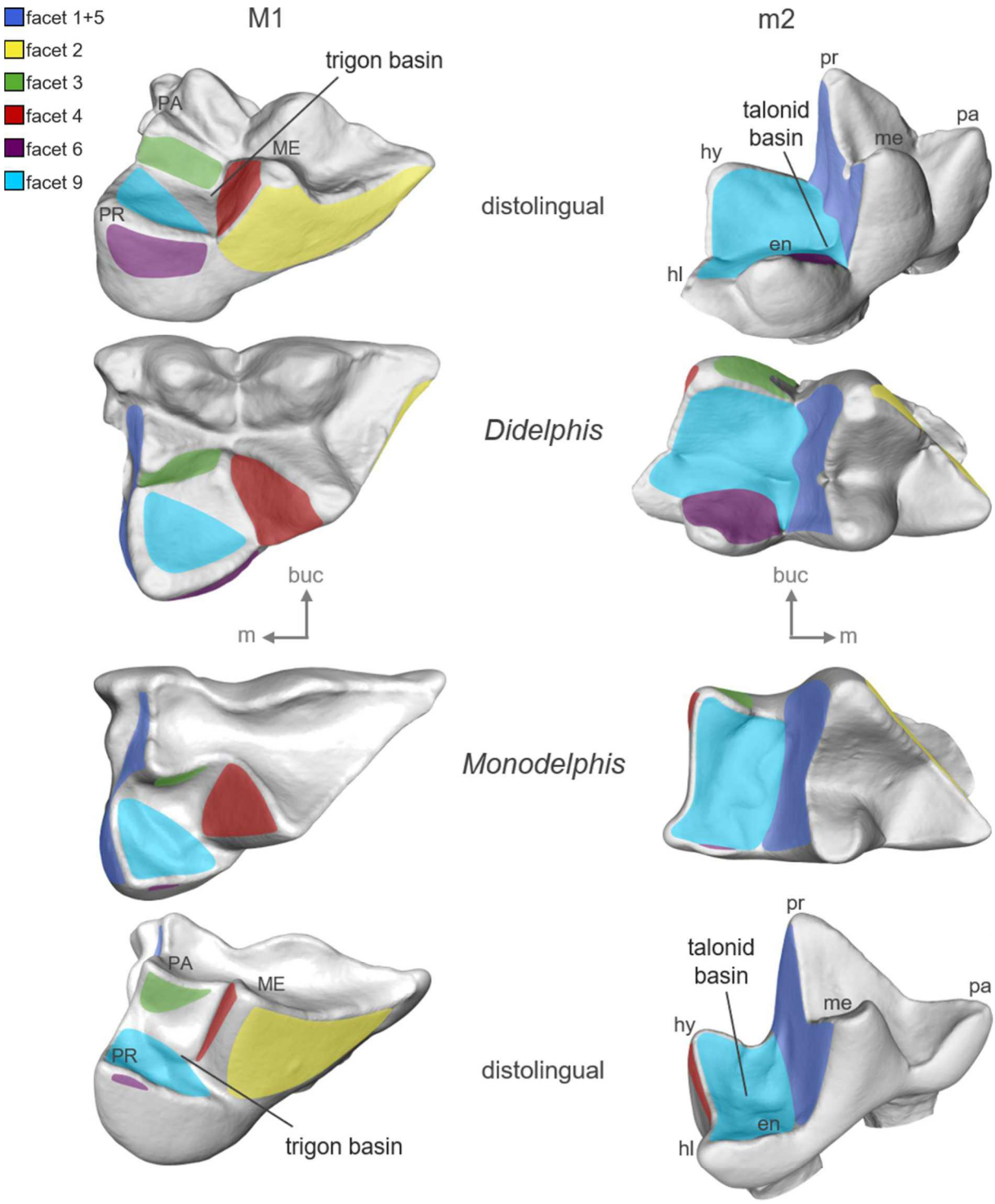

Fig. 54: Facet positions on tribosphenic molars of *Didelphis* (above) and *Monodelphis* (below) (molar models *Didelphis*: SMF 77266, molar models *Monodelphis*: ZMB MAM 35496). The talonid basin of *Monodelphis* is much smaller, shallower and less well-enclosed than that of *Didelphis*, most probably as adaptation to its more insectivorous diet. Additionally, the very small entoconid seldom establishes contact with the protocone, resulting in a much smaller facet 6. Many *Monodelphis* specimens even lack this grinding facet. Note that the wear of the *Monodelphis* molars is concentrated on the basins and does not yet affect the crests. Therefore, its influence on the size of the facets and the functions of the molar is still minor.

ME – metacone, PA – paracone, PR – protocone; en – entoconid, hl – hypoconulid, hy – hypoconid, me – metaconid, pa – paraconid, pr – protoconid

crests also seems to be rather adapted to an insectivorous diet. Nevertheless, both *Monodelphis* and *Haldanodon* still clearly show the basic molar morphology of their respective orders. Therefore, precisely because of their slight deviations in morphology (presumably) as adaptation to insectivory their molar functions are probably better comparable than those of *Didelphis* and *Haldanodon* are.

The *Monodelphis* molars from the OFA project provided by A. H. Schwermann are already quite heavily worn (wear stage IVb out of five wear stages, see also figs. 56 and 57 in Schwermann 2015). However, cusps and crests are only very moderately affected by wear. On the lower molars it is mostly concentrated on the interior of the trigonid and the talonid basin, on the upper molar on the buccal shelf and the trigon basin (fig. 54). Therefore, the surface area of the shearing facets is still more or less unaffected by the progressive wear (see also 6.5.3). The grinding facets are not affected as well since the dentine exposure within the basins does not prevent contact with the antagonistic cusp. Schwermann (2015) even equates the dentine field within the talonid basin with facet 9, a view that is confirmed by the OFA reconstruction. This is why the contact diagram of the *Monodelphis* molars is still well comparable with those of the less heavily worn *Haldanodon* and *Didelphis* molars.

The power stroke of *Monodelphis* is almost identical to that of *Didelphis*: the mesio-lingual movement of phase 1 is directed slightly more lingually, the lingual movement of phase 2 slightly more distally. Just like in *Didelphis*, at the beginning of the power stroke the distal flanks of proto- and metaconid glide along the mesial flanks of para- and protocone in a shear-cutting motion that produces facet 1. At the same time, facet 2 is formed by shear-cutting of the mesial flanks of proto- and paraconid against the distal flanks of metacone and metacrista. Protocone and hypoconid simultaneously also conduct crushing within the talonid respectively trigon basin. In contrast to *Didelphis*, however, the entoconid usually does not contact the disto-lingual flank of the protocone. Therefore, the grinding contact of facet 6 often does not take place in *Monodelphis*. The protocone only commences its grinding function within the talonid basin when the lingual flank of the hypoconid contacts its buccal flank directly before centric occlusion. This grinding contact, which creates facet 9, then again is similar to that of *Didelphis*: it continues in phase 2 until protocone and hypocone lose contact, which marks the end of the power stroke. In *Monodelphis*, too, because of the downward motion no crushing takes place in this phase.

The contact diagram of the *Monodelphis* molars does not show any contacts for facets 3, 4, 5, and 6. Facets 3 and 6 are also not present on the original specimen. The absence of facet 3, usually situated on the buccal flank of the hypoconid, is not a result of the progressive wear, since this flank is still intact. Likewise, the absence of facet 6 is unlikely to result from the

relatively progressive wear within the talonid basin. According to Schwermann (2015), even less worn *Monodelphis* molars often lack those facets. If a specimen actually does show facet 6, it is always very small. This is attributed to the relatively small size of the entoconid – it seldom establishes contact with the protocone. Facet 4, however, is actually present on the original *Monodelphis* lower molar specimens but could not be reproduced with the OFA (see also Schwermann 2015). Facet 5 is present on the original specimen as well but is fused with facet 1. Therefore, it does not appear as a separate facet in the OFA analysis. (For a more detailed analysis of the chewing motion and molar function in *Monodelphis* see Schwermann 2015.)

In *Monodelphis*, the shear-cutting contacts of facets 1 (+5) and 2 take up all of phase 1 (27 out of 27 time steps) (fig. 53). Only 7 % of phase 1 are also used for grinding (2 out of 27 time steps). This is much closer to *Haldanodon* with 12 % accounting for grinding in the first phase than to *Didelphis* with 38 %. Phase 2 of *Monodelphis*, however, very much resembles that of *Didelphis* because all of it is spent on the continuation of this grinding contact (15 out of 15 time steps). This is much more than in *Haldanodon* with 7 % accounting for grinding in the second phase. Referred to the entire power stroke *Monodelphis* spents 60 % (25 out of 42 time steps) solely on shear-cutting – more than *Didelphis* with 48 % and less than *Haldanodon* with 91 %. Grinding takes up 40 % (17 out of 42 time steps) of the power stroke in *Monodelphis* – less than in *Didelphis* with 52 % and much more than in *Haldanodon* with 9%. Therefore, in *Monodelphis* grinding still takes up more time and additionally is better separated from the shear-cutting function than in *Haldanodon*. Nevertheless, the difference in the length of the grinding contact is smaller than that of *Haldanodon* compared to *Didelphis*. That in *Monodelphis* grinding is obviously much less distinct than in *Didelphis* is also shown by the maximum facet sizes: Shearing facet 2 (up to 0.2 mm^2) is much larger and facet 1 (up to 0.07 mm^2) at least slightly larger than grinding facet 9 (up to 0.05 mm^2). This is opposed to *Didelphis* molars on which grinding facets tend to be larger than shearing facets (see 6.5.1). Additionally, *Didelphis* molars possess not only one but two grinding facets. This further emphasizes that the grinding function is much less distinct in *Monodelphis* than it is in *Didelphis*. Nevertheless, the difference in size of shearing and grinding facets is not as distinct as in *Haldanodon*. Therefore, *Monodelphis* molars are still more specialized in grinding than *Haldanodon* molars are.

Unlike grinding, crushing indeed seems to be an important part of phase 1 in *Monodelphis*. Just like in *Didelphis* molars, it is conducted simultaneously to the shear-cutting by the protocone within the talonid basin and by the hypoconid within the trigon basin. Both cusps continue their crushing function until they contact each other immediately before centric occlusion. Therefore, 93 % of phase 1 (25 out of 27 time steps) are used for crushing. This is more or less the same

amount as the 94 % of *Didelphis*. However, both talonid and trigon basin of *Monodelphis* are proportionally distinctly smaller and shallower than those of *Didelphis* are. Additionally, the talonid basin is opening widely towards lingual and the trigon towards distal. In comparison, they are not much better enclosed than the “pseudotalonid” and “pseudotrigon basins” of *Haldanodon*. Nevertheless, the talonid basin of *Monodelphis* is still proportionally distinctly larger than the “pseudotalonid basin” of *Haldanodon*. On the other hand, the “pseudotrigon basin” of *Haldanodon* is distinctly larger than the trigon basin of *Monodelphis*. Therefore, the crushing function probably was at least as distinct in *Haldanodon* molars as in *Monodelphis* molars. If *Haldanodon* indeed had developed a separate upwards directed phase 1b, the importance of the crushing function in this taxon actually is higher than in *Monodelphis* due to the additional crushing taking place in the second phase.

All in all, although *Monodelphis* molars are still more specialized in grinding than those of *Haldanodon* are, *Haldanodon* molars most probably had a crushing function at least as well or even more distinct. Molars of *Hutegotherium* and *Sibirotherium* might even have had a similarly distinct grinding function as *Monodelphis* molars, although in comparison to other docodonts they have relatively high and steep cusps with very sharp crests and therefore most probably also had been insectivorous. This is because like all tegotheriids *Hutegotherium* and *Sibirotherium* possess a comparatively large and very well-enclosed “pseudotalonid basin” as well as a well-enclosed distal basin on the lower molars. They furthermore developed an accessory cusp Z on the upper molars to fit into the distal basin. With this, they gained an additional grinding structure. This not only significantly increased the surface area for the grinding function but also might have prolonged the amount of time spent on grinding during the second phase of the chewing stroke because the distal basin is comparatively deep. Even if the second phase in docodonts consisted of a downward directed chewing stroke, in contrast to *Haldanodon* molars the grinding function of *Hutegotherium* or *Sibirotherium* molars probably would not have lost much of its efficiency. This is because the well-enclosed distal basin much better prevents food from escaping than the distal crests of *Haldanodon*. Therefore, the presence of two well-enclosed basins on the lower molars of *Hutegotherium* and *Sibirotherium* might well have compensated for the (probably not that much) smaller amount of time spent on the grinding function compared to *Monodelphis*. However, whether this is actually the case will remain speculative until it can be tested with an OFA-analysis of the mastication movement of *Hutegotherium* or *Sibirotherium*.

6.5.3 Disparities of molar functions in between tribosphenids and docodonts

Comparisons of “pseudotribosphenic” and tribosphenic tooth morphologies are usually related to the crushing and grinding functions. This is because the development of the talonid basin on the lower molar and the protocone occluding within this basin on the upper molar is widely accepted as the key innovation for tribosphenids. It is believed that this allowed them to very efficiently process a wide range of food, including plant material, which led to their high evolutionary success (Krebs 1988, Luo et al. 2001, Rauhut et al. 2002, Kielan-Jaworowska et al. 2004, Datta 2005, Luo 2007, Luo et al. 2007, Ungar 2010, Schultz and Martin 2014, Wang and Li 2016). Consequently, the tribosphenic molar is the basal tooth morphology from which evolved all molar morphologies of the modern mammals (save the monotremes) (Luo et al. 2001, Kielan-Jaworowska et al. 2004, Ungar 2010). Furthermore, even after more than 160 million years of evolution, the tribosphenic pattern is still present in Recent insectivorous mammalian taxa (e.g. talpids, soricids, erinaceids, golden moles, tenrecs, chiropterans, scandentians, and many marsupials). This is evidence that it still is the most efficient tooth morphology for processing insectivorous diets (Davis 2011, Schultz 2011).

However, this combination of a crushing basin on the lower molar and a cusp occluding within this basin on the upper molar had been independently developed up to three times in mammalian history before the development of the tribosphenic tooth morphology (see also 2.3.1) (Sigogneau-Russell et al. 2001, Luo et al. 2002, Luo 2007, Davis 2011). According to many authors, the crushing and grinding functions of these “pseudotribosphenic” molars probably were less well developed than those of the early tribosphenic molars were (Simpson 1929, Patterson 1956, Rauhut et al. 2002, Sigogneau-Russell 2003, Averianov and Lopatin 2008, Wang and Li 2016). Concerning the “pseudoprotocone”, this is definitely correct at least for docodonts because cusp X does not occlude within the “pseudotalonid basin” but in between two lower molars. This is why it is not a functional homolog to the protocone (see 6.4). The most important “function” of the docodont “pseudoprotocone” is to provide a shear-cutting plane (its mesial flank) and to contribute to the forming of the “pseudotrigon basin”. The tip of cusp X only served to puncture food during jaw closure. Nevertheless, the occlusion of the “pseudoprotocone” within the “pseudotalonid basin” still seems to be a widespread assumption (Hu et al. 2007, Luo 2007, Davis 2011, Rougier et al. 2014), even though this has never been suggested by any study concerning docodont occlusion. Instead, docodonts developed accessory cusp Y to pound into the “pseudotalonid basin” (Crompton and Jenkins 1968, Hopson and Crompton 1969, Jenkins 1969, Gingerich 1973, Kron 1979, Krusat 1980, Kermack et al. 1987, Butler 1988, Pfretzschner et al. 2005, Luo and Martin 2007). Additionally, most

docodonts shifted their main crushing and probably also grinding function to the "pseudotrigon basin" of the upper molar, conducted by cusp b of the lower molar. Other docodonts (*Hutegotherium* and *Sibirotherium*) instead developed an additional distal basin on the lower molar and another accessory cusp (Z) on the upper molar that pounds into it (see 6.4.7). Therefore, at least in slightly worn docodont molars the crushing and even the grinding function might well have been equally distinct as in early tribosphenic molars (see 6.5.1 and 6.5.2).

Concerning the shear-cutting function of docodont molars, some authors such as Butler (1988) and Wang and Li (2016) believe it to be not as well developed as that of tribosphenic molars as well. They postulate that docodonts did neither have really sharp crests nor the very precise occlusion necessary for efficient shear-cutting. It is certainly true that crests on *Haldanodon* molars appear rather blunt and their enamel surface is quickly abraded. Additionally, the high individual variability of occlusion within the species and even within the individual suggests that indeed occlusion in *Haldanodon* might not have been very precise (see 6.3). This is furthermore indicated by the fact that striations on the facets are not always strictly parallel, even if they are caused by the same direction of movement. Facets often have quite blurred outlines as well, although this might also be an effect of the exceptionally high abrasion rates in *Haldanodon*. However, highly variable occlusional patterns also could be verified for the tribosphenic comparison taxon *Didelphis* by Schwermann (2015). Moreover, crests on the molars of some other docodont taxa, e.g. the tegotheriids, are much sharper even in moderately worn molars. Therefore, some docodonts probably had a just as well-developed molar shear-cutting function as early tribosphenids.

However, there is another very important factor influencing the overall efficiency of a molar: the preservation of its functions over the lifespan of the animal. This is because the animal's fitness and reproduction success very much depend on the optimal exploitation of the nutrients in its food. Since abrasion ultimately leads to the loss of any function but simple crushing, enamel thickness has a profound impact on the durability of the molars. The enamel of docodonts is generally much thinner than that of tribosphenids. Therefore, docodont molars probably wore down much faster than those of the tribosphenids did, even though most certainly not all docodont taxa had as exceptionally high abrasion rates as the fossorial *Haldanodon*. The faster abrasion of the molar morphology in docodonts means that they could not maintain their molar functions for as long throughout life as the tribosphenids could. The profound influence of enamel thickness on wear patterns and molar functions has been studied in detail by Schultz (2011) (see also Schultz and Martin 2011). A thick enamel layer does not only wear down more slowly and also better supports the dentine, if exposed, slowing down abrasion even more. Some tribosphenids additionally adapted the thickness of their enamel to ensure a long

maintenance of sharp shear-cutting edges. This is achieved with a combination of thick enamel on one side of the crest and thin enamel on the other. The thin enamel edge as well as the dentine exposed on its side are abraded faster and therefore always are towered over by the thick enamel edge, preventing the crest from getting blunt. This mechanism is used for example in the trigonid of *Monodelphis* and some extant eulipotyphlans (Schultz 2011, Schultz and Martin 2011, Schwermann 2015). Therefore, although the development of the tribosphenic tooth morphology indeed was a very important innovation for the therians, the simultaneous strengthening of the enamel layer might have been just as crucial.

On the other hand, this also shows that the docodont tooth morphology was most certainly able to successfully compete with pretribosphenic molars like that of the dryolestids, which also have comparatively thin enamel (Schultz 2011, Schultz and Martin 2011). Additionally, the power stroke of these pretribosphenic mammals lacks a second phase (Schultz 2011, Schultz and Martin 2014, Schwermann 2015). In any case, the European localities Forest Marble (Middle Jurassic, Great Britain), and Guimarota (Late Jurassic, Portugal), as well as the Asian localities Berezovsk (Middle Jurassic, Russia), Tashkumyr 1 (Middle Jurassic, Kyrgyzstan), and Liuhuanggou (Late Jurassic, China) yielded not only docodonts but also representatives of amphitheriids, and except Liuhuanggou also dryolestidans (Kühne 1968, Freeman 1979, Krebs 1991, 1998, Martin 1999, 2000, Lopatin and Averianov 2009, Averianov et al. 2010, Martin and Averianov 2010, Martin et al. 2010a). In various localities of the Late Jurassic Morrison Formation (USA) *Docodon* was found together with several dryolestid taxa (Kielan-Jaworowska et al. 2004). Both, dryolestids as well as amphitheriids, possess an unicuspid talonid to prevent over-occlusion, but did not yet develop a talonid basin or a protocone (Crompton 1971, Martin 1999, Davis 2011, Schultz and Martin 2011). The only known locality of Early Cretaceous age that yielded a docodont taxon (Shestakovo, Russia) also contained a "peramuran" (Maschenko et al. 2002, Lopatin and Averianov 2009). "Peramurans" developed a bicuspid talonid that confined an incipient basin as well as a lingual cingulum on the upper molar as precursor to the protocone (Crompton 1971, Davis 2011). Interestingly, in the Middle Jurassic locality Daohugou docodonts also coexisted with another "pseudotribosphenic" taxon, the shuotheriids (Luo et al. 2007). If *Itatodon* and *Paritatodon* indeed are not docodonts but shuotheriids as recently postulated by Wang and Li (2016), this is also the case in the Middle Jurassic localities Forest Marble, Berezovsk, and Tashkumyr 1 (Martin and Averianov 2010).

Of course, non-dental characters also play a very important role in interspecific competition. Chow and Rich (1982) as well as Sigogneau (1998), for example, assume that the shuotheriids could not fully exploit the benefits of their "pseudotribosphenic" tooth morphology because the primary jaw joint was still in function, restricting the mandible movement. In docodonts, the

primary jaw joint was already replaced by the secondary ones as the only functional articulation (Henkel and Krusat 1980, Lillegraven and Krusat 1991, Averianov et al. 2005). Furthermore, Krusat (1980) suggested that the flattened and oval form of the secondary jaw joint allowed a great deal of freedom of movement. This is also implicated by the relatively complex masticatory movement of *Haldanodon* determined in the present study (see 6.4). However, docodonts do show other rather plesiomorphic characters, e.g. the presence of a large interclavicle and an unfused coracoid in the shoulder girdle, indicating a sprawling posture like in monotremes (Henkel and Krusat 1980, Krebs 1988, Krusat 1991, Martin 2005, Ji et al. 2006, Kielan-Jaworowska and Hurum 2006, Luo et al. 2015). Furthermore, the wide size range of humeri and femora indicates a lifelong growth (Martin 2005). Therefore, it is very likely that characters influencing for example locomotion, metabolism or reproduction rate also played a significant role in the decline of the docodonts. Kermack et al. (1987) even speculated that the docodonts did only last as long as they did alongside the therians because they at least had the advantage of a more efficient tooth morphology. When the therians finally developed the tribosphenic tooth morphology, the docodonts were no longer able to compete with them and became extinct. That indeed, besides the less durable molar structure, non-dental characters also played a significant role in their decline is strongly suggested by the fact that although the docodonts had no trouble living side-by-side with the pretribosphenic dryolestids, the latter coexisted much longer with the tribosphenids than the docodonts did. Some South American dryolestid taxa even survived the great extinction until the beginning of the Neogene (Chimento et al. 2012) (fig. 2). Docodonts most probably had their highest diversity in the Middle Jurassic with seven known genera (Maschenko et al. 2002, Kielan-Jaworowska et al. 2004, Martin and Averianov 2004, Lopatin and Averianov 2005, Pfretzschner et al. 2005, Ji et al. 2006, Luo and Martin 2007, Davis 2011, Luo et al. 2015, Meng et al. 2015; see also 2.1). As far as is known yet, the first true tribosphenic taxon with a protocone on the upper molars and a fully basined, tricuspid talonid on the lower molars was the Late Jurassic *Juramaia* (Luo et al. 2011). In the Early Cretaceous a first radiation took place within the tribosphenids, leading to the occurrence of the earliest known metatherians and eutherians (Kielan-Jaworowska et al. 2004, Ungar 2010). Docodonts, on the other hand, with five known genera had been still quite abundant in the Late Jurassic but are only known from a single genus (*Sibirotherium*) in the Early Cretaceous (Maschenko et al. 2002, Kielan-Jaworowska et al. 2004, Martin and Averianov 2004, Lopatin and Averianov 2005, Pfretzschner et al. 2005, Ji et al. 2006, Luo and Martin 2007, Davis 2011, Luo et al. 2015, Meng et al. 2015; see also 2.1). It was moreover found in a Siberian locality that totally lacks any tribosphenic taxa (Lopatin et al. 2009, Averianov et al. 2015). Docodont taxa from localities younger than Early Cretaceous are not known so far. In

the tribosphenids, on the other hand, another radiation occurred in the Late Cretaceous during which they gradually began to modify the basal tribosphenic tooth morphology towards the first more specialized dentitions (Ungar 2010). The major radiation of tribosphenids, however, took place not until after the great extinction event at the Cretaceous/Paleogene boundary. During this time most modern mammalian orders appeared and the tribosphenic tooth morphology developed into the various much more specialized patterns known today (Kielan-Jaworowska et al. 2004, Ungar 2010).

7 Summary

The development of the tribosphenic tooth morphology with a crushing basin (talonid basin) on the lower and an interlocking cusp (protocone) on the upper molar is regarded as a key innovation within the therian stem line that allowed a very efficient processing of food by crushing and grinding during mastication. All extant mammals save the monotremes descend from a tribosphenic ancestor (Simpson 1936, Patterson 1956, Mills 1966, Crompton and Hiiemäe 1970, Crompton 1971, Butler 1972, Prothero 1981, Luo et al. 2001, Woodburne et al. 2003, Kielan-Jaworowska et al. 2004, Datta 2005, Lopatin and Averianov 2006, Luo 2007, Luo et al. 2007, Davis 2011). The first fully tribosphenic taxon is known from the Upper Jurassic (Luo et al. 2011). However, the first taxon in mammalian history to develop a very similar tooth morphology with a mesially situated crushing basin on the lower and an interlocking cusp on the upper molar were the mammaliaform docodonts (Middle Jurassic to Early Cretaceous) (Simpson 1929, Crompton & Jenkins 1968, Hopson and Crompton 1969, Jenkins 1969, Gingerich 1973, Krusat 1980, Kermack et al. 1987, Butler 1988, Butler 1997, Wang et al. 1998, Pfretzschner et al. 2005, Luo 2007, Luo and Martin 2007, Luo et al. 2007, Davis 2011, Schultz et al. 2017). To examine whether their "pseudotribosphenic" molar morphology is actually similar to the tribosphenic one, several upper and lower molar rows as well as numerous isolated molars of the Late Jurassic docodont *Haldanodon exspectatus* from the Guimarota coal mine (Leiria, Portugal) were studied in detail.

To quantify the amount of time spend on different mastication functions, a virtual simulation of the chewing stroke of *Haldanodon* was created with the open source software Occlusal Fingerprint Analyser (OFA), using 3D-models of un upper and two lower molars compiled from µ-CT scans. To enable the inclusion of the isolated molar specimens into the material from which to choose the most suitable models, an attempt was made to refer isolated molars to their former tooth position in the dental row. Although mean values of molar length and width of different upper and lower molar positions vary significantly, their range of values overlap to a great extent, probably reflecting relatively high size differences in adult individuals. Therefore, it is almost impossible to distinguish molar positions by a simple plot of length against width.

During the process of taking measurements under the stereomicroscope, an unusual abrasion pattern could be observed in upper as well as lower molar rows. Rows with a low degree of wear are usually mesially stronger worn, rows with a high degree of wear usually distally stronger. This implies a correlation of the direction of increasing wear with ontogenetic age - an initially mesially stronger worn molar row became more and more distally stronger worn in

time. That two juvenile lower jaw specimens are both mesially stronger worn, although one shows a high degree of overall wear, supports this hypothesis. A change of the direction of wear during ontogeny could be explained with a distally situated chewing focus in combination with thin enamel and highly abrasive food. This might have been unique for *Haldanodon*, since such an abrasion pattern could not be observed in other docodont taxa.

The positions of the matching facets on upper and lower molar suggest that the upper molar occludes in between two lower molars. The mesial part of the upper molar contacts the distal half of one lower molar and the distal part of the upper molar the mesial half of the following lower molar. In this position the “pseudoprotocone” cusp X rests in between the lower molars and the more distally situated accessory cusp Y occludes within the “pseudotalonid basin” of the distally situated lower molar. Therefore, cusp X is not a functional homolog to the tribosphenic protocone. This is in accordance with previous studies on various docodont taxa (Crompton and Jenkins 1968, Jenkins 1969, Gingerich 1973, Kron 1979, Krusat 1980, Kermack et al. 1987, Butler 1988, Pfretzschner et al. 2005, Schultz et al. 2017).

To determine the orientation of the movement of the lower molars during the chewing stroke for the OFA simulation, striation patterns were studied on SEM images of a few selected isolated *Haldanodon* molars. Vertical striae that abruptly deflect towards distal on the upper and mesial on the lower molar imply a lateral movement that immediately before centric occlusion gains a considerable proal or palinal component. Striae oriented towards mesial on the upper and distal on the lower molar indicate a second proal or palinal movement in an opposing direction. This was reconstructed as a power stroke with two phases. Phase 1 is a steep upward movement from buccal to lingual of the lower molars into centric occlusion with an abrupt change towards distal at the very end. The second phase is either a downward palinal movement following centric occlusion (phase 2) or a separate upward proal movement (phase 1b). In either case the movement also has a distinct lateral motion component. While the observed leading and trailing edges indicate that phase 1 must have been directed upwards, they are ambiguous for the second phase. They rather seem to imply a downward continuation of the power stroke, which is also more probable from an actualistic point of view. However, they are not distinct enough to clearly rule out an alternatively used upward movement, although this is not known yet from any extant or fossil mammalian taxon. An upward movement would also make more sense form a functional point of view, since shear-cutting can only be performed with significant effort in a downward movement. In any case, the present reconstruction of the power stroke corrects previous studies on various docodont taxa, which either postulated a single chewing stroke ending in centric occlusion (Crompton and Jenkins

1968, Hopson and Crompton 1969, Jenkins 1969, Krusat 1980) or a bi-phased one without change of direction (Butler 1988, Pfretzschner et al. 2005).

In phase 1 the lingual flanks of the upper molar main cusps and the buccal flanks of the lower molar main cusps pass each other in a shear-cutting motion. At the same time, cusp b of the distal lower molar performs extensive crushing within the "pseudotrigon basin" of the upper molar. As soon as the straight mesio-buccal groove of the lower molar loses contact with cusp C of the upper molar, the initially lateral movement becomes palinal. Immediately before centric occlusion, cusp Y slides into the "pseudotalonid basin" to conduct a grinding function. However, as soon as the mesial border of the basin is worn down cusp Y slips out, causing the closure of the gap in between cusp b and the "pseudotrigon basin", which are then able to perform grinding as well. This is indicated by corresponding leading and trailing edges on the mesial border of the "pseudotalonid basin" and the presence of distally inclined striae within the "pseudotrigon basin". Consequently, the majority of crushing and probably even grinding is actually taking place within the large "pseudotrigon basin" of the upper molar. During the palinal downward motion of phase 2, for a very short time cusp Y continues to grind through the "pseudotalonid basin" (respectively cusp b through the "pseudotrigon basin"). At the same time and proceeding throughout the entire phase the distal crests of the mesially situated lower molar pass the mesial flank of cusp X in a "shear-grinding" motion. True shear-cutting is only possible in an upward motion like that of the proal movement in phase 1b. In this case, cusp b of the distal molar simultaneously also conducts crushing within the "pseudotrigon basin" and the grinding of cusp Y trough the "pseudotalonid basin" takes place at the very end of the phase.

The basic molar tooth morphology of other docodonts is generally quite similar to that of *Haldanodon*. Isolated molars of *Dsungarodon*, *Tashkumyrodon*, and *Tegotherium* also show the same main facets. This makes a similar chewing stroke very likely. Nevertheless, due to comparatively minor differences in tooth morphology docodonts can be classified into three different functional groups. Docodonts with mesially opening "pseudotalonid basins" and laterally running lower distal crests (*Borealestes*, *Docodon*, *Docofossor*, *Haldanodon*, *Tashkumyrodon*) mostly relied on shear-cutting and concentrated crushing on the "pseudotrigon basin" of the upper molar, conducted by cusp b. This cusp also was able to perform grinding if cusp Y slipped out of the "pseudotalonid basin". Docodonts with well-enclosed "pseudotalonid basins" and an additional lower distal basin (*Hutegotherium*, *Sibirotherium*, *Tegotherium*) were much more specialized in crushing and grinding, which they focused on the lower molar. Some even developed an additional cusp on the upper molar to pound into the distal basin. Docodonts with well-enclosed "pseudotalonid basins", laterally running lower distal crests or crenulations, and relatively low cusps (*Agilodocodon*, *Castorocauda*, *Dsungarodon*, *Krusatodon*,

Simpsonodon) were best adapted to crushing and grinding, although they were also capable of shear-cutting. This is because cusp b was able to perform crushing and grinding within the "pseudotrigon basin" simultaneously to cusp Y within the "pseudotalonid basin". All in all, crushing and even grinding was much more prominent in docodont molars than postulated in previous studies.

The reconstruction of the chewing movements with the OFA also allowed a comparison of molar functions of the insectivorous *Haldanodon* with those of the tribosphenic taxa *Didelphis* (omnivorous) and *Monodelphis* (insectivorous). In both tribosphenic taxa the protocone conducts grinding within the talonid basin. In *Didelphis* grinding lasts much longer than in *Monodelphis*, but *Haldanodon* spends even less time on this function. *Monodelphis* also lacks one of the didelphid grinding facets, but the remaining one is still comparatively larger than the grinding facet of *Haldanodon*. Therefore, grinding is obviously more distinct in both tribosphenic taxa than it is in *Haldanodon*. This is not necessarily true for crushing. In *Didelphis* and *Monodelphis* it is performed by the protocone within the talonid basin as well as the hypoconid within the trigon basin and just like in *Haldanodon* lasts almost throughout the entire phase 1. In phase 2 crushing cannot take place due to the downward motion of the lower jaw. However, if *Haldanodon* actually used two separate upward movements of the lower molars into occlusion, additionally the entire second phase would have been spent on crushing. Although the basins of *Didelphis* are better enclosed and much larger than those of *Haldanodon*, in this case the amount of crushing performed by their molars does not differ that much. Since the basins of *Monodelphis* are much smaller, shallower and less well-enclosed than those of *Didelphis* are, crushing in *Haldanodon* probably was at least as distinct as in *Monodelphis* even if the second phase of its power stroke was directed downward as well. Other docodont taxa with better enclosed "pseudotalonid" and "pseudotrigon basins" and additional distal basins on the lower molars certainly had a more distinct crushing ability than *Monodelphis* and maybe even an equally distinct one as *Didelphis*, even though some of them most probably also rather were insectivorous.

Although docodont molars might well have been able to compete with early tribosphenic molars in terms of crushing and even grinding function, their thin enamel layer made them much more prone to abrasion and the concomitant loss of function. Additionally, docodonts show some rather basal postcranial characters. Both factors might have played a significant role in their extinction in the Early Cretaceous – at the same time the tribosphenids began to prosper.

8 Acknowledgments

Many heartfelt thanks to Prof. Dr. Thomas Martin for his dedicated supervision and for always having a little time for spontaneous meetings despite his usually full schedule. He also kindly provided all docodont specimens included in this study as well as several valuable tips for literature.

Furthermore, I would like to thank the Deutsche Forschungsgemeinschaft (DFG) for funding my project within the research unit 771 ("Function and performance enhancement in the mammalian dentition - phylogenetic and ontogenetic impact on the masticatory apparatus").

My thanks to the members of the DFG research unit 771 – especially Anne Schubert, Achim and Leonie Schwermann, and Dr. Julia A. Schultz – as well as Romina Hielscher and Maren Jansen for many productive discussions and for always having a sympathetic ear concerning all kinds of questions and problems.

Dr. Julia A. Schultz (Rheinische Friedrich-Wilhelms-Universität Bonn, Bonn, Germany) I also thank for her excellent preparatory work, especially in the domain of methods, for readily providing this knowledge and for the initial training in 3D-reconstruction by means of Avizo and Polyworks and the processing of the 3D-models with the Occlusal Fingerprint Analyser. Moreover, she kindly provided her hard-earned synchrotron data for 3D-reconstruction.

I am very grateful to Dr. Achim H. Schwermann (LWL-Museum für Naturkunde, Münster, Germany) who was a great help in comparing the molar functions of *Haldanodon* with those of *Didelphis* and *Monodelphis* for he did not only discuss this topic at great length with me but also kindly provided the OFA projects for both tribosphenic taxa.

For very productive discussions I also would like to express my gratitude to Dr. Alistair Evans (Monash University, Melbourne, Australia) and Prof. Zhe-Xi Luo (University of Chicago, Chicago, USA).

Thanks also to Romina Hielscher who patiently teached me how to take pictures with the stereomicroscope and was a really big help whenever I had troubles with my figures. I also thank Thomas Engler for diligently 3D-scanning a lot of specimens.

Furthermore, I thank Marga Dietrich Busse, Beate Mühlens-Scaramuzza and Viktoria Kusserow who countless times helped me with administrative matters and acquisition of all kinds of materials as well as Peter Göddertz for technical support and Dorothea Kranz for tips on how to color 3D-prints.

Last but not least I would particularly like to thank my friends and family as well as the members of the Iaido sports club for their unwavering moral support. Especially the love of Florian and his daughter Lili, who decided to step into my life just at the right moment, has been a most needed emotional support. My dear friends Aiyana, Anne, Corinna, Katja, Lilith, Momo, and Romina did their very best to encourage me whenever I felt like giving up. So did my parents, my brother Mitja, and my sister Mascha who also provided me with a little extra money whenever they could afford it. Thus, I was able to concentrate on my study rather than on my wallet. In this regard I will also always be really grateful to Heinz who offered me a little part time job in his working group when I needed it the most. Thank you so very much everybody! Without all of you this study would probably never have been finished!

9 References

Averianov, A. O. (2004). Interpretation of the Early Cretaceous mammal *Peraiocynodon* (Docodonta) and taxonomy of some British Mesozoic docodonts. *Russian Journal of Theriology* 3: 1-4.

Averianov, A. O., A. V. Lopatin, P. P. Skutschas, N. V. Martynovich, S. V. Leshchinskiy, A. S. Rezvyi, S. A. Krasnolutskii, and A. V. Fayngertz (2005). Discovery of Middle Jurassic mammals from Siberia. *Acta Palaeontologica Polonica* 50: 789-797.

Averianov, A. O. and A. V. Lopatin (2006). *Itatodon tatarinovi* (Tegotheriidae, Mammalia), a Docodont from the Middle Jurassic of Western Siberia and Phylogenetic Analysis of Docodonta. *Paleontological Journal* 40: 668-677.

Averianov, A. O. and A. V. Lopatin (2008). “Protocone” in a pretribosphenic mammal and upper dentition of tinodontid “symmetrodontans”. *Journal of Vertebrate Paleontology* 28: 548-552.

Averianov, A. O., A. V. Lopatin, S. A. Krasnolutskii, and S. V. Ivantsov (2010). New docodontants from the Middle Jurassic of Siberia and reanalysis of Docodonta interrelationships. *Proceedings of the Zoological Institute of the Russian Academy of Sciences* 314: 121-148.

Averianov, A. O., A. Lopatin, P. Skutschas, and S. Leshchinskiy (2015). Two new mammal localities within the Lower Cretaceous Ilek Formation of West Siberia, Russia. *Geobios* 48: 131-136.

Barbour, M. E. and G. D. Rees (2006). The role of erosion, abrasion and attrition in tooth wear. *Journal of Clinical Dentistry* 17: 88-93.

Bi, S., X. Zheng, J. Meng, X. Wang, N. Robinson, and B. Davis (2016). A new symmetrodont mammal (Trechnotheria: Zhangheotheriidae) from the Early Cretaceous of China and trechnotherian character evolution. *Scientific Reports* 6: 1-9.

Bonaparte, J. F. (1990). New Late Cretaceous mammals from the Alamitos Formation, Northern Patagonia. *National Geographic Research* 6: 63-93.

Busch, M. and F. O. Kravetz (1991). Diet composition of *Monodelphis dimidiata* (Marsupialia, Didelphidae). *Mammalia* 55: 619-621.

Butler, P. M. (1939). The Teeth of the Jurassic Mammals. *Proceedings of the Zoological Society of London, Series B* 109: 329-356.

Butler, P. M. (1972). Some functional aspects of molar evolution. *Evolution* 26: 474-483.

Butler, P. M. (1988). Docodont Molars as Tribosphenic Analogues (Mammalia, Jurassic). *Mémoires du Muséum National d'Histoire Naturelle, Série C* 53: 329-340.

Butler, P. M. (1997). An alternative hypothesis on the origin of docodont molar teeth. *Journal of Vertebrate Paleontology* 17: 435-439.

Casella, J. and N. C. Cáceres (2006). Diet of four small mammal species from Atlantic forest patches in South Brazil. *Neotropical Biology and Conservation* 1: 5-11.

Chimento, N. R., F. L. Agnolin, and F. E. Novas (2012). The Patagonian fossil mammal *Necrolestes*: a Neogene survivor of Dryolestoidea. *Revista del Museo Argentino de Ciencias Naturales, Nueva Serie* 14: 261-306.

Chow, M. and T. H. V. Rich (1982). *Shuotherium dongi*, n. gen. and sp., a therian with pseudo-tribosphenic molars from the Jurassic of Sichuan, China. *Australian Mammalogy* 5: 127-142.

Clemens, W. A. (1966). Fossil mammals of the type Lance Formation Wyoming – Part II: Marsupialia. *University of California Publications in Geological Sciences* 62: 1-122.

Cornay, R. J. and A. J. Mead (2012). Analysis of enamel hypoplasia in opossums (*Didelphis virginiana*), Baldwin County, Georgia. *Georgia Journal of Science* 70: 87-91.

Costa, R. L. and W. S. Greaves (1981). Experimentally produced tooth wear facets and the direction of jaw motion. *Journal of Paleontology* 55: 635-638.

Crompton, A. W. (1971). The origin of the tribosphenic molar. *Zoological Journal of the Linnean Society* 50(Supp.1): 65-87.

Crompton, A. W. (1974). The dentitions and relationships of the southern African Triassic mammals, *Erythrotherium parringtoni* and *Megazostrodon rudnerae*. *Bulletin of the British Museum (Natural History), Geology series* 24: 397-437.

Crompton, A. W. (1995). Masticatory function in nonmammalian cynodonts and early mammals. In: *Functional Morphology in Vertebrate Paleontology*. Ed: J. J. Thomason. Cambridge, Cambridge University Press: 55-75.

Crompton, A. W. and F. A. Jenkins (1968). Molar occlusion in Late Triassic mammals. *Biological reviews of the Cambridge Philosophical Society* 43: 427-458.

Crompton, A. W. and K. Hiiemäe (1970). Molar occlusion and mandibular movements during occlusion in the American opossum, *Didelphis marsupialis*. *Journal of the Linnean Society of London, Zoology* 49: 21-47.

Crompton, A. W., A. J. Thexton, P. Parker, and K. Hiiemäe (1977). The activity of the jaw and hyoid musculature in the Virginian opossum, *Didelphis virginiana*. In: *The Biology of Marsupials*. Eds: B. Stonehouse and D. Gilmore. London, The MacMillan Press LTD: 287-305.

Datta, P. M. (2005). Earliest mammal with transversely expanded upper molar from the Late Triassic (Carnian) Tiki Formation, South Rewa Bondwana Basin, India. *Journal of Vertebrate Paleontology* 25: 200-207.

Davis, B. M. (2011). Evolution of the tribosphenic molar pattern in early mammals, with comments on the "dual-origin" hypothesis. *Journal of Mammalian Evolution* 18: 227-244.

Eccles, J. D. (1982). Tooth surface loss from abrasion, attrition and erosion. *Dental Update* 9: 373-381.

Evans, A. R. and G. D. Sanson (2003). The tooth of perfection: functional and spatial constraints on mammalian tooth shape. *Biological Journal of the Linnean Society* 78: 173-191.

Flynn, J. J., J. M. Parrish, B. Rakotosamimanana, W. F. Simpson, and A. R. Wyss (1999). A Middle Jurassic mammal from Madagascar. *Nature* 401: 57-60.

Freeman, E. F. (1979). A Middle Jurassic mammal bed from Oxfordshire. *Palaeontology* 22: 135-166.

Gardner, A. L. (1973). The systematics of the genus *Didelphis* (Marsupialia: *Didelphidae*) in North and Middle America. *Special Publications of The Museum, Texas Tech University* 4: 1-81.

Gardner, A. L. (1982). Virginia Opossum – *Didelphis virginiana*. In: *Wild Mammals of North America*. Eds: J. A. Chapman and G. A. Feldhamer. Baltimore, Johns Hopkins University Press: 3-36.

Gidley, J. W. (1906). Evidence bearing on tooth-cusp development. *Proceedings of the Washington Academy of Sciences* 8: 91-110.

Gingerich, P. D. (1973). Molar occlusion and function in the Jurassic mammal *Docodon*. *Journal of Mammalogy* 54: 1008-1013.

Gow, C. E. (1986). A new skull of *Megazostrodon* (Mammalia, Triconodonta) from the Elliot Formation (Lower Jurassic) of southern Africa. *Palaeontologia Africana* 26: 13-23.

Greaves, W. S. (1973). The inference of jaw motion from tooth wear facets. *Journal of Paleontology* 47: 1000-1001.

Grippo, J. O., M. Simring, and S. Schreiner (2004). Attrition, abrasion, corrosion and abfraction revisited: A new perspective on tooth surface lesions. *The Journal of the American Dental Association* 135: 1109-1118.

Hamilton, W. J. (1958). Life history and economic relations of the opossum (*Didelphis marsupialis virginiana*) in New York State. *Cornell University Agricultural Experiment Station Memoir* 354: 1-48.

Harper, T. and G. Rougier (2017). Systematic and functional implications of new material from the Late Cretaceous mammal *Reigitherium*. *Journal of Vertebrate Paleontology, Program and Abstracts* 2017: 125.

Helmdach, F. F. (1971). Stratigraphy and ostracod-fauna from the coal mine Guimarota (Upper Jurassic). *Memórias dos Serviços Geológicos de Portugal, N. S.* 17: 43-88.

Henkel, S. and G. Krusat (1980). Die Fossil-Lagerstätte in der Kohlengrube Guimarota (Portugal) und der erste Fund eines Docodontiden-Skelettes. *Berliner geowissenschaftliche Abhandlungen A* 20: 209–216.

Hiiemäe, K. M. and F. A. Jenkins (1969). The anatomy and internal architecture of the muscles of mastication in the American Opossum *Didelphis marsupialis*. *Postilla* 140: 1-49.

Hiiemäe, K.M., and A.W. Crompton (1971). A cinefluorographic study of feeding in the American opossum, *Didelphis marsupialis*. In: *Dental morphology and evolution*. Ed: A. A. Dahlberg. Chicago, University Chicago Press: 299–334.

Hopson, J. A. and A. W. Crompton (1969). Origin of Mammals. *Evolutionary Biology* 3: 15-72.

Hu, Y.-M., J. Meng, and J. M. Clark (2007). A New Late Jurassic Docodont (Mammalia) from Northeastern Xinjiang, China. *Vertebrata PalAsiatica* 45: 173-194.

Hunter, J. (1778). *The natural history of human teeth*. London, J. Johnson.

Hylander, W. L., C. E. Wall, C. J. Vinyard, C. Ross, M. R. Ravosa, S. H. Williams, and K. R. Johnson (2005). Temporalis function in anthropoids and strepsirrhines: an EMG study. *American Journal of Physical Anthropology* 128: 35-56.

Jenkins, F. A. (1969). Occlusion in *Docodon* (Mammalia, Docodonta). *Postilla* 139: 1-24.

Ji, Q., Z.-X. Luo, C.-X. Yuan, and A. R. Tabrum (2006). A Swimming Mammaliaform from the Middle Jurassic and Ecomorphological Diversification of Early Mammals. *Science* 311: 1123-1127.

Kay, R. F. and K. M. Hiiemäe (1974). Jaw movement and tooth use in recent and fossil primates. *American Journal of Physical Anthropology* 40: 227-256.

Kemp, T. S. (1983). The relationships of mammals. *Zoological Journal of the Linnean Society* 77: 353-384.

Kermack, K. A., F. Mussett, and H. W. Rigney (1973). The lower jaw of *Morganucodon*. *Zoological Journal of the Linnean Society* 53: 87-175.

Kermack, K. A., F. Mussett, and H. W. Rigney (1981). The skull of *Morganucodon*. *Zoological Journal of the Linnean Society* 71: 1-158.

Kermack, K. A., A. J. Lee, P. M. Lees, and F. Mussett (1987). A new docodont from the Forest Marble. *Zoological Journal of the Linnean Society* 89: 1-39.

Kielan-Jaworowska, Z., R. L. Cifelli, and Z.-X. Luo (1998). Alleged Cretaceous placental from down under. *Lethaia* 31: 267-268.

Kielan-Jaworowska, Z., R. L. Cifelli, and Z.-X. Luo (2004). *Mammals from the Age of Dinosaurs: Structure, Relationships, and Paleobiology*. New York, Columbia University Press.

Kielan-Jaworowska, Z. and J. H. Hurum (2006). Limb posture in early mammals: Sprawling or parasagittal. *Acta Palaeontologica Polonica* 51: 393–406.

Krebs, B. (1975). Zur frühen Geschichte der Säugetiere. *Natur und Museum* 105: 147-155.

Krebs, B. (1988). Mesozoische Säugetiere – Ergebnisse von Ausgrabungen in Portugal. *Sitzungsberichte der Gesellschaft Naturforschender Freunde zu Berlin, Neue Folge* 28: 95-107.

Krebs, B. (1991). Das Skelett von *Henkelotherium guimarotae* gen. et sp. nov. aus dem Oberen Jura von Portugal. *Berliner Geowissenschaftliche Abhandlungen, Reihe A* 133: 1–110.

Krebs, B. (1998). *Drescheratherium acutum* gen. et sp. nov., ein neuer Eupantotherier (Mammalia) aus dem Oberen Jura von Portugal. *Berliner Geowissenschaftliche Abhandlungen, Reihe E* 28: 91-111.

Krebs, B. (2000). The excavations in the Guimarota mine. In: *Guimarota – a Jurassic Ecosystem*. Eds: T. Martin and B. Krebs. Munich, Verlag Dr. Friedrich Pfeil: 9-20.

Kretzoi, M. (1946). On Docodonta, a new order of Jurassic Mammalia. *Annales historico-naturales Musei nationalis hungarici* 39: 108-111.

Kron, D. G. (1979). Docodonta. In: *Mesozoic Mammals - The First Two-Thirds of Mammalian History*. Eds: J. A. Lillegraven, Z. Kielan-Jaworowska, and W. A. Clemens. Berkeley, University of California Press: 91-98.

Krusat, G. (1980). Contribuição para o conhecimento da fauna do Kimeridgiano da mina de lignito Guimarota (Leiria, Portugal) - IV parte: *Haldanodon exspectatus* Kühne & Krusat 1972 (Mammalia, Docodonta). *Memórias dos Serviços Geológicos de Portugal* 27: 1-79.

Krusat, G. (1991). Functional morphology of *Haldanodon exspectatus* (Mammalia, Docodonta) from the Upper Jurassic of Portugal. Fifth Symposium on Mesozoic Terrestrial Ecosystems and Biota. Extended abstracts. *Contributions of the Paleontological Museum, University of Oslo* 364: 37–38.

Kühne, W. G. (1950). A symmetrodont tooth from the Rhaeto-Lias. *Nature* 166: 696-697.

Kühne, W. G. (1968). Kimeridge mammals and their bearing on the phylogeny of the Mammalia. In: *Evolution and Environment*. Ed: E. T. Drake. New Haven, Yale University Press: 109-123.

Kühne, W. G. & G. Krusat (1972). Legalisierung des Taxon *Haldanodon* (Mammalia, Docodonta). *Neues Jahrbuch für Geologie, Paläontologie und Mineralogie, Monatshefte* 1972: 300-302.

Lillegraven, J. A. and G. Krusat (1991). Cranio-mandibular anatomy of *Haldanodon exspectatus* (Docodonta; Mammalia) from the Late Jurassic of Portugal and its implications to the evolution of mammalian characters. *Contributions to Geology* 28: 39-138.

Lopatin, A. V. and A. O. Averianov (2005). A New Docodont (Docodonta, Mammalia) from the Middle Jurassic of Siberia. *Doklady Biological Sciences* 405: 434-436.

Lopatin, A. V. and A. O. Averianov (2006). An aegialodontid upper molar and the evolution of mammal dentition. *Science* 313: 1092.

Lopatin, A. V. and A. O. Averianov (2009). Mammals that coexisted with dinosaurs – Finds on Russian territory. *Herald of the Russian Academy of Sciences* 79: 268-273.

Lopatin, A. V., A. O. Averianov, E. N. Maschenko, and S. V. Leshchinskiy (2009). Early Cretaceous mammals of Western Siberia: 2. Tegotheriidae. *Paleontological Journal* 43: 453-462.

Luo, Z.-X. (1994). Sister-group relationships of mammals and transformations of diagnostic mammalian characters. In: *In the shadow of the dinosaurs*. Eds: N. C. Fraser and H.-D. Sues. Cambridge, Cambridge University Press: 98-128.

Luo, Z.-X. (2007). Transformation and diversification in early mammal evolution. *Nature* 450: 1011-1019.

Luo, Z.-X., R. L. Cifelli, and Z. Kielan-Jaworowska (2001). Dual origin of tribosphenic mammals. *Nature* 409: 53-57.

Luo, Z.-X., Z. Kielan-Jaworowska, and R. L. Cifelli (2002). In quest for a phylogeny of Mesozoic mammals. *Acta Palaeontologica Polonica* 47: 1-78.

Luo, Z.-X. and T. Martin (2007). Analysis of Molar Structure and Phylogeny of Docodont Genera. *Bulletin of Carnegie Museum of Natural History* 39: 27-47.

Luo, Z.-X., Q. Ji, and C.-X. Yuan (2007). Convergent dental adaptations in pseudo-tribosphenic and tribosphenic mammals. *Nature* 450: 93-97.

Luo, Z.-X., C.-X. Yuan, Q.-J. Meng, and Q. Ji (2011). A Jurassic eutherian mammal and divergence of marsupials and placentals. *Nature* 476: 442-445.

Luo, Z.-X., Q.-J. Meng, Q. Ji, D. Liu, Y.-G. Zhang, and A. I. Neander (2015). Evolutionary development in basal mammaliaforms as revealed by a docodontan. *Science* 347: 760-764.

Macrini, T. E. (2004). *Monodelphis domestica*. *Mammalian Species* 760: 1-8.

Marsh, O. C. (1880). Notice on Jurassic Mammals representing two new orders. *American Journal of Science* 20: 235-239.

Marsh, O. C. (1881). Notice of new Jurassic Mammals. *American Journal of Science* 21: 511-513.

Marsh, O. C. (1887). American Jurassic Mammals. *American Journal of Science* 33: 326-348.

Martin, T. (1999). Dryolestidae (Eupantotheria, Mammalia) aus dem Oberen Jura von Portugal. *Abhandlungen der senckenbergischen naturforschenden Gesellschaft* 550: 1-119.

Martin, T. (2000). Overview over the Guimarota ecosystem. In: *Guimarota - A Jurassic Ecosystem*. Eds: T. Martin and B. Krebs. Munich, Verlag Dr. Friedrich Pfeil: 143-146.

Martin, T. (2005). Postcranial anatomy of *Haldanodon exspectatus* (Mammalia, Docodonta) from the Late Jurassic (Kimmeridgian) of Portugal and its bearing for mammalian evolution. *Zoological Journal of the Linnean Society* 145: 219-248.

Martin, T. and M. Nowotny (2000). The docodont *Haldanodon* from the Guimarota mine. In: *Guimarota - A Jurassic Ecosystem*. Eds: T. Martin and B. Krebs. Munich, Verlag Dr. Friedrich Pfeil: 91-96.

Martin, T., and A. O. Averianov (2004). A new docodont (Mammalia) from the Middle Jurassic of Kyrgyzstan, Central Asia. *Journal of Vertebrate Paleontology* 24: 195-201.

Martin, T. and O. W. M. Rauhut (2005). Mandible and dentition of *Asfaltomylos patagonicus* (Australosphenida, Mammalia) and the evolution of tribosphenic teeth. *Journal of Vertebrate Paleontology* 25: 414-425.

Martin, T. and A. O. Averianov (2010). Mammals from the Middle Jurassic Balabansai Formation of the Fergana depression, Kyrgyzstan. *Journal of Vertebrate Paleontology* 30: 855-871.

Martin, T., A. O. Averianov, and H.-U. Pfretzschner (2010a). Mammals from the Late Jurassic Qigu Formation in the Southern Junggar Basin, Xinjiang, Northwest China. *Palaeobiodiversity and Palaeoenvironments* 90: 295-319.

Martin, T., M. Nowotny, and M. Fischer (2010b). New data on tooth replacement in the late Jurassic docodont mammal *Haldanodon exspectatus*. *Journal of Vertebrate Paleontology, Program and Abstracts* 2010: 130.

Maschenko, E. N., A. V. Lopatin, and A. V. Voronkevich (2002). A new genus of the tegotheriid docodonts (Docodonta, Tegotheriidae) from the Early Cretaceous of West Siberia. *Russian Journal of Theriology* 1: 75-81.

McManus, J. J. (1974). *Didelphis virginiana*. *Mammalian Species* 40: 1-6.

Menegaz, R. A., D. B. Baier, K. A. Metzger, S. W. Herring, and E. L. Brainerd (2015). XROMM analysis of tooth occlusion and temporomandibular joint kinematics during feeding in juvenile miniature pigs. *Journal of Experimental Biology* 218: 2573-2584.

Meng, Q.-J., Q. Ji, Y.-G Zhang, D. Liu, D. M. Grossnickle, and Z.-X. Luo (2015). An arboreal docodont from the Jurassic and mammaliaform ecological diversification. *Science* 347: 764-768.

Mills, J. R. E. (1966). The functional occlusion of the teeth of the Insectivora. *Zoological Journal of the Linnean Society* 47: 1-25.

Moore, S. J. and G. D. Sanson (1995). A comparison of the molar efficiency of two insect-eating mammals. *Journal of Zoology* 235: 175-192.

Nowotny, M., T. Martin, and M. Fischer (2001). Dental anatomy and tooth replacement of *Haldanodon exspectatus* (Docodonta, Mammalia) from the Upper Jurassic of Portugal. *Journal of Morphology* 248: 268.

Oron, U., and A. W. Crompton (1985). A cineradiographic and electromyographic study of mastication in *Tenrec ecaudatus*. *Journal of Morphology* 185: 155-182.

Osborn, H. F. (1888a). Additional observations upon the structure and classification of the Mesozoic Mammalia. *Proceedings of the Academy of Natural Sciences of Philadelphia* 40: 292-301.

Osborn, H. F. (1888b). The evolution of mammalian molars to and from the tritubercular type. *The American Naturalist* 22: 1067-1079.

Osborn, H. F. (1907). *Evolution of mammalian molar teeth*. New York, Macmillan.

Pascual, R., F. J. Goin, P. Gonzáles, A. Ardolino, and P. F. Puerta (2000). A highly derived docodont from the Patagonian Late Cretaceous: evolutionary implications for Gondwanan mammals. *Geodiversitas* 22: 395-414.

Patterson, B. (1956). Early Cretaceous mammals and the evolution of mammalian molar teeth. *Fieldiana: Geology* 13: 1-105.

Pfretzschner, H.-U., T. Martin, M. W. Maisch, A. T. Matzke, and G. Sun (2005). A new docodont mammal from the Late Jurassic of the Junggar Basin in Northwest China. *Acta Palaeontolgica Polonica* 50: 799-808.

Prasad, G. V. R. and B. K. Manhas (2001). First docodont mammals of Laurasian affinities from India. *Current Science* 81: 1235-1238.

Prasad, G. V. R. and B. K. Manhas (2007). A new docodont mammal from the Jurassic Kota Formation of India. *Palaeontologia Electronica* 10: 1-11.

Prothero, D. R. (1981). New Jurassic mammals from Como Bluff, Wyoming, and the interrelationships of non-tribosphenic Theria. *Bulletin of the American Museum of Natural History* 167: 277-326.

Rauhut, O. W. M., T. Martin, E. Ortiz-Jaureguizar, and P. Puerta (2002). A Jurassic mammal from South America. *Nature* 416: 165-168.

Redford, K. H. and J. F. Eisenberg (1992). *Mammals of the Neotropics: the southern cone – Chile, Argentina, Uruguay, Paraguay*. Illinois, University of Chicago Press.

Rensberger, J. M. (1973). An occlusion model for mastication and dental wear in herbivorous mammals. *Journal of Paleontology* 47: 515-528.

Rensberger, J. M. (1978). Scanning electron microscopy of wear and occlusal events in some small herbivores. In: *Development, function and evolution of teeth*. Eds: P.M. Butler and K. A. Joysey. New York, Academic Press: 415-438.

Rich, T. H., T. F. Flannery, and P. Vickers-Rich (1998). Alleged Cretaceous placental form down under: Reply. *Lethaia* 31: 346-348.

Rougier, G.W., J. R. Wible, and J. A. Hopson (1996). Basicranial anatomy of *Priacodon fruitaensis* (Triconodontidae, Mammalia) from the Late Jurassic of Colorado, and a reappraisal of mammaliaform interrelationships. *American Museum Novitates* 3183: 1-38.

Rougier, G. W. and S. Apesteguia (2004). The Mesozoic radiation of dryolestoids in South America: Dental and cranial evidence. *Journal of Vertebrate Paleontology, Program and Abstracts* 2004: 106.

Rougier, G. W., A. G. Martinelli, A. M. Forasiepi, and M. J. Novacek (2007). New Jurassic Mammals from Patagonia, Argentina: A Reappraisal of Australosphenidan Morphology and Interrelationships. *American Museum Novitates* 3566: 1-54.

Rougier, G. W., A. S. Sheth, K. Carpenter, L. Appella-Guiscafre, and B. M. Davis (2014). A new species of *Docodon* (Mammaliaformes: Docodonta) from the Upper Jurassic Morrison Formation and a reassessment of selected craniodental characters in basal mammaliaforms. *Journal of Mammalian Evolution* 22: 1-16.

Ruf, I., Z.-X. Luo, and T. Martin (2013). Reinvestigation of the basicranium of *Haldanodon exspectatus* (Mammaliaformes, Docodonta). *Journal of Vertebrate Paleontology* 33: 382-400.

Schudack, M. E. (2000). Geological setting and dating of the Guimarota-beds. In: *Guimarota – a Jurassic Ecosystem*. Eds: T. Martin and B. Krebs. Munich, Verlag Dr. Friedrich Pfeil: 21-26.

Schultz, J. A. (2011). *Funktionelle Morphologie und Abnutzungsmuster prätribosphenischer Molaren am Beispiel der Dryolestida (Mammalia, Cladotheria)*. Doctoral dissertation, Rheinische Friedrich-Wilhelms-Universität Bonn.

Schultz, J. A., and T. Martin (2011). Wear pattern and functional morphology of dryolestoid molars (Mammalia, Cladotheria). *Paläontologische Zeitschrift* 85: 269-285.

Schultz, J. A., and T. Martin (2014). Function of pretribosphenic and tribosphenic mammalian molars inferred from 3D animation. *Naturwissenschaften* 101: 771-781.

Schultz, J. A., B.-A. S. Bhullar, and Z.-X. Luo (2017). Re-examination of the Jurassic Mammaliaform *Docodon victor* by Computed Tomography and Occlusal Functional Analysis. *Journal of Mammalian Evolution*: https://doi.org/10.1007/s10914-017-9418-5.

Schwermann, A. H. (2015). *Über die Funktionsweise prätribosphenischer und tribosphenischer Gebisse*. Doctoral dissertation, Rheinische Friedrich-Wilhelms-Universität Bonn.

Sigogneau-Russell, D. (1998). Discovery of a Late Jurassic Chinese mammal in the Upper Bathonian of England. *Comptes Rendus de l'Académie des Sciences Paris, Sciences de la terre et des planètes* 327: 571-576.

Sigogneau-Russell, D. (2001). Docodont nature of *Cyrtlatherium*, an upper Bathonian mammal from England. *Acta Palaeontolgica Polonica* 46: 427-430.

Sigogneau-Russell, D. (2003). Docodonts from the British Mesozoic. *Acta Palaeontolgica Polonica* 48: 357-374.

Sigogneau-Russell, D. and R. Hahn (1995). Reassessment of the Late Triassic symmetrodont mammal *Woutersia*. *Acta Palaeontolgica Polonica* 40: 245-260.

Sigogneau-Russell, D. and P. Godefroit (1997). A primitive docodont (Mammalia) from the Upper Triassic of France and the possible Therian affinities of the order. *Comptes Rendus de l'Académie des Sciences Paris, Sciences de la terre et des planètes* 324: 135-140.

Sigogneau-Russell, D., J. J. Hooker, and P. C. Ensom (2001). The oldest tribosphenic mammal from Laurasia (Purbeck Limestone Group, Berriasian, Cretaceous, UK) and its bearing on the 'dual origin' of Tribosphenida. *Comptes Rendus de l'Académie des Sciences Paris, Sciences de la terre et des planètes* 333: 141-147.

Simpson, G. G. (1925). Mesozoic Mammalia II: Preliminary comparison of Jurassic Mammals except Multituberculates. *American Journal of Science* 10: 559-569.

Simpson, G. G. (1928). Genus *Peraiocynodon* nov. In: *A Cataloge of the Mesozoic Mammalia in the Geological Department of the British Museum*. London, William Clowes & Sons: 125-127.

Simpson, G. G. (1929). *American Mesozoic Mammalia*. London, Yale University Press.

Simpson, G. G. (1933). Paleobiology of Jurassic mammals. *Paleobiologica* 5: 127-158.

Simpson, G. G. (1936). Studies of the earliest mammalian dentitions. *Dental Cosmos* 78: 791-800, 940-953.

Simpson, G. G. (1961). Evolution of Mesozoic mammals. In: *International colloquium on the evolution of lower and nonspecialized mammals*. Ed: G. Vandebroek. Brussels, Koninklijke Vlaamse Academie Voor Wetenschappen, Letteren en Schone Kunsten van Belgie: 57–95.

Spears, I. R. and R. H. Crompton (1996). The mechanical significance of the occlusal geometry of great ape molars in food breakdown. *Journal of Human Evolution* 31: 517-535.

Stern, D., A. W. Crompton, and Z. Skobe (1989). Enamel ultrastructure and masticatory function in molars of the American opossum, *Didelphis virginiana*. *Zoological Journal of the Linnean Society* 95: 311-334.

Stones, H. H. (1948). *Oral and dental diseases*. Edinburgh, E. and S. Livingstone.

Streilein, K. E. (1982). Behavior, ecology, and distribution of South American marsupials. In: *Mammalian biology in South America*. Eds: M. A. Mares and H. H. Genoways. Linesville, University of Pittsburg: 231-250.

Tatarinov, L. P. (1994). An unusual mammal tooth from the Jurassic of Mongolia. *Paleontological Journal* 28: 121-131.

Thenius, E. (1989). *Zähne und Gebiß der Säugetiere*. Berlin, Walter de Gruyter.

Thomason, J. J., A. P. Russell, and M. Morgeli (1990). Forces of biting, body size, and masticatory muscle tension in the opossum *Didelphis virginiana*. *Canadian Journal of Zoology* 68: 318-324.

Ungar, P. S. (2010). *Mammal Teeth – Origin, Evolution, and Diversity*. Baltimore, The Johns Hopkins University Press.

Waldman, M. and R. J. G. Savage (1972). The first Jurassic mammal from Scotland. *Journal of the Geological Society* 128: 119-125.

Wang, Y.-Q., W. A. Clemens, Y.-M. Hu, and C.-K. Li (1998). A probable pseudo-tribosphenic upper molar from the Late Jurassic of China and the early radiation of the Holotheria. *Journal of Vertebrate Paleontology* 18: 777-787.

Wang, Y.-Q. and C.-K. Li (2016). Reconsideration of the systematic position of the Middle Jurassic mammaliaforms *Itatodon* and *Paritatodon*. *Palaeontologia Polonica* 67: 249-256.

Wible, J. R. and J. A. Hopson (1993). Basicranial evidence for early mammal phylogeny. In: *Mammal Phylogeny: Mesozoic Differentiation, Multituberculates, Monotremes, Early Therians, and Marsupials*. Eds: F. S. Szalay, M. J. Novacek, and M. C. McKenna. New York, Springer-Verlag: 45-62.

Wible, J. R. and A. M. Burrows (2016). Does the Jurassic *Agilodocodon* (Mammaliaformes, Docodonta) have any exudativorous dental features? *Palaeontologia Polonica* 67: 289–299.

Williams, S. H., C. J. Vinyard, C. E. Wall, A. H. Doherty, A. W. Crompton, and W. L. Hylander (2011). A preliminary analysis of correlated evolution in mammalian chewing motor patterns. *Integrative and Comparative Biology* 51: 247-259.

Wilson, D. E. and D. M. Reeder (2005). *Mammal Species of the World – A Taxonomic and Geographic Reference (Third Edition)*. Baltimore, Johns Hopkins University Press.

Woodburne, M. O., T. H. Rich, and M. S. Springer (2003). The evolution of tribospheny and the antiquity of mammalian clades. *Molecular Phylogenetics and Evolution* 28: 360-385.

Appendix

Appendix tab. 01: List of upper postcanine *Haldanodon* specimens used for the present study. All listed specimens are presently housed in the collection of the Steinmann-Institut für Geologie, Mineralogie und Paläontologie, Rheinische Friedrich-Wilhelms-Universität Bonn.

taxon	specimen		REM	µ-CT	3D print
Haldanodon	Gui Mam 3107	fr. dP sin			
Haldanodon	Gui Mam 3108	fr. M dex			
Haldanodon	Gui Mam 3109	dP dex			
Haldanodon	Gui Mam 3110	fr. dP sin			
Haldanodon	Gui Mam 3112	fr. dP dex		x	
Haldanodon	Gui Mam 3113	dP sin		x	x
Haldanodon	Gui Mam 3114	fr. dP dex		x	
Haldanodon	Gui Mam 3115	fr. dP dex		x	
Haldanodon	Gui Mam 3116	fr. dP sin		x	
Haldanodon	Gui Mam 3117	fr. dP dex		x	x
Haldanodon	Gui Mam 3118	fr. dP dex		x	
Haldanodon	Gui Mam 3119	fr. ?dP sin		x	
Haldanodon	Gui Mam 3120	M dex		x	
Haldanodon	Gui Mam 3121	fr. dP sin		x	
Haldanodon	Gui Mam 3122	fr. dP dex		x	
Haldanodon	Gui Mam 3123	?M4 dex	x	x	x
Haldanodon	Gui Mam 3124	fr. M sin		x	
Haldanodon	Gui Mam 3125	fr. M sin	x		
Haldanodon	Gui Mam 3126	?dP dex		x	
Haldanodon	Gui Mam 3127	fr. ?M dex		x	
Haldanodon	Gui Mam 3128	fr. M sin		x	
Haldanodon	Gui Mam 3129	dP sin		x	x
Haldanodon	Gui Mam 3130	fr. M sin		x	
Haldanodon	Gui Mam 3131	?M sin		x	
Haldanodon	Gui Mam 3132	M sin			
Haldanodon	Gui Mam 3133	fr. dP dex		x	
Haldanodon	Gui Mam 3134	dP sin		x	x
Haldanodon	Gui Mam 3135	fr. dP dex		x	
Haldanodon	Gui Mam 3136	fr. dP sin		x	
Haldanodon	Gui Mam 3137	fr. dP sin		x	
Haldanodon	Gui Mam 3191	?M4 dex	x		
Haldanodon	Gui Mam 3194	dP sin			
Haldanodon	Gui Mam 3195	fr. dP dex			
Haldanodon	Gui Mam 3196	?dP sin			
Haldanodon	Gui Mam 3197	M sin			
Haldanodon	Gui Mam 3198	fr. dP sin			
Haldanodon	Gui Mam 3221	fr. M sin	x		
Haldanodon	Gui Mam 3222	fr. ?dP dex			
Haldanodon	Gui Mam 3223	fr. M sin			
Haldanodon	Gui Mam 3224	fr. M sin			
Haldanodon	Gui Mam 3225	fr. M sin			
Haldanodon	Gui Mam 3226	fr. M dex			
Haldanodon	Gui Mam 3227	fr. dP dex			
Haldanodon	Gui Mam 3228	fr. M dex			
Haldanodon	Gui Mam 3229	fr. M dex			
Haldanodon	Gui Mam 3230	fr. dP dex			
Haldanodon	Gui Mam 3231	fr. M sin	x		
Haldanodon	Gui Mam 3232	fr. M dex			
Haldanodon	Gui Mam 3233	fr. M sin			

taxon	specimen		REM	µ-CT	3D print
Haldanodon	Gui Mam 3234	fr. M dex			
Haldanodon	Gui Mam 3235	fr. M dex			
Haldanodon	Gui Mam 3236	fr. dP dex			
Haldanodon	Gui Mam 3237	fr. ?dP sin			
Haldanodon	Gui Mam 3239	fr. M sin			
Haldanodon	Gui Mam 3240	fr. M sin			
Haldanodon	Gui Mam 3241	fr. M dex			
Haldanodon	Gui Mam 3242	fr. M sin	x		
Haldanodon	Gui Mam 3243	fr. M dex	x		
Haldanodon	Gui Mam 3244	fr. M dex			
Haldanodon	Gui Mam 3245	fr. M sin	x		
Haldanodon	Gui Mam 3246	fr. M dex			
Haldanodon	Gui Mam 3247	fr. M sin			
Haldanodon	Gui Mam 3248	fr. M dex			
Haldanodon	Gui Mam 3249	fr. M dex			
Haldanodon	Gui Mam 3250	fr. M dex			
Haldanodon	Gui Mam 3251	fr. M sin	x		
Haldanodon	Gui Mam 3252	fr. M sin	x		
Haldanodon	Gui Mam 3253	fr. M dex			
Haldanodon	Gui Mam 3254	fr. M dex			
Haldanodon	Gui Mam 3255	fr. ?M dex			
Haldanodon	Gui Mam 3256	fr. M sin			
Haldanodon	Gui Mam 3257	fr. dP dex			
Haldanodon	Gui Mam 3258	fr. dP sin			
Haldanodon	Gui Mam 3259	fr. M ?dex	x		
Haldanodon	Gui Mam 3260	fr. M dex			
Haldanodon	Gui Mam 3261	fr. M sin	x		
Haldanodon	Gui Mam 3262	fr. M dex	x		
Haldanodon	Gui Mam 3263	fr. M sin			
Haldanodon	Gui Mam 3264	dP sin			
Haldanodon	Gui Mam 3265	fr. M sin	x		

Appendix tab. 02: List of lower postcanine *Haldanodon* specimens used for the present study. All listed specimens are presently housed in the collection of the Steinmann-Institut für Geologie, Mineralogie und Paläontologie, Rheinische Friedrich-Wilhelms-Universität Bonn.

taxon	specimen		REM	µ-CT	3D print
Haldanodon	Gui Mam 3100	m1 dex			
Haldanodon	Gui Mam 3101	m1 sin			
Haldanodon	Gui Mam 3102	m1 dex			
Haldanodon	Gui Mam 3103	m1 dex			
Haldanodon	Gui Mam 3104	m dex	x		
Haldanodon	Gui Mam 3105	m1 dex			
Haldanodon	Gui Mam 3111	m1 dex			
Haldanodon	Gui Mam 3138	?m1 sin		x	
Haldanodon	Gui Mam 3139	m1 sin		x	
Haldanodon	Gui Mam 3140	?m1 dex		x	
Haldanodon	Gui Mam 3141	m1 sin		x	x
Haldanodon	Gui Mam 3142	?m1 dex		x	x
Haldanodon	Gui Mam 3143	dp sin		x	

taxon	specimen		REM	µ-CT	3D print
Haldanodon	Gui Mam 3144	fr. ?m1 sin		x	
Haldanodon	Gui Mam 3145	m1 sin		x	
Haldanodon	Gui Mam 3146	dp dex		x	
Haldanodon	Gui Mam 3147	dp sin		x	
Haldanodon	Gui Mam 3148	dp dex		x	
Haldanodon	Gui Mam 3149	dp dex		x	
Haldanodon	Gui Mam 3150	dp dex		x	
Haldanodon	Gui Mam 3151	dp sin		x	
Haldanodon	Gui Mam 3152	dp dex		x	
Haldanodon	Gui Mam 3153	dp dex		x	x
Haldanodon	Gui Mam 3154	dp sin		x	x
Haldanodon	Gui Mam 3155	dp sin		x	x
Haldanodon	Gui Mam 3156	dp dex		x	
Haldanodon	Gui Mam 3157	dp dex		x	
Haldanodon	Gui Mam 3158	dp dex		x	
Haldanodon	Gui Mam 3159	dp dex		x	
Haldanodon	Gui Mam 3160	dp dex		x	
Haldanodon	Gui Mam 3161	fr. ?m1 dex		x	
Haldanodon	Gui Mam 3162	dp dex		x	
Haldanodon	Gui Mam 3163	dp sin		x	
Haldanodon	Gui Mam 3164	dp sin		x	
Haldanodon	Gui Mam 3165	fr. dp sin		x	
Haldanodon	Gui Mam 3166	?m1 dex		x	
Haldanodon	Gui Mam 3167	m dex	x	x	
Haldanodon	Gui Mam 3168	m dex	x		
Haldanodon	Gui Mam 3169	fr. m dex			
Haldanodon	Gui Mam 3170	m dex	x		
Haldanodon	Gui Mam 3171	?m4 dex			
Haldanodon	Gui Mam 3172	m dex	x		
Haldanodon	Gui Mam 3173	m sin			
Haldanodon	Gui Mam 3174	fr. m dex	x		
Haldanodon	Gui Mam 3175	fr. ?m1 sin			
Haldanodon	Gui Mam 3176	m sin	x		
Haldanodon	Gui Mam 3177	m sin	x		
Haldanodon	Gui Mam 3178	m sin	x		
Haldanodon	Gui Mam 3179	fr. m sin	x		
Haldanodon	Gui Mam 3180	m dex			
Haldanodon	Gui Mam 3181	m sin			
Haldanodon	Gui Mam 3182	?m4 sin			
Haldanodon	Gui Mam 3183	m5 sin			
Haldanodon	Gui Mam 3184	m5 sin			
Haldanodon	Gui Mam 3185	m5 dex			
Haldanodon	Gui Mam 3186	fr. m5 sin			
Haldanodon	Gui Mam 3187	fr. m5 dex			
Haldanodon	Gui Mam 3188	fr. m dex	x		
Haldanodon	Gui Mam 3189	?m1 sin			
Haldanodon	Gui Mam 3200	fr. ?m1 dex			
Haldanodon	Gui Mam 3201	m5 sin			
Haldanodon	Gui Mam 3202	?m5 dex			
Haldanodon	Gui Mam 3203	m dex	x		
Haldanodon	Gui Mam 3205	m5 dex			
Haldanodon	Gui Mam 3206	m dex	x		
Haldanodon	Gui Mam 3207	dp sin			

taxon	specimen		REM	µ-CT	3D print
Haldanodon	Gui Mam 3208	fr. m dex	x		
Haldanodon	Gui Mam 3209	fr. m dex			
Haldanodon	Gui Mam 3210	fr. m5 dex			
Haldanodon	Gui Mam 3211	m5 sin			
Haldanodon	Gui Mam 3212	m4 dex			
Haldanodon	Gui Mam 3213	fr. m dex	x		
Haldanodon	Gui Mam 3214	?m1 sin			
Haldanodon	Gui Mam 3215	fr. m dex			
Haldanodon	Gui Mam 3216	fr. ?m1 sin			
Haldanodon	Gui Mam 3217	fr. ?m1 dex			
Haldanodon	Gui Mam 3218	fr. m ?			
Haldanodon	Gui Mam 3219	fr. ?m1 sin			
Haldanodon	Gui Mam 3220	fr. dp dex			
Haldanodon	Gui Mam 3266	m dex			
Haldanodon	Gui Mam 3267	fr. m sin			
Haldanodon	Gui Mam 3271	m1 sin			
Haldanodon	Gui Mam 3272	fr. m2 / m3 sin			
Haldanodon	Gui Mam 3273	fr. m1 sin			
Haldanodon	Gui Mam 3274	m1 sin	x		
Haldanodon	Gui Mam 3275	?m2 dex	x		
Haldanodon	Gui Mam 3276	?m3 sin	x		
Haldanodon	Gui Mam 3277	?m4 dex			
Haldanodon	Gui Mam 3278	?m5 sin			
Haldanodon	Gui Mam 3279	?m2 / ?m3 dex	x		
Haldanodon	Gui Mam 3280	m2 / m3 dex	x		
Haldanodon	Gui Mam 3281	m2 / m3 dex	x		

Appendix tab. 03: List of docodont taxa and specimens used for comparison with *Haldanodon*. SGP - Sino-German Project; ZIN - Zoological Institute of the Russian Academy of Sciences. All listed specimens are presently housed in the collection of the Steinmann-Institut für Geologie, Mineralogie und Paläontologie, Rheinische Friedrich-Wilhelms-Universität Bonn.

taxon	specimen		REM	µ-CT	3D print
Dsungarodon	SGP 2001/21	m dex			
Dsungarodon	SGP 2001/22	?m5 dex			
Dsungarodon	SGP 2001/23	M dex			
Dsungarodon	SGP 2004/7	?m5 sin			
Dsungarodon	SGP 2004/24	fr. ?m1 dex			
Dsungarodon	SGP 2004/32	fr. M dex			
Dsungarodon	SGP 2005/7	fr. M dex			
Tegotherium	SGP 2001/25	fr. m sin			
Tegotherium	SGP 2004/3	m dex (cast)			
Tegotherium	SGP 2004/5	?m5 dex			
Tegotherium	SGP 2004/11	fr. ?m2+?m3 sin			
Tegotherium	SGP 2004/13	?m5 dex			
Tegotherium	SGP 2004/20	fr. ?m2-?m4 dex			
Tashkumyrodon	ZIN 85279	m sin (cast)			

Appendix tab. 04: List of upper molar row *Haldanodon* specimens used for the present study with details about direction and degree of wear as well as wear gradient. All listed specimens are presently housed in the collection of the Steinmann-Institut für Geologie, Mineralogie und Paläontologie, Rheinische Friedrich-Wilhelms-Universität Bonn.

taxon	specimen		direction of increasing wear	lowest degree of molar wear	highest degree of molar wear	wear gradient	wear of crest X-Y	REM	µ-CT
Haldanodon	Gui Mam 41/75	P3-M3 sin (cast)	mesial	medium (- high)	(medium -) high	small	rather steep		
Haldanodon	Gui Mam 85/75	P2-M3 sin	distal	(medium -) high	high	small	flat		x
Haldanodon	Gui Mam 112/75	?M2-?M4 sin	mesial	low	(medium -) high	large	rather steep		
Haldanodon	Gui Mam 20/76	?M1-?M3 sin	mesial	low (- medium)	medium (- high)	large	steep		
Haldanodon	Gui Mam 60/76	C-M4 dex	mesial	low (- medium)	(low -) medium	small	rather flat		
Haldanodon	Gui Mam 98/76	?M1-?M3 sin	mesial	low	medium	large	rather flat		
Haldanodon	Gui Mam 66/77	C-M3 dex	mesial	low	(medium -) high	large	rather flat		
Haldanodon	Gui Mam 16/78	P1-M4 sin (cast)	mesial	low (- medium)	medium	small	rather flat		
Haldanodon	Gui Mam 42/78	P3-M4 dex	distal (except M4)	medium	(medium -) high	small	flat		x
Haldanodon	Gui Mam 72/78	P1-M4 sin (cast)	distal	medium	medium (- high)	small	rather flat		
Haldanodon	Gui Mam 30/79	C-?M4 sin C-M3 dex	mesial	low	low	small	rather steep		x
Haldanodon	Gui Mam 58/79	?M2-?M4 dex	mesial	low	high	large	rather flat		
Haldanodon	Gui Mam 18/80	P2-M3 sin	mesial	high	high	small	rather steep		x
Haldanodon	Gui Mam 29/80	?M3-?M4 dex							
Haldanodon	Gui Mam 13/82	M1(-)M4 dex	mesial	medium	medium (- high)	small	steep		x
Haldanodon	Gui Mam 25/82	?M1-?M4 dex	distal	medium	(medium -) high	small	rather flat		

Appendix tab. 05: List of lower molar row *Haldanodon* specimens used for the present study with details about direction and degree of wear as well as wear gradient. All listed specimens are presently housed in the collection of the Steinmann-Institut für Geologie, Mineralogie und Paläontologie, Rheinische Friedrich-Wilhelms-Universität Bonn.

taxon	specimen		direction of increasing wear	lowest degree of molar wear	highest degree of molar wear	wear gradient	REM	µ-CT
Haldanodon	Gui Mam 3282	p1-m4 dex	mesial	low (- medium)	low (- medium)	small	x	
Haldanodon	*VJ 1001*	*p1-m4 sin (cast)*	*mesial*	*medium (- high)*	*medium (- high)*	*small*		
Haldanodon	VJ 1002-155	p3-m4 sin	distal	(low -) medium	high	large		
Haldanodon	VJ 1003-155	m3-m4 sin						
Haldanodon	VJ 1004-155	dp4-m1 dex [juv]						
Haldanodon	VJ 1005-155	dp4-m2 dex [juv]	mesial	low	(low -) medium	small		
Haldanodon	VJ 1007-155	m1-m4 dex	distal	high	high	small		
Haldanodon	Gui Mam 14/73	p3-m4 sin	mesial	low (- medium)	(medium -) high	large		
Haldanodon	Gui Mam 7/74	p2-m5 dex	distal (except m1)	low (- medium)	(low -) medium	small		
Haldanodon	Gui Mam 10/74	p1-m4 dex	mesial	(low -) medium	medium (- high)	large		
Haldanodon	Gui Mam 34/74	i2-m6 sin	distal	(medium -) high	high	small		
Haldanodon	Gui Mam 93/74	?c-?m3 sin						
Haldanodon	Gui Mam 106/74	p3-m4 dex	distal	medium (- high)	high	small		
Haldanodon	Gui Mam 107/74	m1-m5 dex	distal (except m1)	medium (- high)	(medium -) high	small		
Haldanodon	Gui Mam 4/75	m1-m4 sin	distal (except m1)	high	high	small		
Haldanodon	Gui Mam 46/75	i3(-)m5 sin	distal	medium (- high)	high	small		
Haldanodon	Gui Mam 47/75	c-m4 sin	mesial	(low -) medium	medium (- high)	large		
Haldanodon	Gui Mam 63/75	i3-m5 dex	mesial	high	high	small		x
Haldanodon	Gui Mam 79/75	p3-m4 dex	mesial	low	low (- medium)	small		x
Haldanodon	Gui Mam 171/75	m4-m5 dex						
Haldanodon	Gui Mam 182/75	c-m6 dex	distal	high	high	small		x
Haldanodon	Gui Mam 10/76	c-m3 dex	distal	(low -) medium	(low -) medium	small		
Haldanodon	Gui Mam 39/76	c-?m3 dex	distal	(low -) medium	medium	small		
Haldanodon	Gui Mam 49/76	p3-m4 sin	distal	(low -) medium	(low -) medium	small		
Haldanodon	Gui Mam 103/76	c-m6 sin	distal	medium (- high)	high	small		
Haldanodon	Gui Mam 122/76	p1-m4 dex	mesial	low (- medium)	low (- medium)	small		
Haldanodon	Gui Mam 125/76	m1-m5 sin	distal (except m4)	high	high	small		
Haldanodon	Gui Mam 141/76	p3-m5 sin	mesial (except m2)	low	low (- medium)	small		

taxon	specimen		direction of increasing wear	lowest degree of molar wear	highest degree of molar wear	wear gradient	REM	µ-CT
Haldanodon	Gui Mam 3/77	p1-m5 sin	mesial	medium	high	large		
Haldanodon	Gui Mam 21/77	m4-m5 sin						
Haldanodon	Gui Mam 33/77	(p3)-m4 sin [juv]	mesial	low	high	large		x
Haldanodon	Gui Mam 82/77	m4-m5 dex						
Haldanodon	Gui Mam 119/77	m1-m4 sin	distal	high	high	small		
Haldanodon	Gui Mam 54/78	c-m3 dex	distal	medium	medium (- high)	small		
Haldanodon	Gui Mam 6/79	m2-(m5) dex						
Haldanodon	Gui Mam 12/79	p2-m5 dex	distal (except m1)	medium	high	large		
Haldanodon	Gui Mam 18/79	c-m3 sin	mesial	low	low (- medium)	small		
Haldanodon	Gui Mam 29/79	p3-m3 dex	mesial	low	(low -) medium	small		
Haldanodon	Gui Mam 30/79	i2-m1 dex						x
Haldanodon	Gui Mam 50/79	?m3-?m4 sin						
Haldanodon	Gui Mam 54/79	p1-m4 sin	distal	(medium -) high	high	small		
Haldanodon	Gui Mam 56/79	p2-m5 dex	mesial	(low -) medium	(medium -) high	large		x
Haldanodon	Gui Mam 76/79	p2-m4 sin	mesial	medium	high	large		
Haldanodon	Gui Mam 97/79	c-m3 sin	mesial	low	medium (- high)	large		x
Haldanodon	Gui Mam 1/80	i2-m5 sin	distal	medium	medium (- high)	small		
Haldanodon	Gui Mam 3/80	m1-m5 sin	distal	high	high	small		
Haldanodon	Gui Mam 4/80	m2-m5 sin	distal	high	high	small		
Haldanodon	Gui Mam 14/80	m1-m4 sin	mesial	low	medium (- high)	large		x
Haldanodon	Gui Mam 23/80	c-m4 dex	distal	medium	high	large		x
Haldanodon	Gui Mam 37/80	i3-m4 sin	mesial	medium (- high)	high	small		
Haldanodon	Gui Mam 11/81	?m3-?m4 sin						
Haldanodon	Gui Mam 6/82	c-m4 sin	mesial	low	(low -) medium	small		x

Appendix tab. 06: List of length and width measurements in mm taken from upper molar rows of *Haldanodon*.

specimen	M1-M3	M1		M2		M3		M4	
	L	L	W	L	W	L	W	L	W
Gui Mam 85/75		1.68	1.77	1.73	2.10				
Gui Mam 112/75				1.93	2.14	1.59	1.75	1.33	1.19
Gui Mam 20/76	4.43	1.60	1.82	1.71	2.11		1.99		
Gui Mam 60/76	4.87	1.76	1.90	1.89	2.26	1.68	2.06	1.62	1.19
Gui Mam 98/76	4.80	1.56	1.67	1.59	2.02	1.93	2.03		
Gui Mam 66/77	3.98	1.69	1.66	1.75	2.28		2.46		
Gui Mam 42/78	4.84	1.73	1.91	1.91	2.35	1.78	1.98		
Gui Mam 30/79 sin		1.67	1.59			1.65	1.71	1.56	1.78
Gui Mam 30/79 dex	3.80	1.54	1.72	1.44	1.71	1.48			
Gui Mam 58/79				1.95	1.95	1.68	1.91	1.32	1.33
Gui Mam 18/80	5.00	1.73	1.82	1.85	2.25	1.94	2.07		
Gui Mam 29/80						1.73	1.88	1.62	1.47
Gui Mam 13/82		1.58	1.65	1.86	2.00	1.75	1.85	1.58	1.34
Gui Mam 25/82	4.73	1.64	1.65	1.75	1.94	1.65		1.73	1.56
cast Gui Mam 41/75	5.00	1.90	2.00	1.90	2.16	1.77	1.81		
cast Gui Mam 16/78	5.71	2.03	1.98	2.13	2.32	1.94	1.96	1.90	1.77
cast Gui Mam 72/78				2.11	2.36	1.96	2.14	1.92	1.45

x.xx uncertain molar position reliable value estimated value

Appendix tab. 07: List of length and width measurements in mm taken form lower molar rows of *Haldanodon*.

specimen	m1-m4	m1		m2		m3		m4		m5		m6	
	L	L	W	L	W	L	W	L	W	L	W	L	W
cast VJ 1001	6.01	1.68	0.94	1.83	1.17	1.56	1.04	1.16	0.85				
VJ 1002-155	6.18	1.55	0.90	1.66	1.03	1.64	1.10	1.36	0.93				
VJ 1003-155						1.93	1.34	1.49	1.17				
VJ 1007-155		1.52	1.01	1.66	1.09	1.63	1.00	1.14	0.87				
Gui Mam 14/73	7.43	1.31	0.83	1.48	1.04	1.82	1.24	1.62	1.14				
Gui Mam 7/74		1.51	0.85	1.68	0.99	1.50	1.07	1.45	0.98	1.17	0.83		
Gui Mam 10/74	6.25	1.63	1.06	1.88	1.26	1.75	1.18	1.23	0.84				
Gui Mam 34/74	6.36	1.56	0.93	1.52	1.18	1.84	1.32	1.68	1.29	1.37	1.06	1.01	0.80
Gui Mam 93/74				1.64	1.02	1.67	1.17						
Gui Mam 106/74	6.53	1.60	0.97	1.71	1.11	1.79	1.18	1.46	1.04				
Gui Mam 107/74	6.42	1.51	1.04	1.87	1.20	1.90	1.26	1.33	0.95	1.18	0.78		
Gui Mam 4/75	5.89			1.70	1.11	1.85	1.23	1.44	0.94				
Gui Mam 46/75	6.48			1.82	1.10			1.38		1.07	0.79		
Gui Mam 47/75		1.67	0.95	1.88	1.22	1.90	1.35	1.57	1.20				
Gui Mam 63/75		1.59	0.83	1.87	1.14	1.75	1.22			1.04	0.75		
Gui Mam 79/75	6.47	1.68	0.98	1.82	1.17	1.73	1.17	1.50	1.03				
Gui Mam 171/75								1.44	1.13	0.98	0.74		
Gui Mam 182/75	6.20	1.60	1.00	1.71	1.15	1.72	1.20	1.37	0.93	1.01	0.82	0.72	0.65
Gui Mam 10/76		1.57	0.85	1.90	1.15	1.94	1.29						
Gui Mam 39/76				1.70	1.07	1.88	1.30	1.87	1.29				
Gui Mam 49/76		1.55	1.00	1.76	1.15	1.73	1.25	1.54	1.12				
Gui Mam 103/76		1.58	0.89			1.72	1.25	1.48	1.13	1.36	1.05	1.11	0.96
Gui Mam 122/76	6.43	1.58	0.92	1.88	1.19	1.29	1.24	1.30	0.91				

specimen	m1-m4	m1		m2		m3		m4		m5		m6	
	L	L	W	L	W	L	W	L	W	L	W	L	W
Gui Mam 125/76	6.71	1.58	0.94	1.83	1.14	1.96	1.32	1.61	1.20	1.01	0.83		
Gui Mam 141/76	6.25	1.50	1.01	1.66	1.26	1.76	1.32	1.58	1.18	1.35	0.95		
Gui Mam 3/77	5.81	1.56	0.92	1.73	1.07	1.54	1.04	1.13	0.78	0.82	0.63		
Gui Mam 21/77								1.31	0.98	1.00	0.76		
Gui Mam 33/77		1.61	0.93	1.75	1.13			1.46	1.00				
Gui Mam 82/77								1.54	1.12	1.21	0.90		
Gui Mam 119/77	6.59	1.57	0.94	1.78	1.11	1.81	1.24	1.57	1.11				
Gui Mam 54/78		1.47	1.00	1.85	1.21	1.89							
Gui Mam 6/79				1.83	1.20	1.82	1.31			1.08	0.82		
Gui Mam 12/79		1.51	0.97	1.91	1.14	1.80	1.26		1.11	1.11	0.88		
Gui Mam 18/79		1.60	0.88	1.85	1.07	1.65	1.14						
Gui Mam 29/79		1.66	0.96	1.93	1.19	1.91	1.28						
Gui Mam 30/79		1.59	0.93										
Gui Mam 50/79						1.86	1.25	1.54	1.15				
Gui Mam 54/79	5.88	1.50	1.02	1.69		1.71	1.12	1.24	0.84				
Gui Mam 56/79	6.29	1.70	1.08	1.86	1.19	1.71	1.23	1.43	0.99	1.10	0.84		
Gui Mam 76/79	6.02	1.57	1.07	1.80	1.15	1.88	1.28	1.33	1.08	0.97	0.83		
Gui Mam 97/79		1.55	0.89	1.64	1.01	1.61	1.11						
Gui Mam 1/80	6.35	1.37	0.90	1.73	1.17	1.80	1.25	1.53	1.13	1.28	0.95		
Gui Mam 3/80	6.46	1.46	1.01	1.73	1.17	1.70	1.20			0.83	0.78		
Gui Mam 4/80	6.90	1.66	1.04	1.92	1.24	2.04	1.45	1.61	1.28	1.18	0.90		
Gui Mam 14/80	6.49	1.63	0.97	1.66	1.11	1.84	1.26	1.54	1.08				
Gui Mam 23/80	7.06	1.70	0.94	1.93	1.15	1.97	1.21	1.55	1.05				
Gui Mam 37/80	6.47	1.60	0.93	1.67	1.14	1.89	1.29	1.55	1.18				
Gui Mam 11/81						1.82	1.19	1.35	0.99				
Gui Mam 6/82	5.95	1.60	0.91	1.81	1.15	1.74	1.14	1.05	0.72				
Gui Mam 3282	5.62	1.29	0.90	1.65	1.00	1.69	1.17	1.17	0.90				

x.xx uncertain molar position reliable value estimated value

Appendix tab. 08: Highest, lowest, and mean values of length and width measurements taken from upper molar positions in *Haldanodon*. Measurements include only well-preserved molars with certainly determinable positions.

	position	maximum	minimum	mean
length in mm	m1	1.70	1.37	1.58
	m2	1.93	1.64	1.80
	m3	2.04	1.29	1.76
	m4	1.68	1.05	1.43
	m5	1.37	0.82	1.12
	m6	1.11	0.72	0.92
width in mm	m1	1.08	0.83	0.95
	m2	1.26	0.99	1.14
	m3	1.45	1.04	1.22
	m4	1.29	0.72	1.03
	m5	1.06	0.63	0.85
	m6	0.96	0.65	0.80

Appendix tab. 09: Highest, lowest, and mean values of length and width measurements taken from lower molar positions in *Haldanodon*. Measurements include only well-preserved molars with certainly determinable positions.

	position	maximum	minimum	mean
length in mm	M1	2.03	1.54	1.73
	M2	2.13	1.73	1.90
	M3	1.96	1.65	1.81
	M4	1.92	1.58	1.75
width in mm	M1	2	1.65	1.84
	M2	2.36	1.94	2.21
	M3	2.14	1.81	1.98
	M4	1.77	1.19	1.46

Appendix tab. 10: Length and width ratios in between M2 and m2 as well as M2 and m3 of *Haldanodon*. Measurements were taken in millimeters and include only well-preserved molars with certainly determinable positions. Note that the length of M2 more or less equals the length of m2 and m3.

	maximum	minimum	mean
L M2 / L m2	1.10	1.05	1.05
L M2 / L m3	1.04	1.34	1.08
W M2 / W m2	1.87	1.96	1.94
W M2 / W m3	1.63	1.87	1.81
L M2 / W m2	1.69	1.75	1.67
L M2 / W m3	1.47	1.66	1.56
W M2 / L m2	1.22	1.18	1.23
W M2 / L m3	1.16	1.50	1.25

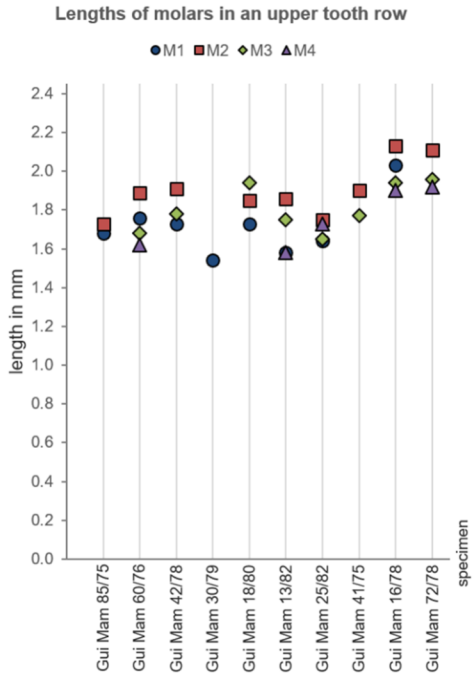

Appendix fig. 01: Length distribution of the molar positions within upper *Haldanodon* tooth rows. Measurements only include well-preserved molars with certainly determinable positions.

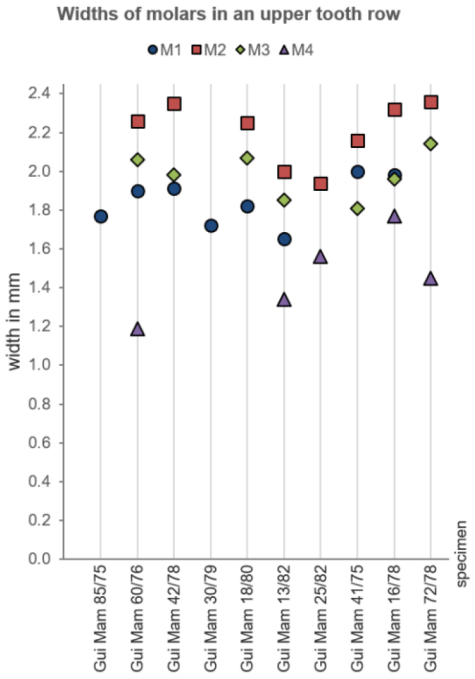

Appendix fig. 02: Width distribution of the molar positions within upper *Haldanodon* tooth rows. Measurements only include well-preserved molars with certainly determinable positions.

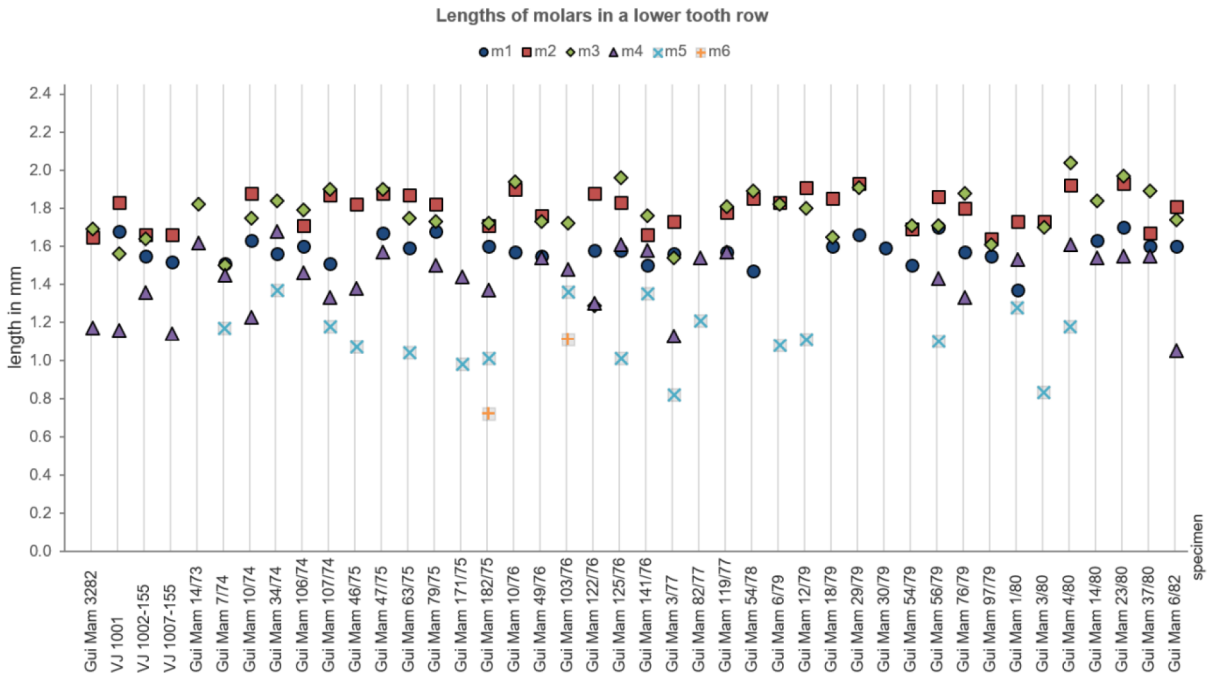

Appendix fig. 03: Length distribution of the molar positions within lower *Haldanodon* tooth rows. Measurements only include well-preserved molars with certainly determinable positions.

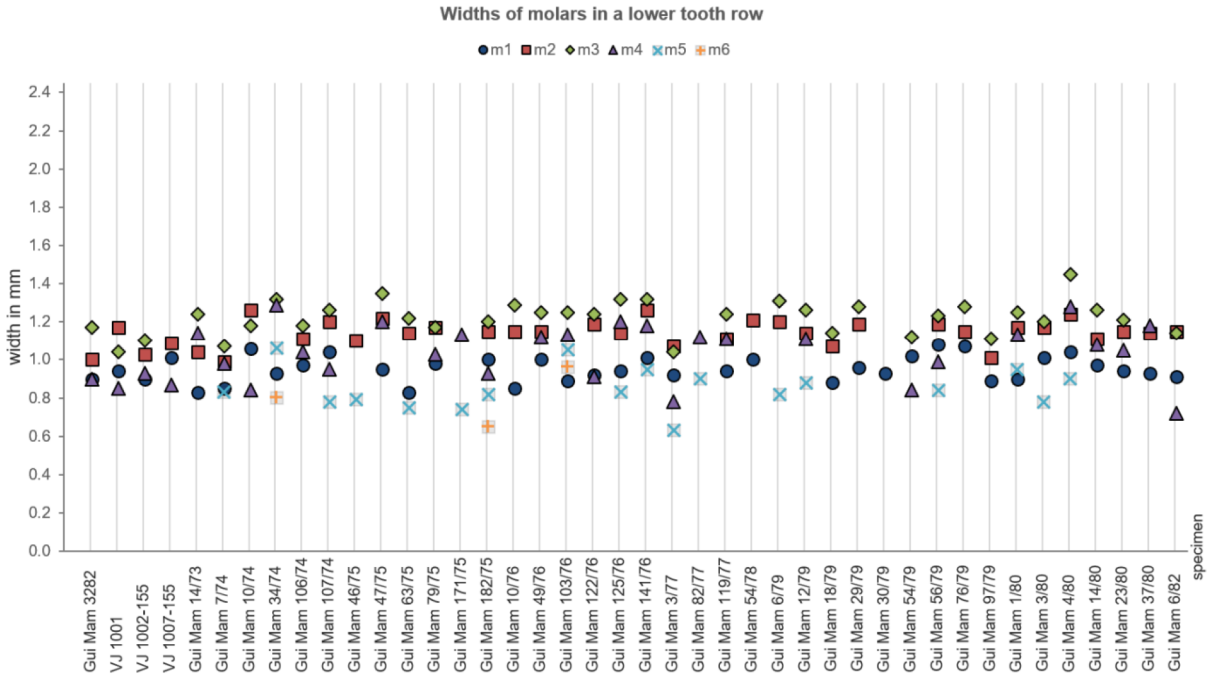

Appendix fig. 04: Width distribution of the molar positions within lower *Haldanodon* tooth rows. Measurements only include well-preserved molars with certainly determinable positions.

Zusammenfassung

Die Entwicklung des tribosphenischen Zahnbaus wird als eine Schlüsselinnovation innerhalb der Stammlinie der Theria angesehen. Sie erlaubt eine sehr effiziente Aufarbeitung der Nahrung schon während des Kauvorgangs. Im Wesentlichen besteht die tribosphenische Zahnmorphologie aus einem distal gelegenen Quetschbecken auf dem unteren Molaren (dem Talonidbecken) und einem dort hineingreifenden Höcker auf dem oberen Molaren (dem Protocon). Somit ist Scherschneiden nicht mehr die einzige Zahnfunktion, sondern wird zusätzlich durch Quetschen und Reiben ergänzt. Alle heute lebenden Säugetiere mit Ausnahme der Monotremen stammen von einem tribosphenischen Vorfahren ab (Simpson 1936, Patterson 1956, Mills 1966, Crompton and Hiiemäe 1970, Crompton 1971, Butler 1972, Prothero 1981, Luo et al. 2001, Woodburne et al. 2003, Kielan-Jaworowska et al. 2004, Datta 2005, Lopatin and Averianov 2006, Luo 2007, Luo et al. 2007, Davis 2011). Das früheste bekannte voll tribosphenische Taxon stammt aus dem Oberjura (Luo et al. 2011). Allerdings wurden auch schon früher in der Stammesgeschichte der Säugetiere Molaren mit einer sehr ähnlichen Zahnmorphologie und einer quetschenden und reibenden Funktion entwickelt. Das erste bekannte Taxon mit solchen „pseudotribosphenischen“ Molaren waren die mammaliaformen Docodonten (Mitteljura bis Unterkreide). Sie besaßen ein mesial gelegenes Quetschbecken auf dem unteren und einen dort hineingreifenden Höcker auf dem oberen Molaren (Simpson 1929, Crompton & Jenkins 1968, Hopson and Crompton 1969, Jenkins 1969, Gingerich 1973, Krusat 1980, Kermack et al. 1987, Butler 1988, Butler 1997, Wang et al. 1998, Pfretzschner et al. 2005, Luo 2007, Luo and Martin 2007, Luo et al. 2007, Davis 2011, Schultz et al. 2017). Das wirft die Frage auf, in wie weit die Funktionsweise dieser „pseudotribosphenischen“ Docodontenmolaren tatsächlich der Funktionsweise tribosphenischer Bezahnungen ähnelt. Um dies zu ermitteln, wurden mehrere obere und untere Molarenreihen sowie zahlreiche isolierte Molaren des Docodonten *Haldanodon exspectatus* aus dem Oberjura der Kohlemine von Guimarota (Leiria, Portugal) detailliert untersucht.

Dabei fiel auf, dass die Molarenreihen ein ungewöhnliches Abnutzungsmuster zeigen. Reihen mit einem niedrigen Abnutzungsgrad sind normalerweise mesial zunehmend stärker abgenutzt, Reihen mit einem hohen Abnutzungsgrad normalerweise distal zunehmend stärker. Das weist auf einen Zusammenhang zwischen Abnutzungsrichtung und ontogenetischem Alter hin. Eine Molarenreihe wurde anfangs mesial stärker abgenutzt, weil die vorderen Molaren früher durchbrachen als die nachfolgenden. Sobald jedoch alle Molaren durchgebrochen waren, wurden die Reihen zunehmend stärker distal abgenutzt. Dass die Unterkiefer zweier juveniler Individuen beide mesial stärker abgenutzt sind, obwohl eines einen insgesamt sehr hohen Abnutzungsgrad der schon vorhandenen Molaren zeigt, unterstützt diese Hypothese. Eine mögliche Erklärung für diesen Wechsel der Abkaurichtung im Laufe des Lebens wäre ein distal gelegener Kauschwerpunkt in Kombination mit dünnem Schmelz und hochabrasiver Nahrung. *Haldanodon* könnte in dieser Hinsicht einzigartig gewesen sein, da solch ein Abnutzungsmuster bisher nicht bei anderen Docodontentaxa beobachtet wurde.

Die Kaubewegung von *Haldanodon* wurde mit der frei verfügbaren Software Occlusal Fingerprint Analyser (OFA) und den aus µ-CT-Scans zusammengestellten 3D-Modellen eines oberen und zweier unterer Molaren virtuell simuliert. Dies ermöglichte nicht nur detaillierte Beobachtungen zum Bewegungsablauf, sondern auch die Quantifizierung der für verschiedene Kaufunktionen aufgewandten Zeit.
Die Position der zusammengehörigen Facetten auf oberem und unterem Molaren zeigt an, dass der obere Molar zwischen zwei unteren okkludiert. Der mesiale Teil des oberen Molaren kontaktiert die distale Hälfte eines unteren Molaren und der distale Teil des oberen Molaren die mesiale Hälfte des nachfolgenden unteren Molaren. In dieser Position okkludiert der „Pseudoprotocon“ (Höcker X) zwischen den unteren Molaren. Deshalb ist Höcker X nicht funktionell homolog zum tribosphenischen Protocon. Stattdessen greift der viel kleinere Höcker Y in das „Pseudotalonidbecken“ des distal gelegenen unteren Molaren. Dies entspricht früheren Studien an anderen Docodontentaxa (Crompton and Jenkins 1968, Jenkins 1969, Gingerich 1973, Kron 1979, Krusat 1980, Kermack et al. 1987, Butler 1988, Pfretzschner et al. 2005, Schultz et al. 2017).
Unter dem REM sichtbare Striationsmuster im Schmelz isolierter *Haldanodon*-Molaren lassen auf die Bewegungsrichtung der unteren Molaren während des Kauvorgangs schließen. Vertikale Striae weisen auf eine laterale Bewegung hin. Auf dem oberen Molaren biegen sie abrupt nach distal und auf dem unteren Molaren nach mesial um. Das deutet darauf hin, dass die Lateralbewegung eine merkliche proale oder palinale Komponente erhält. Striae, die auf dem oberen Molaren mesial und auf dem unteren distal orientiert sind, implizieren eine weitere proale oder palinale Bewegung in die entgegengesetzte Richtung. In der OFA-Simulation wurde der Kauschlag folglich als zweiphasig rekonstruiert. Phase 1 ist eine steile, von bukkal nach lingual verlaufende Aufwärtsbewegung der unteren Molaren in die zentrale Okklusion. Unmittelbar vor der zentralen Okklusion werden sie abrupt nach distal abgelenkt. Die zweite Phase ist entweder eine direkt anschließende palinale Abwärtsbewegung aus der zentralen Okklusion heraus (Phase 2) oder eine separate proale Aufwärtsbewegung (Phase 1b). In beiden Fällen hat die Bewegung auch eine ausgeprägte laterale Komponente. Während die im Dentin beobachteten Leading und Trailing Edges anzeigen, dass Phase 1 aufwärts gerichtet gewesen sein muss, sind sie für die zweite Phase nicht eindeutig. Sie scheinen eher auf eine abwärtsgerichtete Fortsetzung des Kauschlags hinzuweisen, welche auch von einem aktualistischen Standpunkt wahrscheinlicher ist. Allerdings sind sie nicht deutlich genug ausgeprägt, um eine alternativ genutzte Aufwärtsbewegung sicher auszuschließen. Eine solche ist bisher noch von keinem rezenten oder fossilen Säugertaxon bekannt. Sie würde funktionell jedoch mehr Sinn ergeben, weil Scherschneiden und Reiben nur mit einem viel größeren Energieaufwand in einer Abwärtsbewegung ausgeführt werden können und Quetschen gar nicht möglich ist. Die in dieser Studie durchgeführte virtuelle Rekonstruktion des Kauschlags verbessert frühere Studien an anderen Docodontentaxa. Diese gingen entweder von einem einzigen Kauschlag aus, der in zentraler Okklusion endet (Crompton and Jenkins 1968, Hopson and Crompton 1969, Jenkins 1969, Krusat 1980) oder von einem zweiphasigen Kauschlag ohne Richtungsänderung (Butler 1988, Pfretzschner et al. 2005).

In Phase 1 bewegen sich die lingualen Flanken der Haupthöcker des oberen Molaren und die bukkalen Flanken der Haupthöcker der unteren Molaren scherschneidend aneinander vorbei. Dabei wird die mesio-bukkale Grube des distalen unteren Molaren an Höcker C des oberen Molaren entlanggeführt. Zeitgleich nähert sich Höcker b desselben unteren Molaren dem „Pseudotrigonbeckens“ des oberen Molaren, in dem folglich Quetschen stattfindet. Sobald die mesio-bukkale Grube den Kontakt zu Höcker C verliert, wird die anfänglich laterale Bewegung der unteren Molaren palinal abgelenkt. Unmittelbar vor der zentralen Okklusion stellt Höcker Y des oberen Molaren Kontakt zum „Pseudotalonidbecken“ des distalen unteren Molaren her, wodurch Reiben ermöglicht wird. Sobald der mesiale Rand des Beckens jedoch völlig abradiert ist, rutscht Höcker Y aus dem Becken heraus. Dies führt zum Schließen der Lücke zwischen Höcker b und dem „Pseudotrigonbecken“, in dem dann ebenfalls Reiben stattfindet. Darauf deuten entsprechende Leading und Trailing Edges auf dem mesialen Rand des „Pseudotalonidbeckens“ und die Anwesenheit von distal orientierten Striae innerhalb des „Pseudotrigonbeckens“ hin. Somit wird Quetschen und wahrscheinlich sogar Reiben zum Großteil innerhalb des „Pseudotrigonbeckens“ des oberen Molaren ausgeführt. Während der palinalen Abwärtsbewegung von Phase 2 reibt Höcker Y für sehr kurze Zeit weiter durch das „Pseudotalonidbecken“ (bzw. Höcker b durch das „Pseudotrigonbecken“). Zeitgleich und bis zum Ende der Phase bewegen sich die distalen Grate des mesial gelegenen unteren Molaren und die mesiale Flanke von Höcker X des oberen Molaren „scherreibend“ aneinander vorbei. Echtes Scherschneiden ist nur während einer Aufwärtsbewegung möglich, wie es auch während der alternativen proalen Bewegung von Phase 1b der Fall wäre. Höcker b des distalen unteren Molaren würde dann außerdem zeitgleich quetschend in das „Pseudotrigonbecken“ greifen und das Reiben von Höcker Y durch das „Pseudotalonidbecken“ fände ganz am Ende der Phase statt.

Der Grundbauplan der Molaren anderer Docodontenarten ist dem von *Haldanodon*-Molaren sehr ähnlich. Isolierte Molaren von *Dsungarodon*, *Tashkumyrodon* und *Tegotherium* zeigen außerdem die gleichen Hauptfacetten. Dies macht einen ähnlichen Kauschlag wie den von *Haldanodon* sehr wahrscheinlich. Trotzdem können Docodonten aufgrund von vergleichsweise kleinen Unterschieden in der Zahnmorphologie in drei funktionelle Gruppen eingeteilt werden. Docodonten mit mesial geöffnetem „Pseudotalonidbecken“ und lateral verlaufenden distalen Graten auf den unteren Molaren (*Borealestes*, *Docodon*, *Docofossor*, *Haldanodon*, *Tashkumyrodon*) verließen sich wohl hauptsächlich auf Scherschneiden. Sie konzentrierten Quetschen auf das “Pseudotrigonbecken” der oberen Molaren, in das Höcker b der unteren Molaren hineingriff. Auch Reiben konnte dort stattfinden, sobald Höcker Y aus dem geöffneten „Pseudotalonidbecken“ rutschte. Docodonten mit gut abgeschlossenem „Pseudotalonidbecken“ und einem zusätzlichen, distal gelegenen Becken auf den unteren Molaren (*Hutegotherium*, *Sibirotherium*, *Tegotherium*) waren sehr viel mehr auf Quetschen und Reiben spezialisiert. Dieses fokussierten sie jedoch eher auf die unteren Molaren, da das geschlossene Becken ein Herausrutschen von Höcker Y verhinderte und somit die Lücke zwischen Höcker b und dem „Pseudotrigonbecken“ nicht geschlossen werden konnte. Einige entwickelten sogar einen zusätzlichen Höcker auf den oberen Molaren, der in das distale Becken des unteren Molaren fasste. Docodonten mit gut abgeschlossenem „Pseudotalonid-

becken“, lateral verlaufenden distalen Graten oder Krenulierungen und relativ niedrigen Höckern (*Agilodocodon*, *Castorocauda*, *Dsungarodon*, *Krusatodon*, *Simpsonodon*) waren am besten an Quetschen und Reiben angepasst. Das liegt daran, dass aufgrund der niedrigen Höcker Quetschen und Reiben gleichzeitig innerhalb des „Pseudotalonidbeckens“ und innerhalb des „Pseudotrigonbeckens“ stattfinden konnte. Alles in allem waren Quetschen und sogar Reiben bei allen Docodontenarten sehr viel ausgeprägter als in früheren Studien angenommen.
Die Rekonstruktion der Kaubewegungen mit dem OFA ermöglichte außerdem einen Vergleich der Molarenfunktionen von *Haldanodon* (höchstwahrscheinlich insektivor) mit denen der rezenten tribosphenischen Taxa *Didelphis* (omnivor) und *Monodelphis* (insektivor). In beiden tribosphenischen Taxa greift der Protocon in das Talonidbecken, so dass darin zunächst Quetschen und nach Herstellung des direkten Kontakts auch Reiben stattfindet. Bei *Didelphis* nimmt bezogen auf den gesamten Kauschlag Reiben sehr viel mehr Zeit in Anspruch als bei *Monodelphis*. *Haldanodon* verwendet jedoch noch weniger Zeit auf diese Funktion. *Monodelphis* fehlt eine der beiden didelphiden Reibefacetten, aber die noch vorhandene ist relativ gesehen immer noch größer als die Reibefacette von *Haldanodon*. Deshalb ist Reiben offensichtlich in beiden tribosphenischen Taxa stärker ausgeprägt als in *Haldanodon*. Beim Quetschen ist das jedoch nicht unbedingt der Fall. Bei *Didelphis* und *Monodelphis* wird es durch das Ineinandergreifen von Protocon und Talonidbecken sowie von Hypoconid und Trigonbecken ausgeführt. Wie auch bei *Haldanodon* nimmt es fast die gesamte Phase 1 in Anspruch. In Phase 2 kann wegen der Abwärtsbewegung des Unterkiefers Quetschen nicht stattfinden. Falls *Haldanodon* jedoch zwei separate Aufwärtsbewegungen nutzte, würde die gesamte zweite Phase ebenfalls auf Quetschen verwendet worden sein. Obwohl die Becken von *Didelphis* besser geschlossen und viel größer als die von *Haldanodon* sind, würde sich in diesem Fall die Quetschfunktion ihrer Molaren nicht allzu stark unterscheiden. Die Becken von *Monodelphis* sind im Vergleich zu *Didelphis* sehr viel kleiner, flacher und weniger gut geschlossen. Deshalb war Quetschen bei *Haldanodon* wahrscheinlich mindestens ebenso gut ausgeprägt wie bei *Monodelphis*, sogar falls die Bewegung des Unterkiefers während der zweiten Phase ebenfalls abwärtsgerichtet war. Andere höchstwahrscheinlich insektivore Docodontentaxa mit besser geschlossenen „Pseudotalonidbecken“ und „Pseudotrigonbecken“ sowie zusätzlichen distalen Becken auf den unteren Molaren hatten sicherlich eine stärker ausgeprägte Quetschfunktion als *Monodelphis*. Eventuell war sie sogar ähnlich stark ausgeprägte wie bei *Didelphis*. Docodontenmolaren waren also möglicherweise sehr wohl in der Lage mit frühen tribosphenischen Molaren in Hinsicht auf Quetschen und sogar Reiben zu konkurrieren. Allerdings machte sie ihre dünne Schmelzschicht sehr viel anfälliger für Abnutzung und den damit einhergehenden Funktionsverlust. Außerdem besitzen Docodonten einige sehr basale postcraniale Merkmale. Beide Faktoren könnten eine signifikante Rolle bei ihrem Aussterben in der Frühen Kreide gespielt haben – zur gleichen Zeit, als die Tribospheniden sich auszubreiten begannen.